USGS-OFR-96-267

U.S. DEPARTMENT OF THE INTERIOR
U.S. GEOLOGICAL SURVEY

TOWARD ASSESSING THE SEISMIC RISK ASSOCIATED WITH BLIND FAULTS, San Francisco Bay Region, California

Principal Compilers
Onshore area
A. S. Jayko[1]
Offshore area
S. D. Lewis[1]

U. S. Geological Survey Open-file Report 96-267

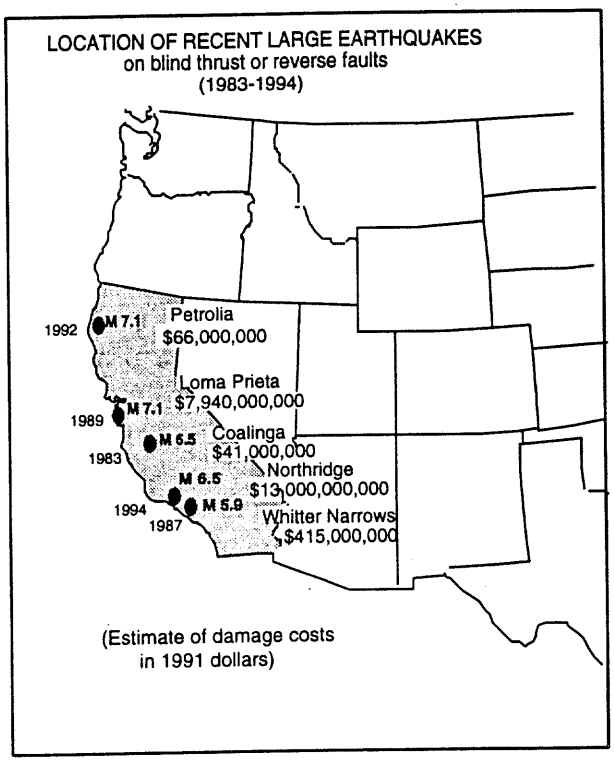

This report is preliminary and has not been reviewed for conformity with U.S. Geological Survey editorial standards or with the North American Stratigraphic Code. Any use of trade, product or firm names is for descriptive purposes only and does not imply endorsement by the U.S. Government.

[1] Menlo Park, California, 94025

1996

This report is a collaborative effort produced by the
Working Group on Active Folding and Blind Thrusting, San Francisco Bay Region
Established May 27, 1994
Organized under the auspices of CONCERT
(Coordinating Organization for Northern California
Earthquake Research and Technology)

In cooperation with IUGG, ILP Project II-2
World Map of Major Active Faults (Western Hemisphere)

Steering Committee

A.S. Jayko[1], coordinator,
Bill Bakun[1], William. R. Lettis[2], Steve Lewis[1]
Dave Schwartz[1], John Sims[1], Dave Wagner[3]
1. U. S. Geological Survey
2. William Lettis and Associates
3. California Division of Mines and Geology

List of Contributors

Angell, M.	Geomatrix Consultants
Anima, R.	U. S. Geological Survey
Arrowsmith, R.	Stanford University
Bonilla, M.G.	U. S. Geological Survey
Buising, A. V.	California State University Hayward
Catching, R. D.	U. S. Geological Survey
Crampton, T.A.	Geomatrix Consultants
Graymer, R. W.	U. S. Geological Survey
Hart, P.E.	Wm Lettis and Associates
Helley, E. J.	U. S. Geological Survey
Hitchcock, C. S	Wm Lettis and Associates
Jachens, R. C.	U. S. Geological Survey
Jayko, A. S.	U. S. Geological Survey
Kelson, K. I.	Wm Lettis and Associates
Kovach, R. L.	Stanford University
Lajoie, K. R.	U. S. Geological Survey
Lettis, W. R.	Wm Lettis and Associates
Lewis, S. D.	U. S. Geological Survey
Marlow, M. S.	U. S. Geological Survey
Mc Laughlin, R. J.	U. S. Geological Survey
McCarthy, J.	U. S. Geological Survey
Nolan, J.	Weber and Associates
Odum, J. K.	U. S. Geological Survey
Oppenheimer, D.	U. S. Geological Survey
Page, B. M.	Stanford University
Parsons, T.	U. S. Geological Survey
Pollard, D.D.	Stanford University
Roering, J.J.	Stanford University
Rymer, M. J.	U. S. Geological Survey
Simpson, G. D.	Wm Lettis and Associates
Sorg, D.H.	U. S. Geological Survey
Unruh, J. R.	Wm Lettis and Associates
Wagner, D.	California Division of Mines and Geology
Wakabayashi J.	Private Consultant
Weber-Band, J.	U. C. Berkeley
Wentworth, C. M.	U. S. Geological Survey
Wesling, J.	Geomatrix Consultants
Williams, P. L.	Berkeley National Lab and U.C. Berkeley
Williams, R. A.	U. S. Geological Survey
Williams, R. T.	University of Tennessee

List of Working Group Participants Appendix III.

Table of Contents

East Bay Area

North Bay and Delta areas

Appendices

Active Folds and Blind Thrusts, San Francisco Bay Region, An Overview

Jayko, A.S., U. S. Geological Survey, 345 Middlefield Rd., Menlo Park, CA 94025

The need for a better understanding of the seismic risk posed by active blind faults is evident from recent damaging earthquakes in northern and southern California, including the Coalinga 1983, Loma Prieta 1989, Petrolia 1992, Northridge 1994, and Whitter Narrows 1987 events. These events are moderate magnitude 6.5 to 7.1 and yet represent a substantial and costly hazard (combined damage estimates of 30.5 billion dollars, Figure 1).

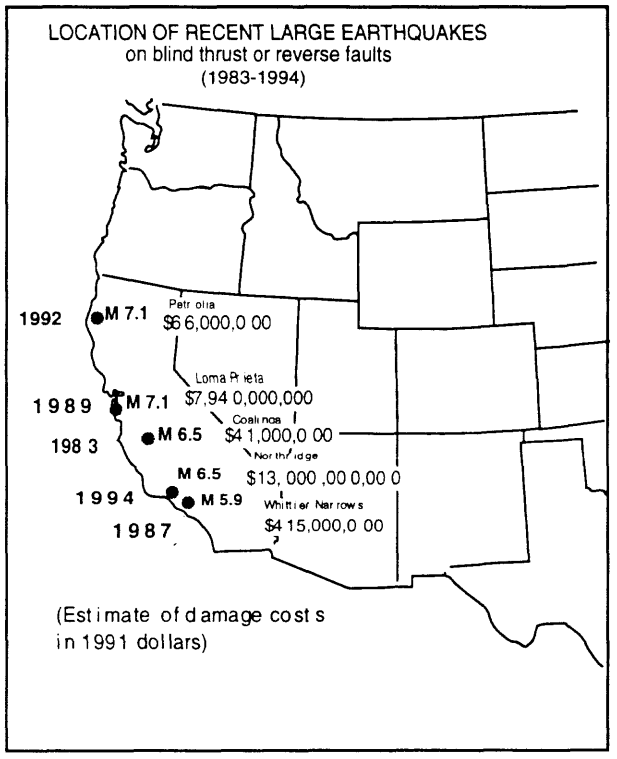

Figure 1 Map showing location of recent large damaging earthquakes in California

Understanding the paleoseismic history of blind faults (Figure 2), the active faults which do not breach the earths surface, and which often terminate at depths of 5-10 kilometers poses a challenging problem to earth scientists because their location and displacement rates, and thus the inferred seismic slip rate, must be derived from inference and cannot be directly measured.

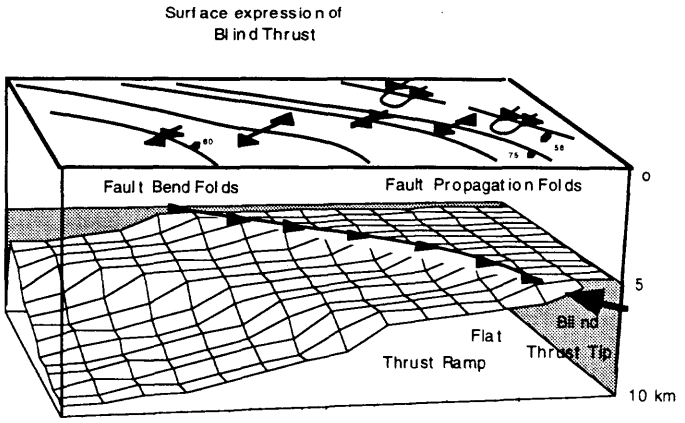

Figure 2 Diagram illustrating blind thrust fault, thrust tip line and associated surface folds.

Active folding and Quaternary vertical displacements are the most direct indicators of the potential location of active blind faults, thus one of the first steps towards understanding the seismic risk posed by blind faults is to gain a thorough understanding of active folds, their structural association, and their structural geometry within the subsurface.

Major aspects to the problem of understanding how active folding can contribute to evaluating seismic risk associated with blind faults are to locate the structures and establish geologic and geomorphic criteria which indicate the recency of displacement, and the rate of deformation. The second is to constrain the

possible fault geometries at depth that give rise to the observed fold sequence.

Blind thrust faults are those faults which, unlike the major strike-slip faults in the bay area, do not produce a rupture at the earth's surface, and thus do not produce a readily mappable fault trace. Such faults must be inferred by geophysical, geomorphologic and/or structural methods. These faults do produce actively growing folds by repeated motion on associated faults (Stein, Ross S., et al, 1992, Ekstrom, et al, 1992; Yeats, Robert S, 1987; Bullard, Thomas F., et al, 1993). Active folds are an indicator of blind faulting, thus an effort to portray the scale and deformation rate of active folds is crucial for developing a complete seismic risk assessment of the region. Vertical displacements provide a good indication of crustal upheaval associated with such folding.

The deformation rates of folds can easily be an order of magnitude or two lower than those found along active strike-slip faults in the San Francisco Bay region (for example, 0.3 mm/yr versus 1.0 to 3.0 mm/yr respectively). A large amount of uncertainty is associated with quantifying the low strain rates of the recent past. The deformation associated with folding will also be more diffuse thus, establishing Holocene displacement per se, especially on large structures is non trivial. Establishing the Holocene-Pleistocene deformation is more realistic for a region, such as the San Francisco Bay area which is characterized by moderate to low crustal shortening rates.

The topographic relief of the San Francisco Bay region is a crude indicator of recent tectonic activity. There is general consensus that major regional topographic highs are structurally controlled. There is also general consensus that most of the topographic relief in the area is fairly youthful, probably late Pliocene and even younger, thus a reasonable expression of Quaternary tectonics (cf. Lawson 1893, Christensen, 1965; Burgmann and others, 1994). The 1989 Loma Prieta event is considered a good analog for indicating the potential scale of a fold structure associated with a medium sized earthquake on a blind thrust. Structures of the size of Ben Lomand Mountain (mountain range scale) are considered to be the primary target scale for identification and compilation as these have the greatest potential for being a seismic source.

CONCERT Working Group

The effort to develop an active fold and blind thrust map for the San Francisco Bay Region was initiated during a CONCERT (Coordinating Organization for Northern California Earthquake Research) workshop on Resolving the Tectonic Framework of the San Francisco Bay Area, held April 18-20 at the U.S. Geological Survey, Menlo Park (Brocher and Furlong, 1994). Participants of this workshop agreed to form a working group (Appendix IV) to help resolve issues regarding active folding and contribute expertise towards the compilation. The impetus to form such a working group is motivated by the need to evaluate the earthquake hazards posed by blind thrust faults.

One of the first objectives was to compile a map from the existing sources that can be used to assess our current understanding of active folding in the region, and that will help define future research needs to adequately address the local hazards due to blind thrusts. Some of the issues for which consensus has been sought are 1.) to define the basic tectonic and geologic features that need to be mapped, 2.) to establish guidelines regarding the quality and confidence rating of the information, 3.) to set up guidelines for database management of fold related information, and 4.) to set up guidelines for compilation priorities and future research activities that address problems related to active folding and blind thrusting.

The scope of the current task includes: 1) proceeding with the available information to produce a database that is essential to urban planners, and 2.) prioritizing a longer term research strategy so that we focus efforts towards improving our understanding of the crustal manifestation of active folds.

This preliminary compilation of a fold map for the San Francisco Bay Region (Plate I) has been compiled from existing published and unpublished geologic data available within the geologic community. The compilation serves the purpose of providing a summary of the current state of knowledge concerning blind faults and active folding in the San Francisco Bay Region. This map will primarily indicate the location of areas where late Cenozoic folding has occurred, further work will be required to determine whether such structures are active in the present tectonic regime, and their relation to subsurface structures. The map will also serve the purpose of indicating the location of regions which require additional study.

Although the emphasis of the project is to identify the seismic hazard posed by potentially active blind thrust faults, any late Cenozoic fold of possible Quaternary age that could be underlain by an active fault, whether that fault has thrust, strike-slip or normal displacement has been characterized on the map. We recognize that the sense of displacement on a fault which underlies an active or late Cenozoic fold may be ambiguous based on surface data alone, and could require further subsurface investigation.

The urgency to compile the best available data concerning active folding was augmented by the need for information on the slip-rate and location of seismically active faults that could be integrated into the probabilistic seismic hazard map. The probabilistic seismic hazard map is one of the sources of data which is used to help define new national and regional building codes and is scheduled for revision in 1995-1996.

This preliminary compilation is an interim product in the sense that the effort to produce an accurate and reliable active fold map indicates some of the paucity of data, and limitations in available means to distinguish active folding from Neogene and Pleistocene folding, as it does a robust understanding of the active tectonics. Thus, the map also serves the purpose of directing attention to high priority areas and topics which require additional study.

This compilation is a cooperative effort between private consulting companies including Cotton and Associates, Dames and Moores, Geomatrix, Harlann, Tait and Associates, Lettis and Associates, Norfleet Consultants, Weber and Associates; academic institutions including Cal State Hayward, U.C. Berkeley, Stanford University, and government institutions including California Division of Mines and Geology, Lawrence Berkeley Labs and the U.S. Geological Survey.

Project Objectives

The primary objective of this project was to compile and provide a source for information concerning the location, and where possible, the rates of deformation of late Cenozoic, in particular, Quaternary folds. The project was narrowly limited to folding, and potentially youthful blind thrusts, as there has previously been extensive work concerning Quaternary surface faulting and fault slip rates. An effort was made to exploit the expertise of the local geologic community, to make available information that exists in unpublished and/or obscure technical reports, and to provide documentation necessary to estimate potential slip-rates on active structures. This report represents a compilation of existing data. Future efforts will be directed towards extracting information, and reinterpreting existing data set with respect to magnitudes and rates of deformation, as well as additional Quaternary studies.

In order to be as systematic and thorough as possible, database forms (Appendix II) that itemize much of the salient information were used by compilers to list characteristics of the folds. This data has been entered into arc-info digital formats. The tabulated data, the fold structures and short abstracts make up the bulk of the report.

Contributions to Database

There is a variety of data and levels of synthesis presented in this report. The primary purpose of the report is to make available the information concerning late Cenozoic folds that is currently known in the geologic community. Some contributors submitted only location information, others submitted complete database information (see database form, Appendix II.), abstracts and a brief synthesis. There was a full spectrum of material submitted for this preliminary compilation. We are very grateful to all the compilers and working group members who volunteered to undertake this task within a short time frame. We welcomed all information that was available and encouraged contributors to make their best estimate of strain rates for the regions they were familiar in spite of the many uncertainties involved. This effort indicates the present state of knowledge concerning active folding in the San Francisco Bay region and helps indicate the direction and location of future studies.

The methods for constraining active folding and blind thrust faulting presented in this report consist of results of Quaternary

marine terrace stratigraphy (Lajoie), regional and detailed geologic mapping and map compilation (Angell, Bonilla, Buising and Wakabayashi, Crampton, Graymer, Kelson, McLaughlin and others, Nolan, Unruh, Wagner, Wesling, and Wentworth), gravity modeling (Jachens; Page and Kovach), seismic reflection profiling (Lewis, Weber-Band, Marlow, McCarthy and others, Williams, P.L.; Williams and others), geomorphology (Kelson and Hitchcock; Jayko) and numeric modeling (Roering and others). Figure 1 shows the location of study areas and Figure 2 shows the location of seismic reflection lines, stream profiles, and published structural sections.

Database Fields

The folds database was designed to accommodate structural and tectonic information as well as that concerning active deformation and potential seismic hazard from blind thrust faulting. The database fields describe the dimensions of the fold, the vertical and horizontal deformation rates, and the accumulated strain, which are the most important information needed to assess the seismogenic potential of the associated thrust system. In most cases the strain quantities are derived from geologic or geomorphic data, principally through determining line-length changes estimated from structural or topographic cross-sections. Fields also describe the type of geologic and geomorphic horizons that define the fold, and the method for dating the horizons. This information can be used to help assess the reliability of the strain data that is inferred from the geologic record. Likewise, database fields describe the availability of drill hole and seismic reflection data which help to constrain the subsurface geometry of folds, and thus the magnitude of displacement.

Many of the database fields contain a value that is derived or inferred. An associated field indicates the confidence in the derived value. The confidence is subjective and made by the compiler based on weighing the quality of the constraints on the various kinds of data input that determine the age of materials and stratigraphic position. Geologic and geomorphic units of a wide range of ages from Holocene to late Miocene were used to constrain the deformation rates and potential location of structures. A wide variety of geochronologic methods have been used to determine the age or age range of geologic horizons, units, members, beds, and geomorphic surfaces. Age determinations have been made from soil stratigraphy, radiocarbon dating, apatite and fission track dating, and floral and faunal remains. The magnitude of uncertainty varies with each method applied, with the quality of material preserved, and with other analytical uncertainties inherent in the methods. For the upper and lower age limit of various structures, different age dating techniques are applied at different horizons. Thus, quantifying the age uncertainty is a formidable problem. Likewise, the strain

rates for many of the structures were determined by change in line lengths determined from structural sections. The quality and accuracy of structural sections is in part a function of available subsurface data including drill hole and seismic reflection. Thus at most localities where deformation rates were determined from geologic data the factors contributing to uncertainties in the derived rate values are numerous. We have not attempted to systematically quantify the error or uncertainty. The confidence ratings used in this database 5 (high) to 1 (low) represents the compilers subjective assessment of these factors.

Table 1 shows the list of categories and definitions that are presented in the tabulated data submitted by the compilers. Figure 3 shows the age range coding 1 - 7 that was entered into the age-min and age-max fields of the tabulated data. Almost all compilers who submitted database forms for structures also submitted short abstracts although there are a couple of exceptions.

Report Format

The contributions in this report have been organized geographically. All of the information for the offshore area was provided by S.D. Lewis. A number of papers address structures in the Santa Cruz Mountains, and in particular, the Monte Vista fault zone which lies along the eastern range front near Los Gatos. There are several papers that describe seismic reflection data from the east bay area along the delta, and less comprehensive coverage of Napa-Sonoma area and the southeastern Diablo Range.

The contributors submitted maps of various scales (scales of the original data and compiled data are entered into the data base) which were scanned and vectorized. Nearly all of the map figures that accompany the abstracts were extracted from the arc-info coverage. The tabulated data was submitted on the database forms and extracted from the arc-info attribute table. Only filled field areas were extracted and tabulated. The arc-line number is listed in the tabulated data and displayed on the accompanying page size maps. In general, only fold structures were submitted and compiled. In the delta area, however; J. Weber-Band mapped the location of the tip-line of buried thrust faults from seismic reflection data, which is an important new contribution. Most of the faults that are shown in the on-shore area were compiled from the 1:750,000 California Division of Mines and Geology, Quaternary Fault Map, some faults were also compiled from the 1:250,000 scale geologic maps.

Coordination with other U.S.G.S. Projects

The results from this report contribute to two U.S.G.S. projects concerning active faulting and seismic hazard assessment, the Major Active Faults of the Western Hemisphere Map that is

being coordinated by Mike Machette, and the Probabilistic Seismic Hazard Map coordinated by Art Frankel which meets national needs for providing input to new national and regional building codes. Both of these regional projects are scheduled for completion during the 1996 calendar year. Data provided by the CONCERT Active Folds working group will be integrated into another consensus group database on slip-rate magnitudes that has evolved in response to needs outlined in the context of the Probabilistic Seismic Hazard Map during a workshop help in Menlo Park on the 3rd of November, 1994.

Internet Access

For those with access to the internet, a FTP directory where files can be transferred and stored has been set up on sierra.wr.usgs.gov. There are two directories, one located in /incoming/bayarea_folds/ where files can be put for temporary storage, the other is located in /outgoing/bayarea_folds/ where text and data files that can be copied or read will be stored. The directories are accessible by anonymous FTP, which means they are accessible to the general public. The incoming is read-copy-write access, the outgoing is read-copy only. Information that should not be modified at random will be kept in the outgoing directory. There is currently the database form in Word 5 and compilation guidelines in the outgoing directory. ARC-INFO export files will be added in the future for those with access to ARC GIS systems.

The results of the initial compilation effort synthesized herein consist of 1.) a structural map showing geologic and geomorphic features indicative of active uplift and potentially, active folding; 2.) an index map showing the location of information provided by compilers; 3.) a postscript file which summarizes information on the structures and is accessible via anonymous ftp on sierra.wr.usgs.gov; and 4.) additional references.

It is hoped that this compilation improves our understanding of the active tectonics of the region and helps to focus future research activities regarding the deformation mechanisms and rates that are responsible for the developments of active folding in the region.

References

Aydin, A., and Page, B. M., 1984, Diverse Pliocene-Quaternary tectonics in a transform environment, San Francisco Bay region, California: Geological Society of America Bulletin, v. 95, p. 1303-1317.

Brocher, T. M., J. McCarthy, Hart, P. E., Holbrook, W. S., Furlong, K. P., McEvilly, T. V., Hole, J. A., and Basix, in press, Seismic evidence for a possible lower-crustal detachment beneath San Francisco Bay: Science,

Bullard, T. F., and Lettis, W. R., 1993, Quaternary deformation associated with blind thrust faulting, Los Angeles Basin, California: Journal of Geophysical Research, v. 98, p. 8349-8369.

Burgmann, R. Arrowsmith, R. Dumitru, T., and Mc Laughlin, R., 1994, Rise and Fall of the southern Santa Cruz Mountains, California: Journal of Geophysical Research, v. p.

Christensen, M. N., 1965, Late Cenozoic deformation in the central Coast Ranges of California: Geological Society of America Bulletin, v. 76, p. 1105-1124.

Ekstrom, Goran, et Al, Seismicity And Geometry Of A 110-Km-Long Blind Thrust Fault; 1, The 1985 Kettleman Hills, California, Earthquake, April 10, 1992, Journal Of Geophysical Research, B, Solid Earth And Planets ; Vol. 97, No. 4, P. 4843-4864.

Haller, K. M., Machette, M. N., and Dart, R. L., 1993, Maps of Major active faults, western Hemisphere, International Lithosphere Program (ILP), Project II-2: U.S. Geological Survey 93-338, 45 p.

Lawson, A. C., 1893, The post-Pliocene diastrophism of the coast of southern California: University of California Press, v. 1, p. 115-160.

Stein, Ross S., et Al, Seismicity And Geometry Of A 110-Km-Long Blind Thrust Fault; 2, Synthesis Of The 1982-1985 California Earthquake Sequence, April 10, 1992, Journal Of Geophysical Research, B, Solid Earth And Planets ; Vol. 97, No. 4, P. 4865-4883.

Yeats, Robert S, Coseismic Folding, Crone, Anthony J., et al. 1987, Open-File Report - U. S. Geological Survey; OF 87-0673, P. 163-172.

Table 1.
The following abbreviations are found in the open-file text tables.

Arc Ln id	Arc Line identity number
Compiler(s)	
Institution	
D of submis	Date of submission to database
Project/Contract	USGS Project or Contract number
Map_scale	Map_scale of submitted compilation
Original_source_scale	
Structure_Name	Fold or Fault Structure_Name
age_min	Minimum age of structure
age_max	Maximum age of structure
Age_control	Source of stratigraphic or geomorphic Age_control
Inclined Geomorphic surface	Inclined or otherwise deformed Geomorphic surface
horiz short (km)	Magnitude of horizontal strain (E) shortening (units km)
c1	c1, confidence in the estimate of magnitude of horizontal strain 1(high) to 5 (low)
Shortening rate mm/yr	Shortening rate, strain rate in the horizontal direction (units in mm/yr)
c2	c2, confidence in the estimate of the shortening rate, 1(high) to 5 (low)
vert rate mm/yr	Vertical displacement rate (units in mm/yr)
c3	c3, confidence in the estimate of the shortening rate, 1(high) to 5 (low)
Initiation of folding (Ma)	Estimate of the timing of the initiation of folding (units Ma)
c4	c4, confidence in the estimate of the timing of the initiation of folding, 1(high) to 5 (low)
Termination of folding (Ma)	Estimate of the timing of the termination of folding (Ma)
c 5	c5, confidence in the estimate of the timing of the termination of folding, 1(high) to 5 (low)
Method	Method of determining strain rates, and magnitude of displacement
Rate ave time length	Lenght of time over which the displacement rate was determined or averaged
Para ss	Does the fold parallel a strike-slip fault? (yes or no)
dist from fault	If the fold parallels a strike-slip fault, what is the average distance from the fault? (units km)
Ave Ori	If the fold does not parallel a strike-slip fault, what is its obliquity with respect to the fault.
Distance fm faults	What distance does the oblique fold lie from the fault?
Ave. Trend	Average Trend of the fold (0 - 360 degrees)

Plunge	Plunge (0 - 90 degrees)
Ave AP strike	Average Axial Plane strike (0 -360 degrees)
AP dip	Axial Plane dip (0 -90 degrees)
AP dip dir	Axial Plane dip direction (n ne e se s sw w nw)
Confidence of location	Confidence of location of the fold trace on the map (Definite, Probable, Possible)
Verge dir	Vergence direction (n ne e se s sw w nw)
Multi or seg	Is the fold part of a larger zone or segmented? (yes or no)
Interlb ang	Interlimb angle (0 - 179 degrees)
Bck-lb strk	Back-limb strike (0 -360 degrees)
Bck-lb dip	Back-limb dip (0 -90 degrees)
Bck-lb dip dr	Back-limb dip direction (n ne e se s sw w nw)
Bck-lb dim (km sq)	Back-limb dimension (units km sq)
Fr-lb strike	Fore-limb strike (0 -360 degrees)
Fr-lb dip	Fore-limb dip (0 -90 degrees)
Fr-lb dip dr	Fore-limb dip direction (n ne e se s sw w nw)
Fr-lb dim (km sq)	Fore-limb dimension (units km sq)
half wvlgth (km)	Half wavelength of the fold (units km)
fold type	fold type, anticline A, syncline, S homocline, H, upright, U, open, O gentle, G, inclined, I, asymmetric AS
fold style	fold style, fault bend fold, fault propagation fold, en echelon, unknown
Geodetic	Geodetic data available? (yes or no)
Reference	Reference for geodetic data
Subsurface data	Subsurface data available? (cite reference)
Structure sections	Structure sections available? (cite reference)
Drill Hole	Drill Hole data available? (cite reference)
Seis Reflct	Seis Reflction data available? (cite reference)
Grav	Gravity data available? (cite reference)
Historical Seismicity	Historical Seismicity (cite reference)
Mag/event	List Magnitude and name of event
Depth	Depth (units km)
Distrib microseis	Distributed microseismicity (cite reference)
Reference or comments	
Additonal References	
Extra	Extra (This space was used to enter an arbitrary end of line character for imported file)

Figure Captions

Figure 1 Map showing location of compilation areas for the Late Cenozoic Folds and blind thrusts of the San Francisco Bay Region.

Figure 2 Map showing sources of profile data used in the fold map compilation.

Figure 3 Time-scale showing age range of folds designated on fold map and in database. Numbers 1-7 show the ranges of age that are used in the tables to indicate age range under age_min and age_max.

Figure 4 Map showing the location of Late Quaternary folds (<750,000 Ma), San Francisco Bay region

Figure 5 Map showing location of Quaternary folds, San Francisco Bay region.

Figure 6 Map showing location of Pliocene and younger folds, San Francisco Bay region.

Figure 7 Estimates of vertical displacement rates in mm/yr, Coastal data from Lajoie, 1994 per. comm. Late Quaternary folds also shown.

Figure 8 Estimates of horizontal displacement rates in mm/yr.

Figure 9 Estimates of the magnitude of horizontal displacement across individual folds, folds shown as dotted line.

Figure 10 Inclination of fold axial planes.

Figure 11 Interlimb angles.

Figure 12 Trend of folds.

Figure 13 Plunge of folds.

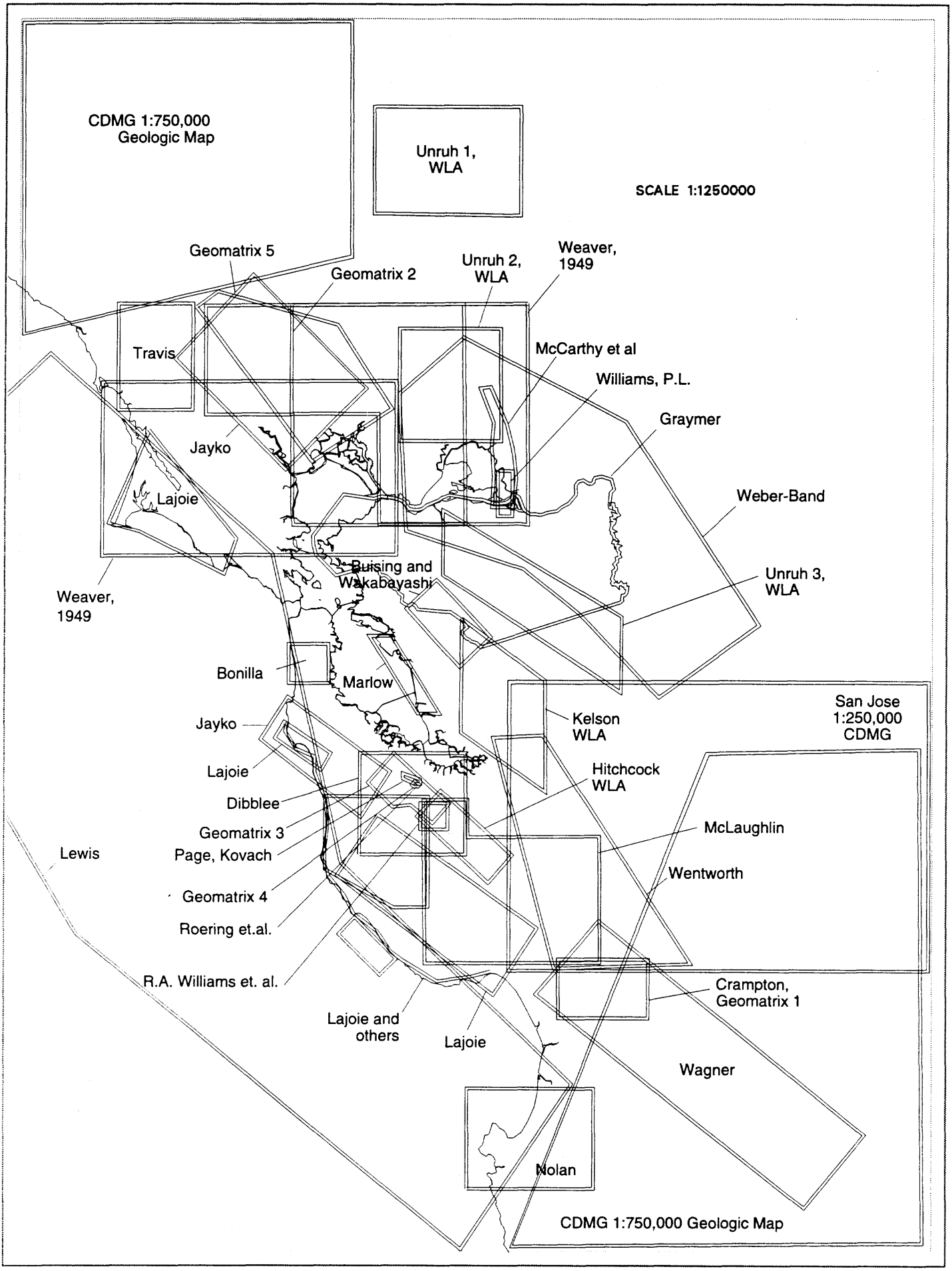
CDMG 1:750,000
Geologic Map
Unruh 1,
WLA
SCALE 1:1250000
Geomatrix 5
Geomatrix 2
Unruh 2,
WLA
Weaver,
1949
Travis
McCarthy et al
Williams, P.L.
Graymer
Jayko
Lajoie
Weber-Band
Ruising and
Wakabayashi
Unruh 3,
WLA
Weaver,
1949
Bonilla
Marlow
San Jose
1:250,000
CDMG
Jayko
Kelson
WLA
Lajoie
Hitchcock
WLA
Dibblee
Geomatrix 3
McLaughlin
Lewis
Page, Kovach
Wentworth
Geomatrix 4
Roering et.al.
R.A. Williams et. al.
Crampton,
Geomatrix 1
Lajoie and
others
Lajoie
Wagner
Nolan
CDMG 1:750,000 Geologic Map

Figure 1

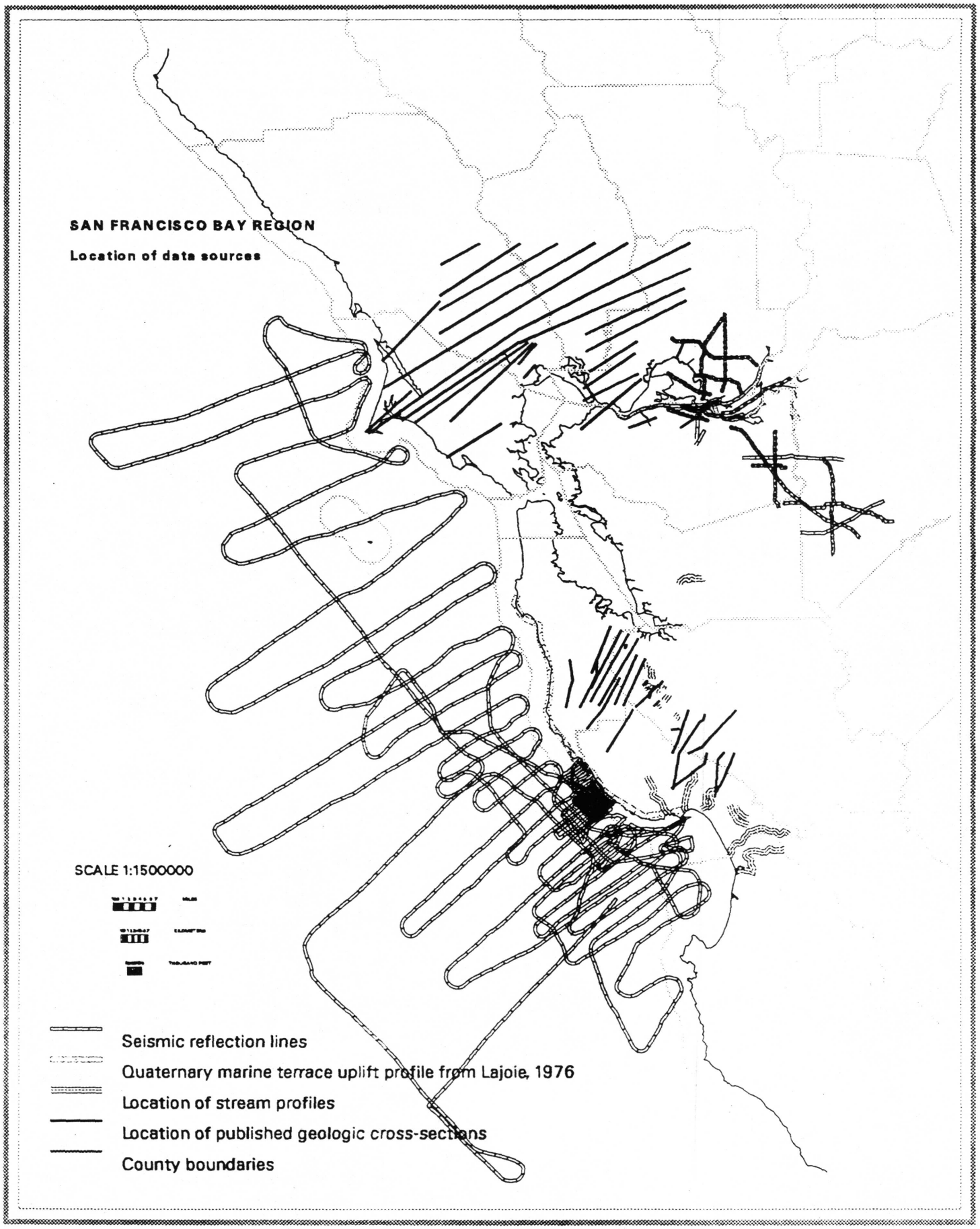
SAN FRANCISCO BAY REGION
Location of data sources
SCALE 1:1500000
Seismic reflection lines
Quaternary marine terrace uplift profile from Lajoie, 1976
Location of stream profiles
Location of published geologic cross-sections
County boundaries

Figure 2

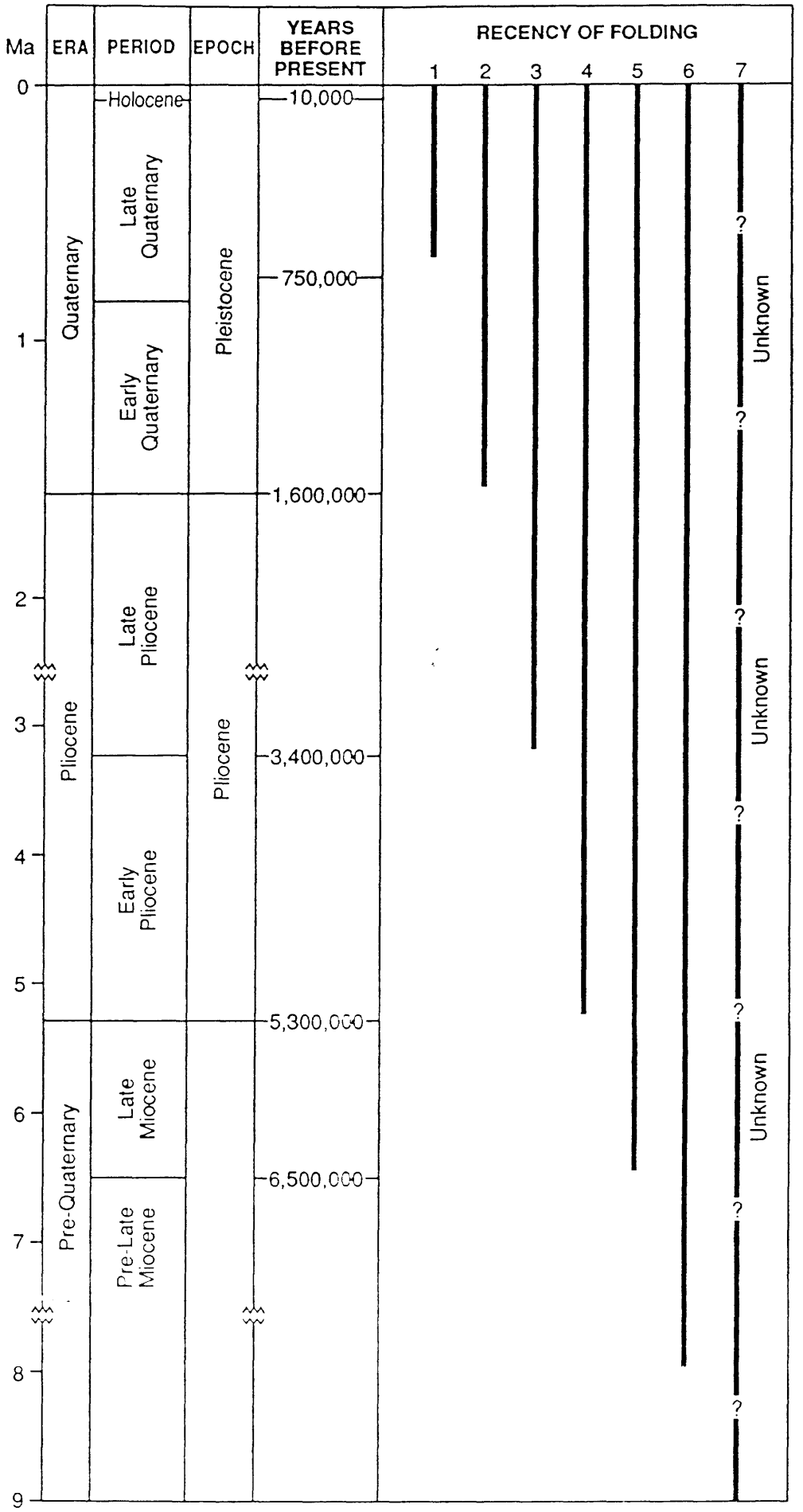
Ma
ERA
PERIOD
EPOCH
YEARS BEFORE PRESENT
RECENCY OF FOLDING
1
2
3
4
5
6
7
0
1
2
3
4
5
6
7
8
9
Holocene
10,000
750,000
1,600,000
3,400,000
5,300,000
6,500,000
Quaternary
Late Quaternary
Early Quaternary
Pleistocene
Pliocene
Late Pliocene
Early Pliocene
Pliocene
Pre-Quaternary
Late Miocene
Pre-Late Miocene
Unknown
Unknown
Unknown

Figure 3

SAN FRANCISCO BAY REGION

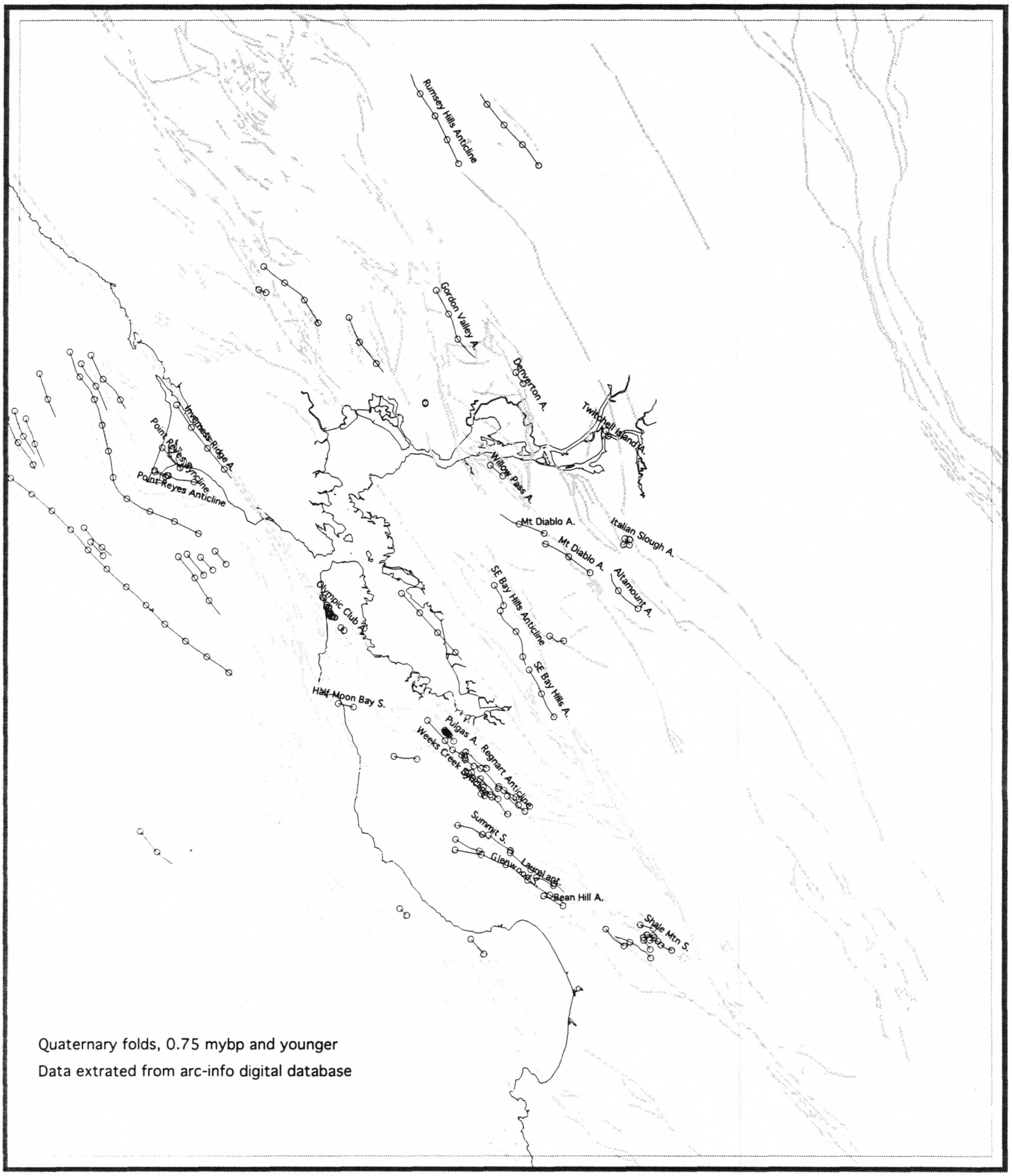

Figure 4

SAN FRANCISCO BAY REGION

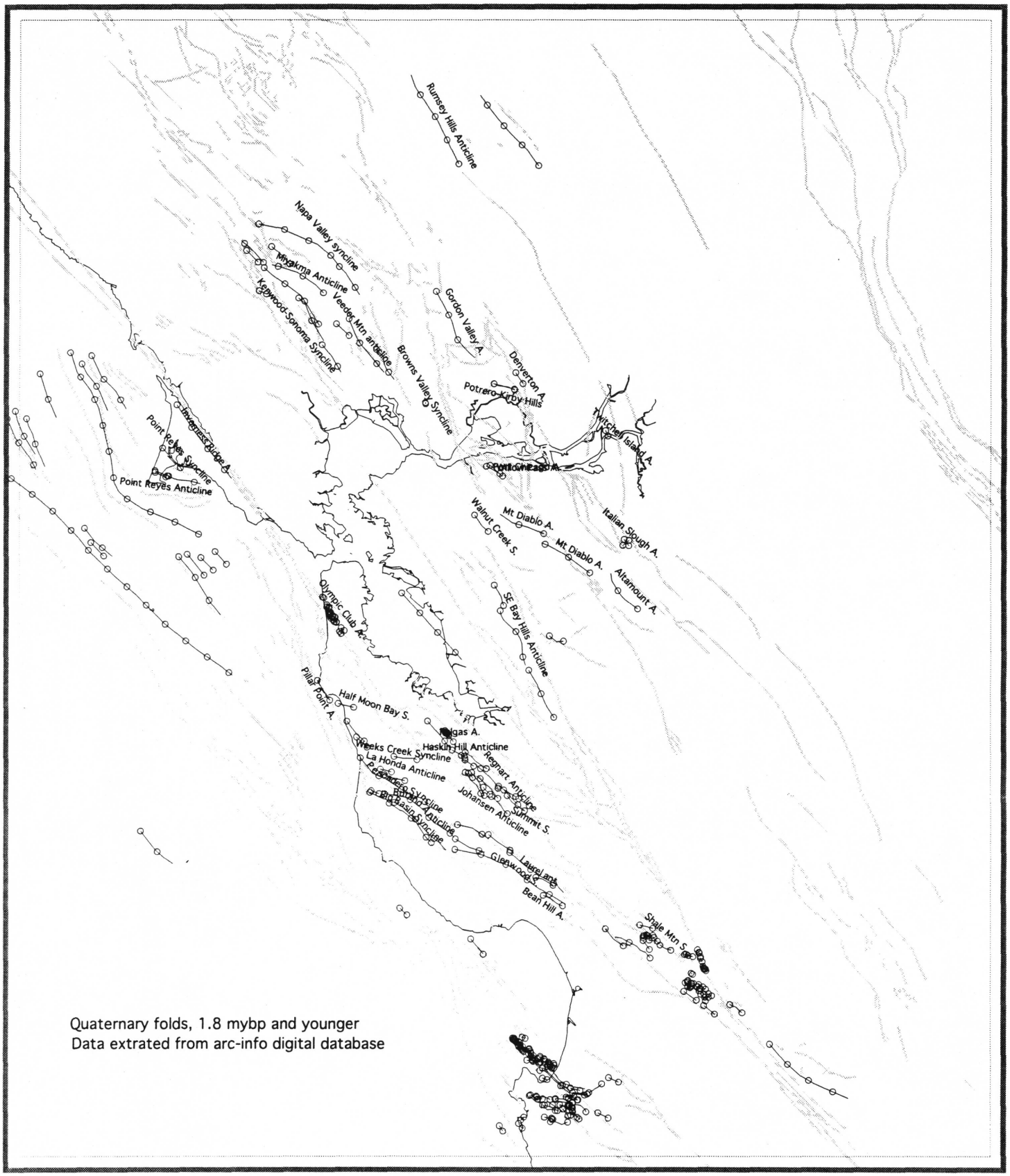

Figure 5

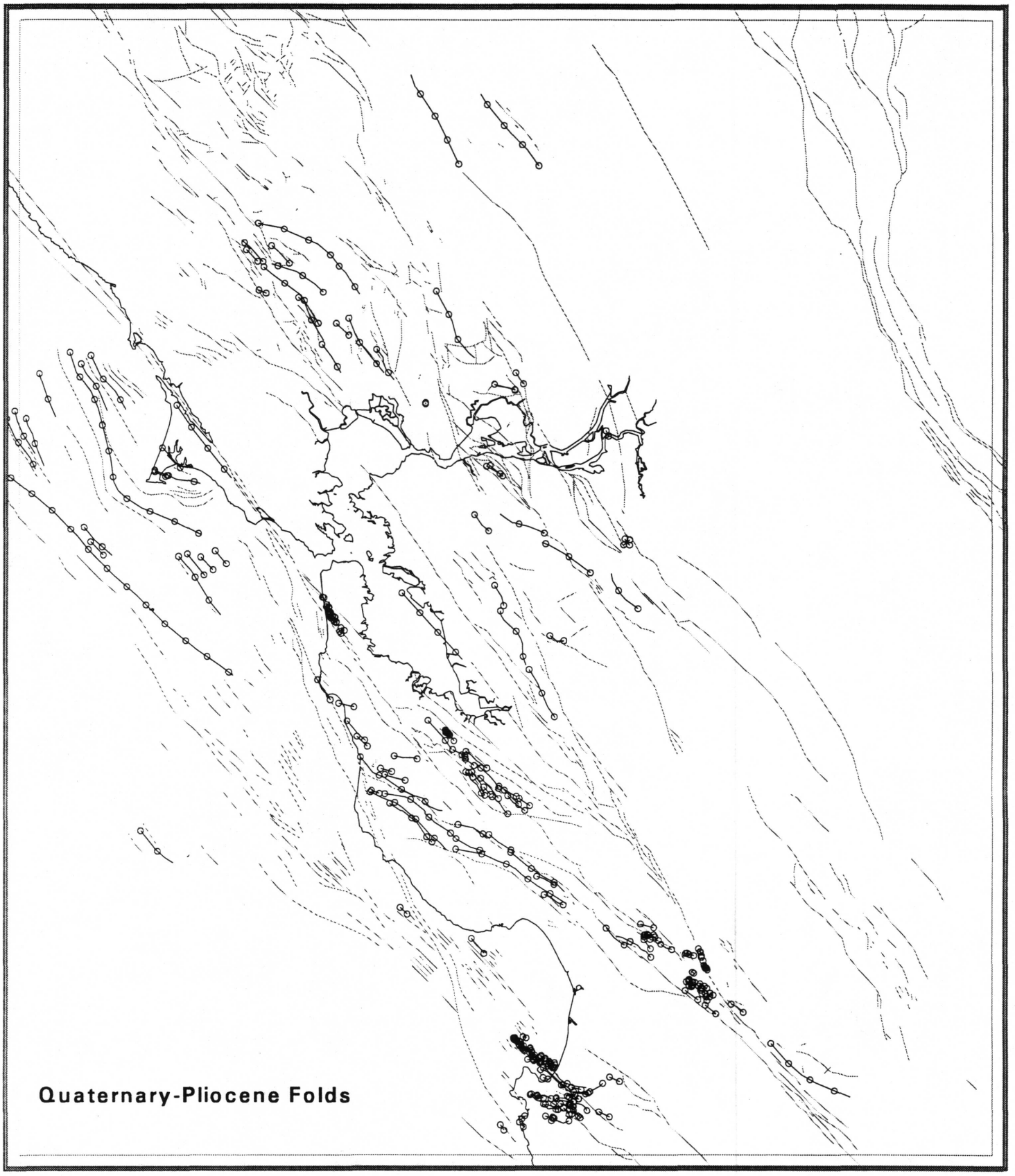

Figure 6

SAN FRANCISCO BAY REGION

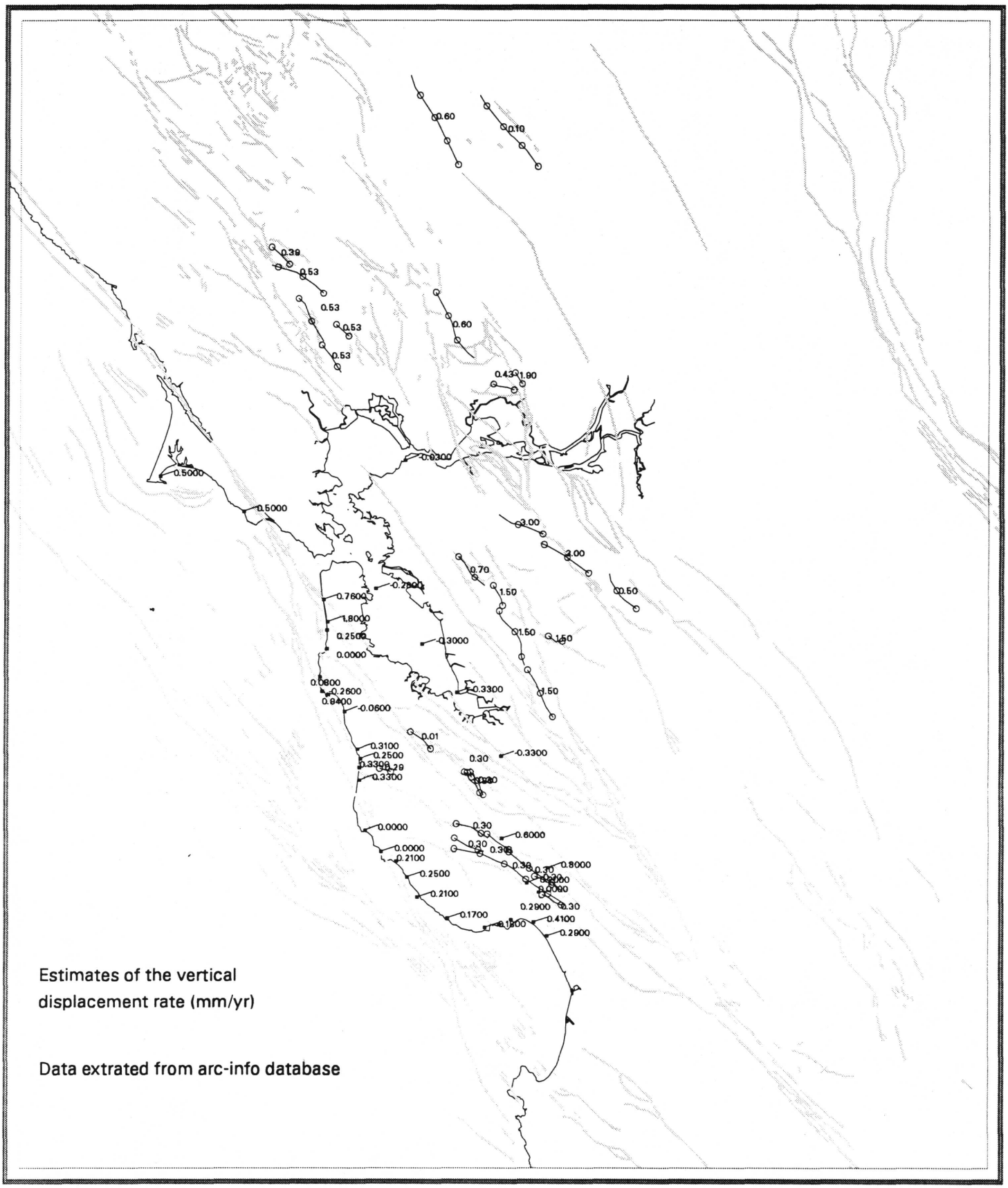

Figure 7

SAN FRANCISCO BAY REGION

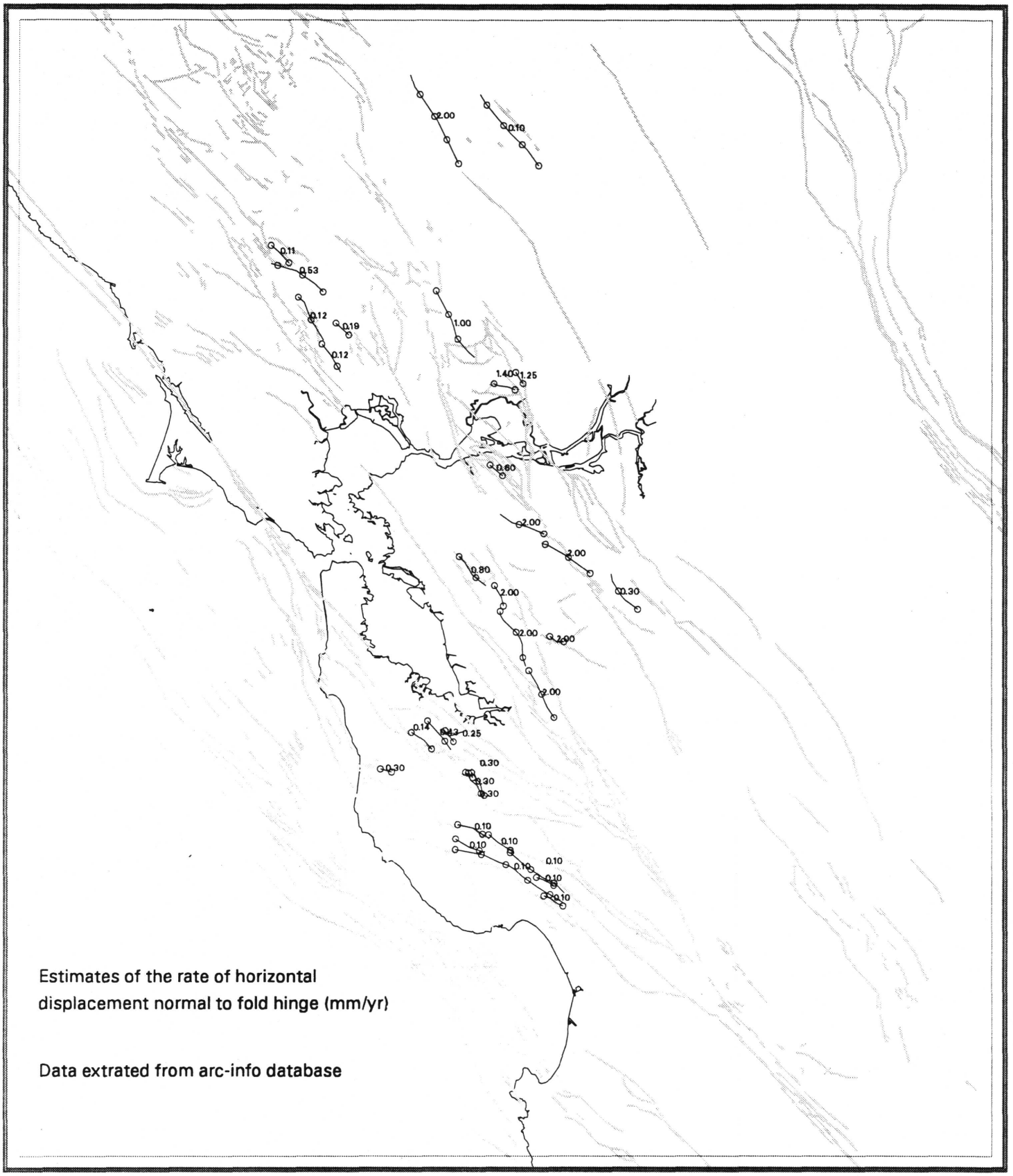

Figure 8

SAN FRANCISCO BAY REGION

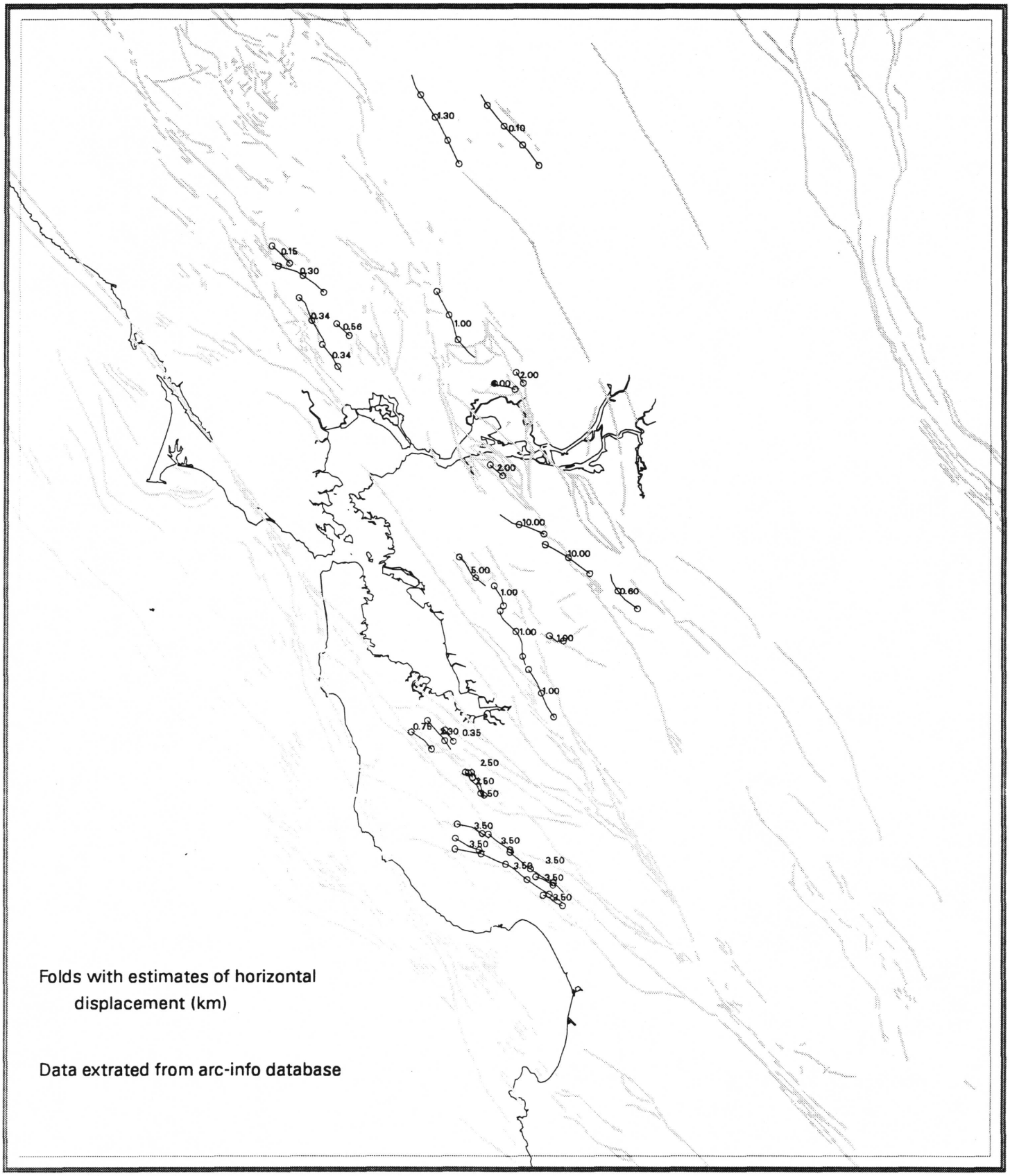

Figure 9

SAN FRANCISCO BAY REGION

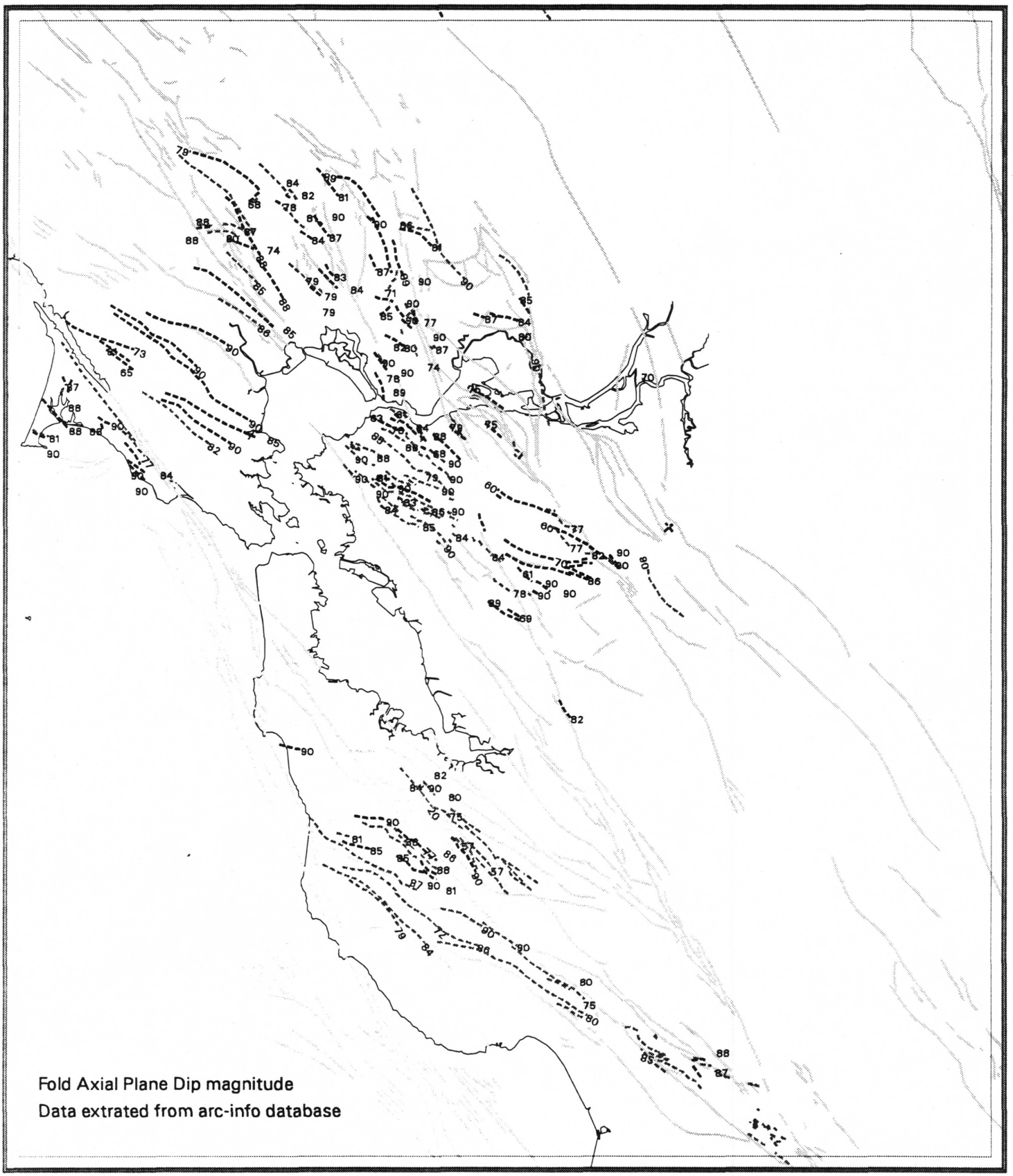

Figure 10

SAN FRANCISCO BAY REGION

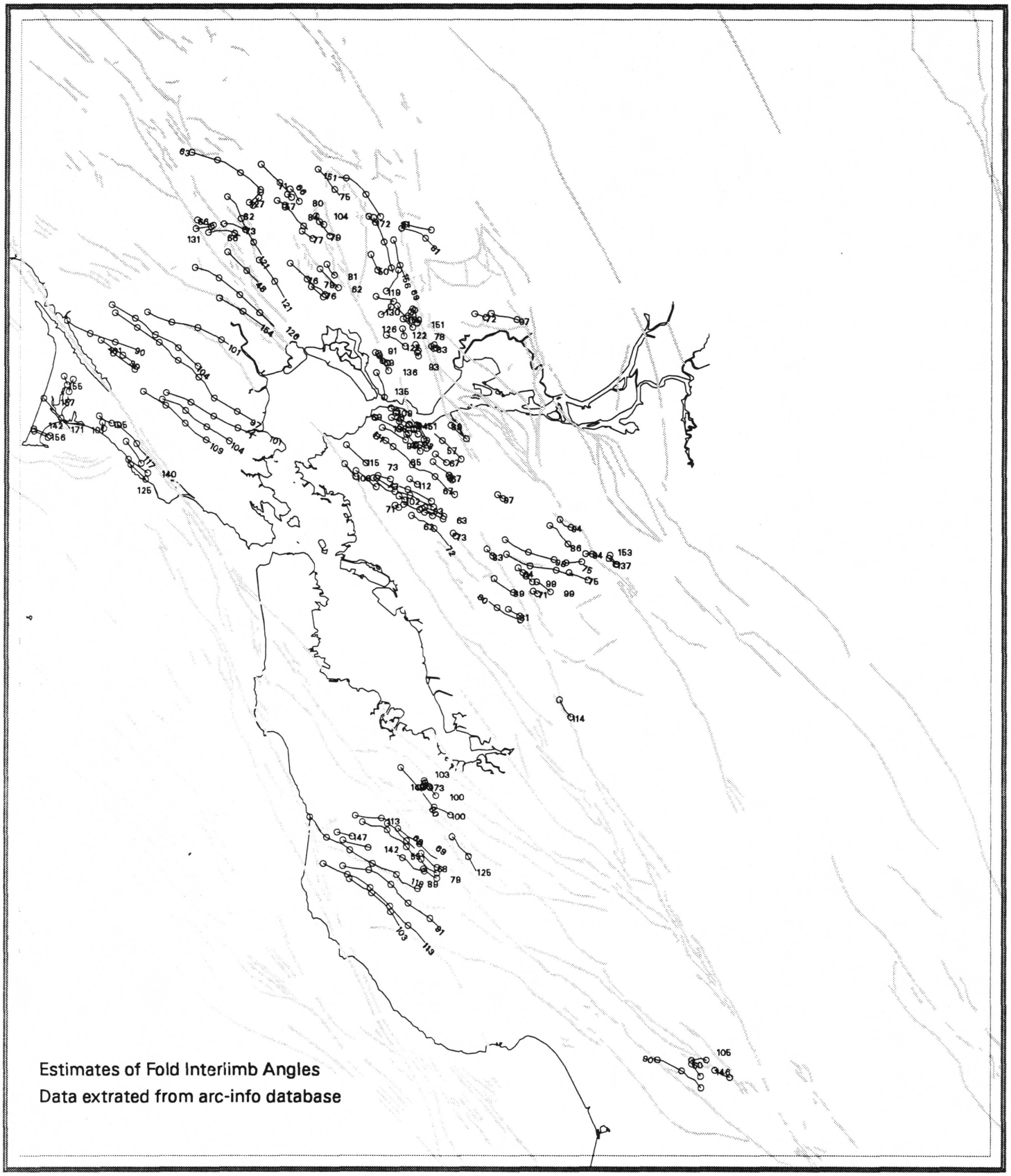

Figure 11

SAN FRANCISCO BAY REGION

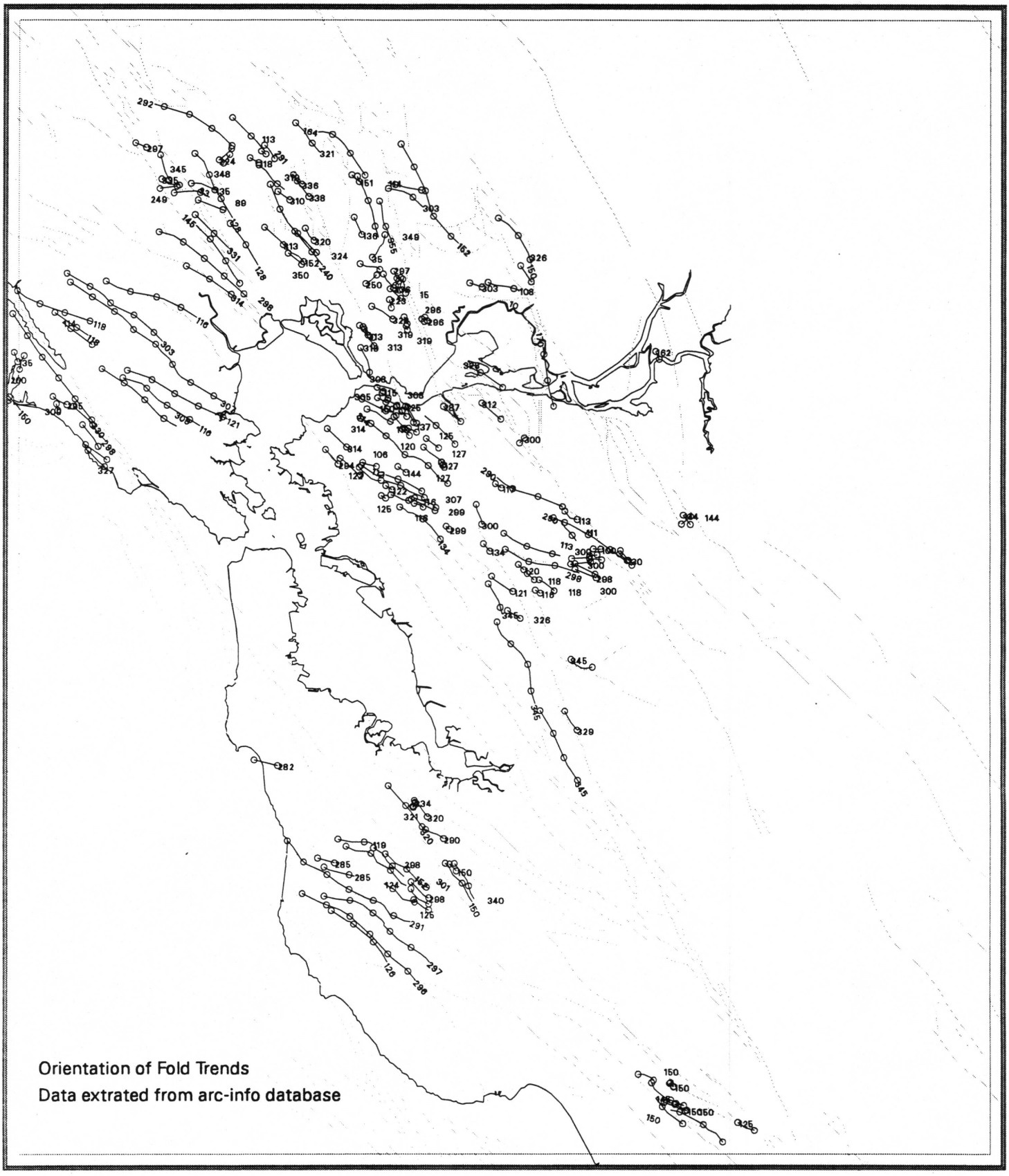

Figure 12

SAN FRANCISCO BAY REGION

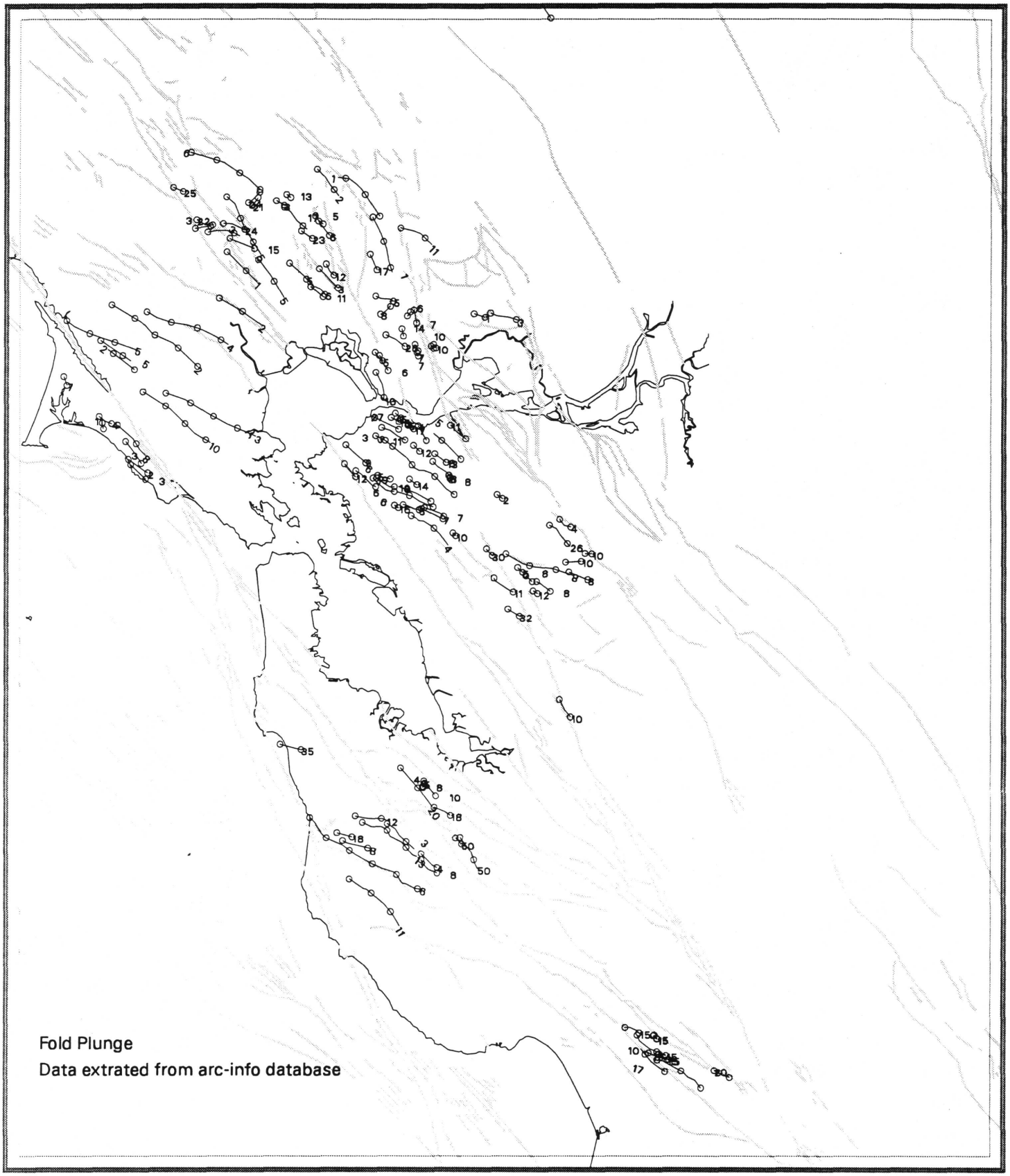

Figure 13

OFFSHORE

Fault and Fold Map of the Central California Continental Margin, San Francisco Bay/Monterey Bay Region

Stephen D. Lewis, U.S. Geological Survey, M.S. 999, Menlo Park, California 94025

One of the most important concepts that has recently developed regarding earthquake hazards in the San Francisco region is that the zone of crustal strain, both coseismic and aseismic, extends over a very broad zone that is loosely centered about the active strands of the Calaveras, Hayward, and San Andreas faults. Outlying features, such as the Concord fault to the east and the San Gregorio fault to the west, are now recognized as important elements that must be included in any attempt to understand regional deformation patterns and mechanisms of strain release.

A regional grid of Common Depth Point seismic reflection profiles acquired by both the USGS and by industry provides the basis for mapping zones of active folding and thrust faulting beneath the continental shelf and slope of the San Francisco Bay-Monterey Bay region. One zone, beneath the inner continental shelf between Santa Cruz and Ano Nuevo, is composed of an imbricate fan of landward-dipping faults with associated folds in the sediment section of the Outer Santa Cruz Basin. The San Gregorio fault zone defines the landward boundary of this zone, which is currently seismically active. Seaward of the San Gregorio fault, the mapped traces of thrust faults trend more westerly than does the San Gregorio fault itself.

Depth-migrated seismic profiles in this region exhibit several horizontal to gently eastward-dipping reflection events. The shallowest event, between 2 and 3 km depth, is probably a detachment related to the San Gregorio and other faults beneath the continental shelf. The deepest event resolved by the pre-stack migration dips eastward from a depth of roughly 8 km beneath the continental slope to a depth of about 16 km (approximately 5-8 s. reflection time) beneath the inner continental shelf. Both pre-stack migrated and DMO stacked profiles also show similar landward-dipping reflectors at depths between 5 km and 10 km. The deepest reflection event probably represents oceanic crust subducted beneath the California continental margin at an unknown time, while the shallower reflectors reflect low-angle faults within Franciscan rock units and Neogene sedimentary rocks deposited on the continental shelf and slope.

A second zone of thrust faults extends for about 75 km along the seaward edge of the continental shelf, but appears to be seismically quiet. This zone is characterized by a narrow zone if discontinous faults and small folds that parallel the continental shelf break from the latitude of Pigeon Point northwestward to the Point Reyes region. A third zone of thrust faulting and folding is present in the Point Reyes Peninsula region, where seafloor erosion has breached actively-growing folds.

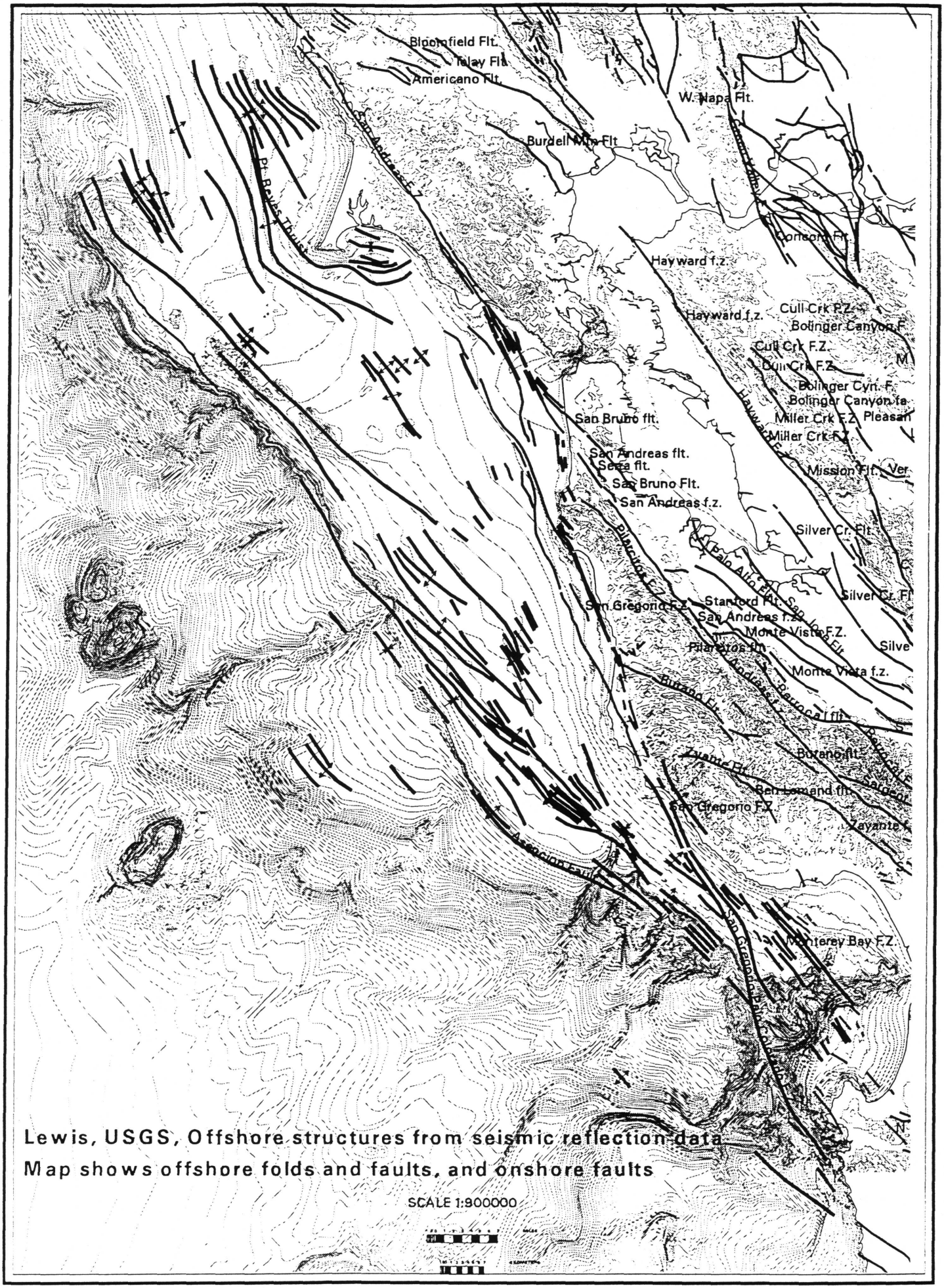

Lewis, USGS, Offshore structures from seismic reflection data

Map shows offshore folds and faults, and onshore faults

SCALE 1:900000

Fold axes for the northern Santa Lucia Mountains

Nolan, J., Weber and Associates

Folds and associated faults in the Santa Lucia Mountains were compiled on a 1:100,000 scale map. In addition, information summarizing fault activities in the area is presented as a close indicator of fold activity. The faults, as a group, are right-lateral reverse oblique and reflect a northeast-southwest crustal shortening. Folds closely associated with faults tend to be tightly oppressed, overturned synclines, while folds between major faults tend to be more open anticlines.

Evidence for active folding includes folding of the Plio-Plistocene Paso Robles Formation with dips ranging up to 28 degrees, tilting or warping of Pleistocene age stream terrace deposits, and youthful flexural slip faulting in the Monterey Formation. There are several folds in the southern portion of Fort Ord, north of Highway 68, that appear to be active. The Pliocene erosional surface on top of the Monterey Formation appears to be folded based on sub-surface contouring (Rosenbertg and Clark, 1994, PLATE 1). This surface is overlain by Paso Robles Formation. Age estimates for the Paso Robles Formation are inprecise in this area as the unit is a poorly defined mixture of various depositional lithologies.

The best estimate of fold rates is $5.2x10^{e-5}$ rad/ka to 3.5x10e rad/ka based on folding of the erosional surface and an assumed age for the surface of 1.12 million years. With regard to younger stream terrace deposits, deformation often appears related to localized deformation along fault zones rather than large scale folding, although a systematic study of terraces might be useful in demonstrating fold activity and fold rates. Flexural slip faulting has not been studied and precious little neotectonic work has been done in the Santa Lucias.

Anderson, R.S., 1990, Evolution of the Santa Cruz Mountains by advection of crust past a San Andreas fault bend, Science, 249, 397-401.

Bowen, O.E., 1969. Geologic Map of Monterey Quadrangle, California Division of Mines and Geology Open File Map.

Clark, J.C., Dibblee, T.W. Jr., Green, H.G., and Bowen, O.E. Jr., 1974, Preliminary Geologic Map of the Monterey and Seaside 7.5 Minute Quadrangles, Monterey County, California with Emphasis on Active Faults. USGS Miscellaneous Field Studies Map MF-577, 2 sheets, 1:24,000 scale

Compton, R.R., 1966, Analyses of Plio-pleistocene Deformation and Stresses in Northern Santa Lucia Range, California. Geol. Soc. Am. Bull. v. 77, pp 1361-1380, Dec. 1966.

Dibblee, T.W. Jr., 1972. Geologic Map of the Jamesburg Quadrangle, California. USGS Open-File Report 74-1021, 1:62,500 scale.

Dibblee, T.W. Jr., 1976. The Riconada and related faults in the southern Coast Ranges, California, and their tectonic significance: U.S. Geological Survey Professional Paper 981, p. 55.

Dibblee, T.W. Jr. and Clark, J.C., 1973. Geologic Map of the Monterey Quadrangle, California. USGS Open-File Report 74-1021, 1:62,500 scale.

Fiedler, W.M., 1944. Geology of the Jamesburg quadrangle, Monterey County, California: California Journal of Mines and Geology, Report XL of the State Mineralogist, v. 40, no. 2, pp. 177-250, 2 map sheets, scale 1:62,500.

Gardner-Taggart, J.M., 1991, Neogene folding and faulting in Southern Monterey Bay, Masters Thesis, San Jose State University, 60 p., 4 map sheets.

Greene, H.G., 1977, Geology of the Monterey Bay Region, California. USGS Open-File Report 77-718, 9 plates, 1:200,000 scale.

Greene, H.G., W.H.K. Lee, D.S. McCulloch and E.E. Brabb, 1973. Fault Map of the Monterey Bay Region, California. USGS Miscellaneous Field Studies Map MF-518, 4 sheets, 1:200,000 scale.

Hall, N.T., A.M. Sarna-Wojcicki and W.R. Dupre, 1974, Faults and Their Potential Hazards in Santa Cruz County, California. USGS Miscellaneous Field Studies Map MF-626, 3 sheets, 1:62,500 scale.

Johnson, D.L., 1993. Geoarcheological, geomorphological, paleoenvironmental, and pedological overview of fort Ord, Monterey county, California -- a working geotechnical report: Unpublished report to U.S. Army construction Engineering Research Laboratory, Champaign, Ill., p. 66, 1 appendix, 4 map sheets.

Lisowski, M., W.H. Prescott, J.C. Savage, and M.J. Johnston, 1990, Geodetic estimate of coseismic slip during the 1989 Loma Prieta California, Earthquake, Geophys. Res. Lett., 17, 1437-1440.

McCulloch, D.S., and Greene, H.G., 1989, Geologic map of the central California continental margin, *in* Green, H.G., and Kennedy, M.P., eds., Geology of the central California continental margin: California Division of Mines and Geology California Continental Margin Geologic Map Series, Map 5A, scale 1:250,0 00.

McKittrick, M.A., 1987. Geologic map of the Tularcitos fault zone, Monterey County, California: Monterey County Planning Department Open-File Report, p. 22, 5 map sheets, scale 1:12,000.

Rosenberg, L.I., and Clark, J.C. 1994. Quaternary faulting of the Greater Monterey Area, California. National Earthquake Hazards Reduction Program, Final technical report. 44 p., 4 map sheets.

Ross, D.C. and E.E. Brabb, 1973, Petrography and structural relations of granitic basement rocks in the Monterey Bay Area, California: U.S. Geological Survey Journal. Res. v. 1, no. 3, pp. 273-282.

Ross, D.C., 1976. Reconnaissance geologic map of pre-Cenozoic basement rocks, northern Santa Lucia Range, Monterey County, California: U.S. Geological Survey Miscellaneous Field studies Map MF-750, p. 7, 2 plates, scale 1:125, 000.

Tuttle, M., Earthquake Potential of the San Gregorio-Hosgri Fault Zone, unpublished thesis, University of California, Santa Cruz, California.

Wagner, D.L., and Pridmore, C.L., 1991. Geologic Map of the Monterey Quadrangle, 2 map sheets, scale 1:100,000.

SUMMARY OF FAULT ACTIVITY

Fault	Activity	
Ord Terrace	Unknown. Most recent documented movement is early Pleistocene.	Mapped from subsurface data, no expression of fault at surface in pre-Holocene dune fields. Offsets earliest Pleistocene Paso Robles Fm.
Seaside	Unknown. Most recent known movement. Early Pleistocene.	Mapped from subsurface data, no expression of fault at surface, offsets Paso Robles Fm.
Chupines	Questionable. Late Pleistocene. Possible Holocene.	Minor vertical separation noted on Paso Robles Fm. Possible offset of Late Pleistocene/Holocene deposits.
Navy	Questionable late. Pleistocene/Holocene. Activity	No direct evidence for Pleistocene offset. Evidence for movement is all inferential.
Sylvan Thrust	Holocene[1]	Thrust fault mapped along base of ridge. Possible landslide origin not ruled out, but appears to be spatially associated with micro seismicity.
Tularcitos	Holocene[1]	Two exposures show offset Holocene age material. Also associated with micro seismicity. Two right reverse oblique focal mechanism solutions.
Holton Canyon Fault	Pleistocene[1]	Has some associated micro seismicity.
Cypress Point Fault	Pre-Quaternary, Questionable Pleistocene (Minor)	Greene found late Pleistocene offset on an offshore fault that aligns with the Cypress Point Fault, but no reliable evidence for Quaternary movement on shore.
Cachagua Fault	Quaternary?[2]	Evidence precludes movement in the last 100,000 years.
Blue Rock Fault (San Clemente Thrust)	Holocene?[3]	Trenching on the over thrust block shows soil cracking/offset that may be indicative of extensional collapse in the thrust block. Soil filling the cracks was dated at 2000-3000 ybp.

SUMMARY OF FAULT ACTIVITY

Palo Colorado Fault	Unknown	Greene (1978) has concluded that the Palo Colorado Fault is the landward extension of the San Gregorio. If true, the Palo Colorado would be Holocene active.
Rocky Creek Fault	Quaternary?	Spatially associated with the M5.2 Big Sur Earthquake of 1984[4]. 1st and 2nd emergent marine terraces appear to be warped (folded?) between the Rocky Creek and Sur faults.[5]
Sur Fault Zone	Quaternary? Holecene?	Preliminary field reconnaissance suggests Pleistocene activity of some elements of the fault system, but no documented Quaternary offsets have been reported. Some researchers[6] consider elements of this fault zone to be the southward continuation of the San Gregorio Fault, in which case it is Holocene active.

1. Rosenberg & Clark 1994.
2. Cotton and Associates, pers. com. 1995.
3. Weber, Hayes & Associates 1995
4. Tuttle 1985.
5. McKittrick, 1988.
6. Hall, 1991.

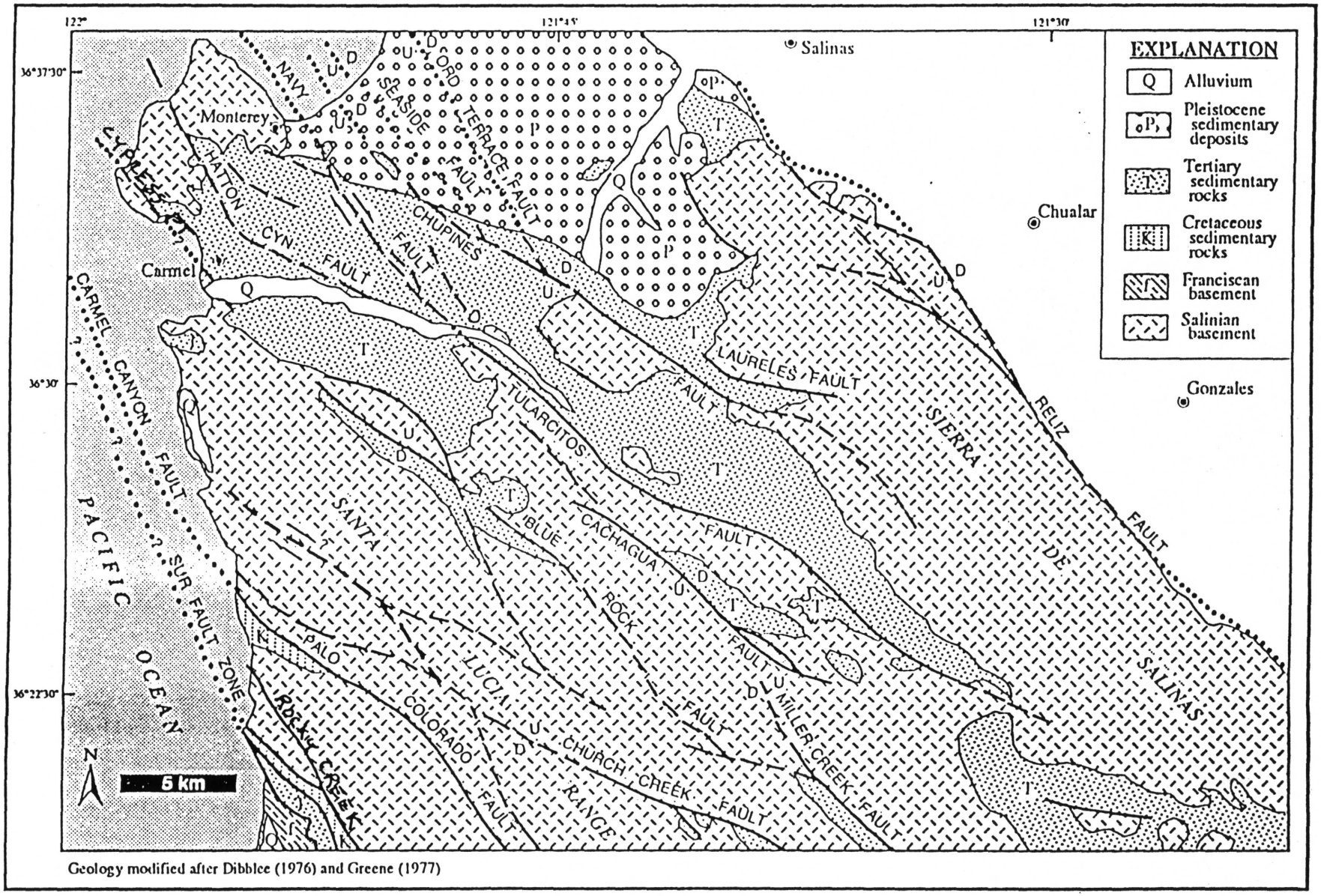

Geology modified after Dibblee (1976) and Greene (1977)

Figure 1. Regional geologic map, northern Santa Lucia Range and Sierra de Salinas, Monterey County, California

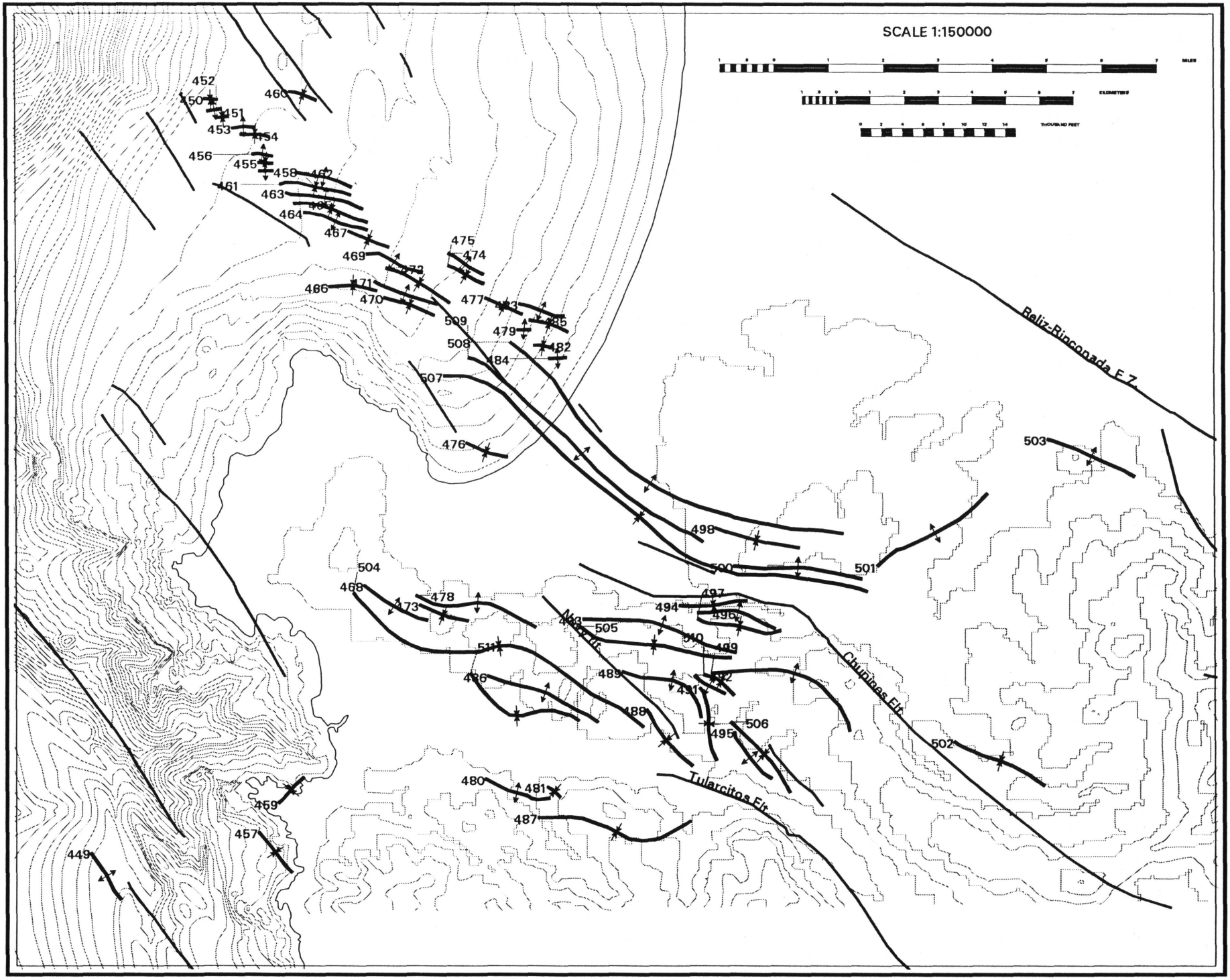
SCALE 1:150000
Baliz-Rinconada F.Z.
Chilpinnes Flt.
Tularcitos Flt.
452
450
460
451
453
454
456
455
458
462
461
463
464
467
469
475
474
466
471
470
477
509
479
485
508
482
484
507
476
503
498
504
468
478
473
494
497
496
505
511
489
491
486
488
506
495
502
480
481
487
459
457
449

Late Cenozoic folds and thrust faults, San Francisco South quadrangle

Bonilla, M., U.S. Geological Survey, 345 Middlefield Rd., MS-977, Menlo Park, Ca., 94025

Northwest-trending folds were identified in the Pleistocene Merced Formation within a band extending some 3 km northeast of the San Andreas fault. Several of these folds are younger than the 0.4 Ma Rockland ash bed. A few of the folds are asymmetrical, verging northeastward, and may reflect the northwestward extension of the Serra thrust fault.

The Serra fault zone cuts the Colma Formation, and one strand probably cuts an A-horizon soil that may be Holocene (Bonilla, 1994). The Colma Formation has been estimated to be on the order of 0.1 Ma (Clifton and Hunter, 1987), but some of it may be younger; a bore-hole sample gave a radiocarbon age of about 34,000 years (Caldwell-Gonzalez-Kennedy-Tudor, 1982; J.R. Powell, 1993, personal communication). A radiocarbon age of 10,540±250 years (Rubin and Alexander, 1960, p. 155) from a stream terrace younger than the Colma formation shows that the Colma is older than 10,000 years. The Serra fault zone is in line with but spatially separated from thrust faults to the southeast which have a similar structural relation to the San Andreas and have earthquakes associated with them. Epicenters of a few small earthquakes have been plotted in the Serra fault zone, but whether these earthquakes are actually on the nearby San Andreas fault is currently unknown (Brabb and Olson, 1986; Zoback and others, 1995).

Brabb, E.E., and Olson, J.A., 1986, Map showing faults and earthquake epicenters in San Mateo County, California: U.S. Geological Survey Miscellaneous Investigations Series Map I-1257-F, 1:62,500.

Bonilla, M. G., 1994, Serra fault zone, San Francisco Peninsula, California [abs.]: EOS, Transactions, American Geophysical Union, v. 75, no. 44, Supplement, p. 681. (1994 Fall Meeting, San Francisco)

Caldwell-Gonzalez-Kennedy-Tudor, 1982, Bayside facilities plan, expanded geotechnical investigation, geotechnical reference report: San Francisco, California, Caldwell-Gonzalez-Kennedy-Tudor Consulting Engineers, 127 p.

Clifton, H.E., and Hunter, R.E., 1987, The Merced Formation and related beds: A mile-thick succession of late Cenozoic coastal and shelf deposits in the seacliffs of San Francisco, California, in Hill, M.L., Cordilleran Section of the Geological Society of America, Centennial Field Guide, v. 1, p. 257-262.

Rubin, Meyer, and Alexander, Corrinne, 1960, U.S. Geological Survey radiocarbon dates V: American Journal of Science Radiocarbon Supplement, v. 2, p. 129-185.

Zoback, M.L., Olson, J.A., and Jachens, R.C., 1995, Seismicity and basement structure beneath south San Francisco Bay, California:, p.31-46 in Sangines, E.M., Andersen, D.W., and Buising, A.V., eds., Recent geologic studies in the San Francisco Bay Area: Pacific Section, SEPM, Book 76, 278 p.

M. Bonilla, San Francisco South area

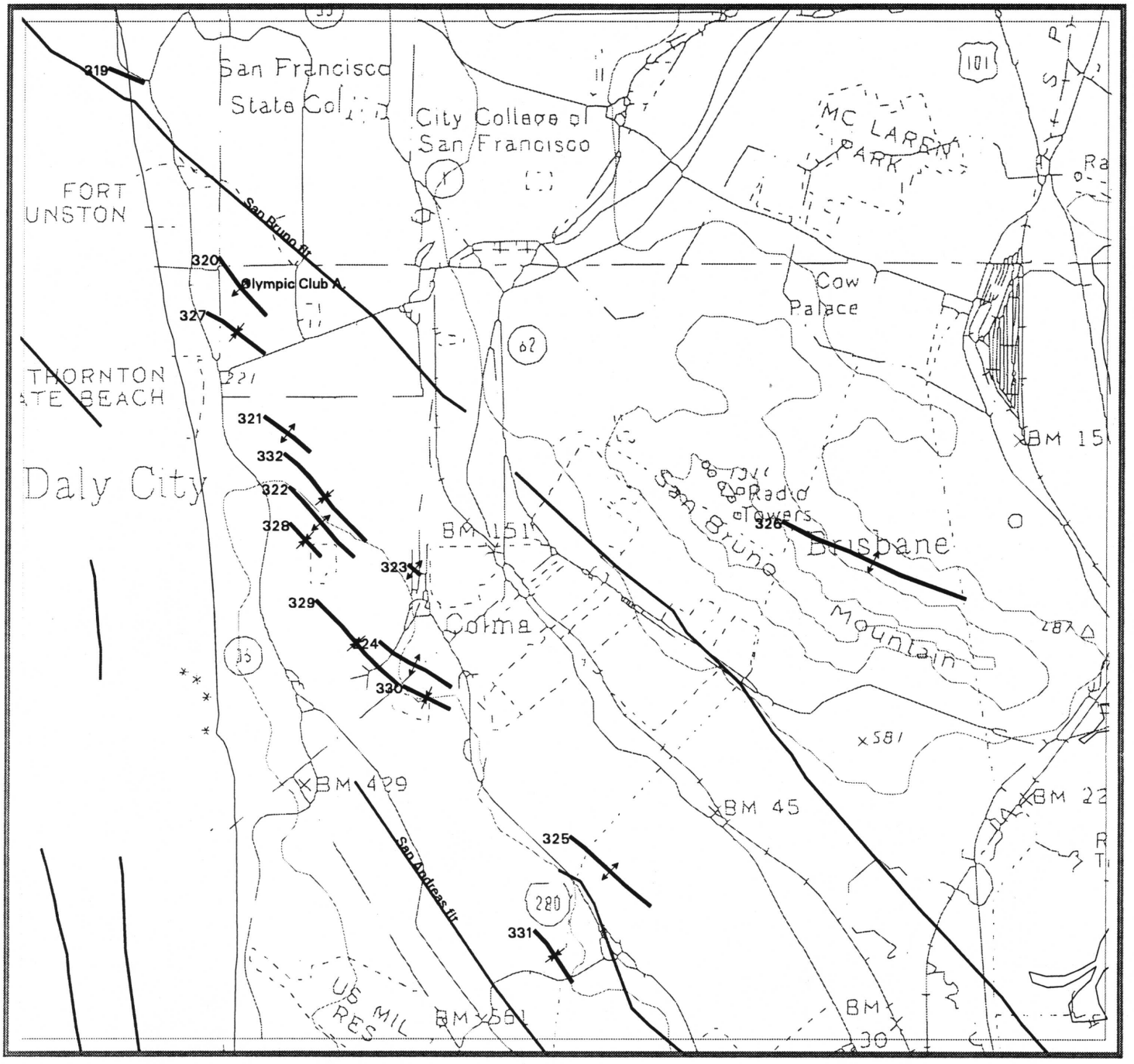

SCALE 1:60000

1 .5 0 1 2 3 4 5 MILES

1 .5 0 1 2 3 4 5 KILOMETERS

0 1 2 3 4 5 6 7 8 9 10 11 THOUSAND FEET

Arc Line identity	319	320	321	322	323	324	325	326	327	328	329	330	331	332
Compiler(s)	Bonilla, Manuel G.	Bonilla, Manuel G.	Bonilla, Manuel G.	Bonilla, Manuel G.	Bonilla, Manuel G.	Bonilla, Manuel G.	Bonilla, Manuel G.	Bonilla, Manuel G.	Bonilla, Manuel G.	Bonilla, Manuel G.	Bonilla, Manuel G.	Bonilla, Manuel G.	Bonilla, Manuel G.	Bonilla, Manuel G.
Structure	1	Olympic Club anticline	4	6	9	13	12	14	3	8	11	13	11a	5, 7
Age minimum	1	1	1	1	1	2	1	6	1	1	2	2	2	1
Age max	1	1					2		1					
Age control	tephrochronology, less than Merced ash	tephrochronology, less than Merced ash	tephrochronology, less than Merced ash	tephrochronology, less than Merced ash	tephrochronology, less than Merced ash	paleontologic, strontium isotope	paleontologic, strontium isotope	lead-alpha	tephrochronology, less than Merced ash	tephrochronology, less than Merced ash	paleontologic, strontium isotope	paleontologi, strontium isotope	paleontologic, strontium isotope	tephrochronology, less than Merced ash
Parallels strike-slip	yes?	yes	yes	yes	yes			no	yes	yes		yes		yes
Distance from fault	3 km, San Andreas	3 km, San Andreas	2.1 km	1.8 km	2.2 km				2.5 km	1.5 km		0.6 km		0.2 km
Average Orientation						24		24			20		24	
Distance from faults						1.4 km	0.2 km	6 km			1.5 km		1.4 km	
Axial Plane strike		320	310	320		295	325	295	305	316	297	237	295	317
Confidence of location	Probable	Definite	Definite	Probable	Possible	Possible	Probable	Probable	Probable	Possible	Possible	Possible	Possible	Probable
Multiple or segmented		yes	yes	yes			no		yes	yes				yes
Fore-limb strike		320	310											
Fore-limb dip		50	45											
Half wavelength (km)		0.2	0.1	0.1					0.2	0.1				0.1
Fold type	monocline	A, AS	A, AS	anticline		syncline	anticline	anticlinorium	syncline	syncline	anticline	syncline	syncline	syncline
Fold style	unknown	unknown	unknown	unknown	monocline?	unknown	unknown	unknown	unknown	unknown		unknown	unknown	unknown
Reference	Hengesh and Wakabayashi, 1994 abst													
Additonal References		Bonilla, 1971, Bonilla, 1953-1995 unpublished data, Sarna-Wojcicki and others, 1991, 1985	Bonilla, 1971, Bonilla, 1953-1995 unpublished data, Sarna-Wojcicki and others, 1991, 1985	Bonilla, 1971, Bonilla, 1953-1995 unpublished data, Sarna-Wojcicki and others, 1991, 1985	Bonilla, 1993, unpublished notes	Bonilla, 1971, Bonilla, 1953-1995 unpublished data, Sarna-Wojcicki and others, 1991, 1985	Bonilla, 1971, Bonilla, 1953-1995 unpublished data, Hunter and others, 1984; Ingram, 1992; Yancey, 1978	Bonilla, 1971, Bonilla, 1953-1995 unpublished data, Marvin and Dobson, 1979	Bonilla, 1971, Bonilla, 1953-1995 unpublished data, Sarna_Wojcicki and others, 1991, 1985	Bonilla, 1971, Bonilla, 1953-1995 unpublished data, Sarna_Wojcicki and others, 1991, 1985	Bonilla, 1971, Bonilla, 1953-1995 unpublished data, Hunter and others, 1984; Ingram, 1992; Yancey, 1978	Bonilla, 1971, Bonilla, 1953-1995 unpublished data, Sarna_Wojcicki and others, 1991, 1985	Bonilla, 1971, Bonilla, 1953-1995 unpublished data, Hunter and others, 1984; Ingram, 1992; Yancey, 1978	Bonilla, 1971, Bonilla, 1953-1995 unpublished data, Sarna_Wojcicki and other, 1991, 1985

Estimates of Deformation Rates and Earthquake Recurrence Intervals, Stanford area

Page, B., and Kovach, R., Department of Geology, Stanford University, Stanford, California

The minimum length of the monocline is 8.5 km. Its vertical amplitude is 8-0 m at Campus Drive West, and 17.4 m at Page Mill Road. Its maximum dip (i.e., slope of the topographic surface) is 2 degrees at these two localities, and is much less in some other laces. The general slope of the Late Pleistocene alluvial fan surface where unaffected by the monocline is less than 1 degree, ranging from 14 to 35 minutes. The monocline involves the Late Pleistocene alluvium, which is estimated to be between 10,000 and 70,000 years old (Helley et al., 1979). We have evidence suggesting that the nearby Coast Ranges, in their present configuration, have risen at an average rate of 1-3 mm/yr, commencing ca. 450,000 years ago (Page, 1992). However, our recent survey of the 100-year-old pavement under the arcade along the east side of the main Stanford quadrangle did not show any deformation ascribable to movement of the monocline, which underlies nearly half of the length of the pavement; hence the current growth rate is very slow or nil.

It is not clear when deformation of the monoclinal began. It could have started 1,000 years ago or 70,000 years ago and we do not know when, or if, it has ceased deforming. Therefore we cannot calculate the strain rate directly.

Our best estimate of the growth rate is based on the likelihood that the monocline did not grow faster than the nearby Coast Ranges, which we believe rose at a rate of 1-3 mm/yr; if so, it only required 17,400 years to reach its height of 17.4 m at Page Mill Road. The 17,400-year growth would easily fall within the probable length of time that has lapsed since deposition of the Late Pleistocene alluvium that is involved in the deformation.

A blind thrust or reverse fault is assumed by us to have produced the monocline. Current subsurface activity in the area between the monocline and the San Andreas fault causes micro-earthquakes which have been studied by J.A. Olson (informal commun., 1994). A number of the micro-earthquakes show reverse-slip mechanisms, and the foci lie within an elongate envelope dipping SW quasi-parallel with some of the focal planes (Kovach and Page, in press). If the monocline was produced by a blind fault dipping 55 degrees, like the aforementioned envelope and some of the focal planes within it, the total slip on the fault was 21.1 m, producing 17.4 m of vertical deformation at Page Mill Road. On the other hand, if the blind fault is a 30-degree thrust, the total slip was 34.8 m. The assumed vertical growth rate of 1 mm/yr for a period of 17,400 years would require an average slip rate of 1.2 mm/yr for the 55-degree fault, and 2 mm/yr for the 30-degree thrust. If the postulated fault is still active, for which there is no compelling evidence, the strain build-up leading to a sudden 200-mm slip and an M 5.5 earthquake would recur every 164 years on the average for the 55-degree fault, and every 100 years for the 30-degree thrust. Such strain rates, if still applicable, would have produced visible 20-cm distortion in the 100-year old Stanford quadrangle. Therefore we tentatively conclude that the postulated blind fault and the monocline itself are not currently active.

Degree of confidence in estimates

The Late Quaternary age of the Stock Farm monocline is definite, inasmuch as the flexure is younger than the Late Quaternary alluvium which it affects. We suppose that our estimates of the growth rate of the monocline, slip rates on the postulated causative fault, and recurrence intervals of earthquakes are probable within subjective error bars of plus 100% and minus 50%. Our tentative conclusion that the monocline and causative fault are inactive needs critical review and a better data base.

Scotese, T.R., 1988, manuscript report on the Lomita Mall tunnel, Stanford. Includes geological sketches and notes along entire length of tunnel within the Stock Farm monocline. File titled "Notes & Reports to accompany Map 'Geological Observations Near Stanford University," locked stack, Branner Earth Sciences Library, Stanford Univ.

Dames & Moore, 1993, et seq., Private report on geology vis-a-vis toxic waste, submitted to Hewlett-Packard Co. Includes logs of drillholes in monocline, and geological cross sections. File titled "Notes & Reports to accompany Map 'Geological Observations Near Stanford University," locked stack, Branner Earth Sciences Library, Stanford Univ.

Page and Kovach, Stanford area

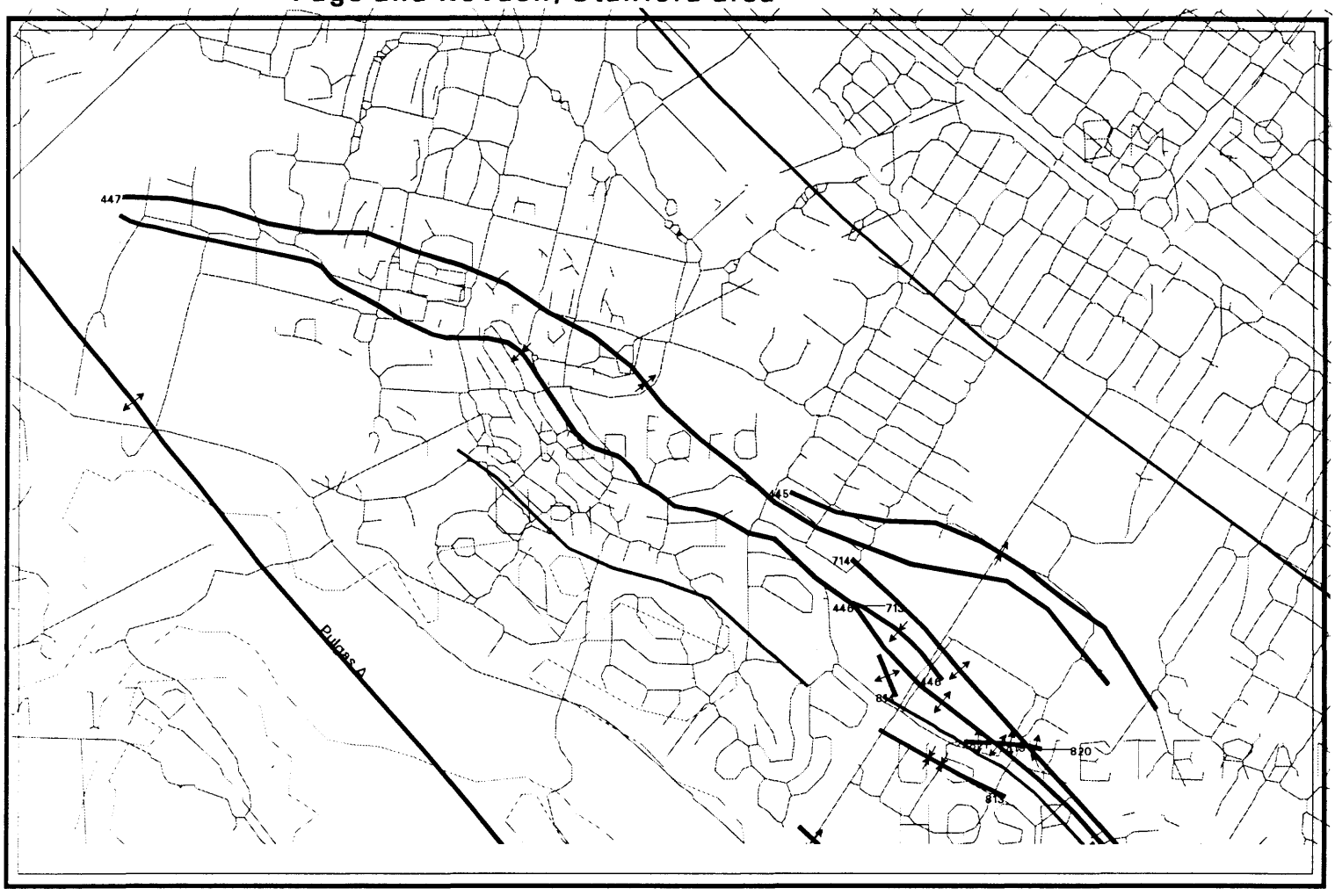

SCALE 1:25000

5 0 1 2

1 .5 0 1 2 3 KILOMETERS

0 1 2 3 4 5 6 7 THOUSAND FEET

Characterizing the Deformation and Seismic Hazard of a Blind Thrust Fault near Stanford, California: Coseismic Elastic Modeling

Joshua J. Roering, J Ramon Arrowsmith, and David D. Pollard, Dept. of Geological and Environmental Science, Stanford University, Stanford, CA 94305-2115

The eastern side of Santa Cruz Mountains, California, has shown high rates of Quaternary uplift. From fission track data, geodesy, and geomorphic analyses, Burgmann et al. (1994) calculate uplift rates of approximately 1 mm/yr. A series of thrust faults including the Monte Vista, Berrocal, Shannon, and Cascade faults, which strike sub-parallel to and dip southwest towards the San Andreas Fault, would have to exhibit a cumulative slip rate of 2-3 mm/yr to accommodate the observed uplift. During the Loma Prieta earthquake of 1989, shortening and upheaval of sidewalks, gutters and concrete paths occurred along the strike of these thrust faults, which will be referred to as the Southwestern Santa Clara Valley (SSCV) thrust belt. This suggests that slip along these faults is related to nearby earthquakes. In addition, a zone of thrust-dominated microseismicity coincides with the position of the thrust belt. Recent geomorphological studies conclude that the SSCV thrust belt includes several poorly characterized blind thrust faults. Because blind thrust faults do not intersect the earth's surface, methods other than conventional geologic field mapping and paleo-seismic investigations must be employed to identify and characterize them. This contribution applies a mechanically-based model to constrain the structural geometry, slip history and seismic hazard of a blind thrust fault near Stanford, California.

The relationship between blind thrust earthquakes and near-surface folding has been documented in several active tectonic areas, including the Central Valley of California, the Los Angeles Basin and the Foothills of the Santa Cruz Mountains, California. Our model assumes that geological structures in active seismic areas are generated from the accumulation of coseismic displacements over the cycle of earthquake events. Deformation generated by faults within the upper 6-10 km of the earth's crust may not be not subject to significant interseismic stress relaxation or isostatic response, so those processes are treated as of secondary importance to the model. Boundary element models that describe the behavior of simplified fault systems can be used to examine deformation associated with blind thrust faults. We apply a model that calculates displacements resulting from the dislocation of a rectangular plane in an elastic half-space. By modeling observed surface displacements above a blind thrust fault, we seek to quantitatively define the geometry of the fault and gain insight about its seismic potential.

The Stockfarm anticline trends northwest from Page Mill Road (between Foothill Expressway and El Camino Real) to the northwestern edge of Stanford campus near

San Francisquito Creek and has a total length of approximately 8.5 km (see Figure 1). Sub-surface studies reveal Quaternary folding in the upper layers of the structure, which are primarily composed of units of the Santa Clara Formation. The northeastern side of the anticline dips northeast at approximately 15 to 17°, while the southwestern side dips southwest at about 50°. Near the crest of the anticline, an angular unconformity indicates episodic deformation and deposition about the same fold axis. Ponded Quaternary alluvium on the flanks of the anticline suggests tectonic-induced deposition from uplifted terrane.

A profile of deformed units in the Stockfarm anticline is modeled with the displacement field of an initially flat surface resulting from slip along a blind thrust fault. Initially, we choose to idealize the buried thrust as a single fault plane. Two distinct fault models predict a fold with morphology similar to that of the Stockfarm anticline (see table). The first model is for a single dislocation plane, the upper end of which is located 0.4 km below the earth's surface. The fault plane dips 20° ±5 to the southwest and has a down-dip width of approximately 0.4 km. The second model has a dislocation plane whose top is 0.25 km below the earth's surface. It dips 60° to the northeast and has a down-dip width of 2 ±1 km. Both models predict regions of subsidence that correspond with observed accumulations of Quaternary alluvium. The displacement field for the northeast-dipping fault model more closely matches the observed deformation field, however, faults of the SSCV thrust belt generally dip to the southwest (See Figure 2).

Based on age estimates of the deformed units and the amplitude of the fold, we calculate the maximum uplift rate of the crest of the anticline to be approximately 0.06 mm/yr. Assuming that the anticline deforms by coseismic slip on the blind thrust fault, we use the model fault dimensions and empirical regressions relating the rupture area, moment magnitude and slip of historical California earthquakes to calculate the recurrence intervals and slip rates of the two fault models (See Table 1). For the fault plane that dips shallowly to the southwest, we estimate a recurrence interval of 700 ±180 years and typical event moment magnitude ≤ 5.0. This fault would experience an average slip rate of 0.28 ±0.1 mm/yr. For the fault plane that dips steeply to the northeast, we calculate a recurrence interval of 2,400 ±500 years, a typical event moment magnitude ≤ 5.7, and an average slip rate of approximately 0.13 mm/yr.

Both fault models produce deformation rates that are consistent with other estimates for uplift, shortening and slip on the Southwestern Santa Clara Valley thrust belt. Uplifted terrace surfaces indicate that deformation rates in the thrust belt may be episodic over the last 3 million years, with the highest rate of uplift (1 mm/year) occurring between 3 and 0.25 million years ago. The fluctuation of these regional

Table 1. Summary of geometry and potential earthquake magnitude for model buried thrust faults underlying the Stockfarm anticline.

Fault Model Summary	Model 1	Model 2
dip	SW 20 deg	NE 60 deg
depth to top (km)	0.4	0.25
Max. uplift rate (mm/yr)	0.06	0.06
fault area (length x width, km)	8.5 x 0.4	8.5 x 2.0
recurrence interval (yr)	700 ± 180	2400 ± 500
moment magnitude (M)*	5.0	5.7
slip rate (mm/yr)	**0.28**	**0.13**

*Based upon empiricial regressions of magnitude vs. rupture area. (Dolan, et al., 1995)

deformation rates may be attributed to the activation and growth of small-scale structures such as the Stockfarm anticline. Because the age of the Santa Clara formation in the study area is poorly constrained, the relationship between regional deformation and the formation of the Stockfarm anticline remains ambiguous.

The shallow depth of the modeled fault planes suggests that the underlying blind thrust fault may not be an isolated seismogenic structure, but instead could be a secondary feature related to deeper thrust faults such as the Berrocal, Cascade, or Monte Vista faults. The analysis of possible mechanical interaction between large faults in the seismogenic zone (e.g. the San Andreas Fault) and small-scale structures (e.g. the Stockfarm anticline) is yet to be completed. Nonetheless, estimated Quaternary deformation rates of the Stockfarm anticline indicate that the Santa Clara Valley near Stanford University could be at risk not only from large strike-slip and reverse mechanism earthquakes, but also from coseismic slip along a blind thrust fault underlying the Stockfarm anticline.

Burgmann, R., Arrowsmith, R., Dumitru, T. & McLaughlin, R. 1994a. Rise and Fall of the southern Santa Cruz Mountains, California, from fission tracks, geomorphology, and geodesy. *Journal of Geophysical Research.* **99**, 20,181-20,202.

Dolan, J. F., Sieh, K., Rockwell, T. K., Yeats, R. S., Shaw, J., Suppe, J., Huftile, G. J. & Gath, E. M. 1995. Prospects for larger or more frequent earthquakes in the Los Angeles metropolitan region. *Science.* **267**, 199-205.

Hitchcock, C. S., Kelson, K. I. & Thompson, S. C. 1994. Geomorphic investigations of deformation along the northeastern margin of the Santa Cruz Mountains. *Open File Report U. S. Geological Survey.* 94-0187.

Kovach, R. L. & Beroza, G. C. 1993. Seismic potential from reverse faulting on the San Francisco Peninsula. *Bulletin of the Seismological Society of America.* **83**, 597-602.

Schwartz, D. P. & Ponti, D. J. 1990. Field guide to neotectonics of the San Andreas fault system, Santa Cruz Mountains, in light of the 1989 Loma Prieta earthquake. *USGS-Open File Report 90-274.* 32-34.

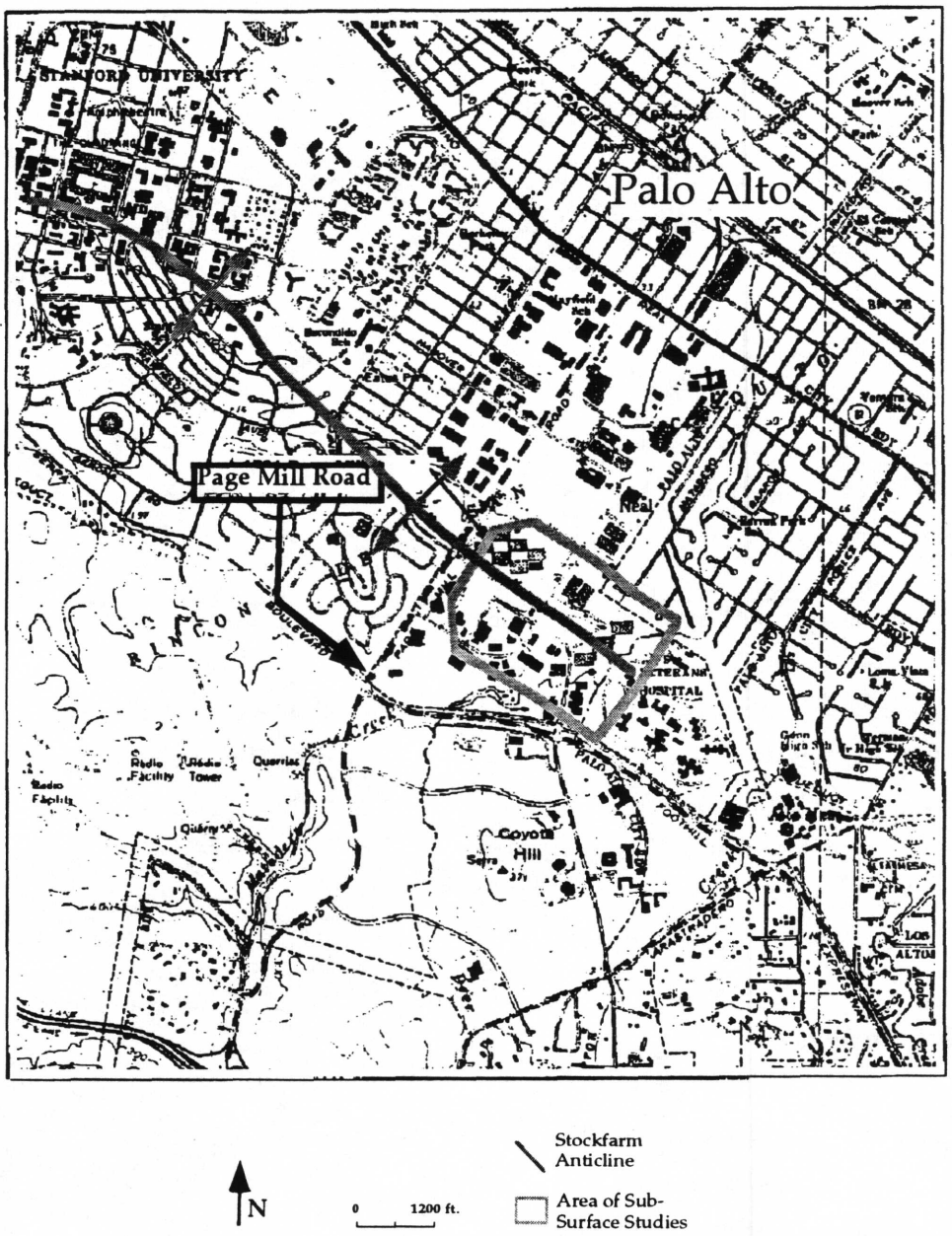

Figure 1. Map of Stanford vicinity with areas of sub-surface investigation and trace of the Stockfarm anticline (after Dames & Moore 1992, Ben Page 1993).

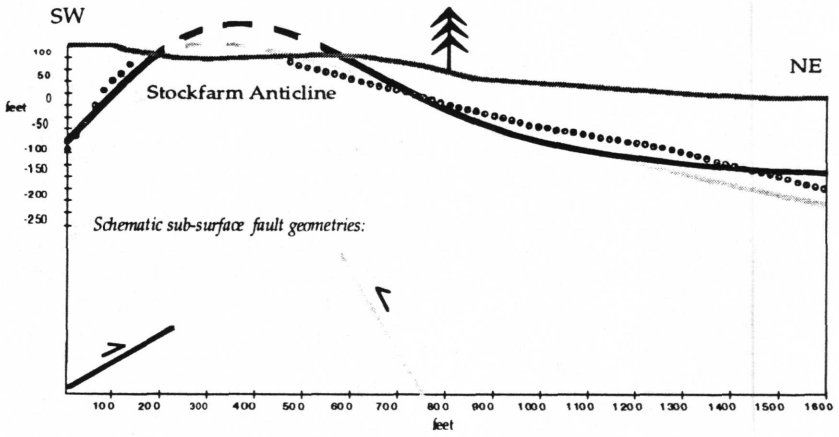

Fig. 2. Cross-section along Page Mill Road illustrating observed (profile of distinctive Santa Clara Fm. bedding; black dots) and modeled (lines) displacement fields. Schematic buried thrust faults reflect sub-surface geometries. Gray and black lines indicate the NE and SW dipping faults and their associated displacement fields, respectively. See Table 1 for model fault geometries and potiential earthquake magnitudes.

Geomorphic Signatures of Potentially Active "Blind" Reverse Faults: Comparison of Santa Clara and San Fernando Valleys

Christopher S Hitchcock and Keith I Kelson (Both at: William Lettis & Assoc., Inc., 1000 Broadway, Suite 612, Oakland, CA 94607; tel. 510 832/3716, e-mail: wla@netcom.com)

The 1994 Northridge earthquake beneath the San Fernando Valley emphasized the need to identify and characterize "blind" reverse faults as potential seismogenic sources. We compare geomorphic evidence for potentially active reverse faults beneath the Santa Clara Valley in northern California to the similar geomorphic signature of known active structures beneath the San Fernando Valley in southern California.

Deformed geomorphic surfaces (see figure, longitudinal profile, Stevens Creek) and probable fault-related lineaments within surficial deposits provide evidence of late Quaternary deformation along the western margin of the Santa Clara Valley. Topographic and vegetation lineaments coincident with changes in stream-channel and stream-terrace gradients, and with the distribution of late Quaternary fan apices, are evidence of deformation within 3 to 5 km-wide northwest-trending zones. These zones coincide with a series of southwest-dipping reverse faults and ground water barriers that parallel the valley margin, and are interpreted as related to potentially active northwest-trending folds. We believe the folds are the surface expression of active deformation within the hanging walls of late Quaternary thrust faults beneath the Santa Clara Valley.

Similar geomorphic features are present along the northern margin of the San Fernando Valley in southern California, in the vicinity of the 1971 San Fernando and 1994 Northridge earthquakes. Vegetation lineaments and changes in stream channel gradients coincide with zones of primary and secondary deformation produced by the 1971 San Fernando Valley earthquake. This deformation is similar in width, discontinuity, and association with a range-front embayment to deformation within the Santa Clara Valley. Although faulting along the northern margin of the San Fernando Valley probably is more common, comparison of the location, pattern, and style of late Quaternary deformation between the two valleys may provide information on the relative activity of structures within the Santa Clara Valley.

Hitchcock and Kelson, W. Lettis and Associates, Los Gatos area

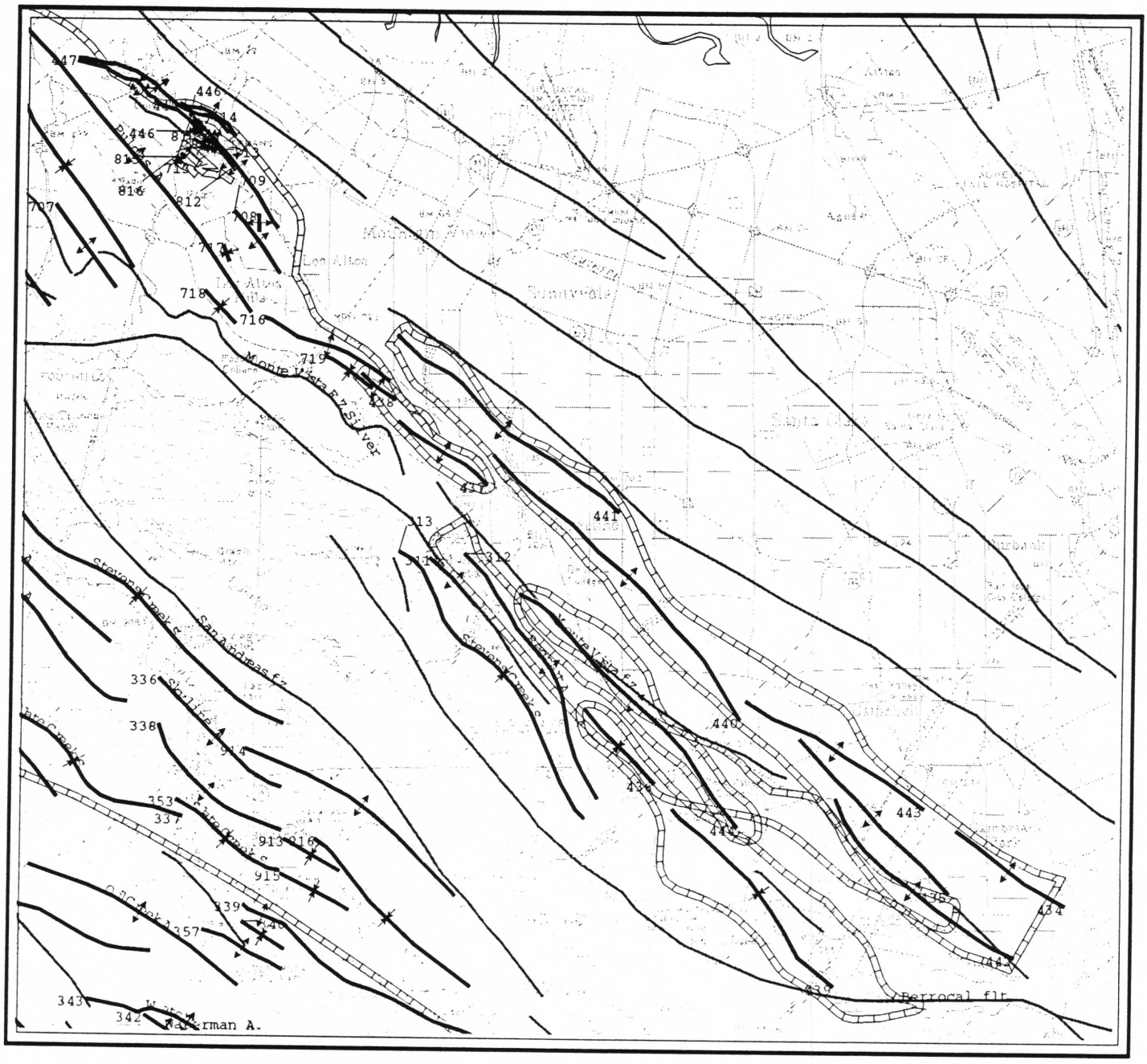

SCALE 1:150000

Location of Stream Profile

Anticlinal area

HITCHCOCK and KELSON Stream Profiles

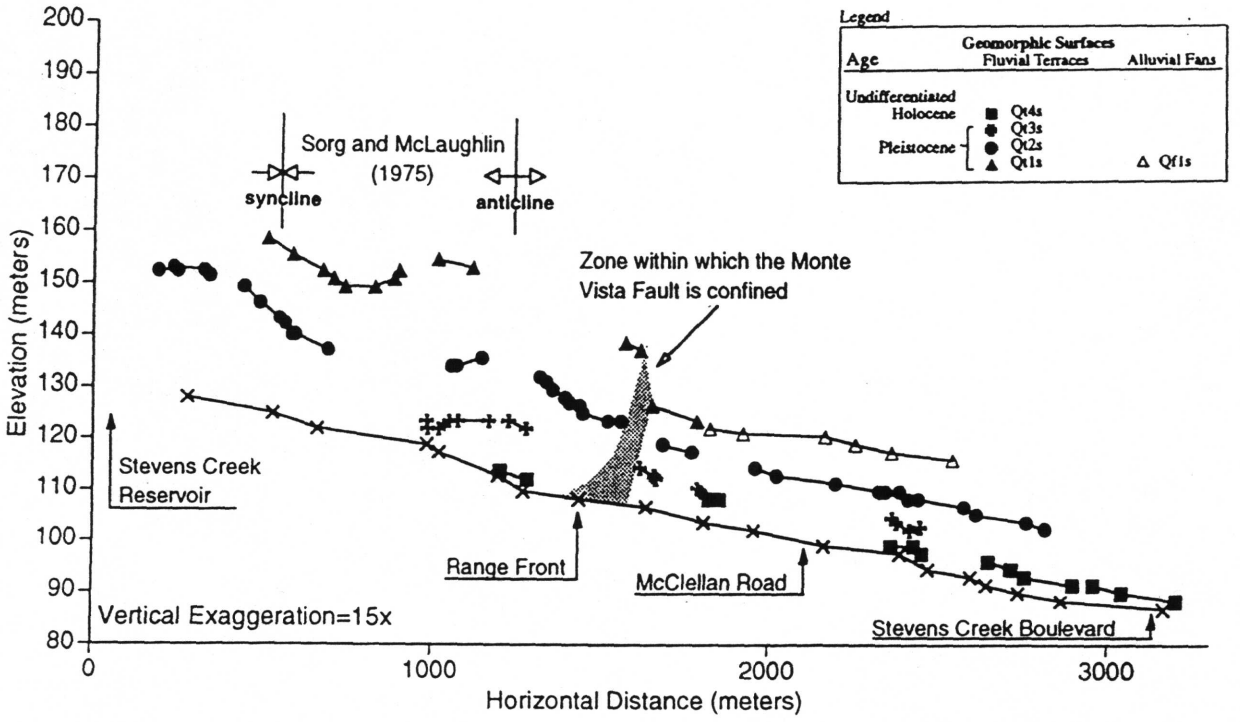

Longitudinal profile of geomorphic surfaces along Stevens Creek east of Stevens Creek Reservoir. Anticline and syncline traces shown on profile are projected from mapping by Sorg and McLaughlin (1975).

Arc Line identity	312	313	434	435	436	437	438	439	440	441	442	443	444
Compiler(s)	Kelson, K. McLaughlin	McLaughlin, R., Kelson, K	Kelson, K. I	Kelson, K. I.	Kelson, K. I.	Kelson, K. I.	Kelson, K. I.	Kelson, K. I.	Kelson, K. I.	Kelson, K. I.	Kelson, K. I.	Kelson, K. I.	Kelson, K. I.
Structure	Regnart anticline	Stevens Creek syncline	Santa Clara Valley folds	Santa Clara Valley folds	Santa Clara Valley folds	Santa Clara Valley folds	Santa Clara Valley folds	Santa Clara Valley folds	Santa Clara Valley folds	Santa Clara Valley folds	Santa Clara Valley folds	Santa Clara Valley folds	Santa Clara Valley folds
Age minimum	1	1	1	1	1	1	1	1	1	1	1	1	1
Age max	4	4	2	2	2	2	2	2	2	2	2	2	2
Age control	paleontologic	paleontologic	paleontologic	paleontologic	paleontologic	paleontologic	paleontologic	paleontologic	paleontologic	paleontologic	paleontologic	paleontologic	paleontologic
Inclined Geomorphic surface	fluvial, lacustrine	lacustrine, fluvial	fluvial	fluvial	fluvial	fluvial	fluvial	fluvial	fluvial	fluvial	fluvial	fluvial	fluvial
Horizontal shortening (km)	2.5	2.5											
c1	1	1											
Shortening rate mm/yr	0.30	0.30											
c2	1	1											
Vertical displacement rate mm/yr	0.3	0.3											
c3		2											
Initiation of folding (Ma)	10 -4.8 m.y.	10 -4.8 m.y.											
c4	1	1											
Termination of folding (Ma)	0.3 - 0.120	0.3 - 0.120											
Method	terrace correlation	terrace correlation											
Rate averaged, time length	125 ka	10m.y. and .12 m.y.											
Parallels strike-slip	yes	yes	yes	yes	yes	yes	yes	yes	yes	yes	yes	yes	yes
Distance from fault	0 - 2, Monte Vista, Shannon	0-2 km, Monte Vista fault											
Trend	340	150											
Plunge	20-90	20-90											
Axial Plane strike	145	145											
Axial Plane dip	57	57											
Axial Plane dip direction	w	w											
Confidence of location	Probable	Probable											
Vergence direction	ne	NE	ne	ne	ne	ne	ne	ne	ne	ne	ne	ne	ne
Multiple or segmented		yes	yes	yes	yes	yes	yes	yes	yes	yes	yes	yes	yes
Half wavelength (km)	0.25- 1.0	0.8											
Fold type	A, S, O, U, I, AS	A, S, O, U, I, AS	A, S, O, U	A, S, O, U	A, S, O, U	A, S, O, U	A, S, O, U	A, S, O, U	A, S, O, U	A, S, O, U	A, S, O, U	A, S, O, U	A, S, O, U
Fold style	fault propagation	fault propagation	fault propagation?	fault propagation?	fault propagation?	fault propagation?	fault propagation?	fault propagation?	fault propagation?	fault propagation?	fault propagation?	fault propagation?	fault propagation?
Geodetic													
Reference													
Drill Hole		yes	CDWR, 1975	CDWR, 1975	CDWR, 1975	CDWR, 1975	CDWR, 1975	CDWR, 1975	CDWR, 1975	CDWR, 1975	CDWR, 1975	CDWR, 1975	CDWR, 1975
Seismic Reflection													
Gravity	yes	yes	yes	yes	yes	yes	yes	yes	yes	yes	yes	yes	yes
Historical Seismicity	yes	yes	Loma Prieta?	Loma Prieta?	Loma Prieta?	Loma Prieta?	Loma Prieta?	Loma Prieta?	Loma Prieta?	Loma Prieta?	Loma Prieta?	Loma Prieta?	Loma Prieta?
Magnitude/event	3.5 -4.0	3.5 -4.0	7.1	7.1	7.1	7.1	7.1	7.1	7.1	7.1	7.1	7.1	7.1
Depth	0-8 km	0-8 km	13	13	13	13	13	13	13	13	13	13	13
Distributed microseismicity	yes	yes											
Reference	Oppenheimer, Olsen, Zoback	Oppenheimer, Olsen, Zoback											
Additonal References	Hitchcock, C.S., Kelson, K. I., and Thompson, S.C., 1994; Sorg and Mc Laughlin, 1975; McLaughlin,and Clark, in prep	Hitchcock, C.S., Kelson, K. I., and Thompson, S.C., 1994; Sorg and Mc Laughlin, 1975; McLaughlin,and Clark, in prep	Hitchcock et al, 1994	Hitchcock et al, 1994	Hitchcock et al, 1994	Hitchcock et al, 1994	Hitchcock et al, 1994	Hitchcock et al, 1994	Hitchcock et al, 1994	Hitchcock et al, 1994	Hitchcock et al, 1994	Hitchcock et al, 1994	Hitchcock et al, 1994

Gravity modeling of the Monte Vista Fault Zone

Jachens, R. C., U.S. Geological Survey, 345 Middlefield Rd., MS-975, Menlo Park, Ca., 94025

The map figure shows an area representing the geophysically defined, concealed Monte Vista Fault Zone in the Los Altos-Los Gatos area at the north-east base of the Santa Cruz Mountains, California. The Monte Vista fault zone where exposed near Los Altos Hills, California according to Sorg and McLaughlin (1975) "is composed of two parallel, closely spaced, northwest- trending fault strands that bound a diapir of unnamed late Miocene sandstone and shale."

The sub-surface fault plane area (hatchered line in map figure) was constructed from gravity data as follows: 1) Gravity data that were collected along a series of 11 profiles normal to the mountain front and spaced 1.0-1.5 km apart, with data points spaced about 0.4 km along the profiles, contain anomalies that are interpreted to reflect the concealed northeast tip of a hanging wall block of Franciscan Complex rocks thrust over the unnamed late Miocene sandstone and shale unit of Sorg and McLaughlin (1975). The southwest edge of the inferred fault plane area is located 0.3 km southwest of the characteristic gravity anomaly, in order to account for uncertainty in the location of the block tip due to the 0.4 km spacing of the gravity data, the 1.0-1.5 km spacing of the profiles, and the inherent uncertainty in gravity interpretations.

Aeromagnetic data collected at a nominal height of 0.3 km above the ground surface along profiles oriented N. 70 degrees E. and spaced 0.8 km apart, with data points spaced about 0.1 km along the profiles, contain anomalies that are interpreted to reflect the concealed juxtaposition of nonmagnetic rocks of the unnamed late Miocene sandstone and shale unit of Sorg and McLaughlin (1975) to the southwest against weakly magnetic Santa Clara Formation or alluvium across a southwest-dipping reverse fault. The northeast edge of the polygon is located 0.3 km northeast of the characteristic magnetic anomaly, in order to account for uncertainty in the location of the fault due to the 0.3 km height of the magnetic survey, the 0.8 km spacing of the profiles, and the inherent uncertainty in magnetic interpretations. To summarize, the magnetic data define the northeast side of the inferred fault plane area and gravity data define the southwest side of the fault area.

Sorg, D.H., and McLaughlin, R.J., 1975, Geologic map of the Sargent-Berrocal fault zone between Los Gatos and Los Altos Hills, Santa Clara County, California: U.S. Geological Survey Miscellaneous Field Studies Map MF-643, scale 1:24,000.

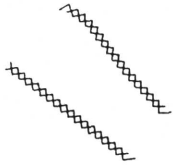

Location of sub-surface fault plane

Gravity data, Jachens, Los Gatos area

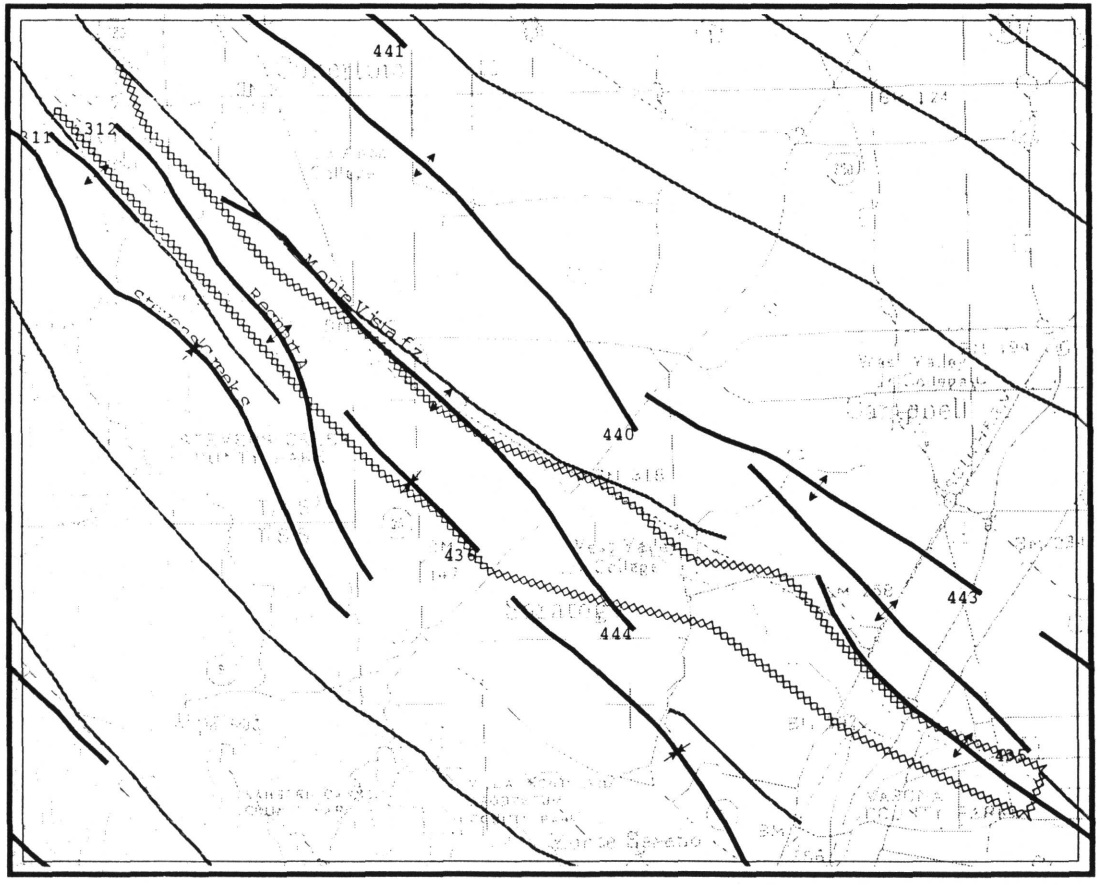

SCALE 1:100000

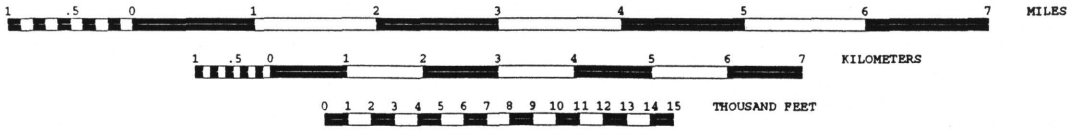

Quaternary Contractional Faulting and Folding Northeast of the San Andreas fault, Portola Valley-Palo Alto, California

Angell, M., and Crampton, T. A., Geomatrix Consultants

In order to help assess the location and intensity of potential surface rupture associated with the Stanford fault and other previously mapped faults that lie between the San Andreas and the northeastern topographic range front of the Santa Cruz Mountains, cross sections extending to mid-crustal depths were constructed using surface geologic data (Dibblee, 1966; Pampeyan 1970; Brabb and Olson, 1986; this report) seismicity data (Brabb and Olson, 1986), and water well and gravity data (Oliver, 1990). The structures are "balanced," meaning they are internally consistent with respect to the geometry and kinematics of fold development by slip on underlying faults, and can be "retrodeformed" or restored to a geologically reasonable pre-contraction geometry. Using this method, the amount of reverse slip responsible for the observed contractional deformation and assessment of the potential intensity and location of future ground rupture in the region is estimated.

Cross section Y-Y' extends from the San Andreas fault at Portola Valley northeast across the foothills to the Stanford fault zone at Palo Alto. The cross section shows two southwest-dipping reverse faults, the Hermit and Stanford faults, that join the San Andreas fault along branch lines at about -4 and -9 km, respectively. Both faults have significant reverse components of slip as indicated by the associated contractional structures that lie in the hanging wall. The amount of lateral slip is not determined.

The smaller fault is the steeply southwest-dipping high-angle (right) reverse Hermit fault (Herd, 1982 in Brabb and Olson, 1986). The surface trace of the Hermit fault splays off the San Andreas fault a few km along strike to the north and crops out about 3 km east of the San Andreas fault along the line of section. Reverse slip on the fault has produced a tightly-folded fault-propagation fold cored by Franciscan Complex basement in the hanging wall. The fault places a moderately to tightly folded anticline of Butano sandstone and Franciscan Complex over a tight to isoclinal syncline in the footwall composed of Monterey Formation and unnamed sandstone. Plio-Pleistocene gravel deposits of the Santa Clara Formation and shallow marine deposits of the Merced Formation are also folded and faulted by the Hermit fault. Very little data are available constraining the displacement history of the Hermit fault. Because of its close proximity and linear trace subparallel to the San Andreas fault, the fault probably accommodates secondary deformation during large rupture events on the San Andreas fault and results from a significant component of right-lateral strike slip, as well as the reverse slip as represented on the cross section.

The larger, deeper fault in section Y-Y' is a compound structure composed of the Pulgas and Stanford faults. The Pulgas fault is a poorly-defined structure at the surface that lies along the range front between Atherton and south of the Stanford campus (Dibblee, 1966; Brabb and Olson, 1986). The fault juxtaposes Tertiary age sedimentary bedrock of the Butano Formation and unnamed sandstone (Ladera Formation?) on the southwest against steeply east-dipping Santa Clara Formation on the northeast. (NB: relationships exposed in Frenchman Road trench excavated by Kovach and Page (1994) are not yet incorporated, but appear consistent with this model). The

Stanford fault is composed of a moderately to steeply southwest-dipping flat and ramp system that has propagated northeastward through the footwall from a pre-existing synformal bend in the Pulgas fault and ends at a blind thrust tip beneath the Stanford anticline. The Stanford anticline and associated deformation front (Stanford fault zone of Brabb and Olson, 1986) are therefore the surface expression of youthful hanging-wall fold deformation associated with northeastward (reverse) propagation of the Stanford fault thrust tip.

Kinematic Interpretation.

The cross section Y-Y' shows that the Pulgas and Stanford faults are part of the same fault system and are kinematically linked. The Pulgas fault is here interpreted as having originated as a southwest-dipping basin-bounding listric normal fault that subsequently has been inverted by reverse slip. Following initial compression, the Stanford fault broke through the footwall of the Pulgas fault, possibly because the Pulgas fault was unable to accommodate further contraction due to its inherently steep dip. Continued slip on the Stanford fault results in hanging-wall deformation due to translation through the anticlinal bend at the junction of the two fault segments. This deformation may be expressed at the surface along the Pulgas fault. It is possible that slip on the lower fault segment beneath the junction is translated entirely to the Pulgas fault and does not reach the Stanford segment.

The subsurface geometry of the reverse fault system includes two phases of compressive deformation, possibly continuous, for both the Stanford-Pulgas faults and the Hermit fault. The relationships between fault geometry , stratigraphy, and regional deformation history suggest some components of the Pulgas fault represent a reactivated previously existing normal fault that was the boundary structure to a half graben developed adjacent to the ancestral San Andreas fault. The initial phase of contraction reactivated the Pulgas normal fault in a reverse sense and produced a major fault-propagation fold in the hanging wall, the Los Altos anticline. A second fault-propagation fold also developed during this period with the initiation of the Hermit fault.

Timing and Amount of Contractional Deformation

The total shortening represented by the cross section is 3800 m ± 10% , or between 3400 and 4200 m. The restored section indicates this contraction has occurred since the top of Monterey time, at about 5-6 ma. The range in rates of total shortening for this section therefore are calculated at 0.6 to 0.8 mm yr. Based on the elevation of bedrock and thickness distribution of the overlying Santa Clara Formation gravel's determined from local well logs and gravity data, approximately 350 meters of reverse slip on the Stanford fault ramp is required to produce the structural relief of the Stanford anticline as shown on the cross section. Regional stratigraphic interpretations of the Santa Clara Formation suggest the deposit formed by alluvial sedimentation due to uplift of the Santa Cruz Mountains. Local stratigraphic and structural relationships to the underlying bedrock indicate the Santa Clara Formation represents sedimentation that records the onset (and progression) of deformation of the Stanford anticline. Unfortunately, the age for the Santa Clara Formation is not well constrained. For the purposes of this assessment we assume an age of between 0.5 ma and 2.5 ma, which is consistent with published

age estimates (Helley and others). If we further assume an uncertainty in the slip estimate of ± 100 m, then we arrive at a range in slip rates for the Stanford fault of 0.1 to 0.9 mm/yr. Also shown are hypocentral locations of well located earthquakes in the vicinity (Brabb and Olson, 1986).

The reverse slip rates are approximately 0.1% to 1.0% of the 12 mm/yr minimum strike slip rate on the adjacent peninsula segment of the San Andreas fault determined by Hall (1984). Therefore, if we assume a maximum of 5 m slip per characteristic event for the San Andreas fault and also assume that events on the San Andreas fault and Pulgas/Stanford fault system are kinematically linked, this results in a maximum of ~5 cm coseismic reverse slip. If this slip reaches the surface, it will likely be manifested as folding and minor fracturing of the Stanford anticline at the deformation front and possibly the Pulgas fault at the range front. In the case of the Hermit fault, where the total reverse component of slip is on the order of 75-±250 m, the same analysis translates to an expected 8 to 17 cm of reverse slip per characteristic event. The amount of slip on the Hermit fault is not well-constrained, though larger and/or more frequent strains should be expected due to the larger amount of total reverse slip indicated by the cross section and its close relationship to the San Andreas fault. Also because of its steep angle and close relationship to the San Andreas fault in both geometry and location the Hermit fault probably has a high strike slip-dip slip ratio and slip will be localized in the vicinity of the surface trade of the fault. High ground motions can be expected in this area during events on adjacent segments of the San Andreas fault, as indicated by the ground motions experienced in this region during the Loma Prieta earthquake.

Conclusions and Implications for Seismic Hazard Assessment

A regionally extensive system of compressive structures lie northeast of the San Andreas fault along the range front of the Santa Cruz Mountains in northern California. Three cross sections have been drawn parallel to the San Andreas fault across this system of structures in the northern, central, and southern regions of the range (the southern X-X' and central, Y-Y' cross sections are shown in this paper). Several characteristic features of the compressive system are common to the cross sections: uplifted Tertiary and/or Quaternary marine sediments are bound by structurally lower Mesozoic Franciscan Complex basement; a southwest-dipping and downward-steepening reverse/right-reverse "floor thrust" terminates at a blind thrust tip along a deformation front northeast of the San Andreas fault; and a topographic range front bounded by a high angle, right-reverse, oblique-slip faults. Cross sectional plots of seismicity form a northeastward-tapering wedge of microearthquake activity, and strongly deformed late Quaternary sediments indicate the system is active in all three locations.

The cross sections are kinematically balanced (i.e. they are consistent with observed structural and geological relationships and distribution of slip on the various segments of the fault systems) and therefore provide a meaningful estimate of the observed contractional strains normal to the San Andreas fault. Deformation represented by the Pajaro Gap cross section (X-X') in the southern Santa Cruz Mountains is calibrated using a well preserved flight of fluvial terraces as a strain gauge. The observed elevations and relative spacings are used to calculate an uplift rate of 0.3 m/yr which

can be produced by about 0.5 mm/yr of dip slip on the underlying reverse fault ramp. Total dip slip (i.e. shortening) for the section determined independently from structural geometry is about 1700 m, or between 1500 and 2000 m. The range in total strain divided by the strain rate suggests the onset of observed contractional deformation began between 3.0 and 4.0 ma for this region. This is consistent with the age of onset of regional transpression along the San Andreas transform system at about 3.4 to 3.9 ma as suggested by plate motion kinematic models (Harbert and Cox).

The Stanford cross section (Y-Y') in the central Santa Cruz Mountains is kinematically balanced and geometrically restored to a half-graben structural configuration of Eocene to Upper Miocene age. The Palo Alto section restores to a Miocene half graben, indicating a pre-existing basement structure controls the location and geometry of contraction for that location. Contraction of the half-graben geometry can explain the local observation of structural and stratigraphic inversion of an elevated Tertiary syncline overthrusting a lowland valley underlain by Franciscan basement near the surface. Stratigraphic evidence for normal growth faulting, structural evidence for down-dropped basement west of the range front, the preservation of a predominantly synclinal structure within the uplifted foothills, erosion of the principal anticline, and youthful breakthrough of the footwall are all consistent with tectonic inversion of a pre-existing normal fault. Tectonic inversion of pre-existing extensional structures may help to explain similar regional observations elsewhere in the Coast Ranges (e.g. Southern Santa Cruz Mts., East Bay Hills, San Luis Range).

The total shortening represented by the cross section (Y-Y') is 3800 m ± 10%, or between 3400 and 4200 m. The restored section indicates this contraction has occurred since the to of Monterey time, at about 5-6 ma. The range in rates of total shortening for this section therefore are calculated at 0.6 to 018 mm/yr. The slip represented by the young blind thrust tip only using the geometry of the overlying Stanford anticline, which is well constrained by bore-hole and gravity data, is about 350 m, or a range of 300 to 400 m. The onset of development 9f the Stanford anticline is constrained by the age of the overlying Santa Clara Formation growth strata at between 0.5 and 2.5 ma. The resulting range in rates for Quaternary deformation is therefore 0.1 to 0.8 mm/yr.

The San Bruno cross section (not shown in this paper) in the northern Santa Cruz Mountains is problematic in that distributed horizontal shear is likely pervasive at short distances from the San Andreas fault. Total contraction parallel to the section can still be reasonably assessed however because the section is approximately normal to the strike of the compressive structures. Also vertical strain is well constrained by bore-hole data that provide the elevation and attitude of the erosional contact between the Merced Formation and underlying Franciscan Complex basement. According to the geometry of the deformed and restored sections, the total contractional strain for this section is about 150 m, or 100 to 200 m, since the top of the Merced Formation at about 400 ka for this area. These ages and shortening strains suggest a range of shortening rates of 0.25 to 0.5 mm/yr.

Based on area/magnitude relationships (Wells and Coppersmith, in review), the mapped lengths of the compressive fault systems intersected by cross sections X-X' (Carnadero/Sargent) and Y-Y'

(Stanford/Pulgas) are 30 and 15 km, respectively, and the average down dip widths suggested by the cross sections (8 and 10 km, respectively) indicate that the floor thrusts to these systems have sufficient area to produce large magnitude seismic events. Using these parameters the calculated Maximum Credible Earthquakes (MCE) for the Carnadero/Sargent fault system is M6.5 and for the Stanford/Pulgas fault system is M6.2, though the parameters are not well constrained. Given the rates cited above the average displacements for the MCE's of about 0.5 to 1.0 for an M6.2 and of about 1.0- to 2.0 m for an M6.5 simple recurrence rates of between 600 and 4000 yrs are implied assuming all observed deformations produced by a succession of MCE's.

Alternatively, because the magnitude of total contractional strain observed in the geologic record for these regions is low, and because the floor thrust and overlying faults in the hanging wall slip during large events on the San Andreas fault, as indicated by observations of secondary contractional deformation along the range front following the 1989 Loma Prieta earthquake (Haugerud and Ellen, 1989), coseismic secondary faulting during large magnitude "characteristic" events on the San Andreas fault may account for all of the local San Andreas fault-normal contraction, precluding the need for independent large magnitude events on the compressive structures. In either case, the strains exhibited by faults between the San Andreas fault and the deformation front must be considered when assessing the seismic potential for that segment of the San Andreas fault.

Geomatrix 1 on regional index map showing location of compiled areas

Angell, Crampton et al, Geomatrix, Pajaro area

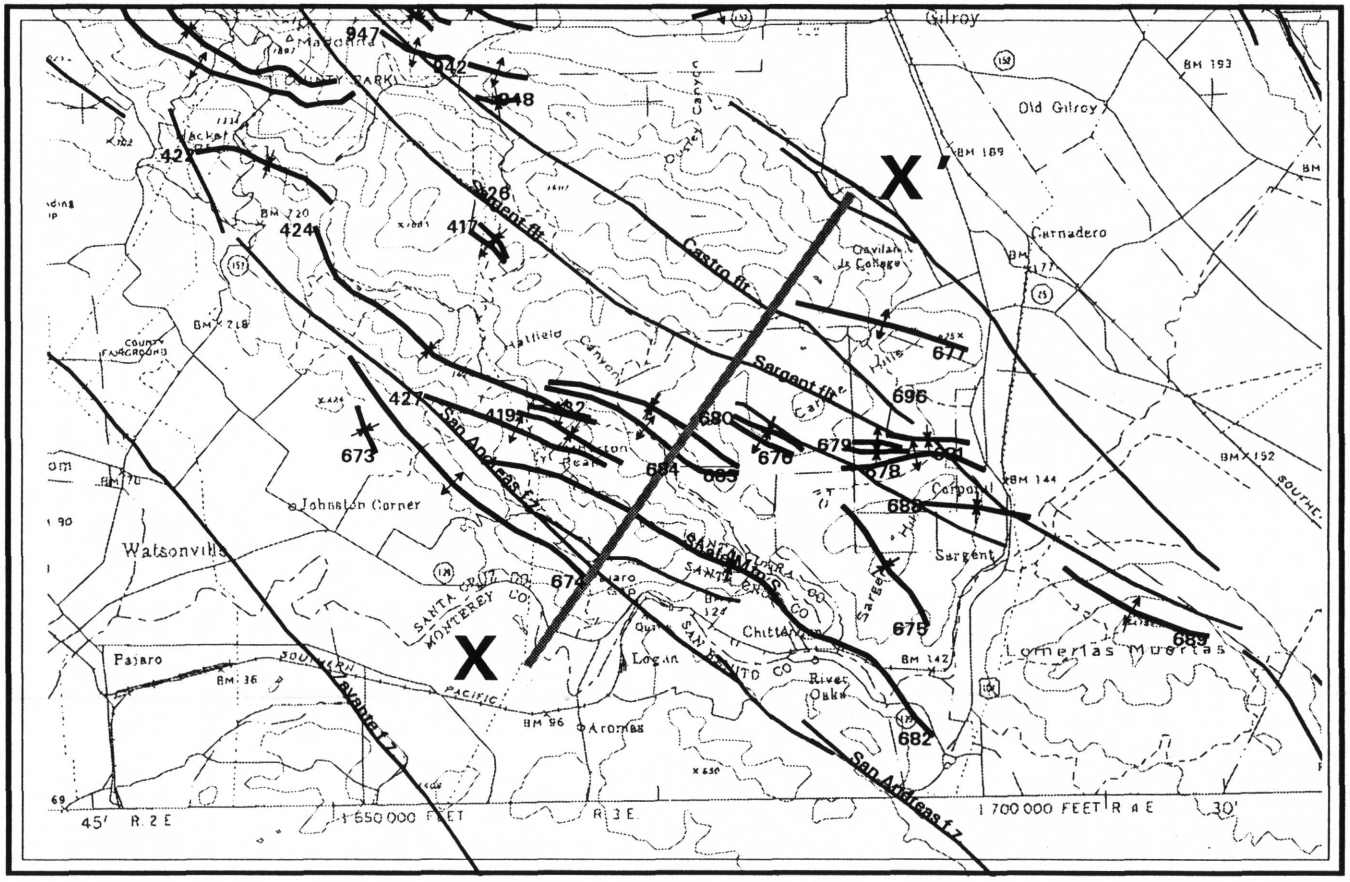

SCALE 1:150000

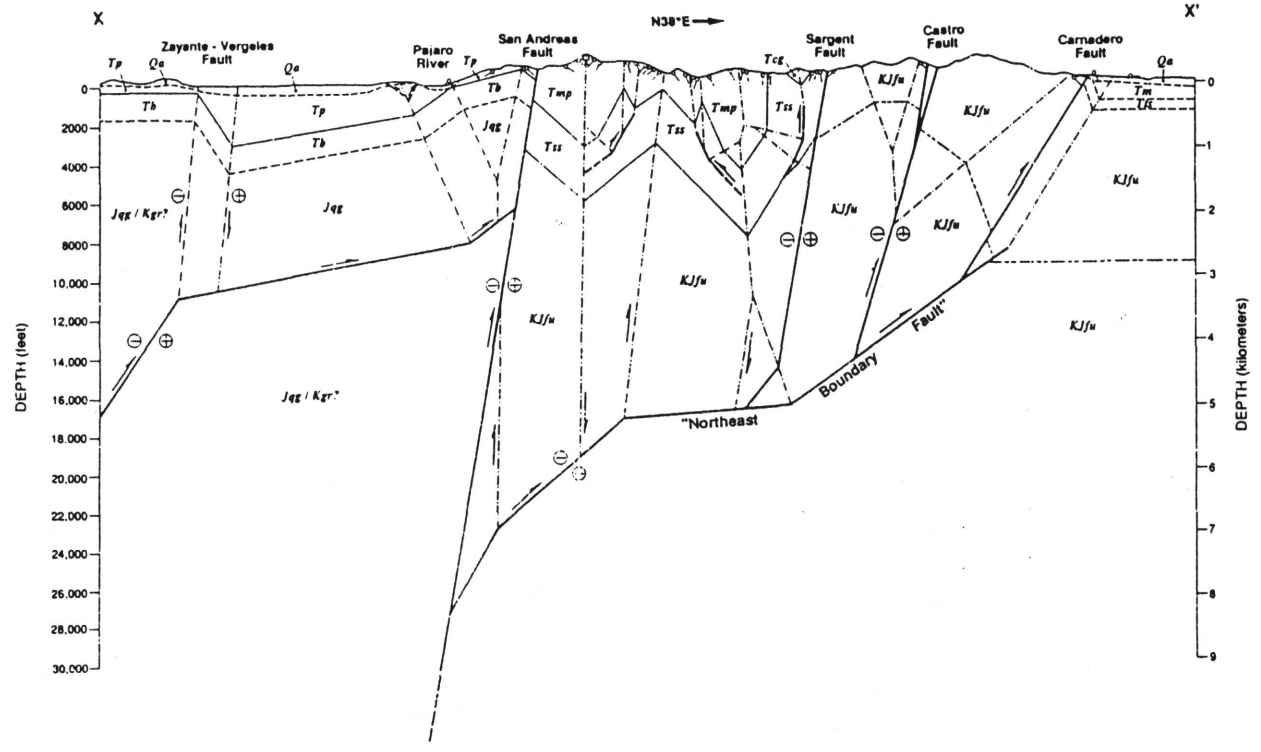

Note

Geology from Dibblee and Brabb,1978; Allen, 1946; Clark and Rietman, 1973.

0 5000 Feet

0 1 Kilometer

GEOLOGIC STRUCTURE SECTION X - X'
Southern Santa Cruz Mountains, California

GEOMATRIX | Project No. 1545 | Figure 9

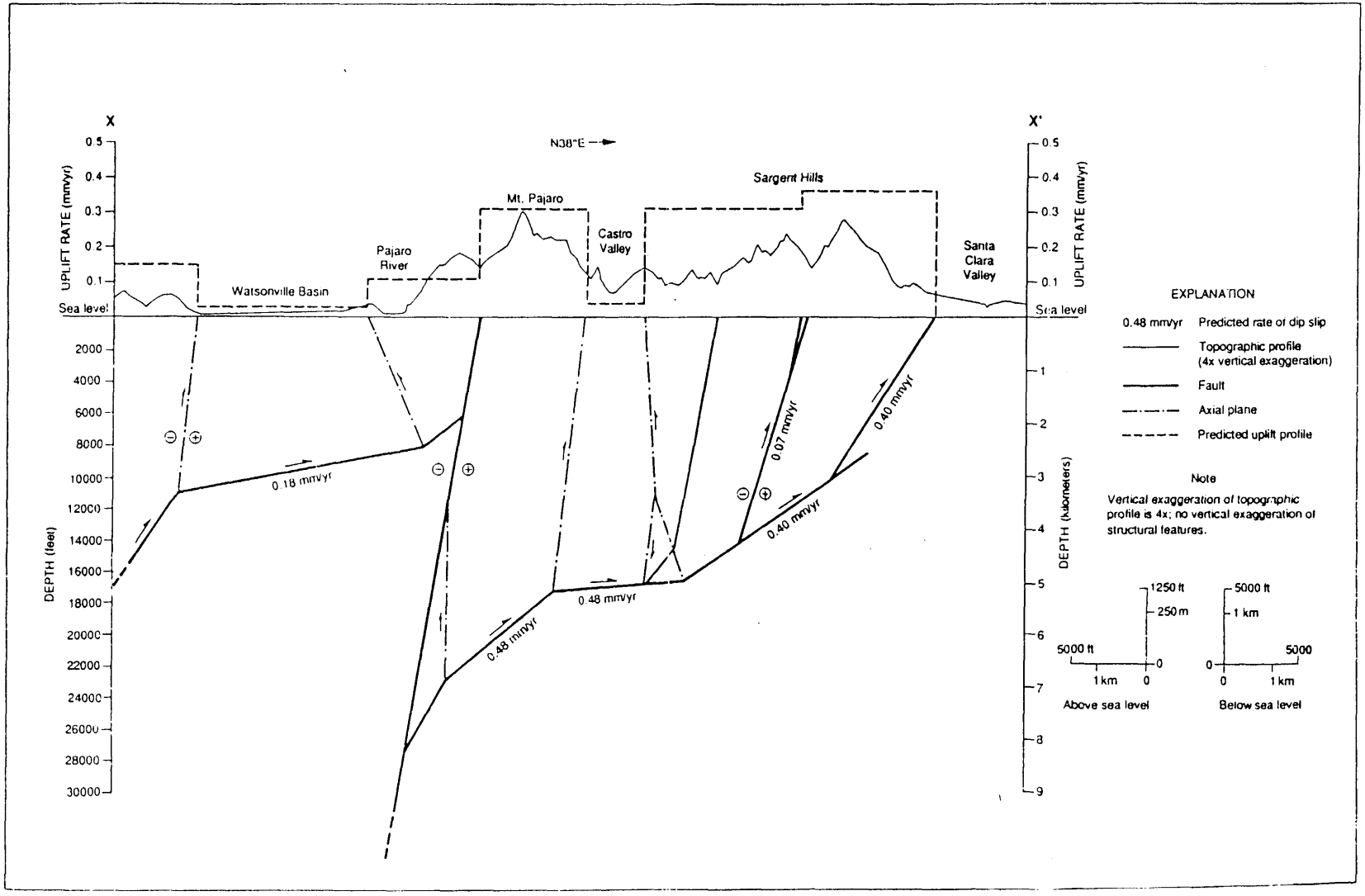
X
X'
N38°E
UPLIFT RATE (mm/yr)
0.5
0.4
0.3
0.2
0.1
Sea level
Watsonville Basin
Pajaro River
Mt. Pajaro
Castro Valley
Sargent Hills
Santa Clara Valley
DEPTH (feet)
2000
4000
6000
8000
10000
12000
14000
16000
18000
20000
22000
24000
26000
28000
30000
DEPTH (kilometers)
1
2
3
4
5
6
7
8
9
0.18 mm/yr
0.48 mm/yr
0.48 mm/yr
0.48 mm/yr
0.07 mm/yr
0.40 mm/yr
EXPLANATION
0.48 mm/yr Predicted rate of dip slip
Topographic profile (4x vertical exaggeration)
Fault
Axial plane
Predicted uplift profile
Note
Vertical exaggeration of topographic profile is 4x; no vertical exaggeration of structural features.
1250 ft
250 m
5000 ft
1 km
0
Above sea level
5000 ft
1 km
5000
Below sea level

Pajaro Area, Angell and Crampton

Arc Line identity	673	674	675	676	677	678	679	680	681	682	688	689
Compiler(s)	Crampton, T.A.,	Crampton, T.A.,	Crampton, T.A.,	Crampton, T.A.,	Crampton, T.A.,	Crampton, T.A. Wagner, D. L.	Crampton, T.A. Wagner, D. L.	Crampton, T.A.,	Crampton, T.A. Wagner, D. L.	Crampton, T. A. Wagner, D. L.	Crampton, T.A.,	Crampton, T.A.,
Age minimum	7	1	1	7	1	1	2	7	2	1	1	1
Age max	7		2	7	2	2	4	7	4	2	4	2
Age control		Paleon-tologic				Paleon-tologic, tephrachron ology, Ethchington Fm	Paleon-tologic, tephrachron ology		Paleon-tologic, tephrachron ology	Paleon-tologic	Paleon-tologic, tephrachronol ogy,	
Inclined Geomorphic surface		flat iron	fluvial		fluvial	fluvial				fluvial		fluvial
Parallels strike-slip		yes	yes		no	no			no	yes	no	yes
Distance from fault		0.5 San Andreas	Sargent FZ							1.5 San Andreas		1.0 Sargent FZ
Average Orientation			20		30 Castro fault	35	35		35	30	35	
Distance from faults			1.0 km							0.5-3 km		
Trend										150		125
Plunge		10 se								0-30		20
Axial Plane strike		45				90	280		280	340	280	125
Axial Plane dip						88 n				85 n		87
Axial Plane dip direction												sw
Confidence of location		Probable			probable	Probable	Probable		Probable	Probable	Probable	probable
Vergence direction		ne	sw			S	N		N	NE	N	ne
Multiple or segmented										Yes		
Interlimb angle			60			105				90		146
Back-limb strike			340			90				60 w		330
Back-limb dip			50 se			35 N				45 sw		14 sw
Back-limb dimension (km sq)						3	3		3		3	
Fore-limb strike			340			90				45		330
Fore-limb dip			70 sw			40 s				47 ne		20 ne
Half wavelength (km)										0.1-3 km		
Fold type		anticline	syncline		anticline	A, O, U	anticline, open, upright		syncline, open, upright	S, U, O	syncline, open, upright	A, Gentle
Fold style		unknown	unknown			fault-bend?	fault-bend?		fault-bend?	unknown	fault-bend?	unknown
Structure sections					Geometric, 1991					Geomatrix, 1991		
Additional References						Allen, J.E., 1946, Geology of the San Juan Bautista quadrangle, California: California Division of Mines Bulletin 133, p. 53-54, Dibble, T. W., Jr., and Brabb, E.E., 1978, Preliminary geologic map of the Chittenden Quadrangle, Santa Clara, Santa Cruz	Allen, J.E., 1946, Geology of the San Juan Bautista quadrangle, California: California Division of Mines Bulletin 133, p. 53-54, Dibble, T. W., Jr., and Brabb, E.E., 1978, Preliminary geologic map of the Chittenden Quadrangle, Santa Clara, Santa Cruz		Allen, J.E., 1946, Geology of the San Juan Bautista quadrangle, California: California Division of Mines Bulletin 133, p. 53-54, Dibble, T. W., Jr., and Brabb, E.E., 1978, Preliminary geologic map of the Chittenden Quadrangle, Santa Clara, Santa Cruz	Allen, J.E., 1946, Geology of the San Juan Bautista quadrangle, California: California Division of Mines Bulletin 133, p. 53-54	Allen, J.E., 1946, Geology of the San Juan Bautista quadrangle, California: California Division of Mines Bulletin 133, p. 53-54, Dibble, T. W., Jr., and Brabb, E.E., 1978, Preliminary geologic map of the Chittenden Quadrangle, Santa Clara, Santa Cruz, San	

Pajaro area continued, Crampton and Angell

Arc Line identity	690	691	683	684	685	686	687
Compiler(s)	Crampton, T.A.,	Crampton, T.A.,	Crampton, T.A.,	Crampton, T.A.,	Crampton, T.A.,	Crampton, T.A.,	Crampton, T.A.,
Age minimum	1	1	7	7	1	1	1
Age max	6	6	7	7	6	6	6

Angell et al, Geomatrix, Los Altos - Palo Alto area
Geomatrix 3 on regional index map showing location of compiled areas

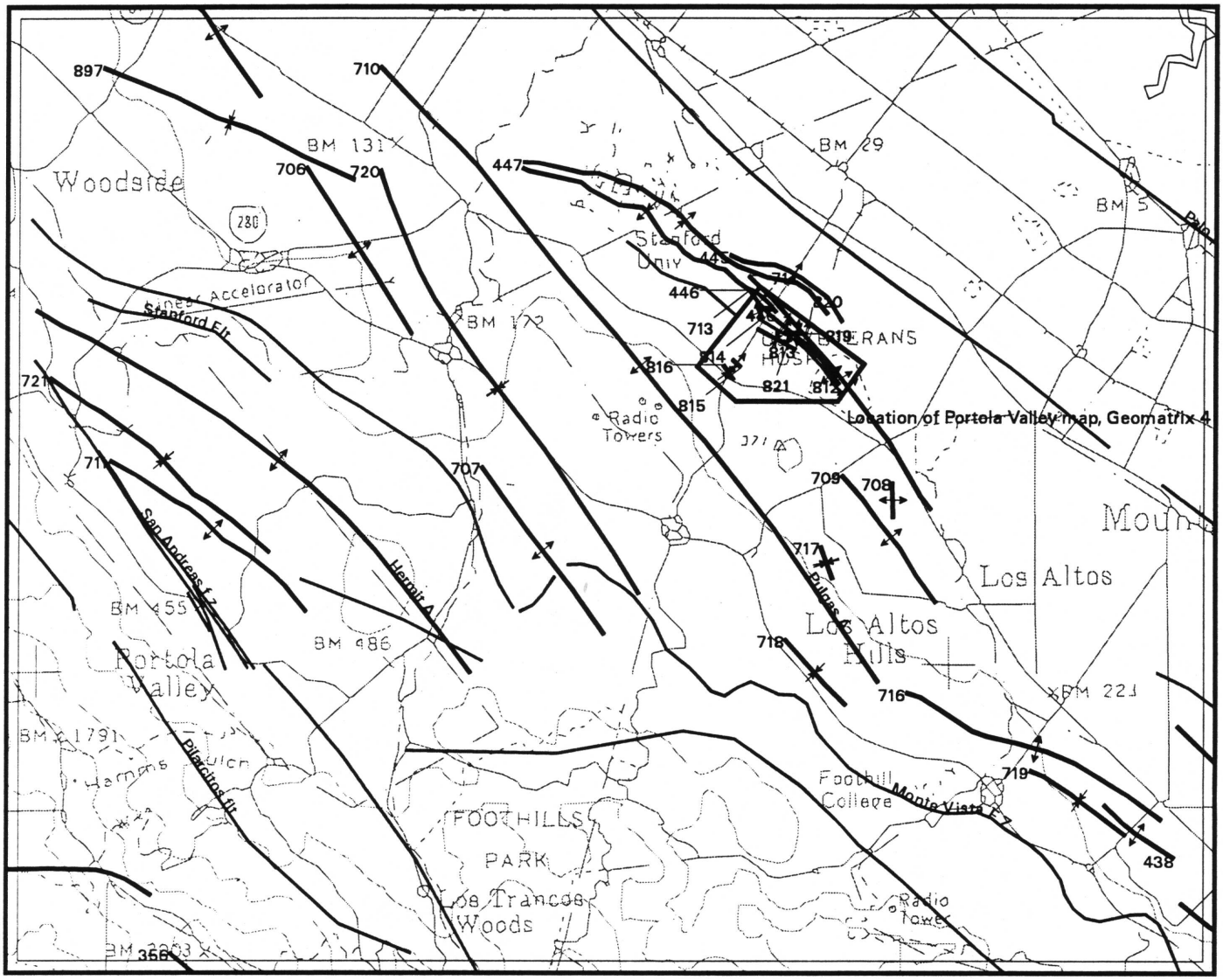

SCALE 1:80000

1 .5 0 1 2 3 4 5 MILES

1 .5 0 1 2 3 4 5 KILOMETERS

0 1 2 3 4 5 6 7 8 9 10 11 THOUSAND FEET

Location Geomatrix 4, index map and section Y-Y

Angell et al, Portola Valley-Los Altos area

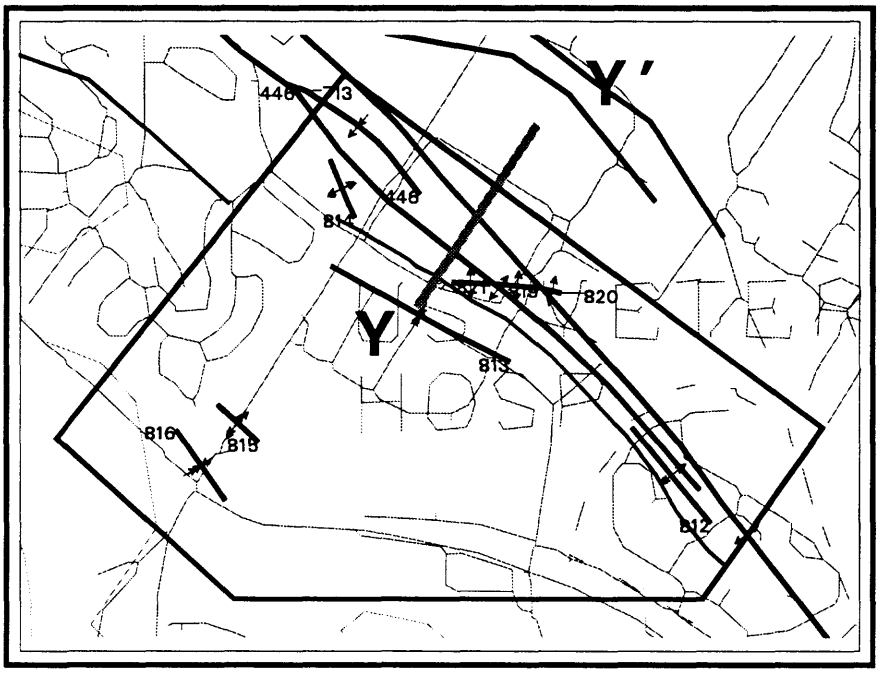

SCALE 1:20000

1 .5 0 1 MILES

1 .5 0 1 KILOMETERS

0 1 2 3 THOUSAND FEET

Cross section Y - Y' from Portola Valley to Palo Alto

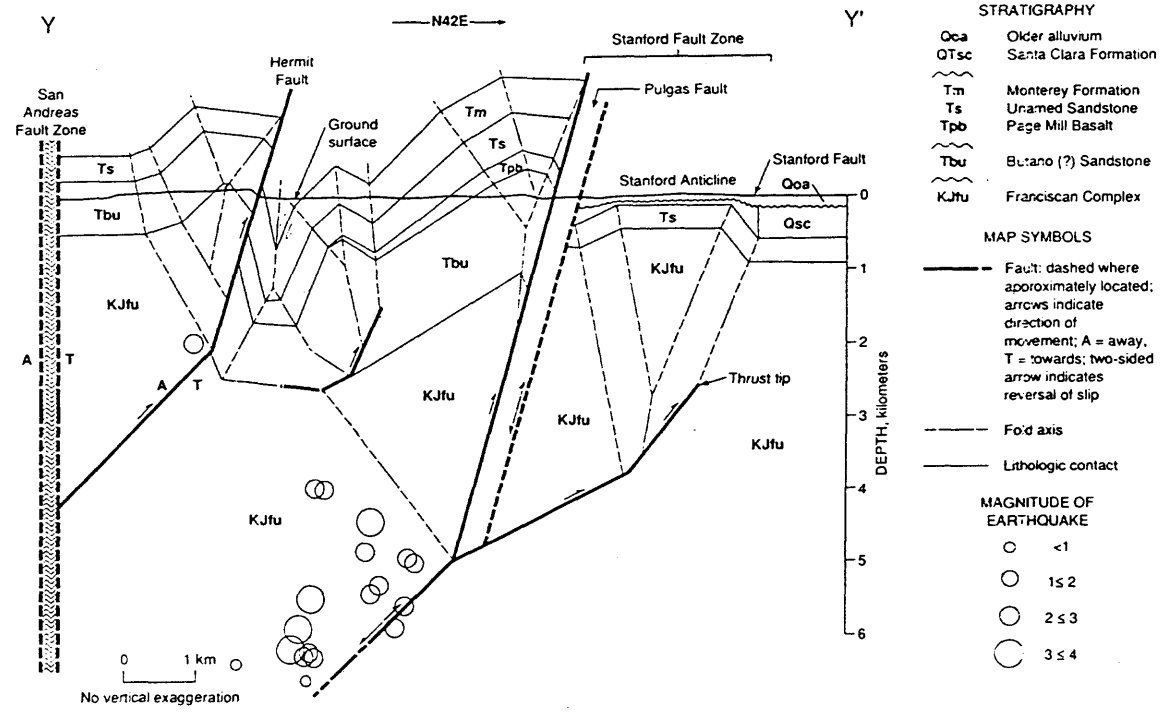

Note: Surface geology from Dibblee, 1966; Pampeyan, 1970. Earthquake data from Brabb and Olson, 1986.

Cross Section Y - Y' Restored to Geometry Prior to Onset of Compressive Deformation at Top of Monterey Time

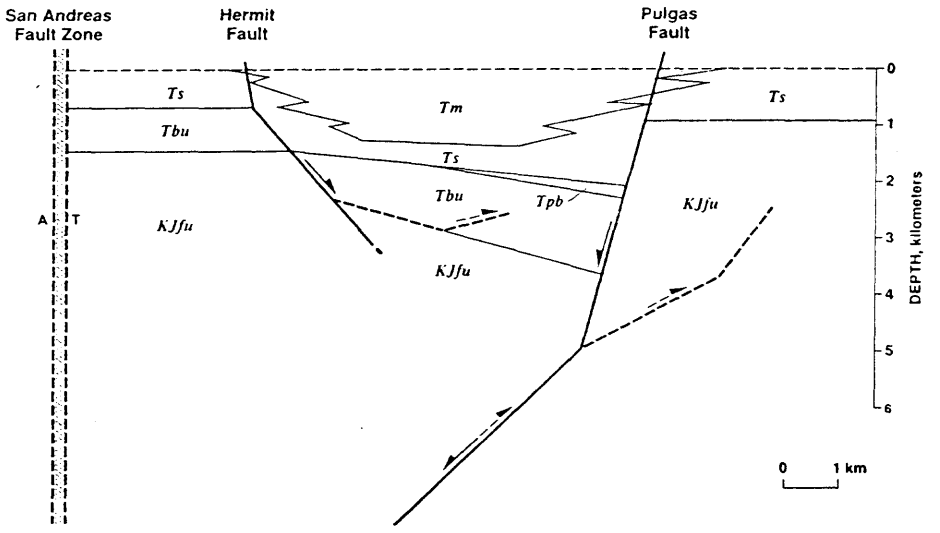

Angell

Arc Ln id	710	714	715	716
Structure_Name	Pulgas Anticline		Hermit anticline	
Age min	1	1	3	1
Age_max	4	3		3
Age_control	paleontologic, Merced Fm	paleontologic	paleontologic Merced Fm	paleontologic, Searsville facies, Santa Clara formation
Inclined Geomorphic surface	fluvial	alluvial	fluvial	alluvial
Horiz shortening (km)	2.3 (2)	0.35 (c2)	0.75 (c2)	
Shortening rate (mm/yr)	0.43	0.25	0.14 (c2)	
vert rate (mm/yr)			.005 (c3)	
Initiation of folding (Ma)	5.5	2.5	5.5 (c3)	2.5 (c3)
Method	balanced x-section	balanced xsection		
Time period for rate averaging		1 - 4 Ma		
Parallels strike-slip	yes	yes		no
Distance from fault (km), fault	6, San Andreas Fault	7.5, San Andreas fault		
Obliquity from fault	5		15	35
Distance from faults, fault			2	8.0, San Andreas fault
Average Trend	320	320		290
Plunge	20	10		18
Average Axial Plane strike	320	320		130
Axial Plane Dip	20 w	80 w		75 sw
Confidence of location	definite	definite		definite
Vergence direction	ne	ne		ne
Multiple or segmented		yes		no
Interlimb angle	80	100		100
Half wavelength (km)	4 km	2.5		
Fold type	Drap	anticline		anticline
Fold style				unknown
Structure sections		Angell and Hall, 1995		
Drill Hole		Brown and Caldwell, 1994		
Seis Reflct		Oliver, 1990		
Grav		Oliver, 1990		
Depth		4 -7 km		
Distrib microseis		Brabb and Olsen, 1986		
Reference				
Additonal References	Brabb and Olsen, 1986			Dibblee, 1966

Constraints On Slip Histories Of Thrust Faults Of The Southwestern San Francisco Bay Area From Geologic Mapping Investigations

McLaughlin, R.J., Sorg, D.H., and Helley, E.J., Office of Western Regional Geology, U.S. Geological Survey MS 975, 345 Middlefield Rd., Menlo Park, California 94025

Eastwardly-vergent thrust and reverse faults that root in the San Andreas fault zone, bound the eastern side of the Santa Cruz Mountains. These faults have been recognized for many hears as having displaced Pleistocene deposits, and locally they display youthful geomorphology. They are considered to be secondary in importance to the San Andreas fault and its major strike-slip branches. However, evidence that coseismic compression and other associated surface deformation was focused along faults of the thrust system during the 1989 Loma Prieta earthquake, has brought new attention and concern over the level of seismic hazard posed by these faults. Information gathered from mapping the various faults of the thrust system, and from numerous site-specific investigations over the time frame of about 1970 to the present, allows a number of constraints to be placed on the slip history of the thrust belt.

In the southwestern Santa Clara Valley, the most well-studied members of this thrust belt include the Sargent, Hooker Gulch, the Berrocal, Shannon, and Monte Vista fault zones. Based on K-Ar ages of hydrothermal K-feldspar formed along the southern parts of the Sargent and the Berrocal faults near Mt. Madonna, both the Sargent and Berrocal faults were active in the early to middle Miocene. These faults were initiated at least 17 to 18 Ma, since field relations indicate that hydrothermal K-feldspar with a 17 Ma K-Ar age was deposited from fluids circulating along the faults. A younger K-Ar age of 10 Ma from hydrothermal K-feldspar deposited along the Loma Prieta thrust segment of the Sargent fault, which displaces Jurassic ophiolite on the southwest, over Cretaceous and Eocene strata, suggests that substantial, if not most up- to the southwest displacement on the Loma Prieta thrust had occurred by 10 Ma. The chronology of slip surfaces in the Sargent fault zone indicates that prominent strike-slip displacement on steep-dipping segments of the fault zone truncate and thus are younger than the low-dipping Loma Prieta thrust segment. The Miocene components of slip on the Sargent fault measured from structure sections include about 1.6 km of vertical displacement, 1 km of shortening, and 2 km of reverse slip. The Hooker Gulch fault, which has displaced the same rock units as the Sargent fault during the same time frame, has accommodated an additional 1.4 km of vertical displacement, 1 km of shortening, and about 2 km of reverse slip. Together, the Sargent and Hooker Gulch fault zones account for about 3 km of vertical displacement, 2 km of shortening, and about 4 km of reverse-slip, most of which occurred in the Miocene.

The component of dextral slip on the Sargent and Hooker Gulch faults, most of which post-dates 10 Ma, is unknown, but probably large. A speculative fault block deformation

model which involves oblique dextral reverse-slip across an ancestral (Miocene) San Andreas fault, suggests that the Sargent fault could accommodate up to 26 km, and the Hooker Gulch fault as much as 10 km of right-slip.

Fission track studies by Bürgmann and others (Journal of Geophysical Research article, in press, 1994) of rocks above and below the Loma Prieta thrust indicate that these rocks have been uplifted an additional 3 to 4 km since 3 to 4 Ma. This displacement is younger and larger than measured displacements across the Sargent and Hooker Gulch faults. The younger uplift therefore may be associated with deeper structures that accommodate compression such as blind thrusts or folds above blind thrusts at depth, or with structurally lower thrusts that surface to the northeast.

Northeast of the Sargent and Hooker Gulch faults are several additional thrusts known to have Pleistocene displacements, and which also root southwestward in the San Andreas fault zone at depths of 10-11 km. These faults include the northwestern part of the Berrocal fault zone, the Shannon fault, and in the Cupertino area, the Monte Vista fault. Because these faults are complexly interwoven, and merge with or diverge from each other along their length, they are collectively treated as one belt of faulting here, termed the Southwestern Santa Clara Valley thrust belt. Faults of the Southwestern Santa Clara Valley thrust belt are part of the same family of thrusts as the Sargent and Hooker Gulch, but the Southwestern Santa Clara Valley thrust belt exhibits evidence of more youthful displacement along its length (ie., these faults displace Plio-Pleistocene and younger deposits). This may indicate that thrust faulting has migrated northeastward, away from the San Andreas fault with time, or alternatively, that Plio-Pleistocene and younger deposits have been completely eroded from upland areas southwest of the thrust belt front.

Earliest slip on the Southwestern Santa Clara Valley thrust belt is not well constrained. However, the Berrocal fault appears to have been active in the early Miocene along with the Sargent fault in the vicinity of Mount Madonna. Faults of the thrust belt displace early to middle Miocene shallow marine strata of the Temblor Sandstone, and other middle Miocene marine strata of the Monterey Group, indicating that major displacements post-date 10 Ma. Uplift and unroofing of the area, perhaps above blind thrusts, apparently began at depth in the Oligo-Miocene, as indicated by the major unconformity at the base of the Temblor Sandstone. Later unroofing and uplift of the Santa Cruz Mountains is signaled by the unconformity at the base of the 3 Ma (Blancan) and younger fluvial Santa Clara Formation. This major tectonic event apparently corresponds to the timing of initiation of major transpression between the North American and Pacific plates.

Several lines of evidence suggest that the slip history of the Southwestern Santa Clara Valley thrust belt has been episodic. Uplifted older fluvial terraces of ancestral Los Gatos Creek, are cut into the folded and tilted Santa Clara Formation. These older terraces are

estimated at 250 ka, based on the degree of weathering of the flat, boulder strewn terrace surface. The elevation of these terraces above the present drainage (152 m) indicates a post-250 ka incision rate (= uplift rate?) of about 0.6 mm/yr; somewhat less than the rate of about 1 mm/yr since 3 Ma derived from fission track data across the Sargent fault.

A gravity investigation for a Masters thesis at Stanford University by R.J. Fleck in the 1960's, concluded that Franciscan Complex rocks of the Black Mountain area override a 2 to 3 km wide belt of buried, lower density Miocene and Plio-Pleistocene strata along a 10 km length of the thrust belt. Assuming a 45° southwest dip for this segment of the thrust belt, yields about 3 km of shortening, 3 km of uplift, and about 4 km of reverse slip. This suggests uplift and shortening rates on the order of 0.3 mm/yr since the late Miocene (10 Ma). However, if most post-early Miocene uplift and shortening has occurred since the beginning of Santa Clara Formation deposition 3 Ma, as the stratigraphic evidence suggest, then Quaternary uplift and shortening rates have approached or exceeded 1 mm/yr episodically.

Near the mouth of Stevens Creek Canyon in the hanging wall block of the Monte Vista fault, another uplifted terrace surface estimated to be 120 ka is displaced about 43 m vertically from the correlative surface north of the fault, yielding an uplift rate of 0.4 mm/yr since 120 ka. Thus, the available data appear to indicate that uplift and shortening rates across the Southwestern Santa Clara Valley thrust belt since 0.25 and 0.125 Ma have been considerably lower than 1 mm/yr. If uplift and shortening rates have approached or exceeded 1 mm/yr episodically, it therefore is likely that these higher rates occurred between 3 and 0.25 Ma.

A tally of total uplift, shortening, and reverse slip from the Sargent fault to the northeastern edge of the Southwestern Santa Clara Valley thrust belt suggests that about 6 km of uplift, 5 km of shortening and 8 km of reverse slip have been accommodated between the San Andreas fault and the southwestern Santa Clara Valley thrust front since about 18 Ma. Since 3 Ma, about 3 km of uplift, 3 km of shortening, and 4 km of reverse slip have occurred.

Thrusting in the southwestern San Francisco Bay Area appears to be migrating northeastward, suggesting the possible presence of buried east-vergent thrusts beneath Santa Clara Valley. As thrusting has migrated eastward to younger, structurally lower faults of the thrust belt, fault members closer to the San Andreas fault are rotated upward to steeper orientations, and accommodate larger components of dextral slip. Larger components of uplift and shortening indicated from field relationships in predominantly Eocene and older rocks of the area require movement on buried flat faults, possibly associated with a tectonic wedge complex and (or) blind thrusts. These hypothetical flat faults that have accommodated long-term regional compression, may account for at least 15 km of uplift, and 220 km of shortening across the Pacific-North American plate boundary.

McLaughlin, Saratoga area

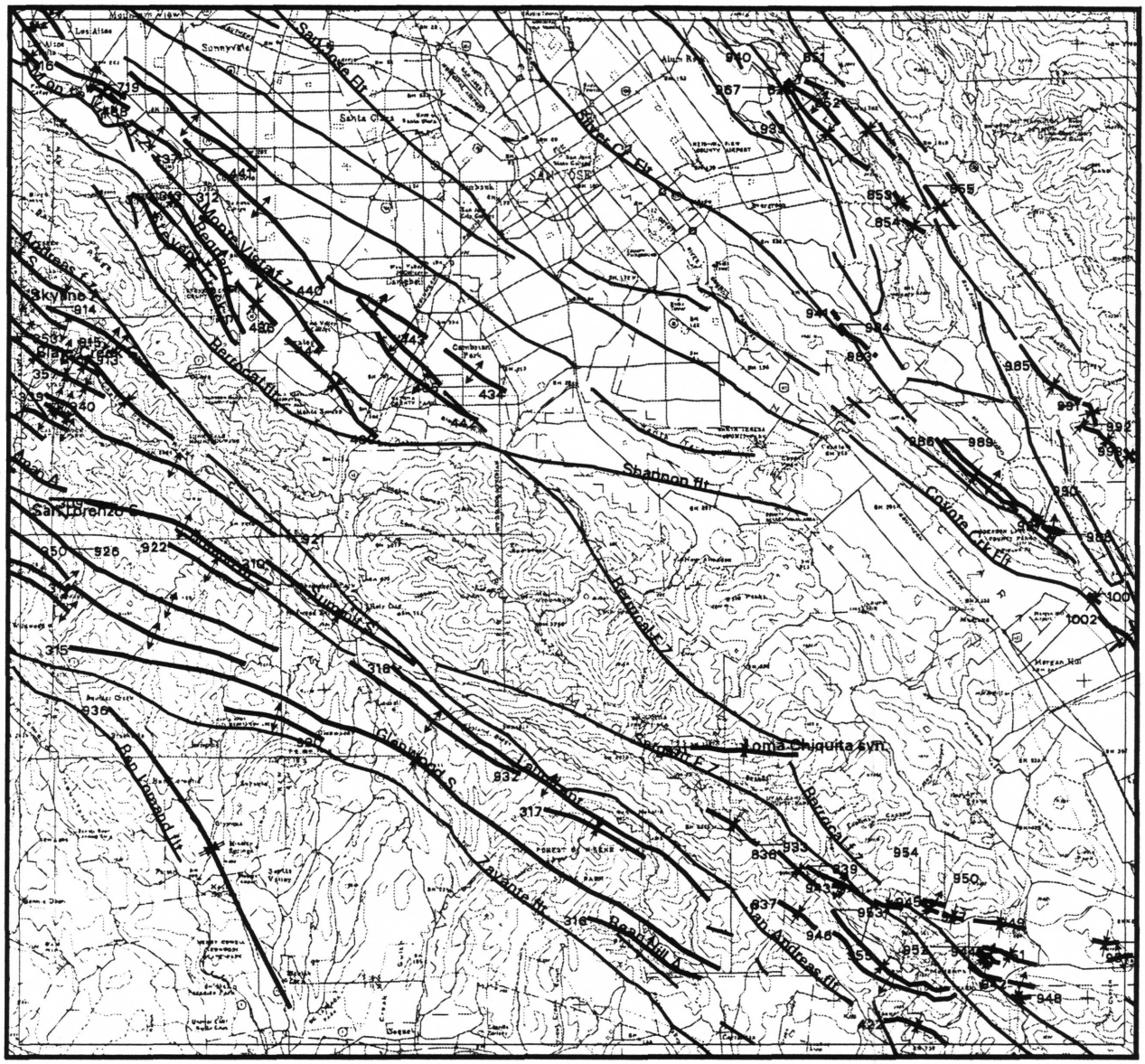

SCALE 1:300000

McLaughlin

Line identity	310	311	312	313	314	315	316	317	318
ıpiler(s)	McLaughlin, R.J.	Mc Laughlin, R.J.	Kelson, K, McLaughlin	McLaughlin, R., Kelson, K	McLaughlin, R.J.	McLaughlin, R.J.	McLaughlin, R.J.	McLaughlin, R.J.	McLaughlin, R.J.
ucture	Summit syncline	anticline	Regnart anticline	Stevens Creek syncline	anticline	Glenwood syncline	Bean Hill anticline	syncline	Laurel anticline
minimum	1	1	1	1	1	1	1	1	1
max		4	4	4					
control	Paleontology, Fission track	paleontologic	paleontologic	paleontologic	Paleontology, Fission track	Paleontology, Fission track	Paleontology, Fission track	Paleontology, Fission track	Paleontology, Fission track
ined Geomorphic surface	marine, fluvial	lacustrine, fluvial	fluvial, lacustrine	lacustrine, fluvial	marine, fluvial	marine, fluvial	marine, fluvial	marine, fluvial	marine, fluvial
izontal shortening (km)	3.5 km	2.5	2.5	2.5	3.5 km	3.5 km	3.5 km	3.5 km	3.5 km
	2	1	1	1	2	2	2	2	2
rtening rate mm/yr	0.1 mm/yr	0.30	0.30	0.30	0.1 mm/yr	0.1 mm/yr	0.1 mm/yr	0.1 mm/yr	0.1 mm/yr
	2	1	1	1	2	2	2	2	2
tical displacement rate /yr	0.3 mm/yr	0.3	0.3	0.3	0.3 mm/yr	0.3 mm/yr	0.3 mm/yr	0.3 mm/yr	0.3 mm/yr
	2	2		2	2	2	2	2	2
ıation of folding (Ma)	20 m.y.	10 -4.8 m.y.	10 -4.8 m.y.	10 -4.8 m.y.	20 m.y.	20 m.y.	20 m.y.	20 m.y.	20 m.y.
	3	1	1	1	3	3	3	3	3
mination of folding (Ma)	active	0.3 - 0.120	0.3 - 0.120	0.3 - 0.120	active	active	active	active	active
hod		terrace correlation	terrace correlation	terrace correlation					
e averaged, time length	5-10 m.yr.	10m.y. and .12 m.y.	125 ka	10m.y. and .12 m.y.	5-10 m.yr.	5-10 m.yr.	5-10 m.yr.	5-10 m.yr.	5-10 m.yr.
allels strike-slip	yes	yes	yes	yes	yes	yes	yes	yes	yes
ance from fault	1 -2 km	0-2 km, Monte Vista fault	0 - 2, Monte Vista, Shannon	0-2 km, Monte Vista fault	1 -2 km	1 -2 km	1 -2 km	1 -2 km	1 -2 km
rage Orientation	10				10	10	10	10	10
ad		150	340	150					
ge		20-90	20-90	20-90					
l Plane strike	305	145	145	145	306	300	297	300	306
l Plane dip	90	57	57	57	86	80	75	80	86
l Plane dip direction		w	w	w	s	n	n	n	s
fidence of location	Definate?	Probable	Probable	Probable	Definate?	Definate?	Definate?	Definate?	Definate?
gence direction	NE	NE	ne	NE	SE	NE	NE	NE	SE
tiple or segmented	yes	yes		yes	yes	yes	yes	yes	yes
f wavelength (km)	0.5-2.0 km	0.25- 1.0	0.25- 1.0	0.8	0.5-2.0 km	0.5-2.0 km	0.5-2.0 km	0.5-2.0 km	0.5-2.0 km
l type	A, S, O, U, I	A, S, O, U, I, AS	A, S, O, U, I, AS	A, S, O, U, I, AS	A, S, O, U, I	A, S, O, U, I	A, S, O, U, I	A, S, O, U, I	A, S, O, U, I
l style	unknown	fault propagation	fault propagation	fault propagation	unknown	unknown	unknown	unknown	unknown
detic	Valensise and Ward, 1991, Burgmann and other, 1994				Valensise and Ward, 1991, Burgmann and other, 1994	Valensise and Ward, 1991, Burgmann and other, 1994	Valensise and Ward, 1991, Burgmann and other, 1994	Valensise and Ward, 1991, Burgmann and other, 1994	Valensise and Ward, 1991, Burgmann and other, 1994
erence									
surface data									
cture sections	Yes	yes	Sorg and McLaughlin, 1975	yes	Yes	Yes	Yes	Yes	Yes
l Hole	Yes,	yes		yes	Yes,	Yes,	Yes,	Yes,	Yes,
mic Reflection	yes				yes	yes	yes	yes	yes
vity	Yes	yes	yes	yes	Yes	Yes	Yes	Yes	Yes
orical Seismicity	Yes, 1989 loma Prieta	yes	yes	yes	Yes, 1989 loma Prieta	Yes, 1989 loma Prieta	Yes, 1989 loma Prieta	Yes, 1989 loma Prieta	Yes, 1989 loma Prieta
gnitude/event	7.1	3.5 -4.0	3.5 -4.0	3.5 -4.0	7.1	7.1	7.1	7.1	7.1
th	17 km	0-8 km	0-8 km	0-8 km	17 km	17 km	17 km	17 km	17 km
ributed microseismicity	yes	yes	yes	yes	yes	yes	yes	yes	yes
erence	Anderson, 1990; Clark and Rietman, 1973	Oppenheimer, Olsen, Zoback	Oppenheimer, Olsen, Zoback	Oppenheimer, Olsen, Zoback	Anderson, 1990; Clark and Rietman, 1973	Anderson, 1990; Clark and Rietman, 1973	Anderson, 1990; Clark and Rietman, 1973	Anderson, 1990; Clark and Rietman, 1973	Anderson, 1990; Clark and Rietman, 1973

litonal References	Lisowski et all, 1990; McLaughlin and others, 1988; McLaughlin and Clark	Hitchcock, C.S., Kelson, K. I., and Thompson, S.C., 1994; Sorg and Mc Laughlin, 1975; McLaughlin,and Clark, in prep	Hitchcock, C.S., Kelson, K. I., and Thompson, S.C., 1994; Sorg and Mc Laughlin, 1975; McLaughlin,and Clark, in prep	Hitchcock, C.S., Kelson, K. I., and Thompson, S.C., 1994; Sorg and Mc Laughlin, 1975; McLaughlin,and Clark, in prep	Lisowski et all, 1990; McLaughlin and others, 1988; McLaughlin and Clark	Lisowski et all, 1990; McLaughlin and others, 1988; McLaughlin and Clark	Lisowski et all, 1990; McLaughlin and others, 1988; McLaughlin and Clark	Lisowski et all, 1990; McLaughlin and others, 1988; McLaughlin and Clark	Lisowski et all, 1990; McLaughlin and others, 1988; McLaughlin and Clark

High-Resolution Geophysical Profiling Across the Monte Vista Fault, Los Altos, California

R.A. Williams, USGS, Denver Federal Center MS 966, Denver, CO 80225; williams@gldvxa.cr.usgs.gov, R.T. Williams Geology Dept., University of Tennessee, Knoxville, TN, 37996, R.D. Catchings, USGS, 345 Middlefield Rd, MS 977, Menlo Park, CA, 94025, K.I. Kelson, and C.S. Hitchcock , both at: Wm Lettis & Assoc., Inc., 1000 Broadway, suite 612, Oakland, CA 94067, M.J. Rymer, USGS, 345 Middlefield Rd, Menlo Park, CA, 94025, J.K. Odum USGS, Denver Federal Center, Denver, CO 80225

The Monte Vista fault is a northwest-trending reverse fault located 5 km northeast of the San Andreas fault, along the eastern margin of the Santa Cruz Mountains, and adjacent to the heavily urbanized Santa Clara Valley. Geologic and geomorphic evidence shows that the fault at this locality has had late Pleistocene and possibly Holocene activity. High-resolution seismic reflection and refraction profiles, and ground-penetrating radar profiles, were acquired obliquely across the mapped trace of the Monte Vista fault in Rancho San Antonio Park, to image the fault at depth and to help identify a specific location for future trenching and other paleoseismological studies (scheduled Sept. '95).

Strong, unbroken reflections from about 600 m depth, are observed immediately southwest of the mapped surface trace of the fault, and continue for a distance of 180 m, with an apparent dip of about 5 degrees to the southwest. These reflections abruptly terminate into non-reflective zones at both north and south ends. An interval of low reflectivity and discontinuous reflections was found from about 10 to 500 m depth. No clear fault plane or rupture zone was observed in the reflection data, but the continuous reflector at about 800 m depth constrains possible dips of the Monte Vista fault to be either vertical or with an apparent south dip of about 75 degrees (about 80o true dip). The refraction data indicate two locations where 2- to 3-m-high stratigraphic warps may exist in the subsurface at a depth of 6 to 8 m. One such warp underlies a 3-m-high scarp at the ground surface. The ground-penetrating radar, which was effective to depths of a few meters, shows discontinuities that also occur about 5 m to the southwest of the surface scarp.

Williams, R.A., et al, USGS, Location of seismic reflection line

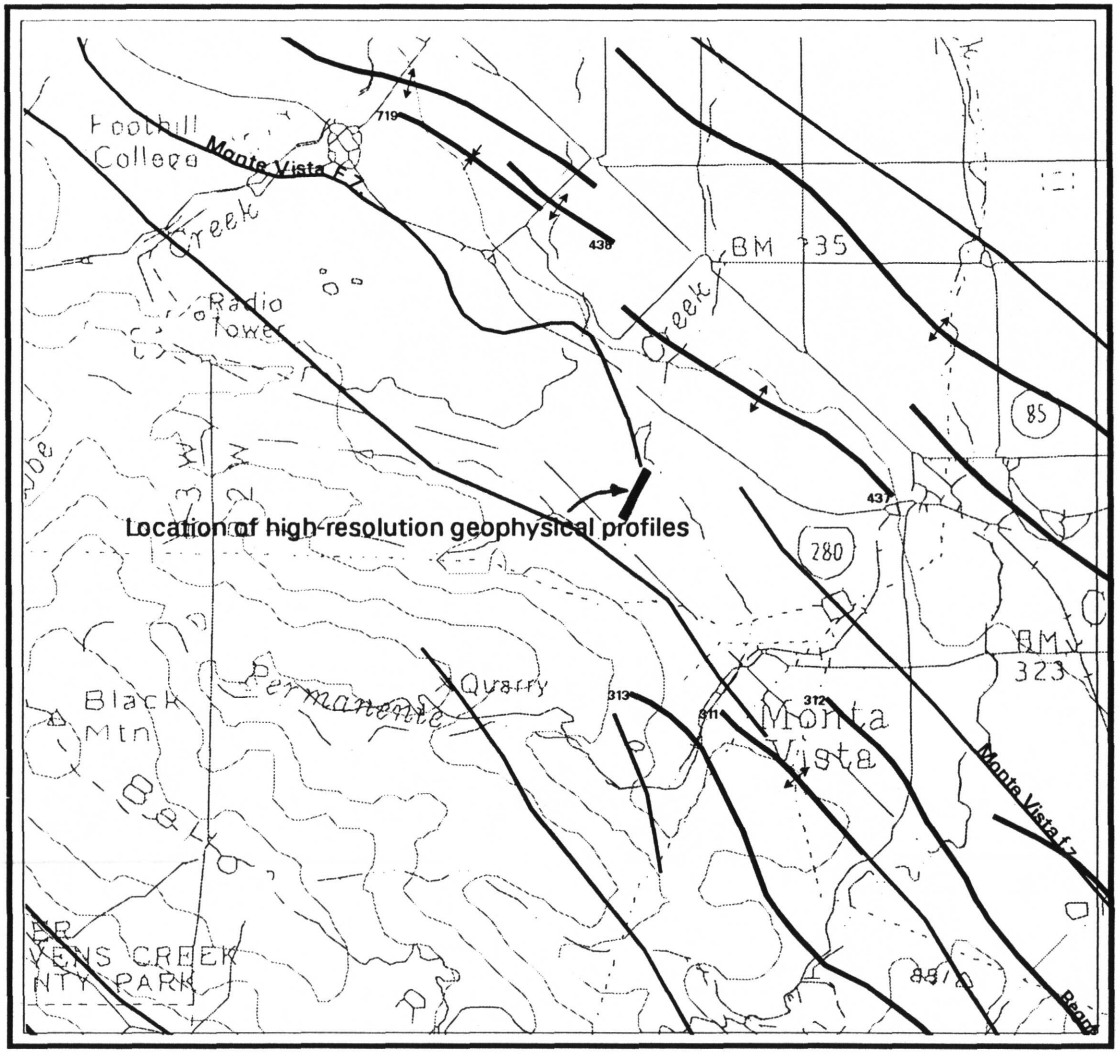

SCALE 1:62500

1 .5 0 1 2 3 4 5 MILES

1 .5 0 1 2 3 4 5 KILOMETERS

0 1 2 3 4 5 6 7 8 9 10 11 THOUSAND FEET

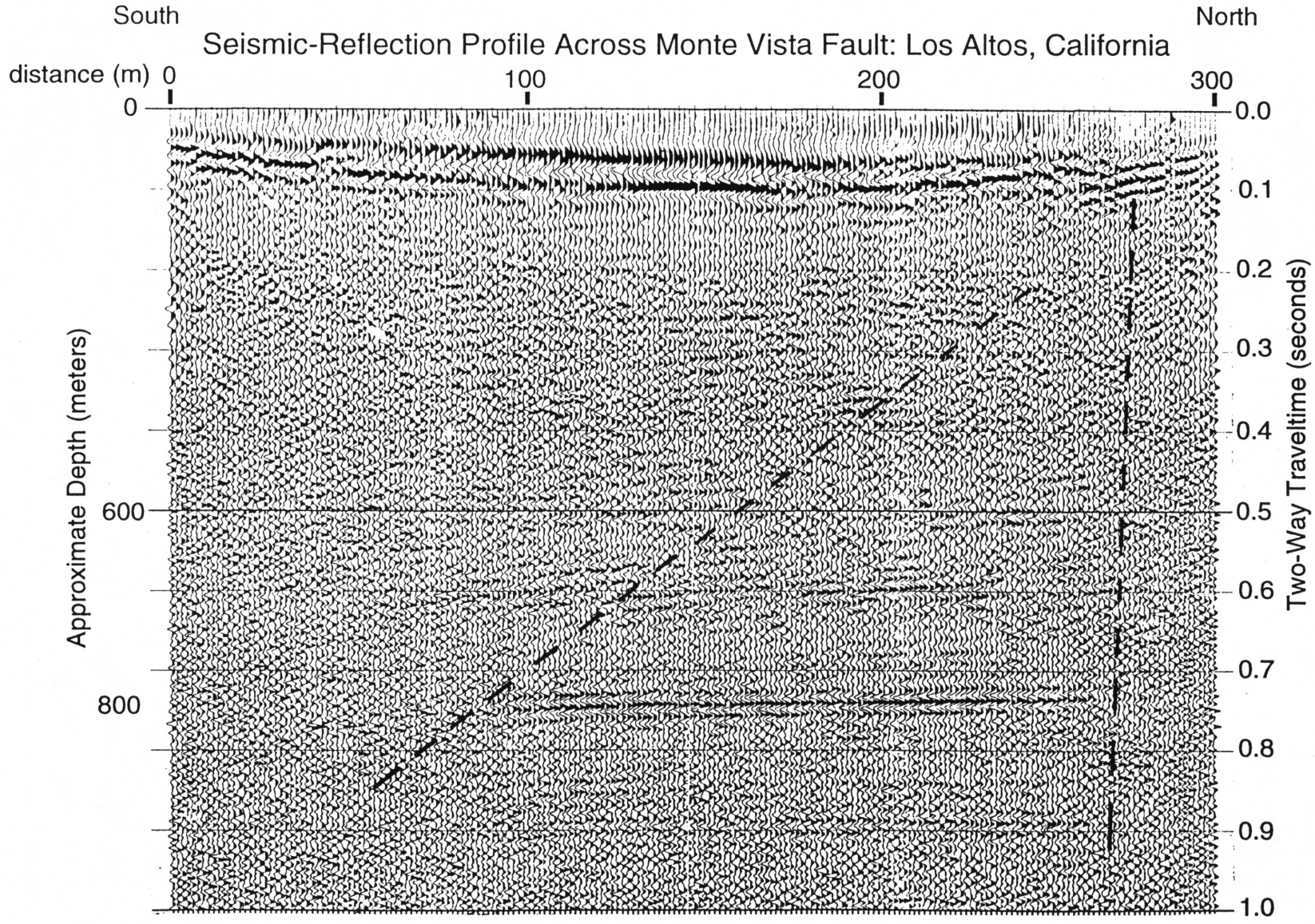

Figure 1. Stacked seismic-reflection profile across the Monte Vista fault, Los Altos, California. Seismic sources used for this profile were 1 lb. charges fired approximately every 10 m into 96 channel geophone spread with 28-Hz sensors spaced at 3-m intervals. Coherent reflection at about 800-m depth abruptly terminates into potential fault zones. Two potential fault orientations (dashed lines) are inferred in the data.

Late Cenozoic strain rates across the La Honda Basin

Jayko, A.S., U.S. Geological Survey, 345 Middlefield Rd., MS-977, Menlo Park, Ca., 94025

The uplift of Late Cenozoic marine deposits (Lawson, 1893, Alexander, 1953, Bradley and Griggs, 1976, Lajoie, et al., 1979b, Lajoie, et al., 1979a) indicates that widespread deformation is on going and involves warping or folding between fault bound blocks. The extent to which this deformation is accommodated by buried faults is a crucial issue to earthquake hazard evaluation. Much of the topography that makes up the San Francisco region and nearby central coast ranges is less than two to four million years old (Lawson, 1893, Higgans, 1960, Higgans, 1961, Christensen, 1965, Anderson, 1990, Montgomery, 1993). Recent geodetic and fault-slip inversion work associated with the Loma Prieta earthquake has led to greater efforts to quantify the rates and mechanisms of structural and thus landscape evolution (Anderson, 1990, Valensise and Ward, 1991). Much geological and geophysical work suggests that the regional scale topographic highs and lows are controlled by the location of actively deforming structures (Lawson, 1893, Christensen, 1965, Montgomery, 1993).

The tectonic style of the San Francisco Bay region has recently been imprinted by passing of the Mendocino triple junction during Late Miocene time prior to development of the present transform fault system. Thus, many structures that developed during this tectonism are favorably oriented to accommodate additional shortening within the present tectonic regime. A period of intense upper Miocene deformation followed by relative quiescence in the lower Pliocene and renewed tectonism in the early Pleistocene has been noted by many earlier workers. The Pacific-Farallon-North America triple junction was in the vicinity of Santa Cruz and the Peninsula area between about 6 to 10 m.y.b.p. during the latest Miocene and possibly earliest Pliocene time (Atwater and Molnar, 1973, Dickinson and Snyder, 1979). During this time Tertiary basins were rapidly uplifted and strongly deformed; in addition, the regional structural fabric characterized by northwest trending faults and folds was established (Graham, et al., 1984). The late Cenozoic tectonics near the Mendocino Triple Junction show that rapid uplift and pervasive deformation are associated with the cessation of subduction and initiation of the transform boundary. The uplift rate in that region is on the order of 2-5 mm/yr (McLaughlin, et al., 1983, Merritts and Bull, 1989, Merritts and Vincent, 1989, Carver, 1987, Lajoie, 1982). The approach of the triple junction was signaled by the development of a regressive sequence associated with emergence of the basins (Blake et al, 1978). Uplift rates taper off quickly to about 0.3 mm/yr by about 60 km south of the triple junction (Merritts and Bull, 1989). The vertical displacement rates determined from Quaternary terraces range

between 0.3 to 0.5 mm/yr through much of northern and central California (Alexander, 1953, Bull, 1986, Bradley and Griggs, 1976, Lajoie, et al., 1979b, Lajoie, 1986, Lettis and Hanson, 1992, Wehmiller, et al., 1977). Assuming that more rapid horizontal deformation rates are associated with the higher uplift rates then it appears that a discreet deformation wave migrates along the continental margin associated with migration of the triple junction and is followed by much less intense deformation associated with the transform faulting.

Results from geodetic surveys in the San Francisco region indicates that much of the relative plate motion (DeMets, et al., 1990) can be measured across the transform system, and that there is little or no measurable convergence during the present time except at localized regions (Sauber, et al., 1989, Lisowski, et al., 1991b). This observation contrasts with crustal thickening and horizontal shortening that were accommodated by folding, thrust faulting, and basin emergence in the late Neogene (Page, 1982, Aydin and Page, 1984, Namson and Davis, 1988, Page, 1990, Jones, et al., 1994). A rigorous examination of Quaternary intra-block structures will provide constraints on the active tectonic style and help determine whether there has been a significant change in rate during the last two or three million years that can account for discrepancies between the geologic and geodetic records..

If the tectonics of the active Mendocino triple junction is an analog to the recent past history of the San Francisco Bay Region, then many structures defined by late Cenozoic strata evolved in the late Neogene, prior to development of the presently active transform. The deformation rates and structure style of the active Mendocino triple junction (Merritts and Bull, 1989, Mc Laughlin and others, 1983) probably serve as indicators of the recent past tectonics that profoundly affected the present structural fabric. Structures which are primarily a consequence of passing of the triple junction (Graham, et al., 1984, Dickinson and Snyder, 1979) about 7.5 m.y.b.p. have not yet been distinguished from those that are presently active.

Preliminary analysis of structural data from the late Cenozoic in the La Honda Basin area suggests that the deformation rate has slowed considerably from about 1.2mm/yr since the Late Miocene to about 0.3 mm/yr in the late Quaternary, and that the highest deformation rates are coincident with passage of the Mendocino fracture zone at this latitude (Figure 1).

Alexander, C. S., 1953, The marine and stream terraces of the Capitol-Watsonville area: University of California Press, v. 10, p. 1-44.

Anderson, R. S., 1990, Evolution of the northern Santa Cruz mountains by advection of crust past a San Andreas Fault Bend: Science, v. 249, p. 397-401.

Atwater, T., and Molnar, P., editors, 1973, Relative motions of the Pacific and North American plates deduced from sea-floor spreading in the Atlantic, Indian, and South Pacific oceans: Proceedings of the Conference on Tectonic problems of the San

Andreas fault system, Stanford University Press, 136-148 p.
Aydin, A., and Page, B. M., 1984, Diverse Pliocene-Quaternary tectonics in a transform environment, San Francisco Bay region, California: Geological Society of America Bulletin, v. 95, p. 1303-1317.
Bradley, W. C., and Griggs, G. B., 1976, Form, geneses, and deformation of central California wave-cut platforms: Geological Society of America Bulletin, v. 87, p. 433-449.
Brocher, T. M., J.McCarthy, Hart, P. E., Holbrook, W. S., Furlong, K. P., McEvilly, T. V., Hole, J. A., and Basix, in press, Seismic evidence for a possible lower-crustal detachment beneath San Francisco Bay: Science,
Bull, W. B., 1986, Inferred ages and uplift rates of global marine terraces near Santa Cruz, California: Geological Society of American Abstracts with Programs, v. 18, p. 90.
Bullard, T. F., and Lettis, W. R., 1993, Quaternary deformation associated with blind thrust faulting, Los Angeles Basin, California: Journal of Geophysical Research, v. 98, p. 8349-8369.
Carver, G. A., editors, 1987, Late Cenozoic tectonics of the Eel River Basin Region, Coastal northern California: Schymiczek, H., and Suchland, R., eds., Tectonics, sedimentation and evolution of the Eel river and associated coastal basins of northern California, San Joaquin Geological Society, 61-72 p.
Christensen, M. N., 1965, Late Cenozoic deformation in the central Coast Ranges of California: Geological Society of America Bulletin, v. 76, p. 1105-1124.
DeMets, C., Gordon, R. G., Argus, D. F., and Stein, S., 1990, Current Plate motions: Geophysical Journal International, v. 101,
Dickinson, W. R., and Snyder, W. S., 1979, Geometry of triple junction related to San Andreas transform: Journal of Geophysical Research, v. 84, p. 561-572.
Furlong, K. P., 1993, Thermal-rheological evolution of the upper mantle and the development of the San Andreas fault system: Tectonophysics, v. 223, p. 149-164.
Furlong, K. P., Hugo, W. D., and Zandt, G., 1989, Geometry and evolution of the San Andreas fault zone in northern California: Journal of Geophysical Research, v. 94,
Graham, S. A., McCloy, C., Hitzman, M., Ward, R., and Turner, R., 1984, Basin evolution during change from convergent to transform continental margin in Central California: American Association of Petroleum Geologists Bulletin, v. 68, p. 233-249.
Haller, K. M., Machette, M. N., and Dart, R. L., 1993, Maps of Major active faults, western Hemisphere, International Lithosphere Program (ILP), Project II-2: U.S. Geological Survey 93-338, 45 p.
Higgans, C. G., 1960, Ohlson Ranch Formation, Pliocene, northwestern Sonoma County, California: University of California Publications in Geological Sciences, v. 36, p. 233-242.
Higgans, C. G., 1961, San Andreas fault, north of San Francisco, California: Geological Society of American Bulletin, v. 72, p. 51-68.
Jones, D. L., Russel, G., Wang, C., McEvilly, T. V., and Lomax, A., 1994, Neogene transpressive evolution of the California Coast Ranges: Tectonics, v. 13, p. 561-574.
Lajoie, K. R., 1982, Emergent Holocene marine terraces at Ventura and Cape Mendocino, California-- indicators of high tectonic uplift rates: Geological Society of American Abstracts with Programs, v. 14, p. 178.
Lajoie, K. R., editors, 1986, Coastal tectonics: Committee, G. S., eds., Active Tectonics, National Academy Press, 95-124 p.
Lajoie, K. R., Kern, J. P., Wehmiller, J. F., Kennedy, G. L., Mathison, S. A., Sarna-Wojcicki, A. M., Yerkes, R. F., and McCrory, P. F., editors, 1979a, Quaternary marine shorelines and crustal deformation, San Diego to Santa Barbara: Abbott, P. L., eds., Geological Excursions Southern California Area, San Diego State University, 3-15 p.
Lajoie, K. R., Weber, G. E., Mathieson, S. A., and Wallace, J., editors, 1979b, Quaternary tectonics of coastal Santa Cruz and San Mateo Counties, California, as indicated by deformed marine terraces and alluvial deposits: Weber, G. E., Lajoie, K. R., and Griggs, G. B., eds., 1979b, Geological Society of America Guidebook,
Lawson, A. C., 1893, The post-Pliocene diastrophism of the coast of southern California: University of California Press, v. 1, p. 115-160.
Lettis, W. R., and Hanson, K. L., 1992, Quaternary tectonic influences on coastal morphology, south central California: Quaternary International, v. 15/16, p. 135-148.
Lisowski, M., Savage, J. C., and Prescott, W. H., 1991a, The velocity field along the San Andreas fault in central and southern California: Journal of Geophysical Research, v. 96, p. 8369-8389.
Lisowski, M., Savage, J. C., and Prescott, W. H., 1991b, The velocity field along the San Andreas fault in northern California:
McLaughlin, R. J., Lajoie, K. R., Sorg, D. H., Morrison, S. D., and Wolfe, J. A., 1983, Tectonic uplift of a middle Wisconsin marine platform near the Mendocino triple junction, California: Geology, v. 11, p. 35-39.
Merritts, D., and Bull, W. B., 1989, Interpreting Quaternary uplift rates at the Mendocino triple

junction, northern California, from uplifted marine terraces: Geology, v. 17, p. 1020-1024.
Montgomery, D. R., 1993, Compressional uplift in the central California Coast Ranges: Geology, v. 21, p. 543-546.
Mount, V. S., and Suppe, J. S., 1987, State of stress near the San Andreas fault: implications for wrench tectonics: Geology, v. 15, p. 1143-1146.
Namson, J. S., and Davis, T. L., 1988, Seismically active fold and thrust belt in the San Joaquin Valley, central California: Geological Society of America, v. 100, p. 257-273.
Page, B. M., editors, 1982, Modes of Quaternary tectonic movement in the San Francisco Bay Region, California: Proceedings- conference on earthquake hazards in the Eastern San Francisco Bay Area, California Division of Mines and Geology, 1-10 p.
Page, B. M., 1990, Evolution and complexities of the transform system in California, U.S.A.: Annales Tectonicea, v. IV, p. 53-69.
Sauber, J., Lisowski, M., and Soloman, S. C., Sauber, J., Lisowski, M., and Soloman, S. C.S, 1989, Geodetic measurement of deformation east of the San Andreas fault in central California:
Smith, D., 1978, Compound erosion surface on the San Francisco Peninsula, California: Geological Society of America, Abstracts with Programs,
Valensise, G., and Ward, S. N., 1991, Long-term uplift of the Santa Cruz Coastline in response to repeated earthquakes along the San Andreas fault: Bulletin of the Seismological Society of America, v. 81, p. 1694-1704.
Wehmiller, J. F., Lajoie, K. R., Kvenvolden, K. A., Peterson, E., Belknap, D. F., Kennedy, G. L., Addicott, W. O., Vedder, J. G., and Wright, R. W., 1977, Correlation and chronology of Pacific Coast marine terrace deposits by fossil amino acid sterochemistry-- techniques evaluation, relative ages, kinetic model ages, and geologic interpretations: 77-680, p.

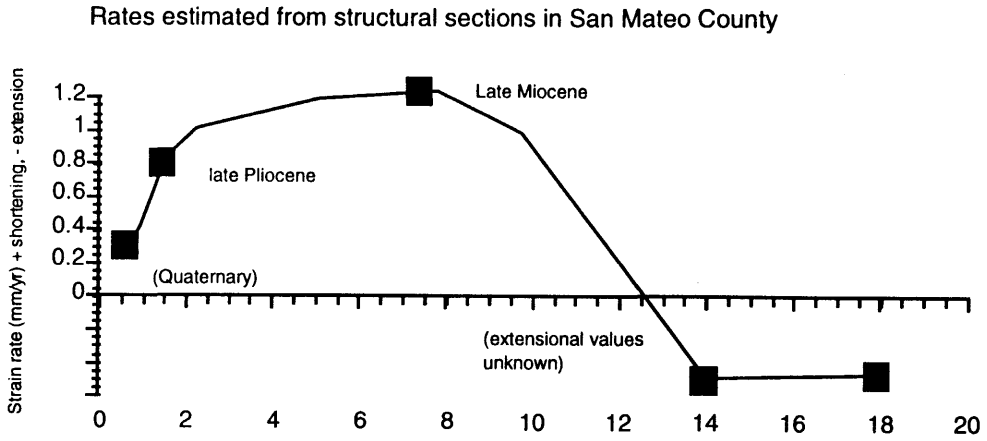
Rates estimated from structural sections in San Mateo County
Strain rate (mm/yr) + shortening, - extension
1.2
1
0.8
0.6
0.4
0.2
0
Late Miocene
late Pliocene
(Quaternary)
(extensional values
unknown)
0
2
4
6
8
10
12
14
16
18
20

Figure 1

Jayko, La Honda-San Gregorio area

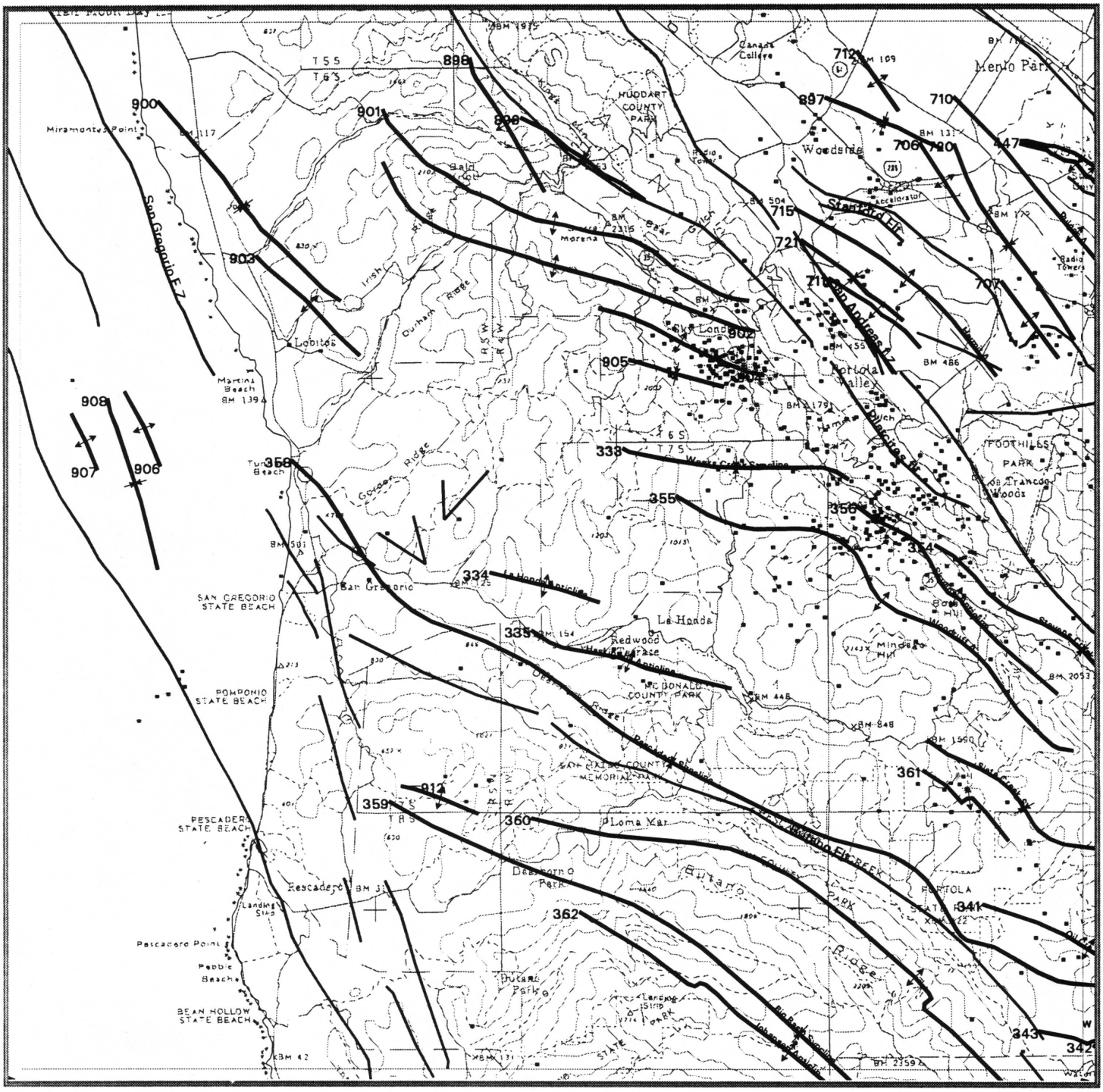

Location of earthquake epicenters SCALE 1:150000

1 .5 0 1 2 3 4 5 6 7 MILES

1 .5 0 1 2 3 4 5 6 7 KILOMETERS

0 2 4 6 8 10 12 14 THOUSAND FEET

JAYKO

LINEID	334
COMPILER	Jayko A.S., Green Nylen N.
INSTITUT	USGS
SUBMISSION	4/25/95
PROJECT	9540-10200
COMMAPSCALE	250000
ORIMAPSCL	62500
STRUCTURE	La Honda Anticline
MINAGE	2
MAXAGE	5
AGECONTROL	Purisima Fm.
GEOMORPH	marine terrace, 80kybp
EHORZ	0
CONF1	0
ERATEH	0.3
CONF2	4
ERATEV	0.29
CONF3	3
FOLDINIT	7
CONF4	2
FOLDEND	0.01
CONF5	0.2
METHOD	time average
DURRAVE	2
PAPASS	no
TREND	285
PLUNGE	18
APSTRIKE	284
APDIP	81
APDIPDR	N
CONF	
VERG	N
SEGMENTED	no
ILIMBA	147
BLSTRIKE	140
BLDIP	30
BLDIPDR	W
BLDIM	0
FLSTRIKE	221
FLDIP	20
FLDIPDR	W

Half Moon Bay Syncline and Pillar Point Dome

K.R. Lajoie, U.S. Geological Survey, MS-977, Menlo Park, California, 94025

Half Moon Bay Syncline

The Half Moon Bay syncline is expressed by a gentle downwarp in the emergent Half Moon Bay marine terrace (105 or 82ka) on the central coast of San Mateo County (Figure 1). Generalized structural contours on the buried wave-cut platform and the longitudinal profile of the shoreline angle delineate a broad westward-plunging syncline flanked by two minor anticlines. The syncline plunges obliquely into the northwest-trending, right-lateral Seal Cove fault, suggesting a drag-fold relationship.

Neither the wave-cut platform nor the shoreline angle of the next higher Miramar terrace (probably 124ka) is exposed, but the longitudinal profile of its topographic surface reveals synclinal warping slightly tighter than that expressed by the Half Moon Bay terrace, indicating progressive deformation. Well developed, but widely separated remnants of at least three higher marine terraces notch the hillsides above Half Moon Bay, but their longitudinal profiles are too poorly constrained to provide independent evidence of synclinal warping. However, the broad embayment of Pilarcitos Creek east of Half Moon Bay, in which some of the high terrace remnants occur, and the saddle in the ridge crest at the head of the embayment might reflect long term synclinal folding.

The local drainage pattern clearly reflects the synclinal warping expressed by the Half Moon Bay terrace. The high reaches of the major streams draining the hills above Half Moon Bay trend southwestward (Figure 1), roughly following linear joints in the underlying Pliocene marine sedimentary rocks of the Purisima Formation. However, where the streams leave the hills and cross the Half Moon Bay terrace their courses deflect toward the synclinal axis (Figure 1). Exceptions to this general pattern occur at the northern and southern ends of the terrace where the stream courses trend down the back sides of the two minor adjacent anticlines.

The Holocene depositional and erosional patterns also reflect the synclinal warping expressed by the Half Moon Bay terrace. The Holocene rise in sea level raised the base level of the streams crossing the central, downwarped part of the Half Moon Bay terrace, forming Half Moon Bay and causing the streams entering it to deposit alluvial fans over the Pleistocene terrace sediments. In marked contrast, the mid-Holocene stabilization of sea level resulted in sea-cliff erosion along the uplifted southern limb of the syncline, locally lowering base level and causing the major streams crossing the terrace to deeply incise their late Pleistocene to early Holocene floodplains, the Pleistocene terrace sediments and the underlying Pliocene bedrock. However, minor streams unable to incise the bedrock cascade over the sea cliffs as seasonal water falls.

Pillar Point Dome

The Pillar Point dome is expressed geomorphically by the narrow ridge, Seal Cove bluff, northwest of Half Moon Bay (Figures 1A and 2); Pillar Point, the prominent headland at the southeast end of the ridge, defines the northern end of the Half Moon Bay. An uplifted and warped remnant of the Half Moon Bay terrace truncates the crest of the ridge forming a flat summit surface (Figure 2). The wave-cut platform and its thin veneer of overlying terrace

sediments are exposed high in the modern sea cliff along the southwest side of the ridge. Two relict sea stacks protrude through the terrace sediments at the center of the ridge (Figure 2) and at its southern end (Pillar Point).

Detailed bathymetry reveals upturned and faulted beds of the Pliocene Purisima Formation on the active wave-cut platform (Jack, 1969). The areal extent of these deformed beds probably reflect the lateral dimensions of the Pillar Point dome (Figure 1A). Poorly constrained structural contours on and projected from the uplifted remnant of the wave-cut platform of the Half Moon Bay terrace reveal that the dome is probably a narrow, northwest-trending structure truncated along its northeast side by the Seal Cove fault. The configuration of the dome is so poorly constrained that its axes cannot be determined with confidence. However, its major axis probably lies adjacent and parallel to the fault, while its minor axis probably trends southwestward away from the fault at a high angle.

Projecting the structural contours onto a vertical extension of the fault plain yields an approximate longitudinal profile of the Pillar Point dome (Figure 1B). This profile contrasts markedly from the profile of the Half Moon Bay syncline northeast of the fault. Because no piercing points can be identified, neither local slip directions nor slip rates can be determined.

The southern extent of the Seal Cove fault is not known. However, linear scarps revealed in the detailed bathymetry of Half Moon Bay (Jack, 1969) indicate the fault side steps and bends to the south at Pillar Point (Figure 1). The fault might extend offshore to Pescadero and connect with a strand of the onshore San Gregorio fault. In any event, the Pillar Point dome and the opposing Half Moon Bay syncline probably reflect structural complexities at the bend in right-lateral Seal Cove fault. As such, both structures are minor features superimposed on the broader antliclinal uplift of the Santa Cruz mountains.

BIBLIOGRAPHY

Bloom, A.L., and Yonekura, N.,1985, Coastal terraces generated by sea-level change and tectonic uplift: in Wodenberg, Michael J. (ed.), Models in Geomorphology, Boston, Allen and Unwin, p. 139-154.

Jack, R.N., 1969, Quaternary sediments at Montara, San Mateo County, California: California University, Berkeley, M. A. thesis, 131 p.

Kennedy, G.L., Lajoie, K.R., Blunt, D.J., and Mathieson, S.A., 1981, Half Moon Bay terrace, California, and the age of its Pleistocene invertebrate faunas: Southern California Mallacologists Proceedings, 1981.

Lajoie, K.R., Ponti, D.P., Powell II, C.L., Mathieson, S.A., and Sarna-Wojcicki, A.M., 1991, Emergent marine strandlines and associated sediments, coastal California; a record of Quaternary sea-level fluctuations, vertical tectonic movements, climatic changes, and coastal processes, *in* Morrison, R.B., ed., Quaternary non-glacial geology: Conterminous U.S.: Boulder Colorado, Geological Society of America, The Geology of North America, v. K-2, p. 190-203.

FIGURE 1:

Map and profiles of the Half Moon Bay terrace showing the Half Moon Bay syncline and the Pillar Point dome (PP: Pillar Point). Amino-acid and molluscan faunal data correlate the Half Moon Bay terrace with either the 105 or 82ka sea-level highstands (Kennedy and others, 1981). A: Generalized structural contours on the buried wave-cut platform define the broad Half Moon Bay syncline and two minor anticlines northeast of the Seal Cove fault, and the narrow Pillar Point dome (actually half dome) southwest of the fault. Platform elevation data are from shallow bore holes and sea-cliff exposures. The contours defining the dome are projected over an area of deformed beds of the Pliocene Purisima Formation (Tp) exposed on the Holocene wave-cut platform. Note that stream channels deflect toward the axis of the syncline where they leave the hills and cross the warped Half Moon Bay terrace. B: Longitudinal profiles of the wave-cut platform of the Half Moon Bay terrace. The profile of the shoreline angle (solid line) delineates the broad syncline and two minor adjacent anticlines northeast of the fault. The concave upward profile (dashed line) delineates the intersection of the platform northeast of the fault with the projected vertical fault plain. The convex upward profile (dash-dot line) delineates the intersection of the platform southeast of the fault (Pillar Point dome) with the projected fault plain. Uplift is referenced to the 105 and 82ka sea-level highstands, 0m and -7m, respectively (Bloom and Yonekura, 1985). Because no piercing points can be identified neither local slip directions nor slip rates can be determined. See Figure 2 for cross-section A - A. Modified from Lajoie and others (1991).

FIGURE 2:

Cross-section A - A northeast of Half Moon Bay showing offset of the Half Moon Bay terrace across the right-lateral Seal Cove fault. The Pillar Point dome is defined by structural contours projected from the uplifted remnant of the terrace platform (PWCP) truncating the summit of Seal Cove bluff. The lateral extent of the dome is constrained by the extent of deformed Pliocene Purisima beds exposed in the Holocene platform (HWCP) (Jack, 1969). The maximum vertical separation of the platform across the fault is 49m, but because there are no definable piercing points, the actual vertical displacement is not known. Uplift is referenced to the 105 and 82ka sea-level highstands, 0m and -7m, respectively. See Figure 1 for location.

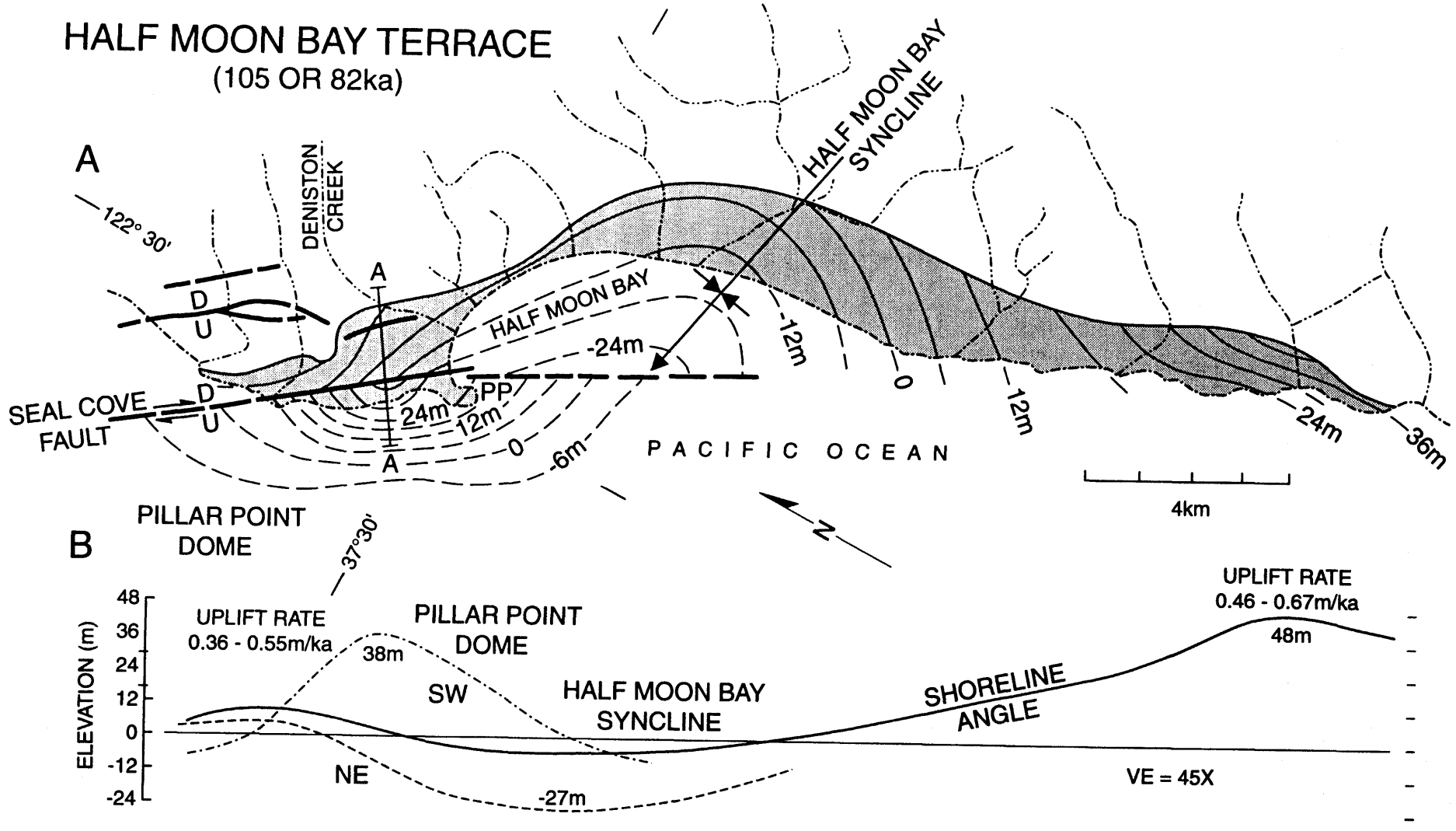
HALF MOON BAY TERRACE
(105 OR 82ka)
A
122° 30'
DENISTON CREEK
HALF MOON BAY SYNCLINE
HALF MOON BAY
-24m
-12m
0
12m
24m
36m
D
U
SEAL COVE FAULT
24m
12m
0
-6m
PP
PACIFIC OCEAN
4km
N
B
PILLAR POINT DOME
37°30'
UPLIFT RATE
0.36 - 0.55m/ka
38m
PILLAR POINT DOME
SW
HALF MOON BAY SYNCLINE
NE
-27m
SHORELINE ANGLE
UPLIFT RATE
0.46 - 0.67m/ka
48m
VE = 45X
ELEVATION (m)
48
36
24
12
0
-12
-24
HALF MOON BAY TERRACE
24m CONTOUR ON PLATFORM
FAULT
A A CROSS SECTION
PLATFORM PROFILES
SHORELINE ANGLE
NE NE SIDE FAULT
SW SW SIDE FAULT
HYDROLOGY
SHORELINE
STREAM

FIGURE 1

HALF MOON BAY TERRACE

(105 OR 82ka)

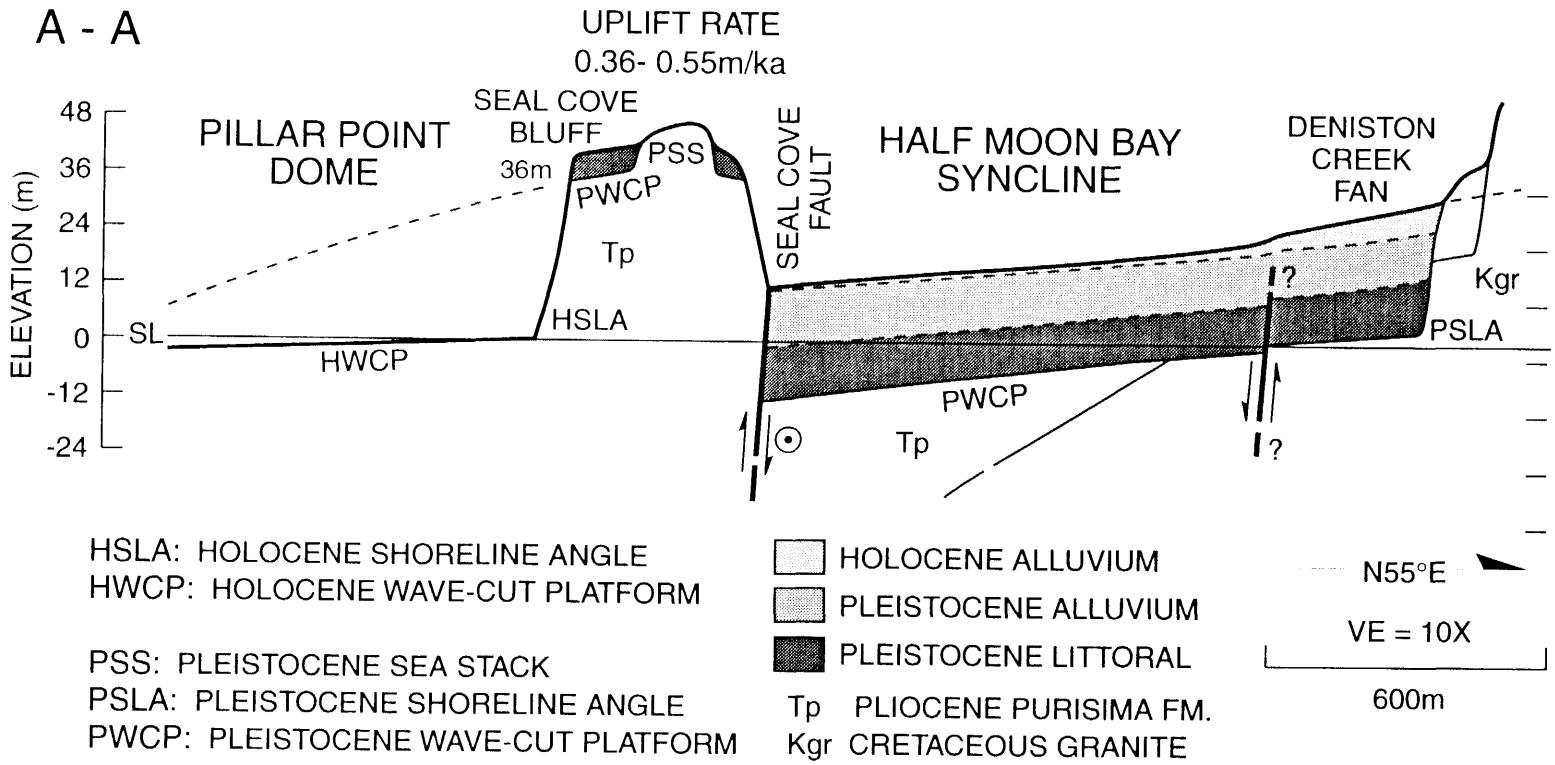

FIGURE 2

Northeast Santa Cruz Mountains Thrust/Fold Belt

K. R. Lajoie, U.S. Geological survey, MS-977, Menlo Park, California, 94025

The northeast Santa Cruz Mountains thrust/fold belt comprises the recently uplifted hilly to mountainous terrain northeast of the San Andreas fault (Figures 1 to 4) that extends from San Francisco in the northwest to the Pajaro River in the southeast. Structurally, the belt consists of numerous southwest-dipping high-angle reverse and thrust faults, and related folds that collectively form a complex hemi-antiform (Figures 7 to 11). The belt reflects northeast-southwest crustal shortening adjacent to the San Andreas fault, which in turn reflects minor plate convergence across the fault (Figure 2). Topographically, the belt divides into a foothill region with ridge crests below 300m and an upland region with ridge crests ranging from 700 to 1200m (Figures 5 and 6). The Monta Vista and Berrocal faults separate the regions, with precipitous relief across the faults.

BIBLIOGRAPHY

Bonilla, M.G., 1971, Preliminary geologic map of the San Francisco South quadrangle and part of the Hunters Point quadrangle, California: U.S. Geological Survey Miscellaneous Field Studies Map MF-311, scale 1:24,000.

Brabb, E.E., and Pampeyan, E.H., 1983, Geologic map of San Mateo County, California: U.S. Geological Survey Miscellaneous Investigations Series, I-1257-A, scale 1:62,500.

Burgmann, R., Arrowsmith, R., Dumitru, T., and McLaughlin, R.J., 1994, Rise and fall of the southern Santa Cruz Mountains, California, from fission tracks, geomorphology, and geodesy: Journal of Geophysical Research, 99, B10, p. 20,181-20,202.

Chin, J.L., Morrow, J.R., Ross, C.R., and Clifton, H.E., 1993, Geologic maps of upper Cenozoic deposits in central California: U.S. Geological Survey Miscellaneous Investigations Series I-1943, scale 1:250,000.

Clifton and Hunter, 1987, The Merced Formation and related beds: a mile-thick succession of late Cenozoic coastal and shelf deposits in the sea cliffs of San Francisco, California: Geological Society of America Centennial Field Guide-Cordilleran Section, p. 257-262.

Cummings, J.C., 1972, The Santa Clara Formation on the San Francisco peninsula, *in* Frizzell, Virgil, ed., Progress Report on the USGS Quaternary studies in the San Francisco Bay area: Friends of the Pleistocene Guidebook, Oct. 6-8, 1972, p. 3-10.

DeMets, C., Gordon, R.G., Argus, D.F., and Stein, S., 1990, Current plate motions: Geophysical Journal International, v. 101, p. 425-478.

Glen, 1959, Pliocene and Lower Pleistocene of the Western Part of the San Francisco peninsula: University of California publications in Geological Sciences, v. 36, no. 2, p. 147-198.

Hall, N.T., 1966, Late Cenozoic stratigraphy between Mussel Rock and Fleishacker Zoo, San Francisco Peninsula: California Division of Mines and Geology, Mineral Information Service, v. 19, no. 11, p. S22-S25.

Haugerud, R.A., and Ellen, S.D., 1990, Coseismic ground deformation along the northeast margin of the Santa Cruz Mountains, *in* Schwartz, D.P., and Ponti, D.J., eds. Field guide to neotectonics of the San Andreas fault system, Santa Cruz Mountains, in light of the Loma Prieta earthquake: U.S. Geological Survey, Open File Report 90-274, p. 32-37.

Hitchcock, C.S., Kelson, K.I., and Thompson, S.C., 1994, Geomorphic investigations of deformation along the northeastern margin of the Sant Cruz Mountains: U.S. Geological Survey Open File Report 94-187, 50 p.

Ingram, B.L., 1992, Paleoclimatic and paleoceonographic studies of estuarine and marine sediments using strontium isotopes: Stanford, Calif., Stanford University, Ph.D. dissertation, 236 p.

Jennings, C.W., 1994, Fault activity map of California and adjacent areas: California Division of Mines and Geology, Geologic Data Map No. 6, scale 1:75,000.

Kovach, R.L., and Page, B.M., 1995, Seismotectonics near Stanford University: California Geology, July/August, p. 91-98.

Lawson, A.C. chm., 1908, The California earthquake of April 18, 1906: Report of the State Earthquake Investigation Commission: Carnegie Institute of Washington Publication 87, v. 1, 451 p., atlas.

Lisowski, M., Savage, J. C., and Prescott, W. H., 1991, The velocity field along the San Andreas fault in central and southern California: Journal of Geophysical Research, v. 96, no. B5, p. 8369-8389.

McLaughlin, R.J., 1974, The Sargent-Berrocal fault zone and its relation to the San Andreas fault system in the southern San Francisco Bay region and Santa Clara Valley, California: U.S. Geological Survey Journal of Research, v. 2, no. 5, p. 593-598.

Page, B.M., Ingle, J.C., and Kovach, R.L., 1996, Quaternary diapir of claystone in faulted anticline, Stanford California: California Geology, May/June, p. 55-67.

Pampeyan, E.H., 1993, Geologic map of the Palo Alto and part of the Redwood Point 7-1/2' quadrangles, San Mateo and Santa Clara Counties, California: U.S. Geological Survey Miscellaneous Field Investigations I-2371, scale 1:24,000.

Pampeyan, E.H., 1994, Geologic map of the Montara Mountain and San Mateo 7-1/2' quadrangles, San Mateo County, California: U.S. Geological Survey Miscellaneous Field Investigations Map I-2390, scale 1:24,000.

Sarna-Wojcicki, A.M., 1976, Correlation of Late Cenozoic tuffs in the central coast ranges of California by means of trace- and minor-element chemistry: U.S. Geological Survey Professional Paper 972.

Sarna-Wojcicki, A.M., Meyer, C.E., Bowman, H.R., Hall, N.T., Russell, P.C., Woodward, M.J., and Slates, J.L., 1985, Correlation of the Rockland ash bed, a 400,00-year-old stratigraphic marker in northern California and western Nevada, and implications for middle Pleistocene paleogeography of central California: Quaternary Research, 23, p. 236-257.

Smith, D.D., 1960, The geomorphology of part of the San Francisco Peninsula, California: Stanford, Calif., Stanford University, Ph.D. dissertation, 365 p.

FIGURE 1

Structurally, the northeast Santa Cruz Mountains thrust/fold belt comprises a series of southwest-dipping high-angle reverse and thrust faults that deform sediments ranging in age from Mesozoic to Holocene. The Monta Vista (MV) and Berrocal (BE) faults separate the foothill region from the upland region (Figures 5 and 6), with precipitous relief across the faults. For example, the elevation near Felt Lake (FL) is 250m, while just 9km to the southeast it is 850m at Black Mountain (BM). Locally, the Serra (SE) and Monta Vista (MV) faults appear to define a structural boundary between foothill region and the alluvial plain to the northeast. However, other thrust faults buried beneath the Pleistocene to Holocene basin sediments probably lie to the northeast of this apparent boundary. Possible evidence for a buried thrust beneath the alluvium is the Stock Farm Monocline trending northwestward across a Pleistocene fan surface on the Stanford campus in Palo Alto (Figure 10) (Kovach and Page, 1995). Other examples are the zones of surface lineations, stream-terrace convexities and topographic scarps trending northwestward across the Los Gatos embayment (Hitchcock and others, 1994; J. Coakley, 1996, personal communication). Locally, the Serra (SE) and Monta Vista (MV) faults overthrust and deform late Pleistocene and possibly Holocene sediments (Smith, 1960; Bonilla, 1971; McLaughlin, 1974; Pampeyan, 1993, 1994; Hitchcock and others, 1994). Displacement across all the faults in the thrust/fold belt is probably right oblique, not pure thrust. Ground-surface deformation occurred between the Monta Vista and Berrocal faults during the 1906 San Francisco Earthquake (Lawson, 1914), and along the same and related faults during the 1989 Loma Prieta earthquake (Haugerud and Ellen, 1990). Scattered micro-seismicity , some with oblique solutions, persists throughout the thrust/fold belt (M. L. Zoback, 1996, personal communication; Kovach and Page (1995) (Figure 10). Folds involving Mesozoic to late Pleistocene sedimentary rocks are associated with most of the high-angle reverse and thrust faults shown here, and some of the faults originate in sheared folds. Fault data generalized from Bonilla (1971), McLaughlin (1974), Chin and others (1993), Pampeyan (1993, 1994), Hitchcock and others (1994) and Kovach and Page (1995). See Figures 7 to 11 for cross sections A - A to E - E.

FIGURE 2

Map of the northeast Santa Cruz Mountains thrust/fold belt showing North American-Pacific plate convergence across the San Andreas fault. The NUVEL-1 model predicts that the tangent to the circle of rotation between these plates strikes about N34° W in the San Francisco Bay region (DeMets and others, 1990). The predicted right-lateral relative plate motion is 48mm/a, with about 17mm/a concentrated on the San Andreas fault (Lisowski and others, 1991). At Daly City, the San Andreas strikes N35° W, yielding a plate convergence angle of 1° and a convergence rate of 0.3mm/a normal to the Nuvel-1 plate boundary. Near Loma Prieta, the fault strikes N52° W, yielding a convergence angle of 18° and a convergence rate of 5.5mm/a. The height and width of the thrust belt increases to the southeast as the convergence angle increases (Figures 5 and 6). If the bend in the San Andreas formed when the Coast Ranges began to rise about 3.5 million years ago, the total crustal shortening across the thrust/fold belt has been about 10km normal plate boundary near Loma Prieta. There the belt is 19km wide, indicating about 30% crustal shortening between Coyote and the San Andreas fault. However, summation of crustal shortening across the thrust faults themselves yields an estimate of 5km (R. McLaughlin, 1996, written communication). The 5km difference in these estimates might indicate that the bend has evolved through time.

FIGURE 3

Map of the northeast Santa Cruz Mountains thrust/fold belt showing crest elevations and uplift rates. The crest of the foothills region lies below 300m, while the crest of the uplands region lies between 700 and 1200m. These elevations, which inrease nonlinearly to the southeast as the plate-convergence angle increases (Figures 2, 5 and 6), most likely reflect relative long term uplift rates. The Colma terrace (CT), here tentatively correlated with the 124ka sea-level highstand (6m), crops out at 26m in the modern sea cliff at Daly City (Hall, 1966; Bonilla, 1971). The elevation and assumed age of this terrace yield an uplift rate of 0.16m/ka. If instead, the Colma terrace correlates with either the 105ka (0m) or 82ka (-7m) highstand, the uplift rate would be 0.40 or 0.25m/ka, respectively. The Rockland ash (RA), dated at 400ka (Sarna-Wojcicki and others, 1985), crops out at 150m in the upper part of the shallow-marine Merced Formation at Daly City (M. Bonilla, 1994, personal comunication), and at 180m in the Woodside facies of the alluvial (?) Santa Clara Formation in Woodside (Cummings, 1972; Sarna-Wojcicki,1976). At both localities, the beds containing the ash are tilted and erosionally truncated, indicating that the outcrop elevations represent minimal uplift. Assuming the ash was deposited near present sea level, the uplift rates would be $\geq$ 0.38m/ka at Daly City and $\geq$ 0.45m/ka at Woodside. Six sedimentary apatite samples from a transect near Loma Prieta yield fission track ages averaging 4.6Ma (Bü rgmann and others, 1994). This age dates the time of crustal cooling below 110° C and suggests that about 3km of unroofing has occurred in the upland region over the last 4.6ka. Allowing for the present elevation of about 1km, these data suggest a long-term uplift rate of 0.87m/ka.

FIGURE 4

Map of the northeast Sant Cruz Mountains thrust/fold belt showing its regional structural axes. Both topographically and structurally, the Santa Cruz Mountains form an elongate, doubly plunging antiform that reflects compressional uplift at the broad left bend in the San Andreas fault. The San Andreas asymmetrically bisects the antiform along its major axis, producing two hemi-antiforms, the thrust belt to the northeast and the tilted block to the southwest. The axes of these structures lie along the zones of maximum uplift adjacent to the fault, and their minor axes plunge away from it. The uplifted thrust/fold belt is the most conspicuous element of the general, northeastward tilted San Francisco Bay block between the San Andreas and Hayward faults. The northeastward tilt of this block produced the the asymmetrical basin now partly flooded by San Francisco Bay.

FIGURE 5

Elevations of selected sites along the crest of the northeast Santa Cruz Mountains thrust/fold belt plotted as a function of distance from the coastline at Daly City (•); the projection plain lies along the NUVEL-1 plate boundary, trending N34° W. In the foothill region the crest lies below 300m, while in the upland region it lies between 700 and 1200m. The precipitous scarp separating the foothill and upland regions between Felt Lake (FL, 250m) and Black Mountain (BM, 850m) reflects the vertical component of displacement on the Berrocal and Monta Vista faults, shown here diagramatically. Also plotted is the width of the thrust belt as a function distance from the coastline (Δ). In general, both the elevation and width of the belt increase to the southeast, as the convergence angle between the North American and Pacific plates increases along the eastward bend in the San Andreas fault. These trends are not linear because NE-SW crustal shortening

represented by the belt occurs mainly along discrete failure surfaces, not as plastic deformation. See Figures 1 through 4 for site localities.

FIGURE 6

Elevations of selected sites along the crest of the northeast Santa Cruz Mountains thrust/fold belt plotted as a function of the convergence angle between the North American and Pacific plates across the San Andreas fault (•); the projection plain lies along the NUVEL-1 plate boundary, trending N34° W. In the foothill region the crest lies below 300m, while in the upland region it lies between 700 and 1200m. The precipitous scarp separating the foothill and upland regions between Felt Lake (FL. 250m) and Black Mountain (BM, 850m) reflects the vertical component of displacement on the Berrocal and Monta Vista faults, shown here diagramatically. Also plotted is the width of the thrust belt as a function distance from the coastline (Δ). In general, both the elevation and width of the thrust belt increase to the southeast as the convergence angle increases along the eastward bend in the San Andreas fault. These trends are not linear because the NE-SW crustal shortening represented by the thrust belt occurs mainly along discrete failure surfaces, not as plastic deformation. See Figures 1 through4 for site localities.

FIGURE 7

Cross section A - A at Daly City (Figure 1). A virtually uninterrupted, 1800m section of the predominantly shallow-marine Plio-Pleistocene Merced Formation crops out in the modern sea cliff in this area (Glen, 1959; Hall, 1966; Clifton and Hunter, 1989). Strontium-isotope data date the Merced at 3.2 to 0.2Ma (Ingram, 1992). The Rockland ash, in the upper part of the Merced, is dated at 400ka (Sarna-Wojcicki and others, 1985). This ash crops out at an elevation of 150m in Daly City (M. Bonilla, 1994, personal communication). Assuming the ash was deposited near present sea level, the minimum uplift rate at that site is 0.38m/ka.

FIGURE 8

Cross section B - B at San Bruno (Figure 1), showing rocks of the Mesozoic Franciscan Formation (KJf) thrust northeast over the late Pleistocene Colma Formation along the Serra fault (Bonilla, 1971). The Colma Formation and terrace are here tentatively correlated with the 124ka sea-level highstand. The erosional Buri Buri surface forms an irregular summit plateau along the crest of Buri Buri ridge, the local topographic manifestation of the northeast Santa Cruz Mountains thrust/fold belt. The Buri Buri surface extends as far south as Palo Alto (Smith, 1960), and possibly as far south as Coyote, along the crest of the foothills region. The age of the Buri Buri surface is not known, but its northernmost remnant truncates beds of the Merced Formation that might be as young as 400ka.

FIGURE 9

Cross section C - C in Burlingame, southeast of Daly City (Figure 1), showing rocks of the Mesozoic Franciscan Formation (KJf) thrust northeast over sediments of the Plio-Pleistocene Merced Formation along the Serra and related faults (Smith, 1960; Pampeyan, 1994). This section clearly illustrates the complex thrust faulting that accomodates the NE-SW crustal shortening accross the northeast Santa Cruz Mountains thrust/fold belt. Southeast of the San Andreas fault, the crest of the Santa Cruz Mountains rises to 500m, which illustrates the sharp topgraphic and structural contrast across the fault.

FIGURE 10

Cross section D - D through Palo Alto (Figure 1) showing the close relationship between the high-angle reverse

and thrust faults, and the folds in the northeast Santa Cruz Mountains thrust/fold belt. Sedimentary rocks involved in the deformation range in age from Mesozoic to late Pleistocene, and possibly Holocene. Some of the microseismis in this area show oblique ruptures (black dots). The southwestward dipping zone of microseismicity extends to a depth of eight kilometers. Modified from Kovach and Page (1995).

FIGURE 11

Cross section E - E through Loma Prieta (Figure 1), showing the complex faults that comprise the northeast Santa Cruz Mountains thrust/fold belt. At this locality, the vertical component of displacement on the Berrocal fault produced the steep scarp separating the foothill and upland regions. It is possible, as shown here, that not all the thrust faults merge with the San Andreas at depth. Six sedimentary apatite samples yield fission track ages averaging 4.6Ma (Bü rgmann and others, 1994). This age dates the time of crustal cooling below 110° C and suggests that about 3km of unroofing has occurred in the upland region over the last 4.6ka. Allowing for the present elevation of about 1km, these data suggest a long-term uplift rate of 0.87m/ka. Modified from Bü rgmann and others (1994).

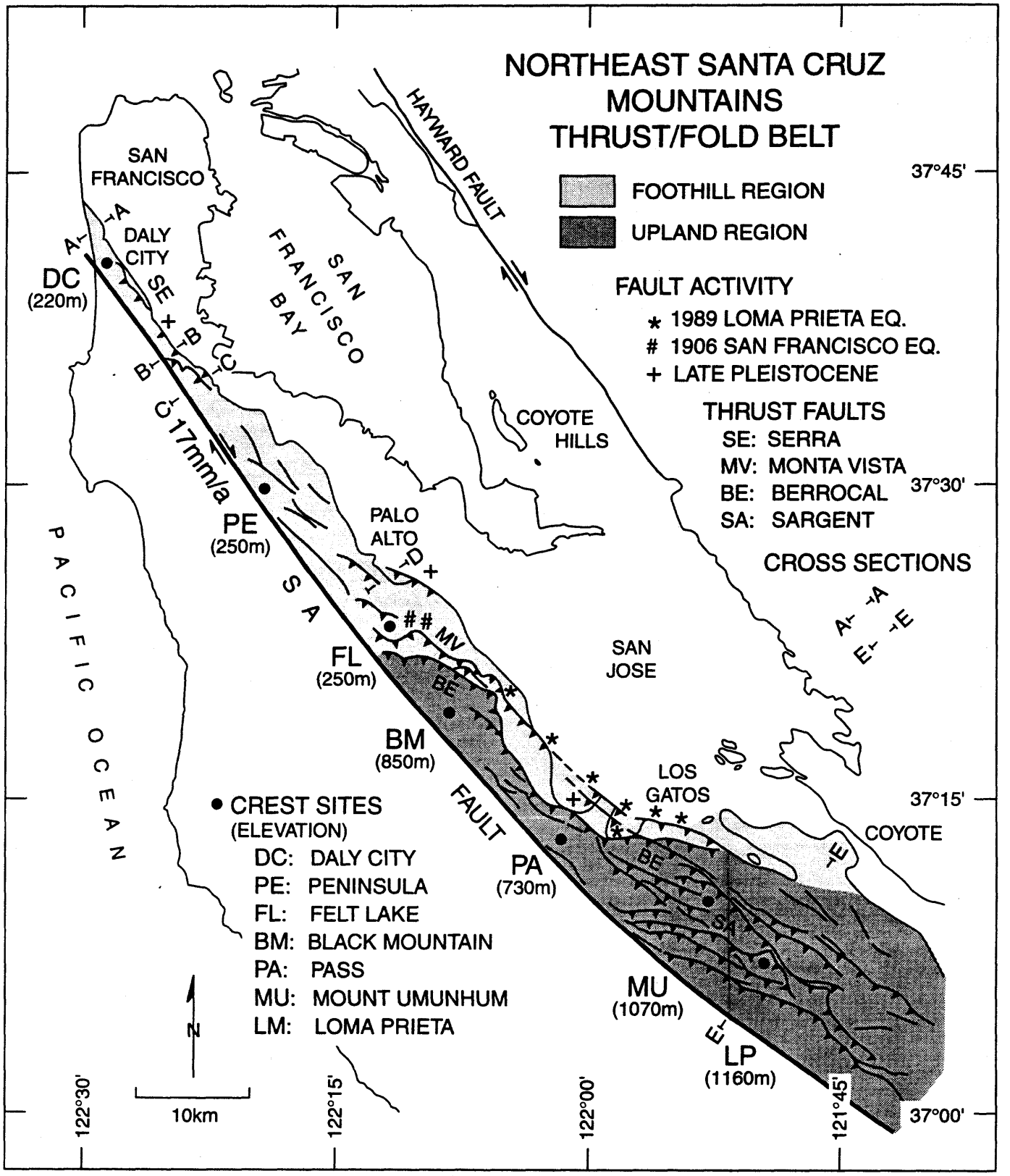
NORTHEAST SANTA CRUZ MOUNTAINS THRUST/FOLD BELT
FOOTHILL REGION
UPLAND REGION
FAULT ACTIVITY
* 1989 LOMA PRIETA EQ.
# 1906 SAN FRANCISCO EQ.
+ LATE PLEISTOCENE
THRUST FAULTS
SE: SERRA
MV: MONTA VISTA
BE: BERROCAL
SA: SARGENT
CROSS SECTIONS
SAN FRANCISCO
DALY CITY
DC (220m)
SAN FRANCISCO BAY
HAYWARD FAULT
COYOTE HILLS
17mm/a
PE (250m)
PALO ALTO
PACIFIC OCEAN
FL (250m)
BM (850m)
SAN JOSE
LOS GATOS
COYOTE
PA (730m)
MU (1070m)
LP (1160m)
SAN ANDREAS FAULT
CREST SITES (ELEVATION)
DC: DALY CITY
PE: PENINSULA
FL: FELT LAKE
BM: BLACK MOUNTAIN
PA: PASS
MU: MOUNT UMUNHUM
LM: LOMA PRIETA
N
10km
37°45'
37°30'
37°15'
37°00'
122°30'
122°15'
122°00'
121°45'

FIGURE 1

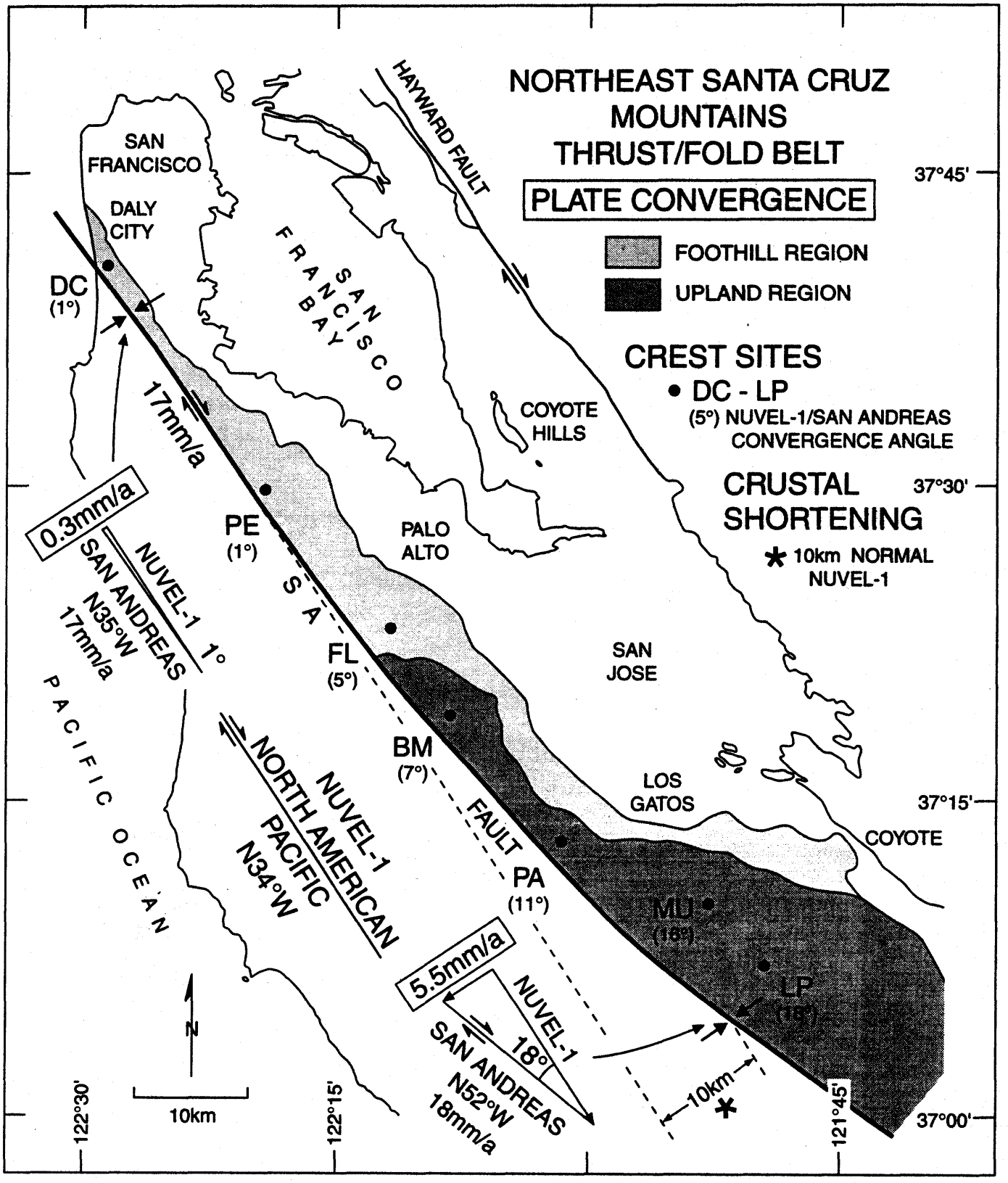
NORTHEAST SANTA CRUZ MOUNTAINS THRUST/FOLD BELT
PLATE CONVERGENCE
FOOTHILL REGION
UPLAND REGION
CREST SITES
• DC - LP
(5°) NUVEL-1/SAN ANDREAS CONVERGENCE ANGLE
CRUSTAL SHORTENING
✱ 10km NORMAL NUVEL-1
HAYWARD FAULT
SAN FRANCISCO
DALY CITY
SAN FRANCISCO BAY
COYOTE HILLS
PALO ALTO
SAN JOSE
LOS GATOS
COYOTE
DC (1°)
PE (1°)
FL (5°)
BM (7°)
PA (11°)
MU (16°)
LP (18°)
17mm/a
0.3mm/a
SAN ANDREAS N35°W 17mm/a
NUVEL-1 1°
NUVEL-1 NORTH AMERICAN PACIFIC N34°W
FAULT
5.5mm/a
NUVEL-1 18°
SAN ANDREAS N52°W 18mm/a
PACIFIC OCEAN
N
10km
10km
37°45'
37°30'
37°15'
37°00'
122°30'
122°15'
121°45'

FIGURE 2

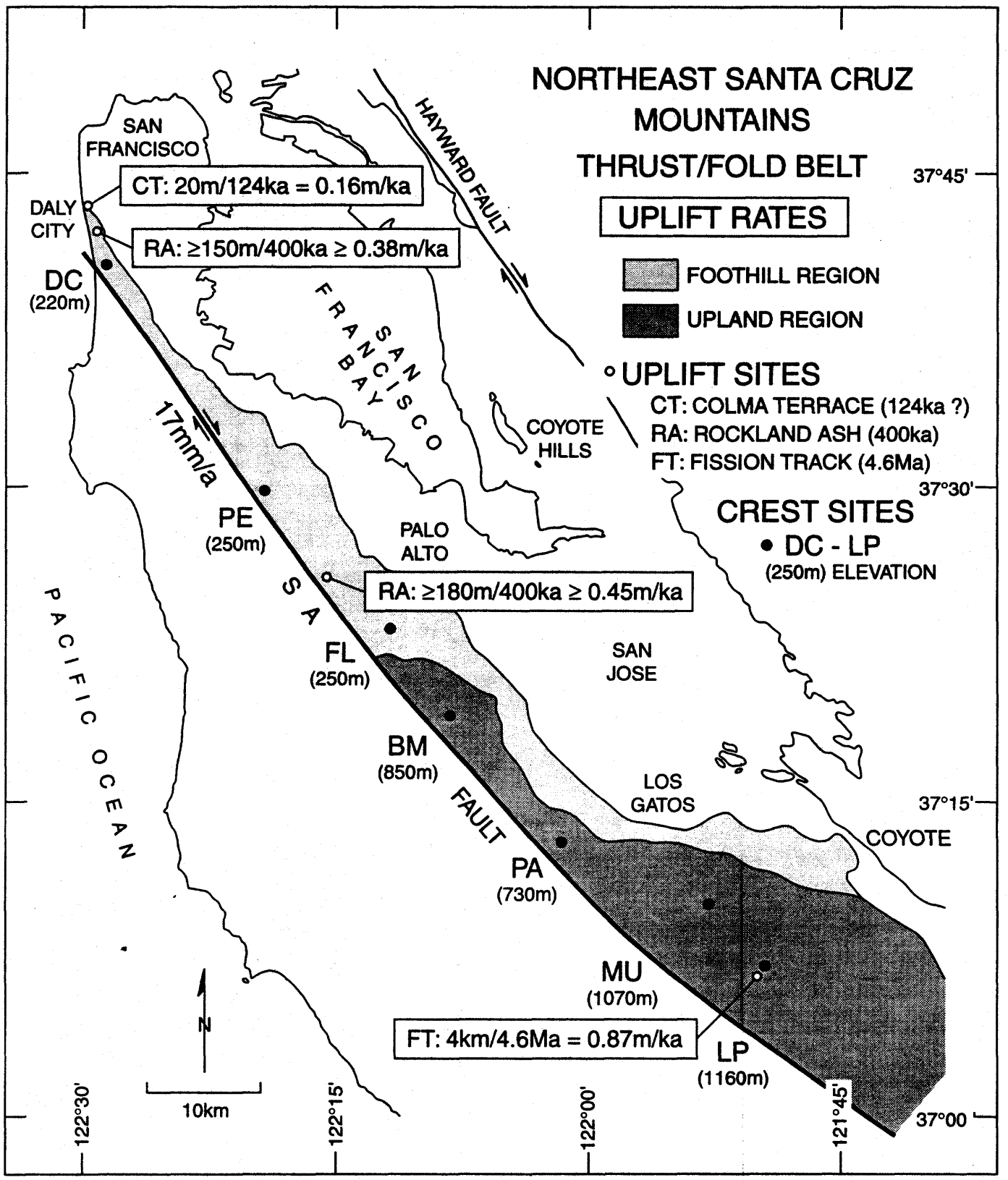
NORTHEAST SANTA CRUZ MOUNTAINS THRUST/FOLD BELT
UPLIFT RATES
FOOTHILL REGION
UPLAND REGION
UPLIFT SITES
CT: COLMA TERRACE (124ka ?)
RA: ROCKLAND ASH (400ka)
FT: FISSION TRACK (4.6Ma)
CREST SITES
• DC - LP
(250m) ELEVATION
CT: 20m/124ka = 0.16m/ka
RA: ≥150m/400ka ≥ 0.38m/ka
RA: ≥180m/400ka ≥ 0.45m/ka
FT: 4km/4.6Ma = 0.87m/ka
SAN FRANCISCO
DALY CITY
DC (220m)
HAYWARD FAULT
SAN FRANCISCO BAY
COYOTE HILLS
17mm/a
PE (250m)
PALO ALTO
SAN JOSE
FL (250m)
BM (850m)
LOS GATOS
COYOTE
PA (730m)
MU (1070m)
LP (1160m)
SAF
FAULT
PACIFIC OCEAN
N
10km
37°45'
37°30'
37°15'
37°00
122°30'
122°15'
122°00'
121°45'

FIGURE 3

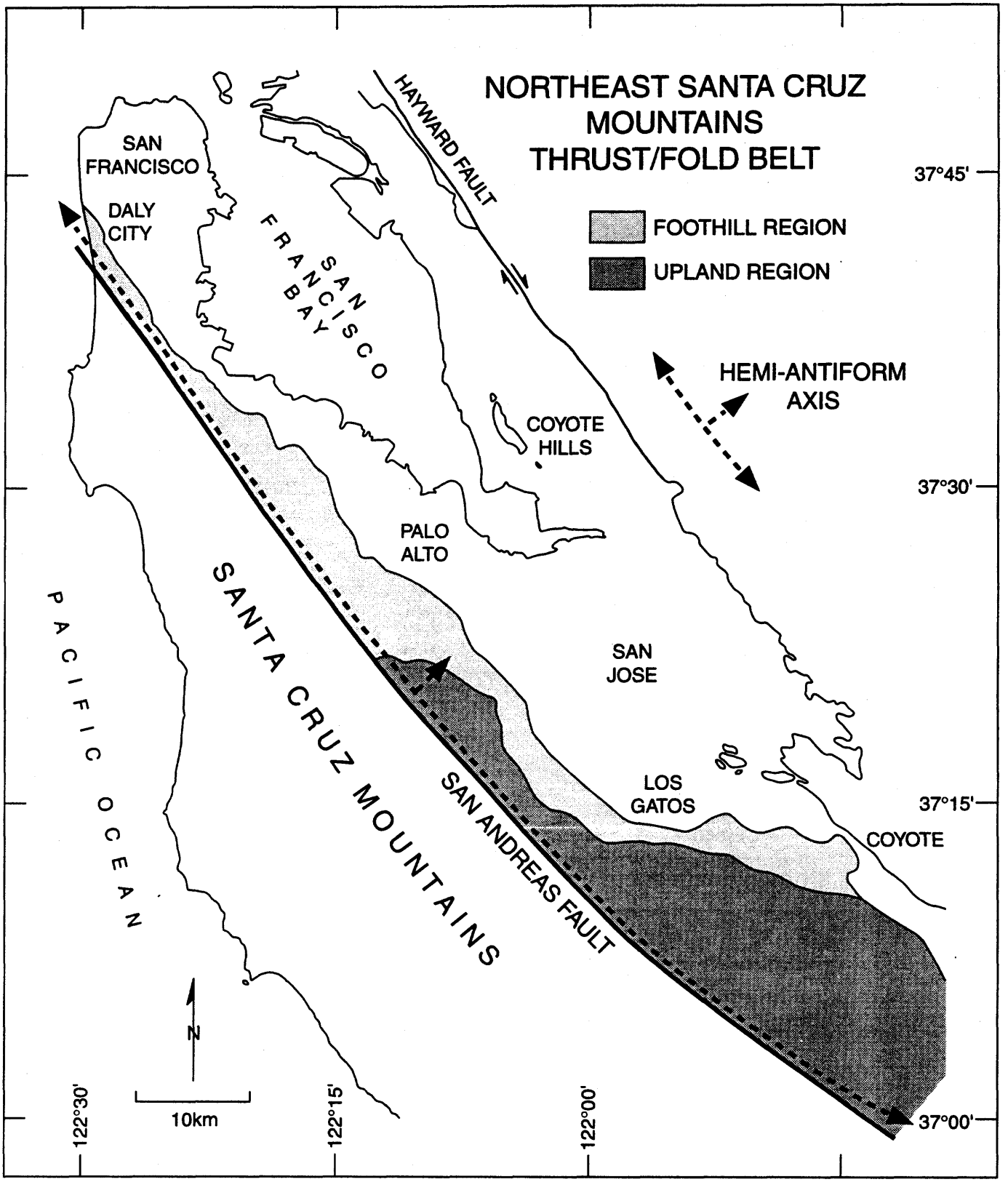
NORTHEAST SANTA CRUZ MOUNTAINS THRUST/FOLD BELT
HAYWARD FAULT
FOOTHILL REGION
UPLAND REGION
HEMI-ANTIFORM AXIS
SAN FRANCISCO
DALY CITY
SAN FRANCISCO BAY
COYOTE HILLS
PALO ALTO
SAN JOSE
LOS GATOS
COYOTE
SANTA CRUZ MOUNTAINS
SAN ANDREAS FAULT
PACIFIC OCEAN
N
10km
37°45'
37°30'
37°15'
37°00'
122°30'
122°15'
122°00'

FIGURE 4

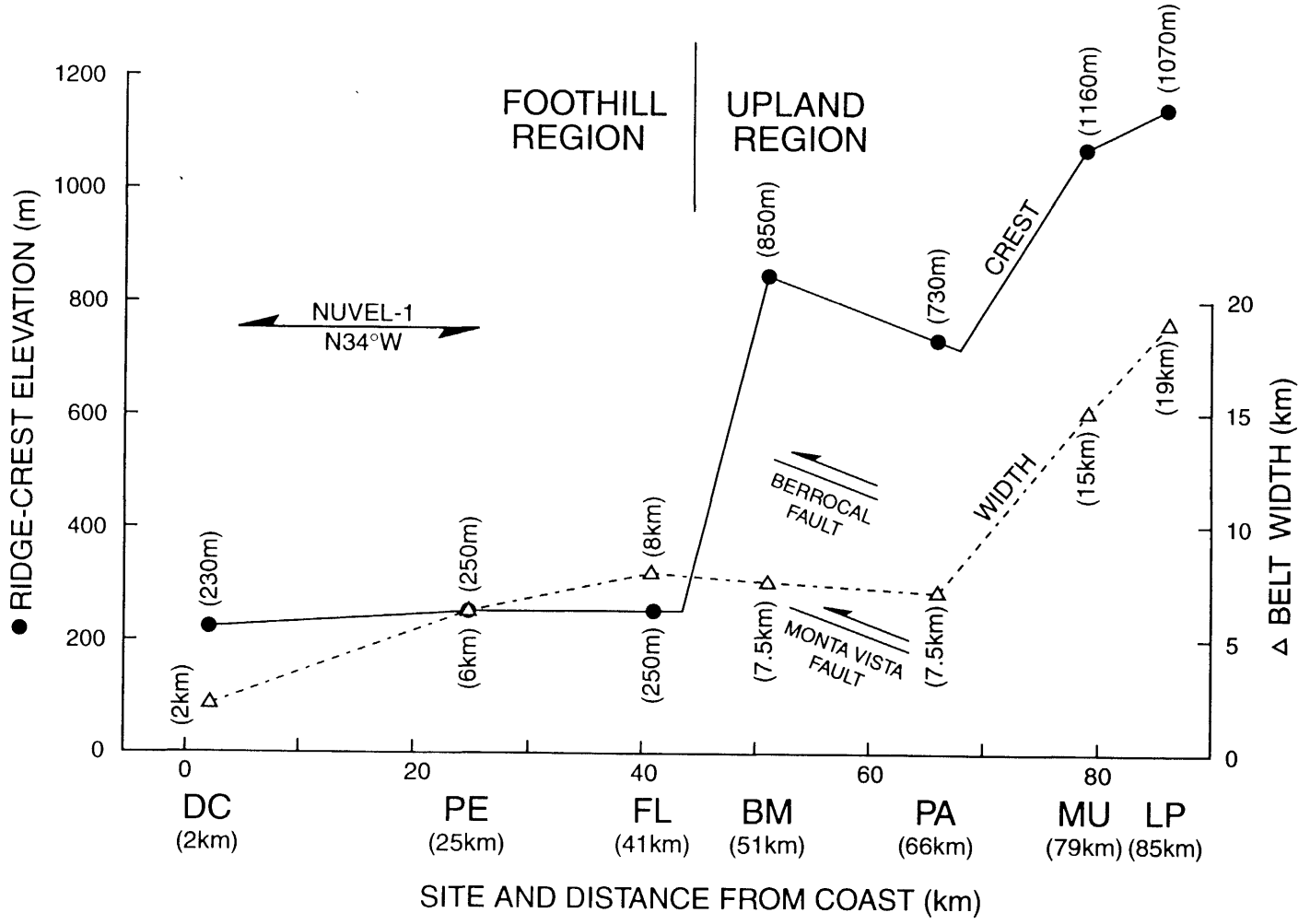
FOOTHILL REGION
UPLAND REGION
NUVEL-1
N34°W
BERROCAL FAULT
MONTA VISTA FAULT
CREST
WIDTH
(230m)
(250m)
(850m)
(730m)
(1160m)
(1070m)
(2km)
(6km)
(8km)
(250m)
(7.5km)
(7.5km)
(15km)
(19km)
● RIDGE-CREST ELEVATION (m)
△ BELT WIDTH (km)
0
200
400
600
800
1000
1200
0
5
10
15
20
0
20
40
60
80
DC (2km)
PE (25km)
FL (41km)
BM (51km)
PA (66km)
MU (79km)
LP (85km)
SITE AND DISTANCE FROM COAST (km)

FIGURE 5

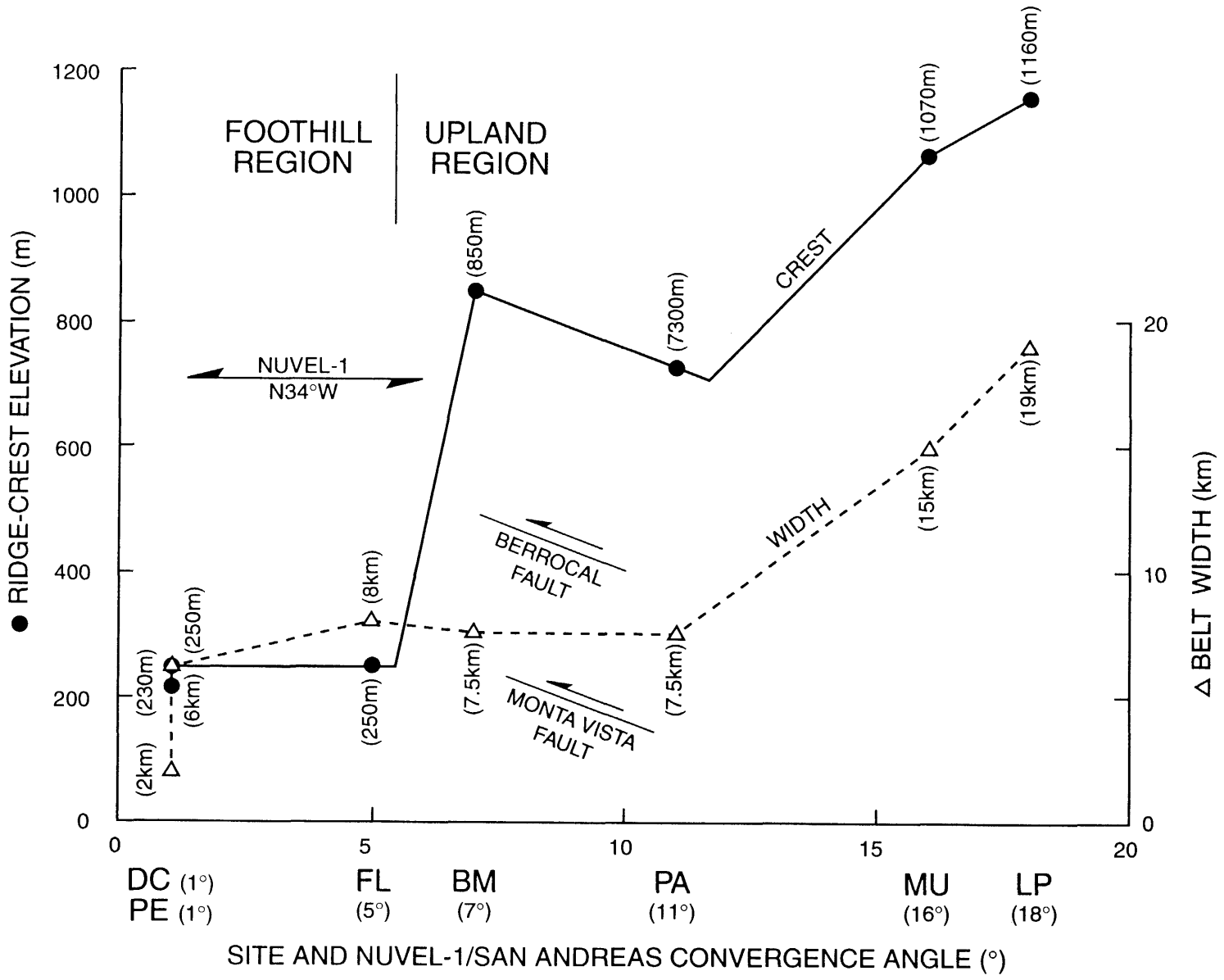
FOOTHILL REGION
UPLAND REGION
NUVEL-1
N34°W
CREST
WIDTH
BERROCAL FAULT
MONTA VISTA FAULT
(1160m)
(1070m)
(850m)
(7300m)
(250m)
(230m)
(2km)
(6km)
(8km)
(250m)
(7.5km)
(7.5km)
(15km)
(19km)
● RIDGE-CREST ELEVATION (m)
△ BELT WIDTH (km)
1200
1000
800
600
400
200
0
20
10
0
0
5
10
15
20
DC (1°)
PE (1°)
FL (5°)
BM (7°)
PA (11°)
MU (16°)
LP (18°)
SITE AND NUVEL-1/SAN ANDREAS CONVERGENCE ANGLE (°)

FIGURE 6

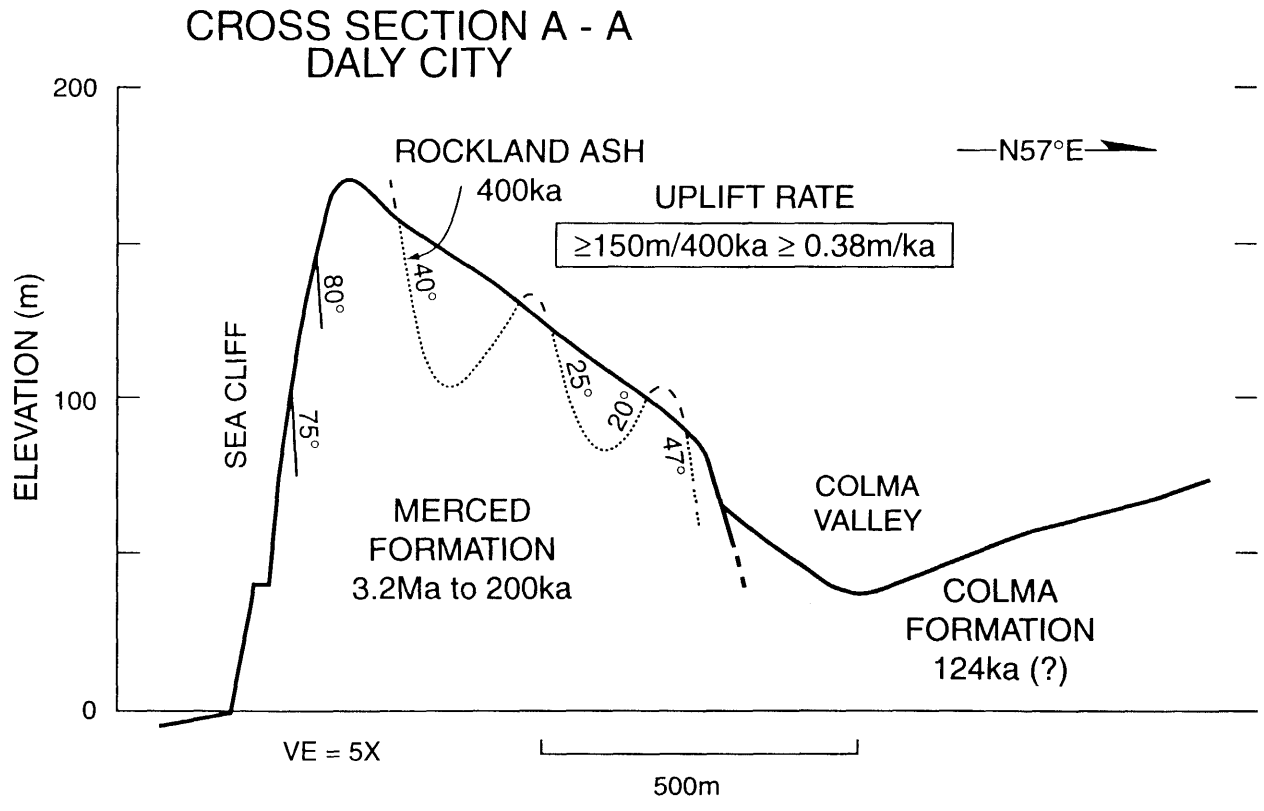
CROSS SECTION A - A
DALY CITY
200
100
0
ELEVATION (m)
ROCKLAND ASH
400ka
N57°E
UPLIFT RATE
≥150m/400ka ≥ 0.38m/ka
80°
40°
75°
25°
20°
47°
SEA CLIFF
MERCED
FORMATION
3.2Ma to 200ka
COLMA
VALLEY
COLMA
FORMATION
124ka (?)
VE = 5X
500m

FIGURE 7

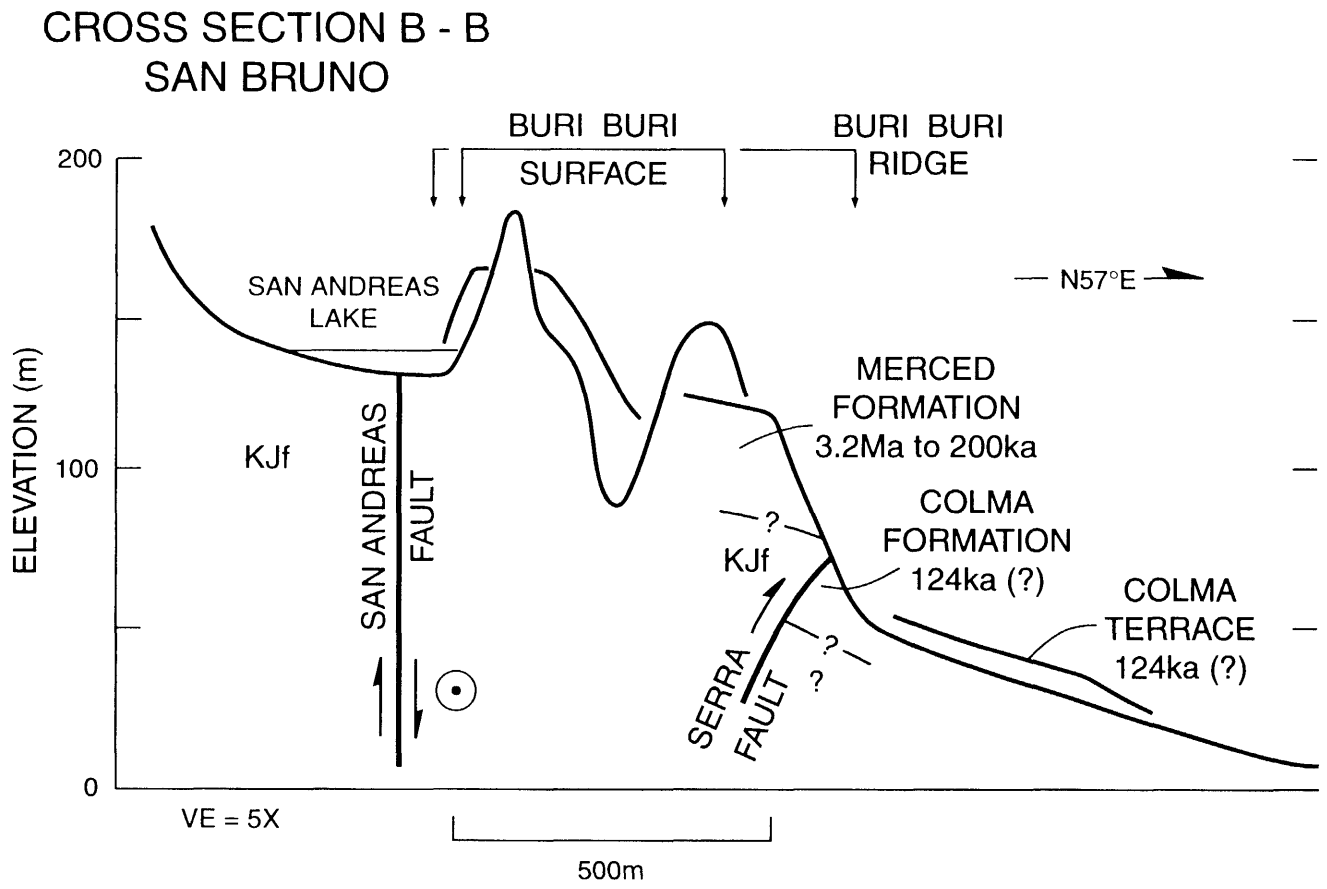
CROSS SECTION B - B
SAN BRUNO
BURI BURI
SURFACE
BURI BURI
RIDGE
200
100
0
ELEVATION (m)
SAN ANDREAS
LAKE
N57°E
KJf
SAN ANDREAS
FAULT
MERCED
FORMATION
3.2Ma to 200ka
COLMA
FORMATION
124ka (?)
KJf
SERRA
FAULT
COLMA
TERRACE
124ka (?)
VE = 5X
500m

FIGURE 8

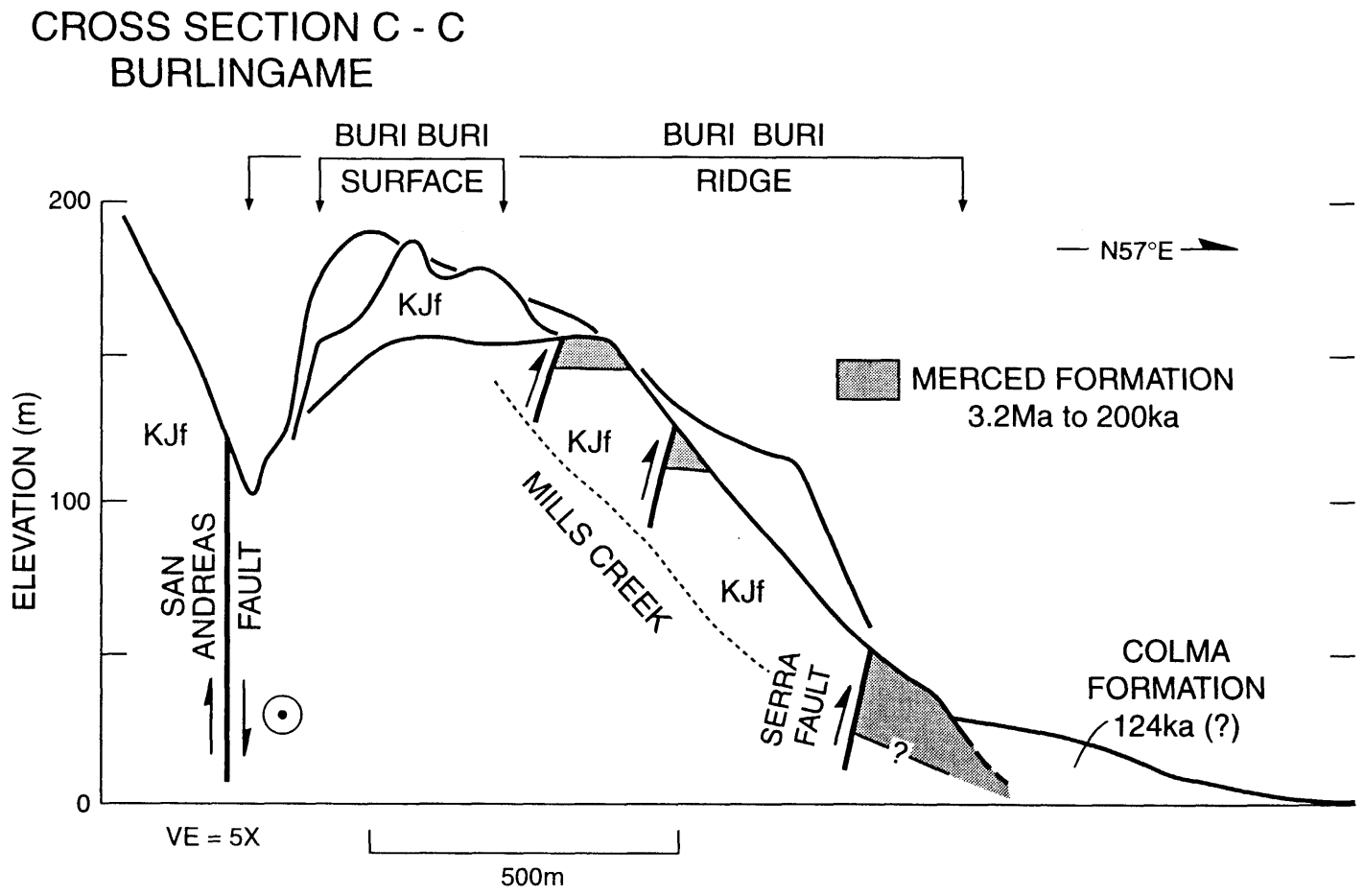
CROSS SECTION C - C
BURLINGAME
BURI BURI
SURFACE
BURI BURI
RIDGE
200
100
0
ELEVATION (m)
N57°E
KJf
KJf
KJf
KJf
MERCED FORMATION
3.2Ma to 200ka
SAN ANDREAS FAULT
MILLS CREEK
SERRA FAULT
?
COLMA FORMATION
124ka (?)
VE = 5X
500m

FIGURE 9

CROSS SECTION D - D
PALO ALTO

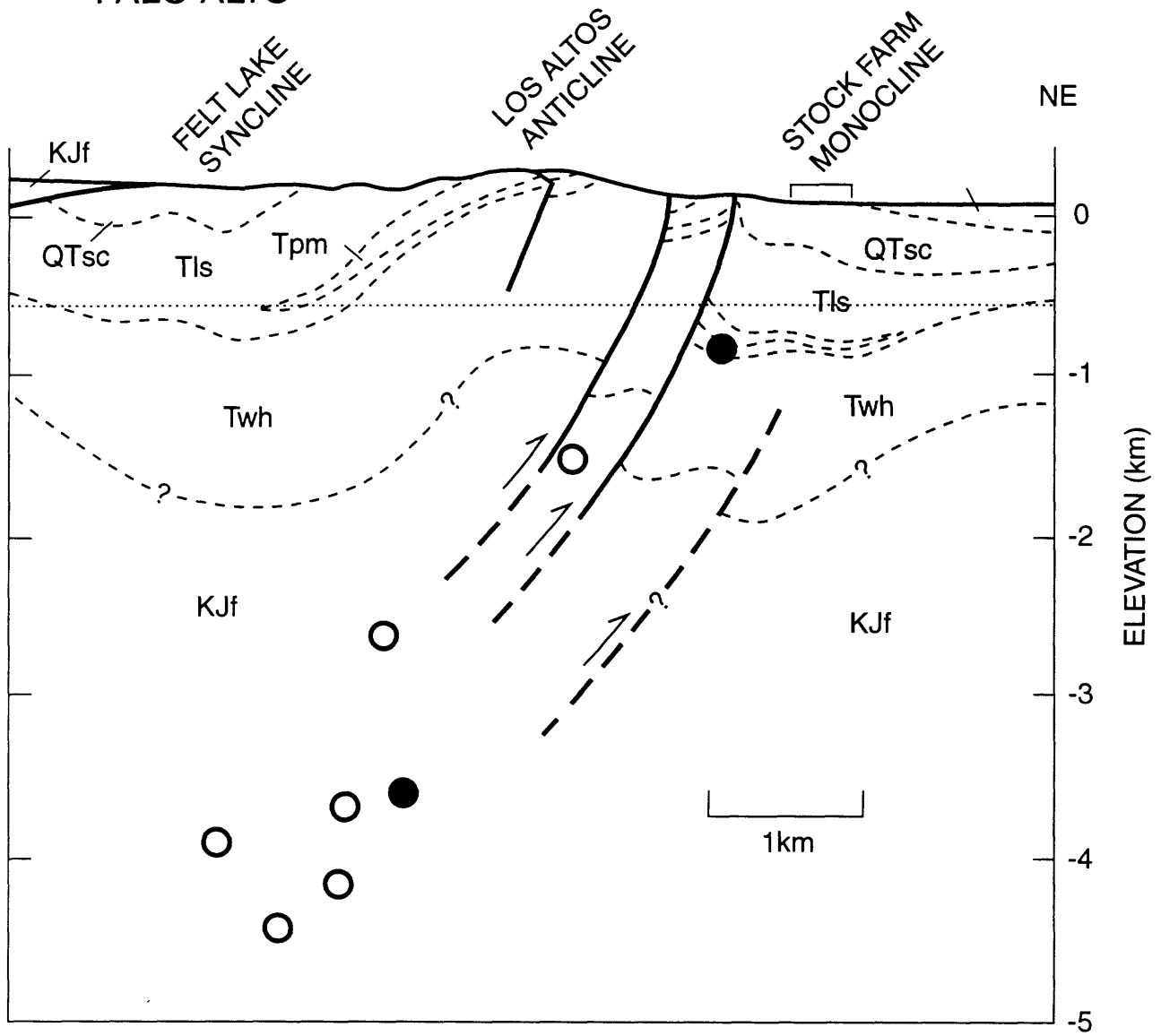

Qal	ALLUVIUM (QUATERNARY)
QTsc	SANTA CLARA FM. (PLIO-PLEISTOCENE)
Tls	LADERA FM. (MIOCENE)
Tpm	PAGE MILL BASALT (MIOCENE)
Twh	WHISKEY HILL FM. (EOCENE)
KJf	FRANCISCAN FM. (MESOZOIC)

○ HYPOCENTER
● HYPOCENTER WITH OBLIQUE COMPONENT

FIGURE 10

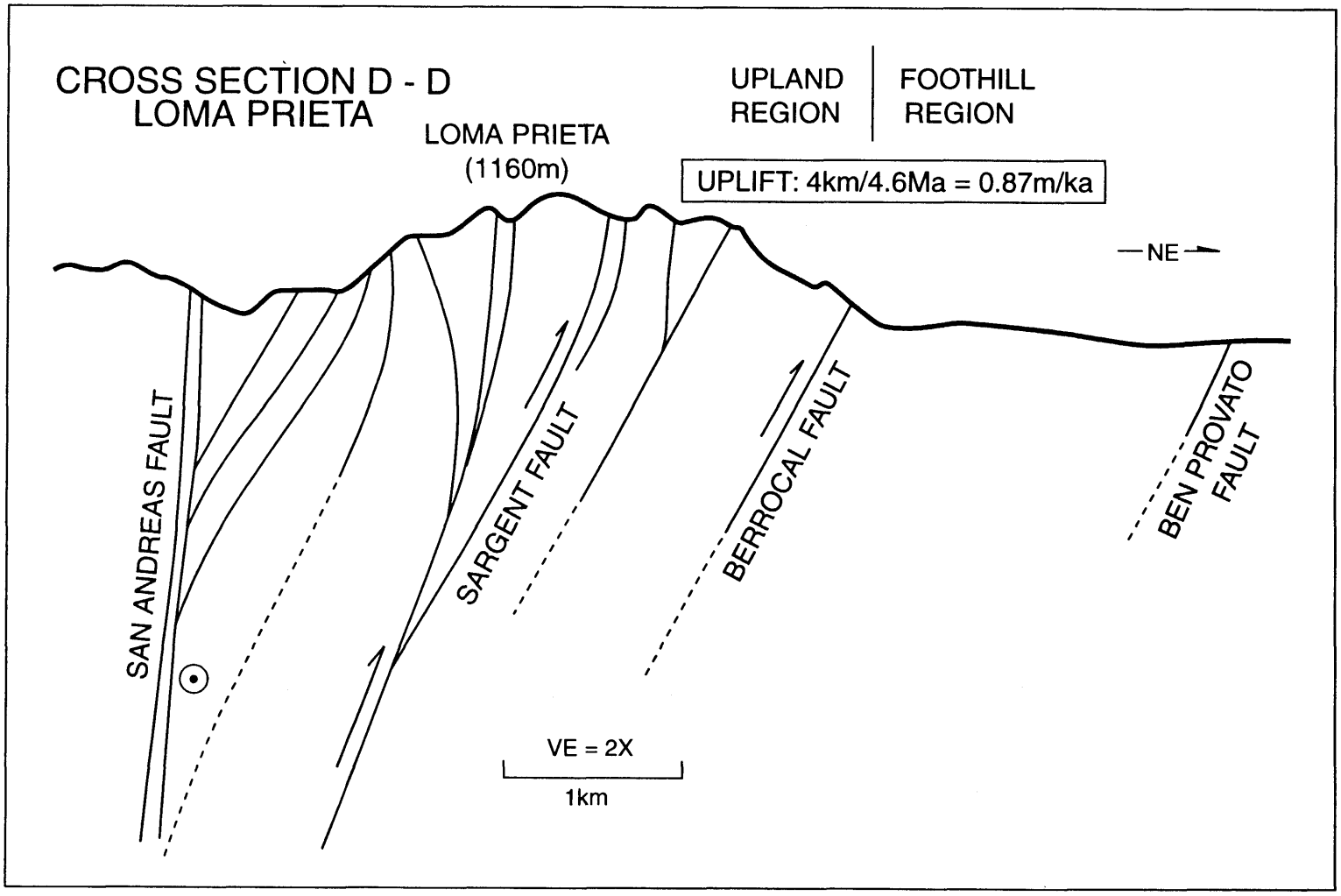
CROSS SECTION D - D
LOMA PRIETA
UPLAND REGION
FOOTHILL REGION
LOMA PRIETA
(1160m)
UPLIFT: 4km/4.6Ma = 0.87m/ka
NE
SAN ANDREAS FAULT
SARGENT FAULT
BERROCAL FAULT
BEN PROVATO FAULT
VE = 2X
1km

FIGURE 11

Lajoie, Half Moon Bay area

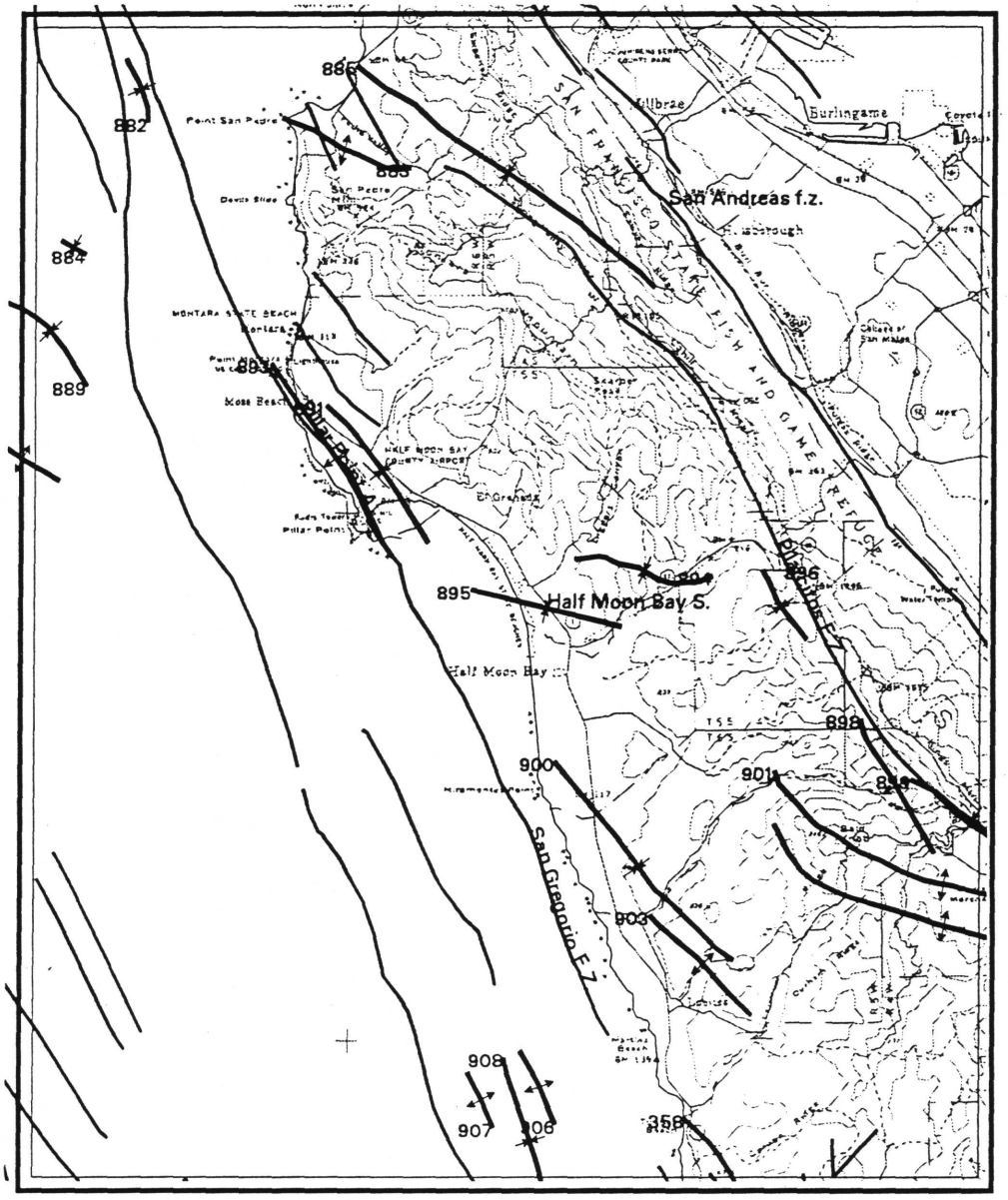

SCALE 1:200000

SAN FRANCISCO BAY REGION

Estimates of the amount of vertical displacement rates from various Quaternary datums, (mm/yr), K.R. Lajoie

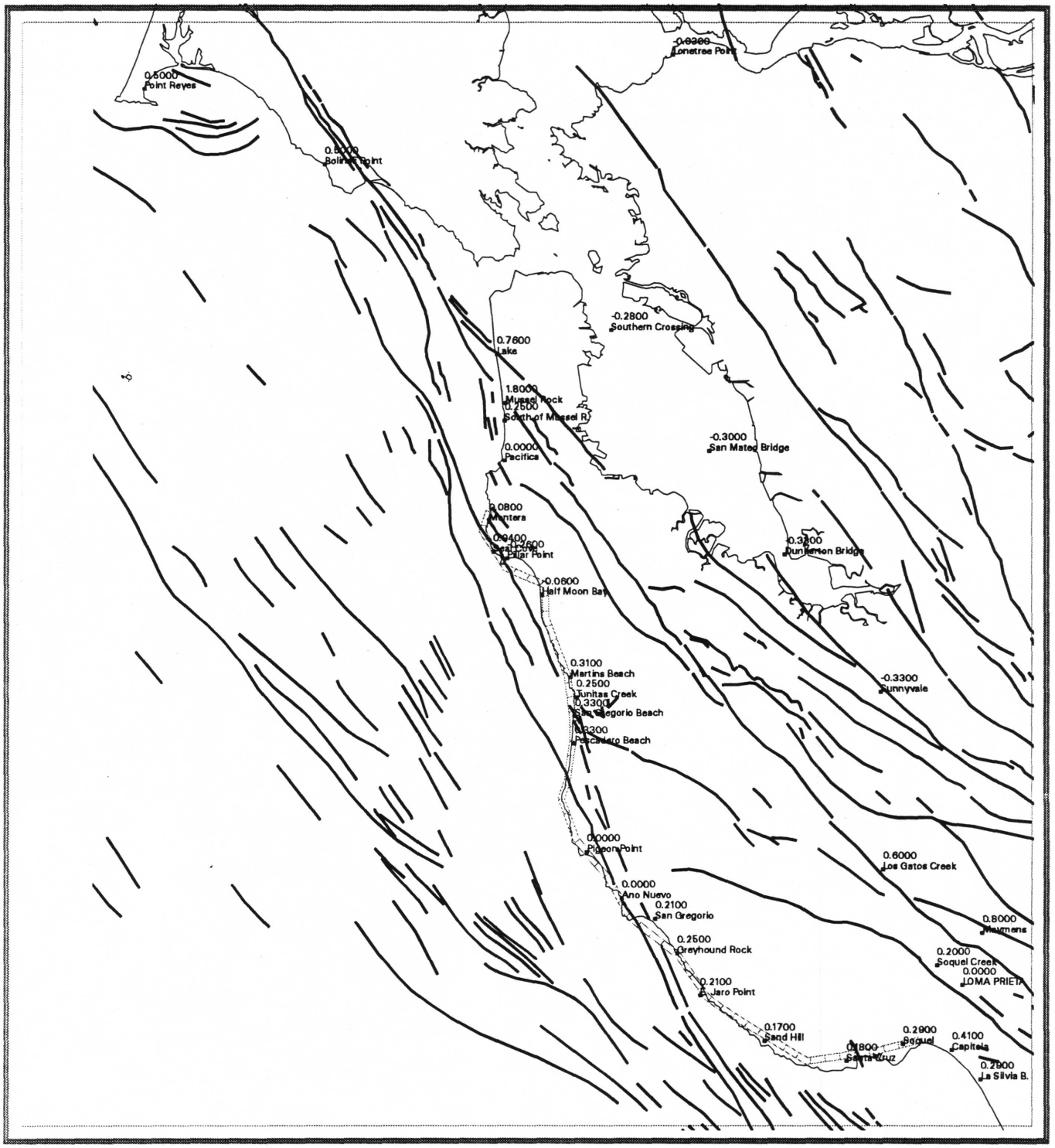

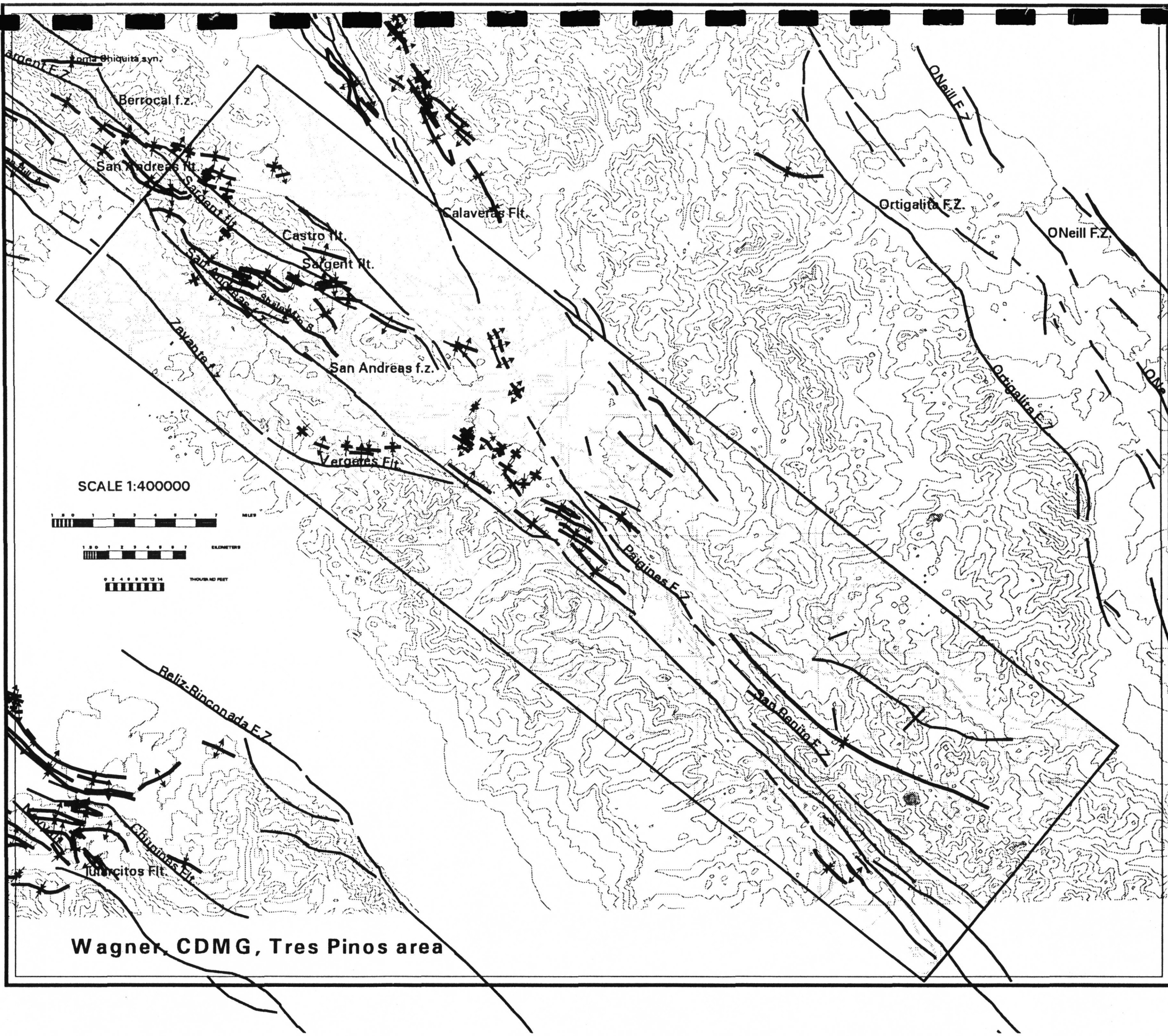
Berrocal f.z.
San Andreas flt.
Sargent flt.
Castro flt.
Sargent flt.
Calaveras Flt.
ONeill F.Z.
Ortigalita F.Z.
ONeill F.Z.
Ortigalita F.Z.
San Andreas f.z.
Zayante f.
Vergeles Flt.
Paicines F.Z.
San Benito F.Z.
Reliz-Rinconada F.Z.
Chupines Flt.
SCALE 1:400000
Wagner, CDMG, Tres Pinos area

Off-shore structures from southern San Francisco Bay

Michael S. Marlow, U.S. Geological Survey MS-999, 345 Middlefield Road, Menlo Park, CA 94025 USA

The eastern south bay is underlain by a major unconformity at a subbottom depth of about 300 m, whose age is unknown. Sedimentation rates derived from recent drilling at the Bay Bridge suggest an age of about 200,000 BP for the burial of the unconformity. Beds below the unconformity dip steeply to the east and are the remaining synformal limb of a major fold structure beneath the east half of south San Francisco Bay. This synform is overlain by 300 m of flat-lying beds and the entire section extends to at least 800 m beneath the bay and forms the San Leandro "basin", which is characterized by a prominent gravity low. The approximate end points of the fold are based on gravity data (Bob Jachens, per. comm.) and limited seismic reflection data We have no seismic directly over the synclinal axis, only estimates from the gravity data.

Marlow, South San Francisco Bay - San Leandro area

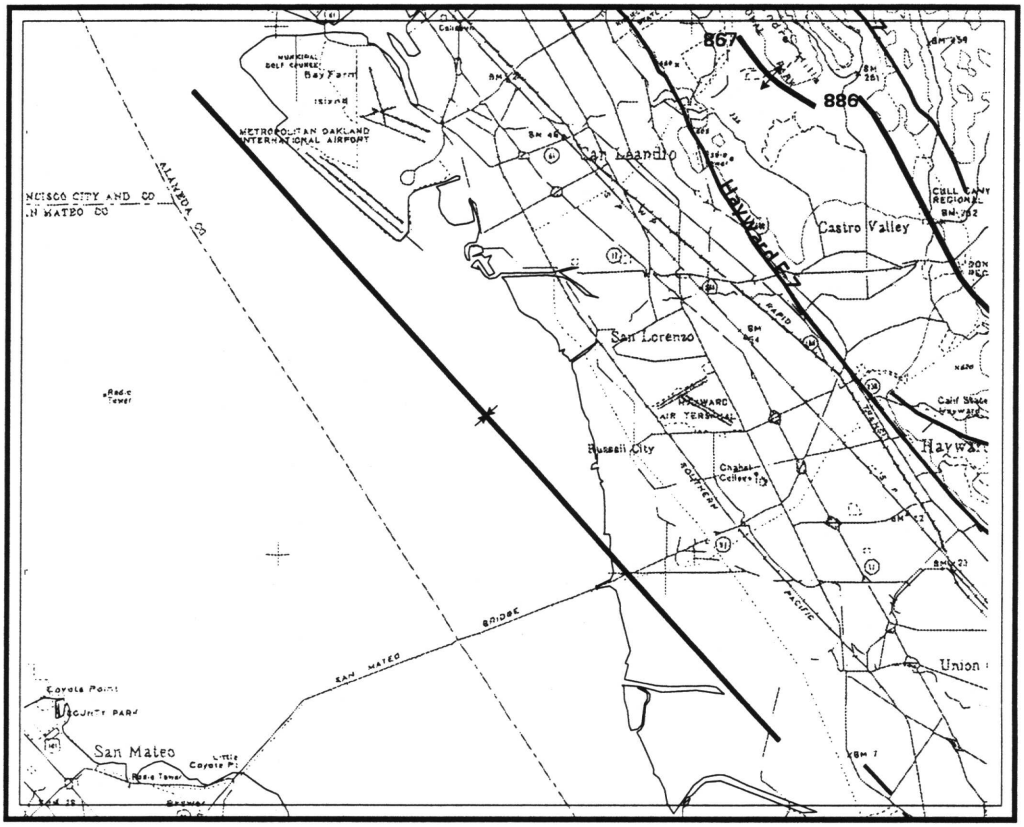

SCALE 1:200000

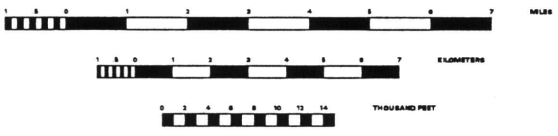

Preliminary Neogene fold and thrust map of Contra Costa County

Graymer, Russell W., U. S. Geological Survey, 345 Middlefield Rd., Menlo Park, CA 94025

Contra Costa County is divided into seven areas, each containing a distinct stratigraphic assemblage (in the manner of Graymer, Jones, and Brabb, 1994). In general, the youngest mapped (pre-Quaternary) units are intensely folded and faulted. The age of the youngest unit has been used to constrain the maximum age of folding and thrusting within each of the seven areas. In four areas the youngest unit is early Pliocene, and in one area (north of Mount Diablo) it is late Pliocene. For the most part, because Quaternary units are undifferentiated, the presence or absence of Quaternary compressive deformation is not known. But given that faults with documented Holocene offset, such as the Hayward fault, show good evidence for Quaternary compressive deformation in Alameda County, and that the youngest mapped units throughout the county are deformed by compressive structures, it is possible that active compressive deformation could lead to seismogenic stress on one or more reverse faults (emergent or blind) in the county.

The only mapped unit that is not involved in folding and reverse faulting is the Quaternary Montezuma Formation, which crops out in a small patch in the Hercules area. The unfolded nature of this unit indicates that compressive deformation, which folded the early Pliocene (5.2 Ma) Pinole Tuff, was for the most part complete before the deposition of the Montezuma Formation (Pleistocene) in that area. However, the uplift of the Pleistocene deposits to their current position up to 80 feet above sea level may indicate continuing, but broader, deformation.

Graymer, R.W., Jones, D.L., and Brabb, E.E., 1994, Preliminary geologic map emphasizing bedrock formations in Contra Costa County, California: A digital database: U.S. Geological Survey Open-file Report 94-622.

Graymer, Contra Costa County

SCALE 1:400000

Late Quaternary Deformation of the Southern East Bay Hills, Alameda County, CA

Kelson, Keith I., and Gary D. Simpson, William Lettis & Associates, Inc.,
1000 Broadway, Suite 612, Oakland, CA 94607
510/ 832-3716, wla@netcom.com

The southern East Bay Hills provide a means to assess late Quaternary surficial deformation in the area bordered by the northern Calaveras and Hayward faults. The substantial topographic relief of the range is related, in part, to interactions between these two active, predominantly right-lateral structures. Based on mapping of fluvial terraces along Alameda Creek and analysis of range topography, we estimate the pattern, location, and rate of late Quaternary deformation within the southern East Bay Hills.

Alameda Creek, which represents the only subaerial drainage that crosses the structural grain of the range, flows westward across the range within the deeply incised Niles Canyon. The distribution of remnants of four fluvial terraces along Alameda Creek suggest broad anticlinal deformation of the range. Upstream of Niles Canyon, terrace profiles are convergent and suggest subsidence within Sunol Valley. In the eastern part of the canyon, high terraces have flat or slightly eastward (upstream) gradients likely related to uplift of the range. Terrace heights and apparent terrace spacing are greatest in the core of the range. In the western (downstream) part of the canyon, terraces converge and higher terrace-profiles have progressively steeper gradients. Based on a radiocarbon age-estimate of 20 ka for the second-highest terrace and a maximum height of 30 to 34 m, a late Pleistocene uplift rate of 1.5 to 1.7 mm/yr is estimated. A 21-m-high terrace is less than 13 ka, which provides a maximum uplift rate of 1.6 mm/yr. We estimate an average late Pleistocene uplift rate of 1.5 ± 0.5 mm/yr for the southern East Bay Hills.

Generalized topographic (envelope, subenvelope, and residual) maps suggest broad anticlinal deformation of the range as a whole, as well as two distinct loci of uplift north and south of Mission Pass. Because the rim of Niles Canyon is topographically higher than the lowest part of the range at Mission Pass (4 km to the south), deformation of the range may include development of a structural saddle at Mission Pass. The presence of discontinuous gravel remnants near the rim of Niles Canyon, which may be the middle Pleistocene upper Livermore Gravel, suggests that the ancestral Alameda Creek may have begun incising into the range during the middle Pleistocene. Thus, much of the observed deformation of the range may have occurred within the past half-million years or so.

comprises sandstone, pebbly sandstone, pelecypod coquina, and associated siltstone. Bedding style and fossil assemblages suggest shelfal and/or estuarine deposition. Clast composition in pebbly beds implies mixing of sediments derived from both Franciscan and Sierran source terranes. Although Ham (1952) applied the name "Neroly Formation" to the upper part of the San Pablo Group at San Leandro Reservoir, the lithic-rich andesitic bluesands generally considered characteristic of the Neroly are absent in this area

The San Pablo Group is conformably overlain by the Contra Costa Group (Fig. 1). In our study area, the two units locally intercalate and are locally in gradational contact. Buising (e.g., 1992) has distinguished five complexly intercalated lithofacies in the Contra Costa Group at San Leandro Reservoir. The conglomerate-dominated, sandstone-dominated, and interbedded conglomerate, sandstone, and siltstone lithofacies represent fluvial channel and floodplain deposits; the sandstone + mudstone lithofacies represents lacustrine-deltaic and shallow-lacustrine deposits; the shale lithofacies records open-lacustrine deposition. The proportion of conglomerate in the Contra Costa Group increases slightly from east to west across Upper San Leandro watershed. This is a gradual trend and appears to be unrelated to known faulting in the study area. Fluvial deposits are volumetrically dominant in the Contra Costa Group in our study area; open-lacustrine shales occur in stratigraphically isolated lenses ranging from >1 km to <100 m along strike. This suggests numerous small lakes on a broad fluviodeltaic drainage plain which probably emptied into an estuary roughly analogous to the modern San Francisco Bay (see Liniecki-Laporte and Andersen, 1988; Buising and Walker, 1995). Clast composition in both sand and coarse-clast fractions of the Contra Costa Group suggests mixing of Franciscan- and Sierran-derived sediment (Buising, 1995).

Folds

The most important fold in the study area is the Kaiser Creek syncline, which trends ~335° and plunges ~0°. The Kaiser Creek syncline has an along-trend length of approximately 6-7 km and a wavelength on the order of 5 km; balanced cross sections of Wakabayashi and others (1992) suggest an amplitude of 3-4 km. Many parasitic folds occur on both limbs of the Kaiser Creek syncline. Outcrop geometries suggest that parasitic folds have wavelengths ranging from a few m or 10's of m to as much as 0.8 km; amplitudes of the larger parasitic folds probably approach 0.5 km. The Kaiser Creek syncline itself is nearly upright but shows minor asymmetry with the northeast limb slightly steeper. Stratal attitudes in much of the study area, particularly the western half, require rather tight folding, and stereo net plots of attitude data suggest chevron-like folds (Wakabayashi and others, 1992). No chevron geometry is evident on our maps; however, map outcrop patterns

are greatly complicated by the fact that stratigraphy in the Upper Cenozoic units of Upper San Leandro watershed, particularly the Contra Costa Group, is extremely lenticular.

Northwest-striking (reverse) faults

This category includes several structures whose map patterns reflect a northwest strike and southwest dip. At least two of these structures have demonstrable reverse separation: the Miller Creek fault places sandstone and siliceous units of the Monterey Group over sandstone and conglomerate of the younger Contra Costa and San Pablo groups west of Upper San Leandro Reservoir, while the Bollinger fault places sandstone of the San Pablo Group over sandstone and conglomerate of the Contra Costa Group east of the reservoir. The Cull Creek fault is very similar to the Miller Creek fault in terms of strike, direction of dip, and apparent magnitude of dip, and, although separation is more difficult to ascertain on the Cull Creek fault because it is entirely within the stratigraphically complex Contra Costa Group, we infer that it is also a northeast-vergent reverse-separation fault. Similarly, Dibblee (1980) shows west-side-up separation on the Las Trampas fault.

The mapped traces of all of the NW-striking faults cut fairly straight across rugged, high-relief topography, suggesting steep fault dips. Trench investigations carried out by Earth Sciences Associates (see Wakabayashi and others, 1992) confirm near-surface dips of 60-80 degrees for the Miller Creek fault in the vicinity of the Kaiser Creek arm of Upper San Leandro Reservoir. Further south along the Miller Creek fault, 1:12,000 (unpublished data) has documented multiple arcuate fault strands resembling the classic imbricate fan' thrust geometry described by Boyer and Elliott (1982). A similar model may apply to the multiple "braided" strands of the Cull Creek fault as well (Buising, unpublished mapping).

Northeast-striking (strike-slip?) faults

The northeast-striking faults documented within our study area are primarily minor structures. The only one large enough to show on the compilation map has an along-strike length of approximately 0.8 km (see original mapping by Ham, 1952); mapped lengths of a few 10's to 100's of m and strike separations of several m to 10's of m are more common. Straight map traces suggest steep dips. We interpret these features as strike-slip-dominated tear faults associated with NE-SW-directed (plate-boundary normal) shortening.

Age Of Structures and Shortening Rate for Study Area

Cross-cutting relationships and ages of folded and faulted strata point to a latest Miocene or younger age for the initiation of movement on all of the structures described above. Paleogeographic reconstructions of

Buising and Walker (1995) suggest that widespread uplift began in the greater East Bay region sometime between 10 and 5 Ma; the youngest strata in the Upper San Leandro Reservoir area known to be affected by folding belong to the upper portion of the Contra Costa Group and are probably on the order of 6 Ma (Liniecki-Laporte and Andersen, 1988) or possibly slightly younger (A. Buising, unpublished data). Fold hinge traces are locally cut by NW-striking reverse faults. The NW-striking faults thus must post-date folding at least slightly, although folds and NW-striking faults could be essentially coeval because their similarity in orientation suggests that they may have been cogenetic. Based on geomorphic and trench evidence, Wakabayashi and others (1992) have suggested that both the Miller Creek and Cull Creek faults may have undergone late Quaternary motion. The age of the NE-striking faults is likely similar to that of the NW-striking set (particularly if they are in fact genetically related!).

Balanced cross-sections published by Wakabayashi and others (1992) provide a means of estimating net shortening and approximate shortening rates across the East Bay Hills fold and thrust belt at the latitude of Upper San Leandro Reservoir. Based on these section, we estimate net shortening across our study area as ~5 km. Using a 6-Ma start date for the onset of contraction, this gives an approximate shortening rate of 0.8 mm/yr. A 3.5-Ma contraction start date gives an approximate shortening rate of 1.4 mm/yr. However, there is abundant evidence to suggest that the partitioning of strike slip on faults of the San Andreas system has changed significantly since Miocene time (Wakabayashi and Hengesh, 1995); the same is likely true for contractile structures in the greater Bay area. Thus, long-term or average shortening rates may differ significantly from Holocene rates, and the estimates given above should be used cautiously in seismic risk assessment: present-day shortening rates (and associated seismogenic potential) may be either greater or lesser than the above estimates.

References cited

Boyer, S. E., and Elliott, D., 1982, Thrust systems: American Association of Petroleum Geologists Bulletin, v. 66, p. 1196-1230.

Buising, Anna V., 1992, Sedimentologic evidence for structural and topographic evolution following the onset of strike slip, E. San Francisco Bay area, California: Geological Society of America Abstracts with Programs, v. 24, no. 7, p. A276.

Buising, A. V., 1995, Mixed-provenance sands in the Upper Miocene Contra Costa Group, Upper San Leandro Watershed and Cull Canyon, Alameda-Contra Costa Counties, CA [abs.]: American Association of Petroleum Geologists Bulletin, in press.

Buising, Anna V., and Walker, James P., 1995, Preliminary palinspastic paleogeographic reconstructions for the greater San Francisco Bay area, 15 Ma-5 Ma, in Sangines, E. M., Andersen, D. W., and Buising, A. V., eds., Recent geologic studies in the San Francisco Bay area: Pacific Section SEPM, v. 76, p. 141-160.

Dibblee, T. W., Jr., 1980, Preliminary geologic map of the Las Trampas Ridge quadrangle, Alameda and Contra Costa Counties, California: United States Geological Survey Open-File Report 80-545, scale 1:24,000.

Ham, C. K., 1952, Geology of Las Trampas Ridge, Berkeley Hills, California: California Division of Mines Special Report 22, 27 p.

Liniecki-Laporte, M., and Andersen, D. W., 1988, Possible new constraints on late Miocene

depositional patterns in west-central California: Geology, v. 16, p. 216-220.
Wakabayashi, J., and Hengesh, J. V., 1995, Distribution of Late Cenozoic displacement on the San Andreas fault system, northern California: in Sangines, E. M., Andersen, D. W., and Buising, A. V., eds., Recent geologic studies in the San Francisco Bay area: Pacific Section SEPM, v. 76, p. 19-30.
Wakabayashi, J., Smith, D. L., and Hamilton, D. H., 1992, The Miller Creek and related structures: Neogene kinematics of a potentially active thrust system in the East Bay Hills, California, in Borchardt, G., Hirschfeld, S. E., Lienkaemper, J. J., McClellan, P., Williams, P. L., and Wong, I. G., eds., Proceedings of the second conference on earthquake hazards in the eastern San Francisco Bay area: California Division of Mines and Geology Special Publication 113, p. 345-354.

Kelson and Simpson, W. Lettis and Associates, Niles Canyon area

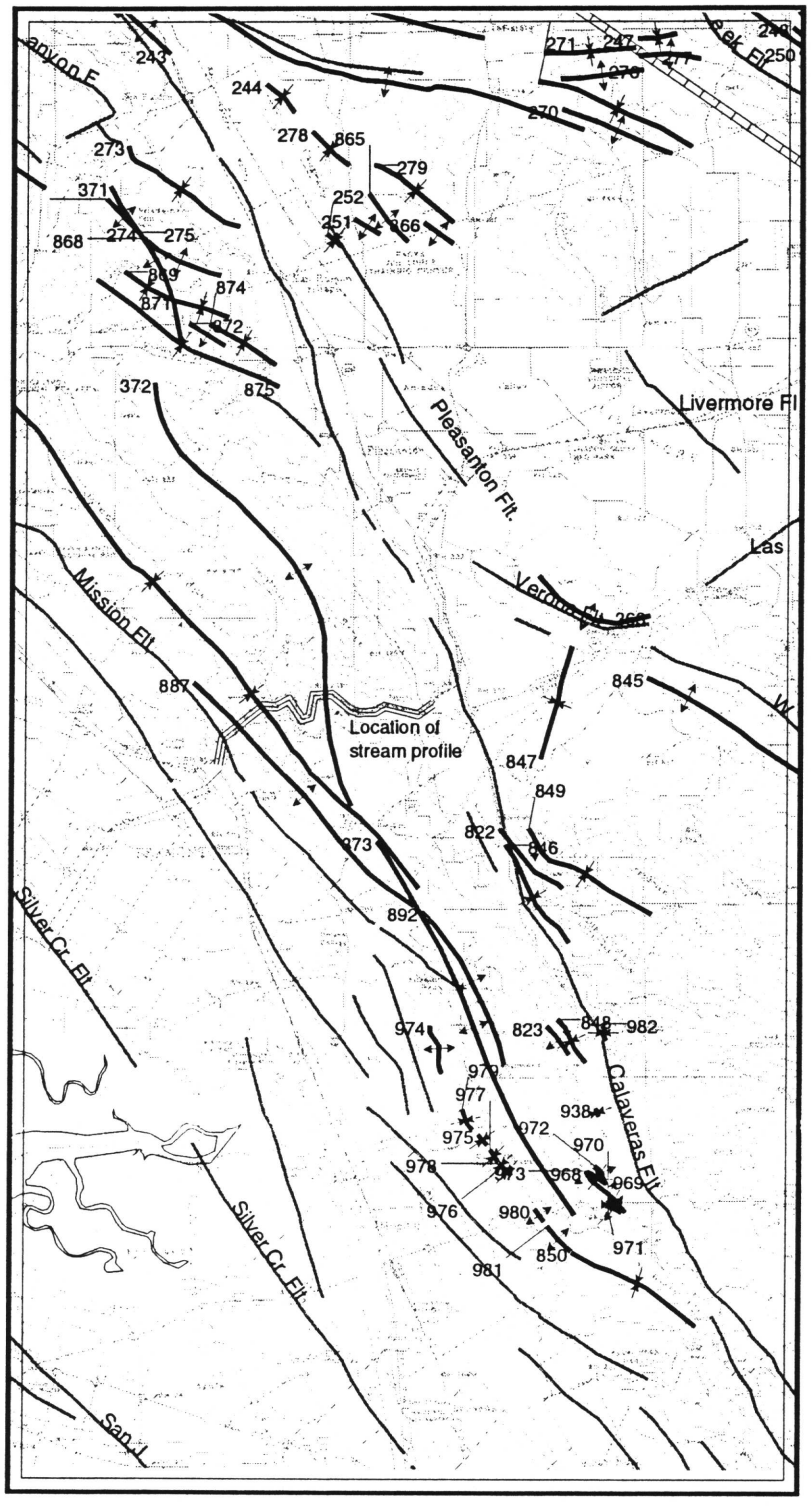

SCALE 1:250000

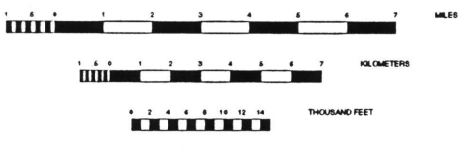

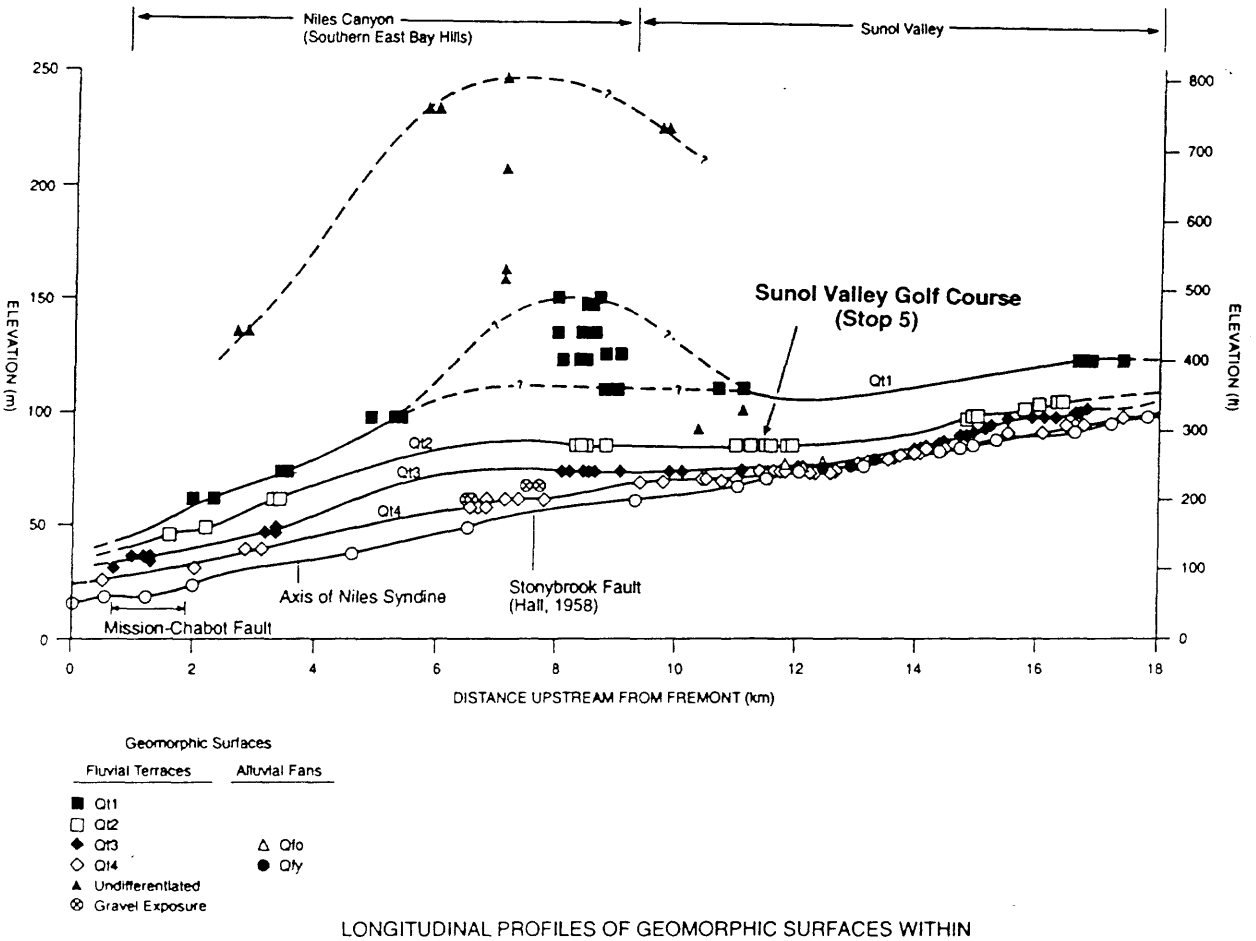

LONGITUDINAL PROFILES OF GEOMORPHIC SURFACES WITHIN SUNOL VALLEY AND NILES CANYON, SHOWING INTERPRETATION OF POSSIBLE DEFORMATION ACROSS THE SOUTHERN EAST BAY HILLS

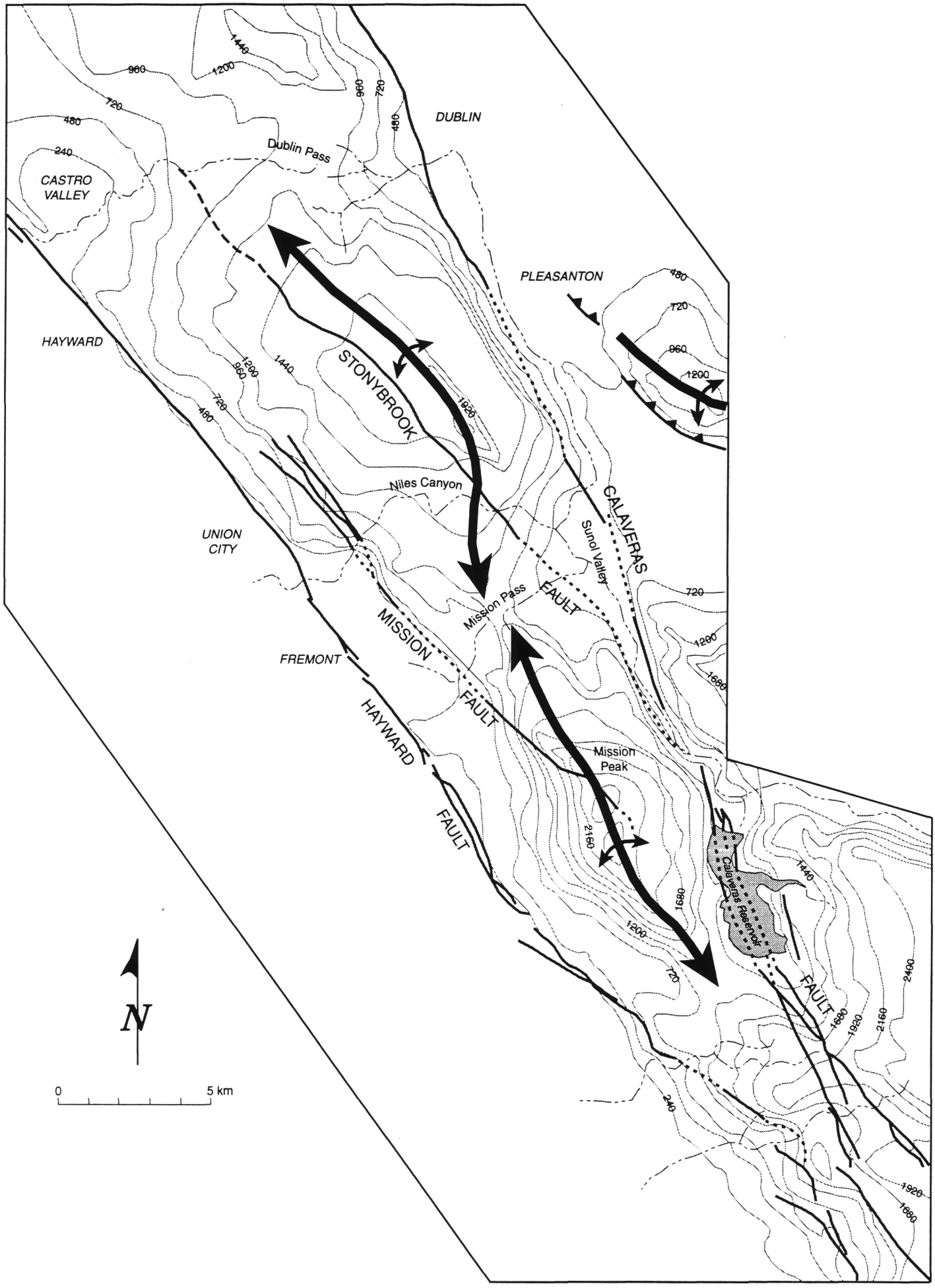
DUBLIN
Dublin Pass
CASTRO VALLEY
PLEASANTON
HAYWARD
STONYBROOK
Niles Canyon
GALAVERAS
Sunol Valley
FAULT
UNION CITY
Mission Pass
MISSION
FREMONT
HAYWARD
FAULT
FAULT
Mission Peak
Calaveras Reservoir
FAULT
N
0
5 km

Kelson

Arc Line identity	363	371	372	373
Compiler(s)	Kelson, K	Kelson, K	Kelson, K	Kelson, K
Structure	Southern East Bay Hills Anticline	Southern East Bay Hills Anticline	Southern East Bay Hills Anticline	Southern East Bay Hills Anticline
Age minimum	1	1	1	1
Age max				
Age control	post Livermore gravel, C14	post Livermore gravel, C14	post Livermore gravel, C14	post Livermore gravel, C14
Inclined Geomorphic surface	fluvial, residual map	fluvial, residual map	fluvial, residual map	fluvial, residual map
Horizontal shortening (km)	1	1	1	1
c1	4	4	4	4
Shortening rate mm/yr	2.00	2.00	2.00	2.00
c2	4	4	4	4
Vertical displacement rate mm/yr	1.5	1.5	1.5	1.5
c3	2	2	2	2
Initiation of folding (Ma)	?	?	?	?
c4				
Termination of folding (Ma)	active	active	active	active
Method	geomorphic	geomorphic	geomorphic	geomorphic
Rate averaged, time length	20 ka average	20 ka average	20 ka average	20 ka average
Parallels strike-slip	yes	yes	yes	yes
Distance from fault	2.5 -5.0 km, Calaveras, 4 Hayward	2.5 -5.0 km, Calaveras, 4 Hayward	2.5 -5.0 km, Calaveras, 4 Hayward	2.5 -5.0 km, Calaveras, 4 Hayward
Trend	345	345	345	345
Plunge	dome	dome	dome	dome
Axial Plane strike	?	?	?	?
Axial Plane dip	?	?	?	?
Axial Plane dip direction	?	?	?	?
Confidence of location	Probable	Probable	Probable	Probable
Vergence direction	?	?	?	?
Multiple or segmented	yes	yes	yes	yes
Half wavelength (km)				
Fold type	A, U	A, U	A, U	A, U
Fold style	unknown	unknown	unknown	unknown
Geodetic	level-line	level-line	level-line	level-line
Reference	Alt, J.N., 1979	Alt, J.N., 1979	Alt, J.N., 1979	Alt, J.N., 1979
Drill Hole				
Seismic				
Reflection				
Gravity				
Historical Seismicity	Wong and Hemple-Haley, 1992	Wong and Hemple-Haley, 1992	Wong and Hemple-Haley, 1992	Wong and Hemple-Haley, 1992
Magnitude/event				
Depth				
Distributed microseismicity				
Reference				
Additonal References	Andrews et al, 1993; Kelson et al, 1993	Andrews et al, 1993; Kelson et al, 1993	Andrews et al, 1993; Kelson et al, 1993	Andrews et al, 1993; Kelson et al, 1993

Late Cenozoic Structures Between Upper San Leandro Reservoir And Dublin Canyon, Eastern San Francisco Bay Area, California

Buising, Anna V., Department of Geological Sciences, California State University, Hayward, CA 94542, email abuising@darwin.sci.csuhayward.edu, and Wakabayashi, John, Independent Consultant, 1329 Sheridan Lane, Hayward, CA 94544

Introduction

We describe Late Cenozoic structures in an area of approximately 220 km^2 between the northern edge of East Bay Municiple Utilities District (EBMUD's) Upper San Leandro watershed and Dublin Canyon (I-580). Our primary source of data is our own detailed mapping, but we draw also on published mapping by Ham (1952) and Dibblee (1980) and on unpublished mapping by Kurt Vollbrecht. Late Cenozoic structures in our study area include northwest-trending folds, northwest-striking faults, and northeast-striking faults. Northwest-striking faults include structures with demonstrable reverse slip, such as the Miller Creek fault, and structures interpreted as reverse faults based on similarity in orientation and general outcrop style to known reverse faults, such as the Cull Creek fault. Sense of separation on the northeast-striking faults is difficult to establish because of the extreme stratigraphic variability of the units they typically offset (continental sediments of the Contra Costa Group); we interpret these structures as tear faults associated with contractile deformation.

Neogene stratigraphy of the Upper San Leandro Reservoir area

The oldest Neogene strata exposed in our study area belong to the Monterey Group (Fig. 1) and are inferred to be of mid-Miocene age based on tentative correlation with lithologically similar units in the Berkeley Hills and on the western flank of Mt. Diablo. In the Upper San Leandro Reservoir area, the Monterey Group consists of very thin-bedded chert and porcellanite with interbeds of dark-colored, locally siliceous shale, overlain by medium- and thick-bedded sandstones. Although minor differences exist (some or all of which may be due to stratigraphic disruption by multiple, closely spaced fault strands) Monterey stratigraphy east and west of the Miller Creek fault is grossly similar. We interpret the siliceous rocks and associated shale of the Monterey Group as deposits of a largely starved deep-marine environment; fossil assemblages and general sedimentologic style suggest a shallow-marine (shelfal) environment of deposition for the overlying sandstones.

The Monterey Group is overlain by the San Pablo Group (Fig. 1); the contact between the two is conformable and locally gradational. In the vicinity of Upper San Leandro Reservoir, the San Pablo Group comprises sandstone, pebbly sandstone,

pelecypod coquina, and associated siltstone. Bedding style and fossil assemblages suggest shelfal and/or estuarine deposition. Clast composition in pebbly beds implies mixing of sediments derived from both Franciscan and Sierran source terranes. Although Ham (1952) applied the name "Neroly Formation" to the upper part of the San Pablo Group at San Leandro Reservoir, the lithic-rich andesitic bluesands generally considered characteristic of the Neroly are absent in this area

The San Pablo Group is conformably overlain by the Contra Costa Group (Fig. 1). In our study area, the two units locally intercalate and are locally in gradational contact. Buising (e.g., 1992) has distinguished five complexly intercalated lithofacies in the Contra Costa Group at San Leandro Reservoir. The conglomerate-dominated, sandstone-dominated, and interbedded conglomerate, sandstone, and siltstone lithofacies represent fluvial channel and floodplain deposits; the sandstone + mudstone lithofacies represents lacustrine-deltaic and shallow-lacustrine deposits; the shale lithofacies records open-lacustrine deposition. The proportion of conglomerate in the Contra Costa Group increases slightly from east to west across Upper San Leandro watershed. This is a gradual trend and appears to be unrelated to known faulting in the study area. Fluvial deposits are volumetrically dominant in the Contra Costa Group in our study area; open-lacustrine shales occur in stratigraphically isolated lenses ranging from >1 km to <100 m along strike. This suggests numerous small lakes on a broad fluviodeltaic drainage plain which probably emptied into an estuary roughly analogous to the modern San Francisco Bay (see Liniecki-Laporte and Andersen, 1988; Buising and Walker, 1995). Clast composition in both sand and coarse-clast fractions of the Contra Costa Group suggests mixing of Franciscan- and Sierran-derived sediment (Buising, 1995).

Folds

The most important fold in the study area is the Kaiser Creek syncline, which trends ~335° and plunges ~0°. The Kaiser Creek syncline has an along-trend length of approximately 6-7 km and a wavelength on the order of 5 km; balanced cross sections of Wakabayashi and others (1992) suggest an amplitude of 3-4 km. Many parasitic folds occur on both limbs of the Kaiser Creek syncline. Outcrop geometries suggest that parasitic folds have wavelengths ranging from a few m or 10's of m to as much as 0.8 km; amplitudes of the larger parasitic folds probably approach 0.5 km. The Kaiser Creek syncline itself is nearly upright but shows minor asymmetry with the northeast limb slightly steeper. Stratal attitudes in much of the study area, particularly the western half, require rather tight folding, and stereo net plots of attitude data suggest chevron-like folds (Wakabayashi and others, 1992). No chevron geometry is evident on our maps; however, map outcrop patterns are greatly complicated by the fact that

stratigraphy in the Upper Cenozoic units of Upper San Leandro watershed, particularly the Contra Costa Group, is extremely lenticular.

Northwest-striking (reverse) faults

This category includes several structures whose map patterns reflect a northwest strike and southwest dip. At least two of these structures have demonstrable reverse separation: the Miller Creek fault places sandstone and siliceous units of the Monterey Group over sandstone and conglomerate of the younger Contra Costa and San Pablo groups west of Upper San Leandro Reservoir, while the Bollinger fault places sandstone of the San Pablo Group over sandstone and conglomerate of the Contra Costa Group east of the reservoir. The Cull Creek fault is very similar to the Miller Creek fault in terms of strike, direction of dip, and apparent magnitude of dip, and, although separation is more difficult to ascertain on the Cull Creek fault because it is entirely within the stratigraphically complex Contra Costa Group, we infer that it is also a northeast-vergent reverse-separation fault. Similarly, Dibblee (1980) shows west-side-up separation on the Las Trampas fault.

The mapped traces of all of the NW-striking faults cut fairly straight across rugged, high-relief topography, suggesting steep fault dips. Trench investigations carried out by Earth Sciences Associates (see Wakabayashi and others, 1992) confirm near-surface dips of 60-80 degrees for the Miller Creek fault in the vicinity of the Kaiser Creek arm of Upper San Leandro Reservoir. Further south along the Miller Creek fault, 1:12,000 (unpublished data) has documented multiple arcuate fault strands resembling the classic imbricate fan' thrust geometry described by Boyer and Elliott (1982). A similar model may apply to the multiple "braided" strands of the Cull Creek fault as well (Buising, unpublished mapping).

Northeast-striking (strike-slip?) faults

The northeast-striking faults documented within our study area are primarily minor structures. The only one large enough to show on the compilation map has an along-strike length of approximately 0.8 km (see original mapping by Ham, 1952); mapped lengths of a few 10's to 100's of m and strike separations of several m to 10's of m are more common. Straight map traces suggest steep dips. We interpret these features as strike-slip-dominated tear faults associated with NE-SW-directed (plate-boundary normal) shortening.

Age Of Structures and Shortening Rate for Study Area

Cross-cutting relationships and ages of folded and faulted strata point to a latest Miocene or younger age for the initiation of movement on all of the structures described above. Paleogeographic reconstructions of Buising and Walker (1995) suggest that

widespread uplift began in the greater East Bay region sometime between 10 and 5 Ma; the youngest strata in the Upper San Leandro Reservoir area known to be affected by folding belong to the upper portion of the Contra Costa Group and are probably on the order of 6 Ma (Liniecki-Laporte and Andersen, 1988) or possibly slightly younger (A. Buising, unpublished data). Fold hinge traces are locally cut by NW-striking reverse faults. The NW-striking faults thus must post-date folding at least slightly, although folds and NW-striking faults could be essentially coeval because their similarity in orientation suggests that they may have been cogenetic. Based on geomorphic and trench evidence, Wakabayashi and others (1992) have suggested that both the Miller Creek and Cull Creek faults may have undergone late Quaternary motion. The age of the NE-striking faults is likely similar to that of the NW-striking set (particularly if they are in fact genetically related!).

Balanced cross-sections published by Wakabayashi and others (1992) provide a means of estimating net shortening and approximate shortening rates across the East Bay Hills fold and thrust belt at the latitude of Upper San Leandro Reservoir. Based on these section, we estimate net shortening across our study area as ~5 km. Using a 6-Ma start date for the onset of contraction, this gives an approximate shortening rate of 0.8 mm/yr. A 3.5-Ma contraction start date gives an approximate shortening rate of 1.4 mm/yr. However, there is abundant evidence to suggest that the partitioning of strike slip on faults of the San Andreas system has changed significantly since Miocene time (Wakabayashi and Hengesh, 1995); the same is likely true for contractile structures in the greater Bay area. Thus, long-term or average shortening rates may differ significantly from Holocene rates, and the estimates given above should be used cautiously in seismic risk assessment: present-day shortening rates (and associated seismogenic potential) may be either greater or lesser than the above estimates.

References cited

Boyer, S. E., and Elliott, D., 1982, Thrust systems: American Association of Petroleum Geologists Bulletin, v. 66, p. 1196-1230.

Buising, Anna V., 1992, Sedimentologic evidence for structural and topographic evolution following the onset of strike slip, E. San Francisco Bay area, California: Geological Society of America Abstracts with Programs, v. 24, no. 7, p. A276.

Buising, A. V., 1995, Mixed-provenance sands in the Upper Miocene Contra Costa Group, Upper San Leandro Watershed and Cull Canyon, Alameda-Contra Costa Counties, CA [abs.]: American Association of Petroleum Geologists Bulletin, in press.

Buising, Anna V., and Walker, James P., 1995, Preliminary palinspastic paleogeographic reconstructions for the greater San Francisco Bay area, 15 Ma-5 Ma, in Sangines, E. M., Andersen, D. W., and Buising, A. V., eds., Recent geologic studies in the San Francisco Bay area: Pacific Section SEPM, v. 76, p. 141-160.

Dibblee, T. W., Jr., 1980, Preliminary geologic map of the Las Trampas Ridge quadrangle, Alameda and Contra Costa Counties, California: United States Geological Survey Open-File Report 80-545, scale 1:24,000.

Ham, C. K., 1952, Geology of Las Trampas Ridge, Berkeley Hills, California: California Division of Mines Special Report 22, 27 p.

Liniecki-Laporte, M., and Andersen, D. W., 1988, Possible new constraints on late Miocene depositional patterns in west-central California: Geology, v. 16, p. 216-220.

Wakabayashi, J., and Hengesh, J. V., 1995, Distribution of Late Cenozoic displacement on the San Andreas fault system, northern California: in Sangines, E. M., Andersen, D. W., and Buising, A. V., eds., Recent geologic studies in the San Francisco Bay area: Pacific Section SEPM, v. 76, p. 19-30.

Wakabayashi, J., Smith, D. L., and Hamilton, D. H., 1992, The Miller Creek and related structures: Neogene kinematics of a potentially active thrust system in the East Bay Hills, California, in Borchardt, G., Hirschfeld, S. E., Lienkaemper, J. J., McClellan, P., Williams, P. L., and Wong, I. G., eds., Proceedings of the second conference on earthquake hazards in the eastern San Francisco Bay area: California Division of Mines and Geology Special Publication 113, p. 345-354.

Schematic stratigraphic column:
Upper Cenozoic units, vicinity of Upper San Leandro Reservoir, Alameda and Contra Costa counties, California

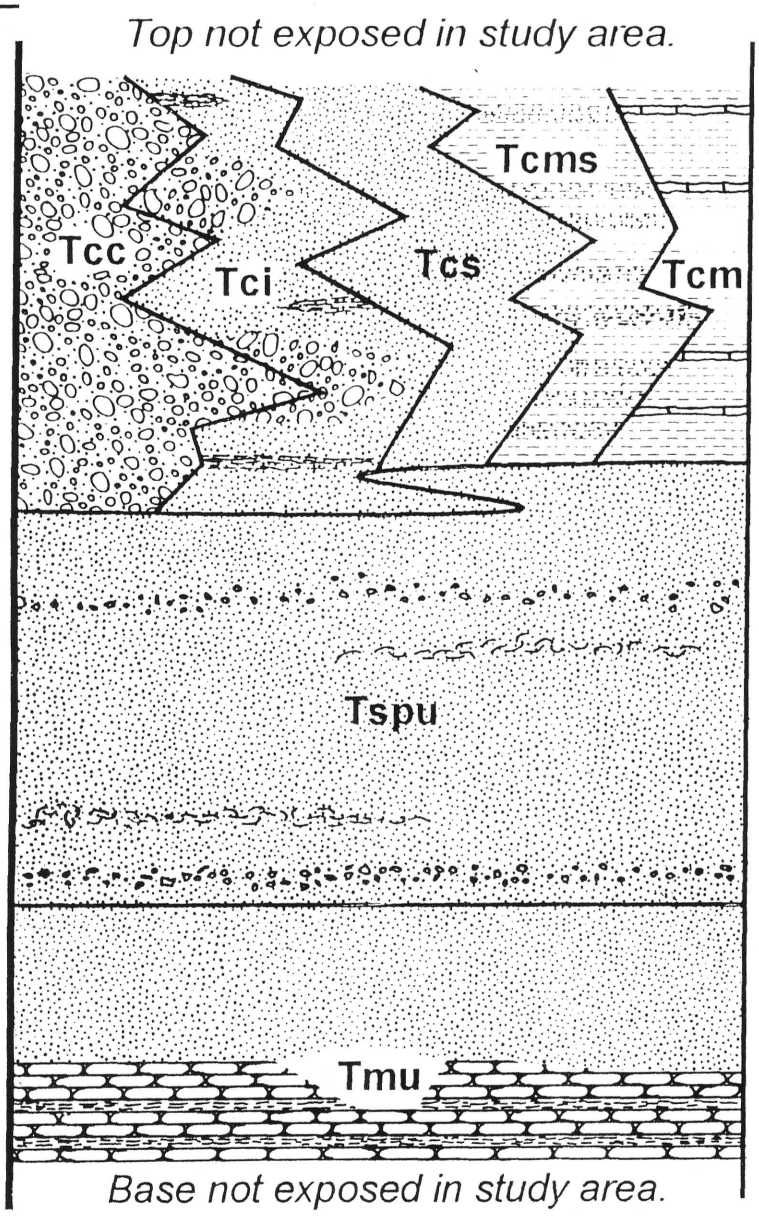

Tc -- Contra Costa Group

Tcc: Conglomerate-dominated lithofacies. Includes minor sandstone and conspicuous local packets of pervasively bioturbated red siltstone. Conglomerates and sandstones represent fluvial channel deposits; siltstones are floodplain deposits. **Tcs: Sandstone-dominated lithofacies.** Locally includes pebbly sandstone and granule conglomerate. Fluvial deposits. **Tci: "Interbedded" lithofacies.** Intimately intercalated conglomerate, sandstone, and siltstone/mudstone. Fluvial deposits. **Tcms: Mudstone and sandstone lithofacies.** Decimeter-scale sandstones with interbedded mudstones. Sandstones contain abundant symmetrical ripple marks. Shallow-lacustrine and lacustrine-deltaic deposits.
Tcm: Mudstone/shale lithofacies. Blue, gray, and olive mudstone and shale locally including decimeter-scale interbeds of sandstone and/or micrite. Mudstone/shale represents open lacustrine deposition; sandstones are mass-flow deposits; micrites are likely algal deposits.

Tspu -- San Pablo Group, undivided

Sandstone, pebbly sandstone, shell hash and siltstone. Shallow-marine and estuarine deposits.

Tmu -- Monterey Group, undivided

Basinal siliceous sediments (Claremont Shale equivalent) overlain by shallow-marine sandstone.

Buising and Wakabayashi, East Bay Hills

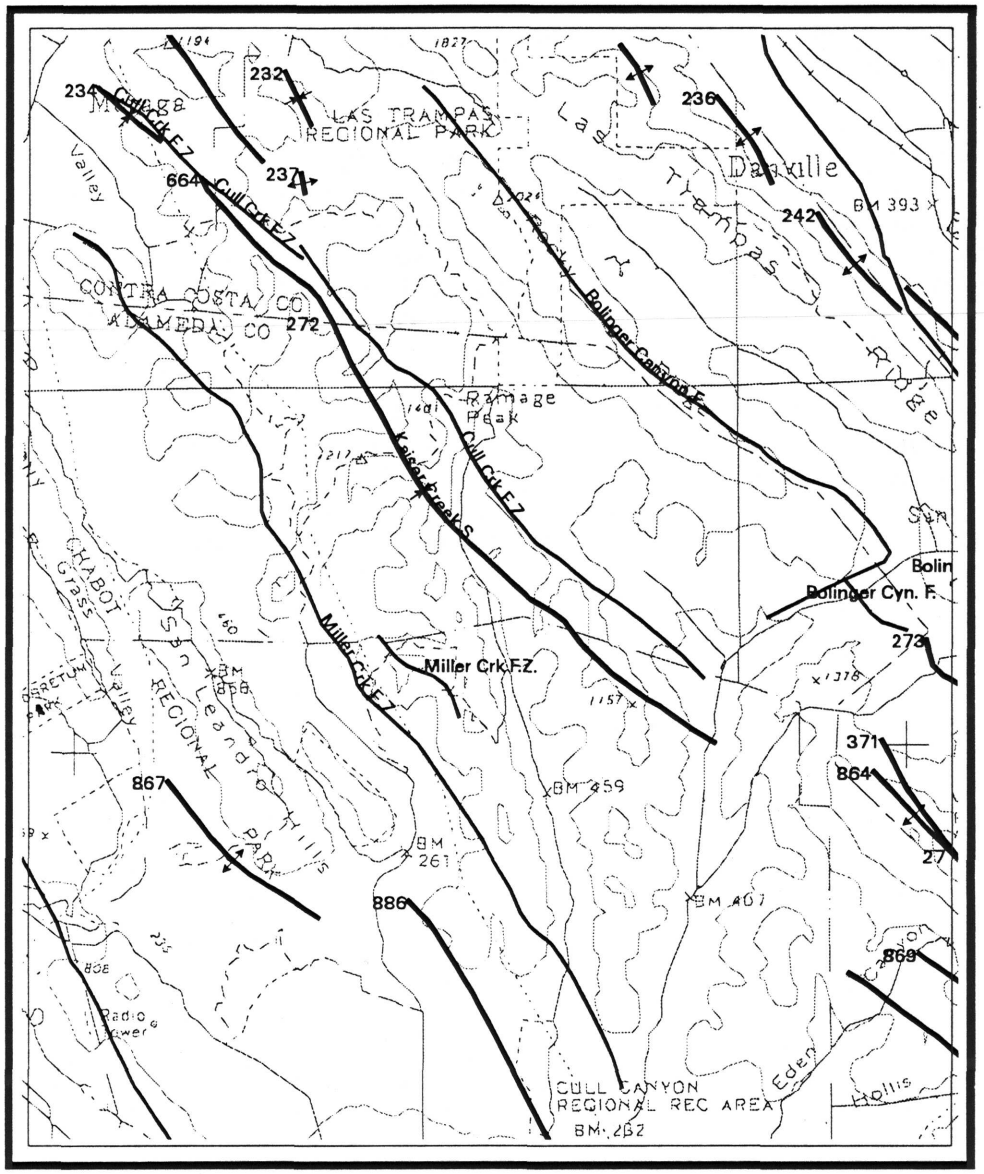

SCALE 1:100000

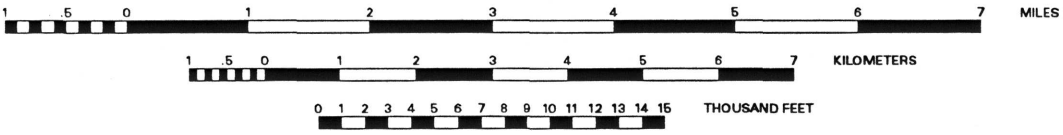

Buising and Wakabayashi

Arc Line identity	**664**
Compiler(s)	Buising, A., Wakabayashi, J.
Structure	Kaiser Creek syncline
Age minimum	5
Age_control	paleontologic, Ar30/Ar40 on plag in volcani-clastic interbed
Horizontal shortening (km)	5 (2)
Shortening rate mm/yr	0.8 (3)
vert rate mm/yr	0.7 (3)
Initiation of folding (Ma)	6 (3)
Termination of folding (Ma)	active? (3)
Method	Balanced x-section
Rate averaged, time length	6 M.y.
Parallels strike-slip	yes
Distance from fault	5.6 km, Hayward fault
Trend	335
Plunge	0
Axial Plane strike	335
Axial Plane dip	90
Confidence of location	Definite
Multiple or segmented	yes
Fold type	A,S,U,A,S
Subsurface data	Yes, Wakabayashi and others 1992

The Pittsburg/Kirby Hills Reverse Fault

Patrick L Williams, Berkeley National Laboratory and, Department of Geography, University of California, Berkeley California, 94720, 510/486-7156 plw@ccs.lbl.gov

High-resolution seismic-reflection images within the Sacramento River, near Pittsburg, California, reveal a discrete, kilometer-wide, west-facing monoclinal fold within Pleistocene and younger strata (Anima and Williams, 1991; Anima et al., 1992). Activity of this feature manifests ongoing shortening of the northern California Coast Ranges. This zone of deformation is the surface expression of the "Pittsburg/Kirby Hills reverse fault" (P-KH), an unknown active structure prior to the 1991 BASIX experiment. Within a 20-km radius of the P-KH fault are located two-major toll-bridges, a large weapons-storage facility, a petroleum-fired power plant, several oil refineries, the seismically vulnerable Sacramento Delta lowlands, a significant proportion of the SF-Bay-area's lifelines, and a population of greater than 300,000 persons.

Interpretation of various marine and on-land seismic reflection data indicates the presence of a fault-propagation fold above the termination of a steeply east-dipping reverse fault. Distributed deformation imaged in the marine sections consists of a one-km-wide west-facing monocline centered on the town of Pittsburg, the uplift and erosional truncation of beds immediately to the east, and subsidence and sediment accumulation in the area immediately to the west of the fold. In cross section, the fold's boundaries are narrow and straight, and beds within and beside the monocline are essentially planar. The abrupt change of attitude at the fold's boundaries may identify faulting along the fold's axial surfaces. Beds appear to be traceable through the folds western fold axial surface, but the eastern fold axis may be faulted subsequent to folding. The geometry of folding is consistent with westward vergence, and a locus of uplift to the east. Reflection imaging of the upper crust in the BASIX experiment verified the existence of the P-KH reverse fault, dipping about 60° to the east in this location (Karageorgi et al., 1992; Hart and McCarthy, 1992), consistent with shallow reflection data collected by LBL and UC Berkeley, and by the USGS (particularly McCarthy et al., 1994). McCarthy et al.'s high-resolution data set indicates that the P-KH reverse fault was active during Holocene time.

Geometric Analysis and Slip Rate of the Fold.

The apparent dip of sedimentary layers adjacent and outside the fold is 0.5 to 2 degrees to the west. Within the monocline apparent dips of these same beds reach a maximum of 17 degrees to the west, and apparent dips of 11 to 13 degrees dominate across the fold. Within the fold, Pleistocene sedimentary strata are truncated and capped

unconformably by Holocene alluvial deposits. To the east of the monocline the nearly flat lying Pleistocene beds are disconformably mantled by Holocene deposits.

At least 80±10 m of probable Pleistocene strata has been removed from the eastern limb of the fold. This illustrates relative uplift of the eastern side of the structure, and indicates that much of the preHolocene section is entirely missing there. The High resolution reflection data, particularly those of McCarthy et al. (1994), suggest that the youngest of the deformed beds are of late Pleistocene and Holocene age, but this estimate needs to be verified. Imaging of the near-surface folding of these young deposits infers youthful, apparently continuing compressional deformation of the eastern Coast Ranges in the Pittsburg Area. Age determination of the youngest deformed strata and of significant time horizons within the imaged section has been instigated by UC Berkeley, and will provide new bounds on the youthfulness and rate of thrusting across the eastern front of the California Coast Ranges.

Structural constraints from deeper profiling.

Without additional evidence, it would be impossible to distinguish whether the Pittsburg monocline was produced by fault propagation or fault-bend folding. Fortunately, profiling of the upper crust verifies the existence of the P-KH reverse fault at depth, projecting to the surface near the base of the monocline [Karageorgi et al., 1992; Hart et al., 1992]. The deep reverse fault dips 60° to the east beneath the Sacramento River. This direct confirmation of the fault's attitude and location greatly improves our ability to characterize its past motions. Agreement of fault location in the high resolution and upper crustal profiling demonstrates that the shallow folding results from fault-propagation, not fault-bend folding. Knowledge of the fault's attitude under the Sacramento River (dipping 60° East and striking N05°W) [Karageorgi et al., 1992], provides primary data for the calculation of fold evolution.

Seismic activity.

Earthquake epicenters in the Pittsburg area are concentrated in a N- trending band passing through the deformed zone [Wong et al., 1988]. The coincidence of the pattern of seismicity with the deformation discovered by the BASIX experiment supports our interpretation of a major structure near Pittsburg. Comparison of the Pittsburg structure with classical models of fault-bend and fault-propagation folding suggest that the surface folding probably results from activity of a steeply east-dipping reverse fault. The abundance of strike-slip and reverse focal mechanisms in the area suggest that the P-KH fault is, at present, an oblique slip structure.

Use of Pittsburg core to measure the Quaternary shortening rate of the P-KH fault.

To further these investigations, UC Berkeley participated with a Caltrans bay area drilling program to acquire a continuous sediment core to a depth of 63 meters beneath the Sacramento River-bottom at Pittsburg. The core was obtained from the relatively downward-moving (footwall) side of the fault, along the path of our seismic reflection line. The chronostratigraphy at this site, in combination with analysis geometry of folding recorded by seismic reflection data, allows the recovery of the P-KH fault's late Quaternary deformation history (over a period of ca. 0 to 0.2 ma). In order for this goal to be accomplished, an ambitious multidisciplinary study of the core is required.

References

Anima R.J. and P.L. Williams, High-resolution marine profiling in BASIX: complex faulting at major East Bay faults, 1991, *EOS Trans. AGU*, 72, 446.

Anima R.J., P.L. Williams and J. McCarthy, 1992, High-resolution marine seismic reflection profiles across East Bay faults, in Proceedings, Second Conference on Earthquake Hazards of the Eastern San Francisco Bay Area, 1991-92, G. Borchardt, S. Hirschfeld, J. McClellan, P. Williams, and I. Wong, eds.

Hart, P.E., J. McCarthy, E. Karageorgi, K. Williams, and T. McEvilly, Crustal Structure from the San Francisco Bay Area: REsults from the 1991 Bay Area Seismic Imaging eXperiment (BASIX), EOS Trans AGU, 73, 404, 1992.

Karagorgi, E., J. Weber Band and K. Williams, Crustal Structure of the San Francisco Bay REgion from CALCRUST and BASIX data, EOS Trans AGU, 73, 404, 1992.

McCarthy, J., Hart P.E., Anima R., Oppenheimer, D., and Parsons T., Seismic evidence for faulting in the western Sacramento Delta region, Pittsburg, California, (abstract) EOS Trans. AGU, 75, p. 684, 1994.

Wong, I. G., R.W. Ely, A.C. Kollmann, 1988, Contemporary seismicity and tectonics of the northern and central Coast Ranges-Sierran Block boundary zone, California, Jour. Geophysical Res., v. 93, no. B7, p. 7813-7833.

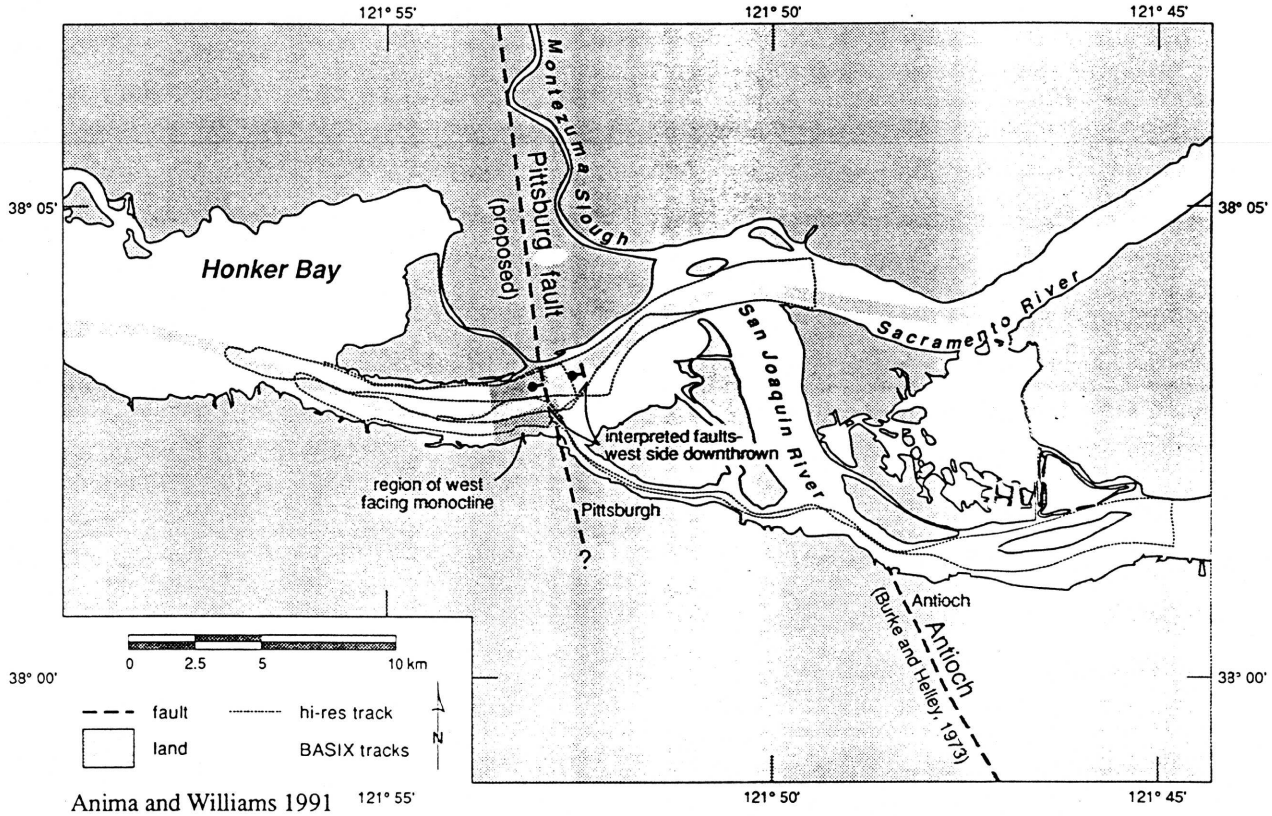

Figure 6. High-resolution tracklines in the vicinity of Antioch and Pittsburgh. Deformation was detected to the north of Pittsburgh and is assigned to a structure referred to here as the "Pittsburg fault".

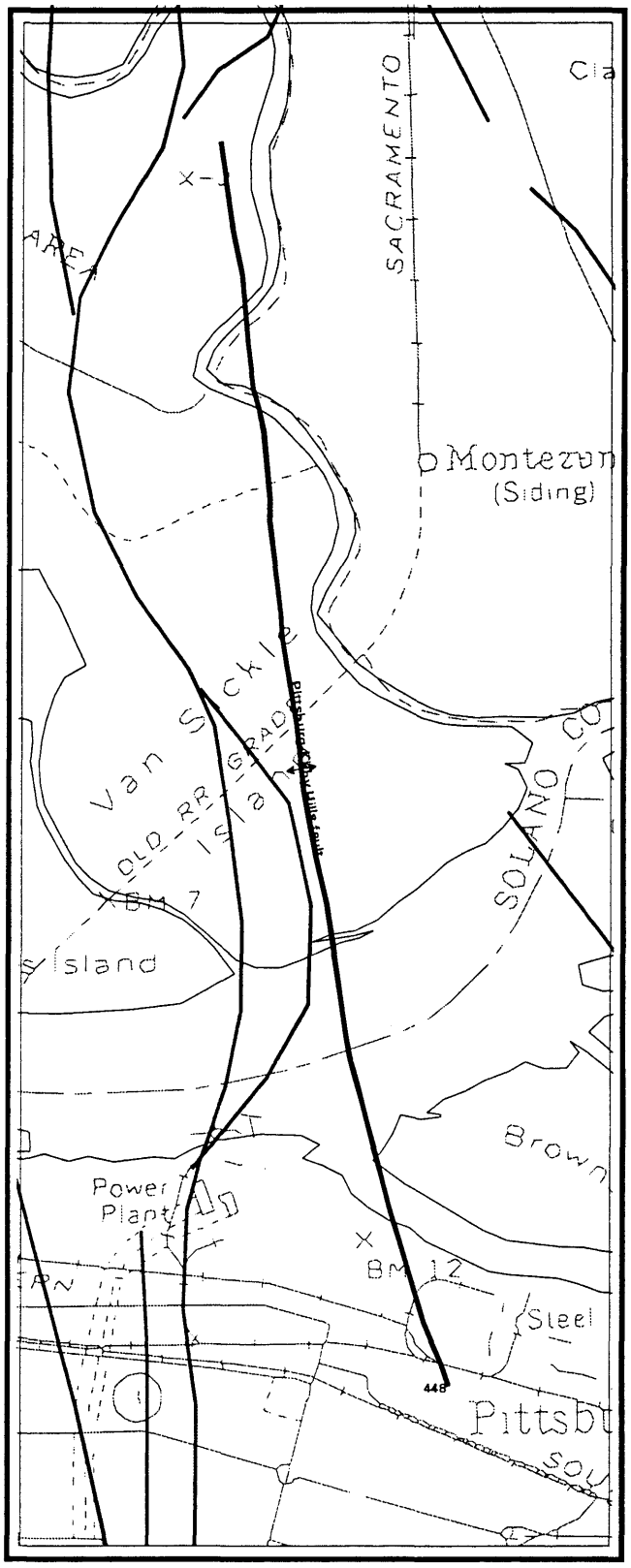

SCALE 1:60000

1 .5 0 1 2 3 4 5 MILES

1 .5 0 1 2 3 4 5 KILOMETERS

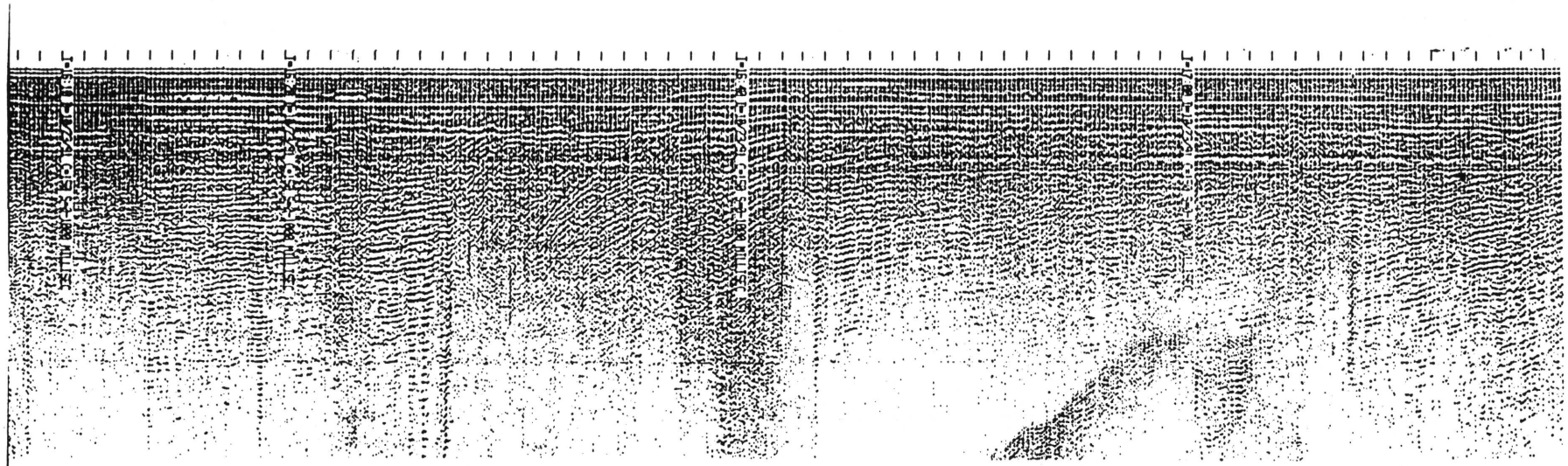

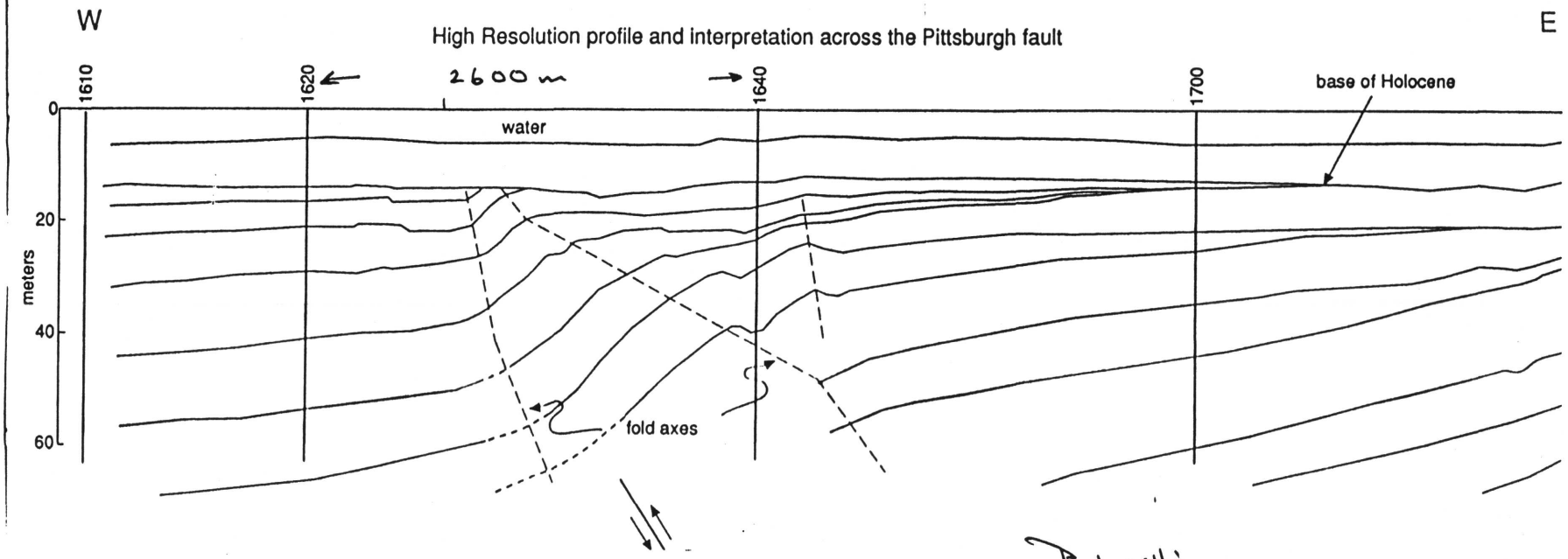

P. Williams
Unpublished Data, 1995

Williams, P.L.

Arc Line identity	**448**
Compiler(s)	Williams, P.
Structure	Pittsburg-Kirby Hills fault sone
Age minimum	1
Age control	seismic strat, corehole lithology
Inclined Geomorphic surface	buried fluvial and marine strata
Horizontal shortening (km)	0.01 (c1)
Shortening rate mm/yr	0 (c2)
Vertical displacement rate mm/yr	0 (c2)
Initiation of folding (Ma)	5
Termination of folding (Ma)	active
Method	x-section, geomorph
Rate averaged, time length	0.12 Ma
Parallels strike-slip	yes
Distance from fault	15, Concord
Trend	350
Axial Plane strike	350
Axial Plane dip	70
Axial Plane dip direction	e
Confidence of location	Definite
Vergence direction	w
Half wavelength (km)	1.5
Fold type	A, O, U, I, AS
Fold style	fault propagation
Reference	Williams et al, 1994; Anima and Williams
Drill Hole	205 ft.
Seismic Reflection	yes
Historical Seismicity	yes
Distributed microseismicity	yes

Seismic Evidence for Faulting in the Western Sacramento Delta Region, Pittsburgh, California

McCarthy, J., Hart, P.E., Anima, R., Oppenheimer, D. and Parsons, T. (all at : U.S. Geological Survey, 345 Middlefield Rd., Menlo Park, CA 94025)

In an effort to identify and characterize the faults of the San Francisco Bay Area, the U.S. Geological Survey has been conducting marine seismic reflection surveys in the shallow waters of the Bay and western Sacramento Delta. Both high-resolution, ~100-m penetration Uniboom data and deeper-penetrating multichannel seismic reflection data have been acquired. These variably penetrating acoustic profiles provide evidence for faulting and deformation beneath the Sacramento River in the vicinity of Pittsburgh, California. The Uniboom data reveal a 1.0-km-wide zone of 3-5° west-dipping strata unconformably overlain by a 30- to 40-m-thick package of westward-thickening prograding sediments. The localized nature of these dipping strata and the prominent angular unconformity that separates them suggest a recent episode of tilting and erosion. The deeper seismic reflection profiles show this zone of deformation extending downward to at least 2 km depth, based on a series of reflector offsets in the upper 2 to 3 s (two-way traveltime).

The faulting and deformation in the vicinity of Pittsburgh is also associated with unusually deep seismicity, ranging between 15 and 23 km. This seismicity is distributed across a 4-km-wide belt that coincides with, and extends east of, the zone of deformation imaged in the upper crust. Together these observations define a near vertical or steeply east-dipping (>75-90°) fault zone that extends from the near surface down almost to the base of the crust. Focal mechanisms indicate predominantly strike-slip faulting.

The earthquake activity near Pittsburgh extends ~25 km north and ~5 km south of the Sacramento River. To the north, in the vicinity of Kirby and Potrero Hills, the seismicity is coincident with the mapped Kirby Hill fault. To the south it dies out near the northern limit of the Kirker fault at the northern edge of the Diablo Range. These results support the interpretation of Krug et al. (1992), who proposed that the Kirby Hills and Kirker faults are linked together in a ~65-km-long system of faults which they labeled the Kirby Hills fault system. The Kirby Hills fault system may thus be an important element in the ongoing crustal deformation in the East Bay.

McCarthy, J., Hart, P.E., Anima, R., Oppenheimer, D., and Parsons, T., 1994, Seismic evidence for faulting in the western Sacramento Delta region, Pittsburgh, California [abs.]: EOS, Transactions of the American Geophysical Union, v. 75, no. 44, p. 684. Logged into BWTR 9/94.

McCarthy, J., Hart, P.E., and Oppenheimer, D., 1995, High angle faulting in the western Sacramento Delta region, Pittsburgh, California [abs.]: AAPG Abstracts with Programs, Pacific Section (in press). Logged into BWTR 11/94.

McCarthy et al, Sacramento Delta area

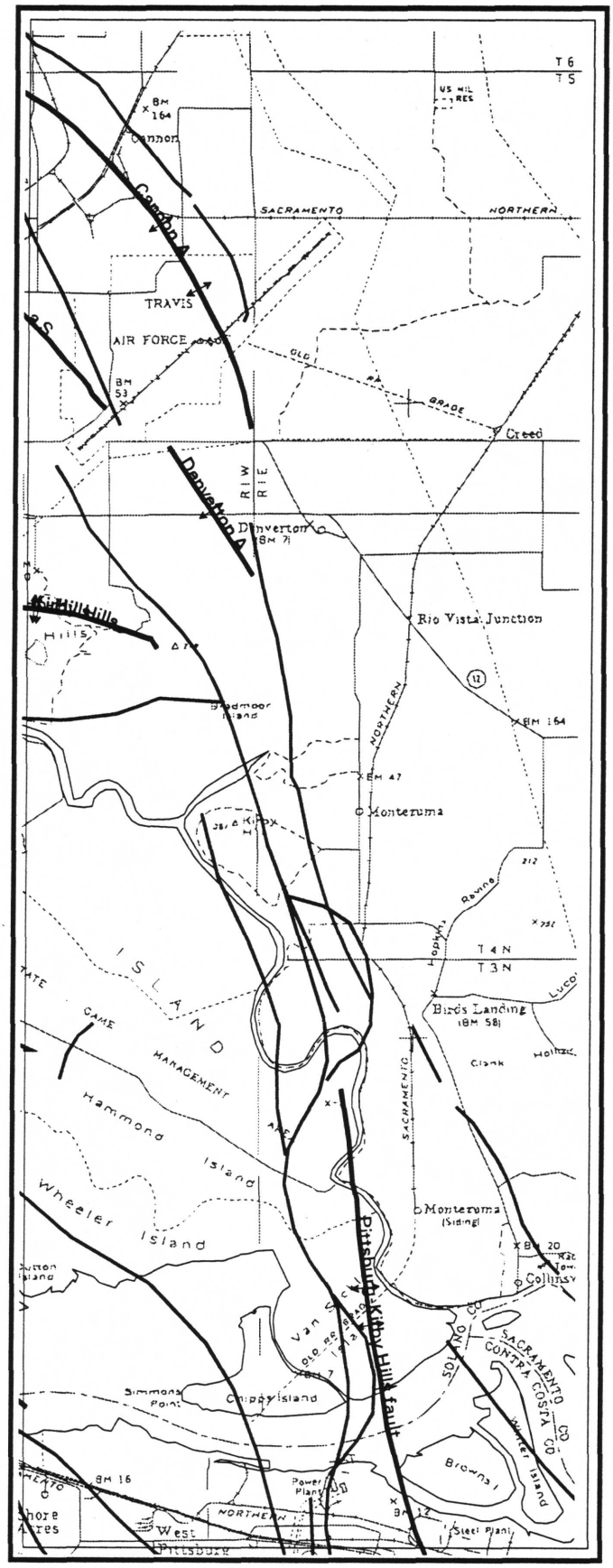

SCALE 1:150000

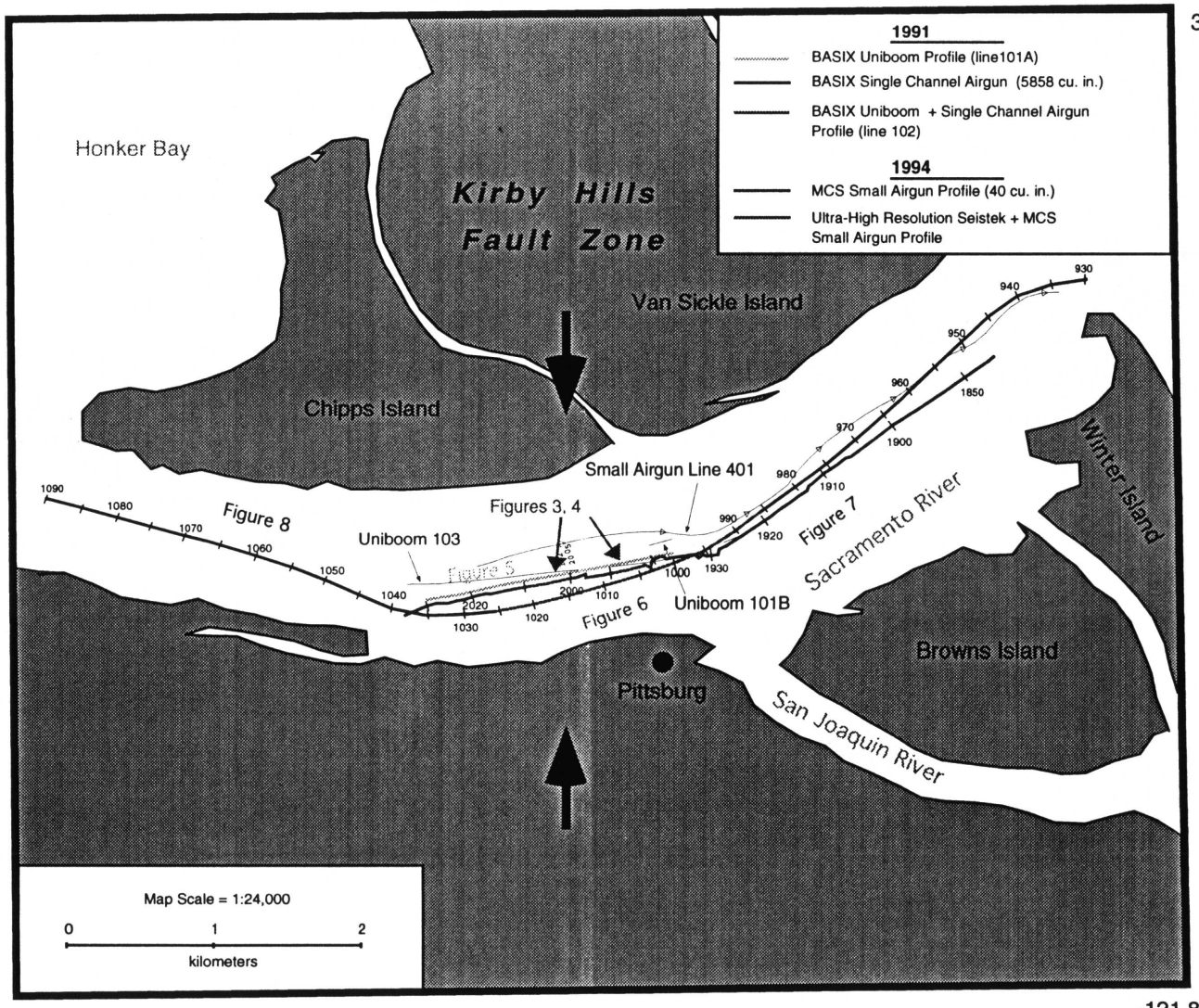

MAP SCALE 1 / 24000.00

NAUTICAL MILES

0 1

KILOMETERS

0 1 2

TRANSVERSE MERCATOR PROJECTION
STANDARD MERIDIAN = -123.0000
DISTANCE BETWEEN GRID MARKS:
LATITUDE = 6'
LONGITUDE = 6'

NAVIGATION LEGEND

CRUISE 1
Nav line
SAMPLE RATE EVERY 2.00 MINUTES

CRUISE 2
Nav line
SAMPLE RATE EVERY 2.00 MINUTES

CRUISE 3
Nav line
TIME SYMBOL EVERY 5 MINUTES
LINE LABEL
SAMPLE RATE EVERY 5 POINTS

Location of seismic profiles from the 1991 BASIX experiment and the 1994 small airgun survey. Four different seismic profiling tools were used during these two studies, providing images over a range of depths in the crust. The Seistek provided an image of the shallow upper crust (~10 meter penetration), the Unibooom imaged reflectors to depths of ~100 m, the small airguns penetrated to ~1 km, and the large airgun array penetrated to 3-5 km depth. These images are shown in Figures 3-9.

(5)

UNIBOOM LINE 101A
WEST
EAST
0.0
0.05
0.10
Two-Way Traveltime (Sec)
Kirby Hills Fault Zone
B
Multiple
Multiple
Vertical Exaggeration = 7.5:1
200 meters
37
75
Approximate Depth (meters)

(6)

UNIBOOM LINE 102
WEST
EAST
0.0
0.05
0.10
Two-Way Traveltime (Sec)
Kirby Hills Fault Zone
B
Multiple
Multiple
Multiple
Vertical Exaggeration = 7.5:1
200 meters
37
75
Approximate Depth (meters)

137

72

location not shown on attached figure

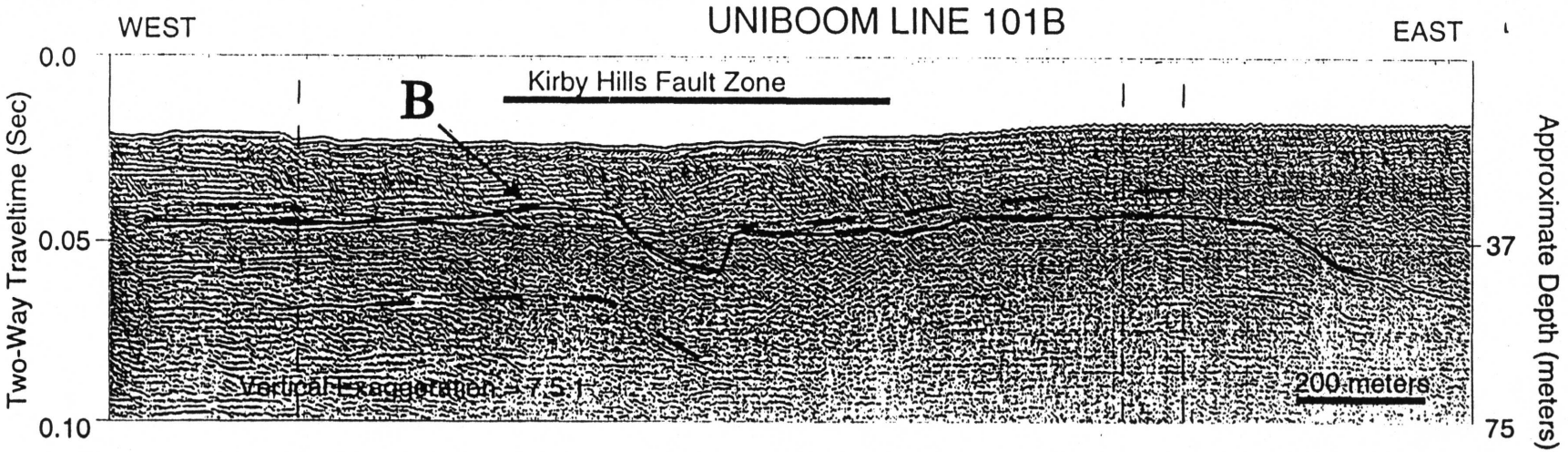

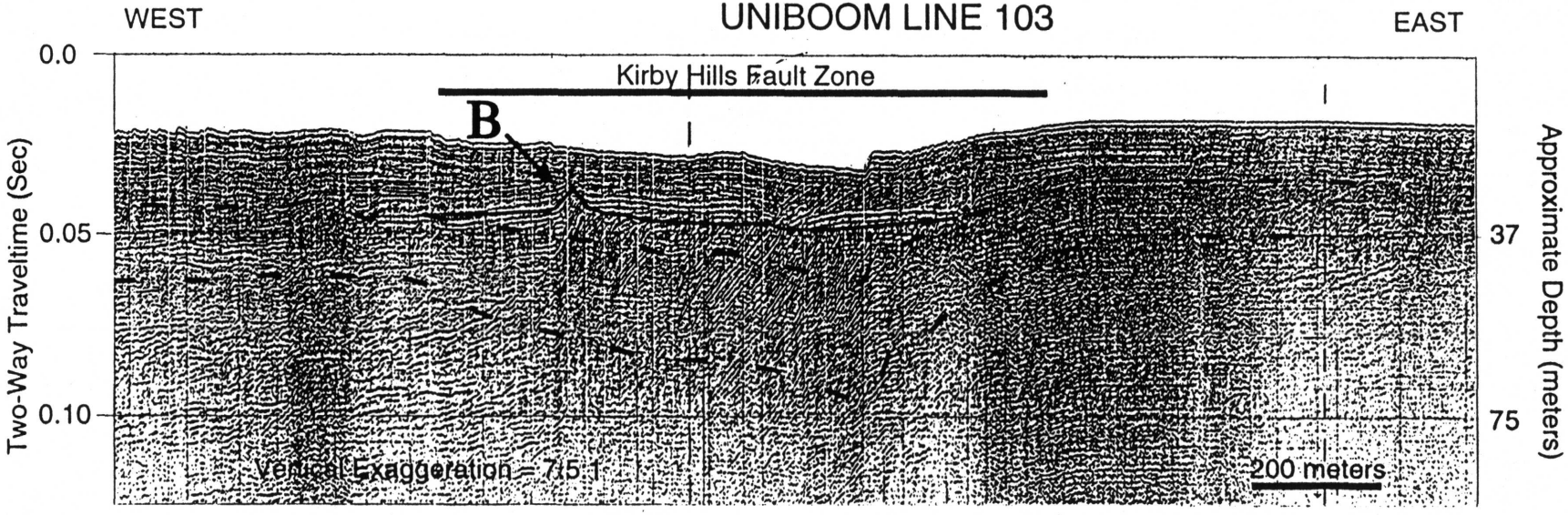

(3)

Seistec Very High Resolution Profile, Part II

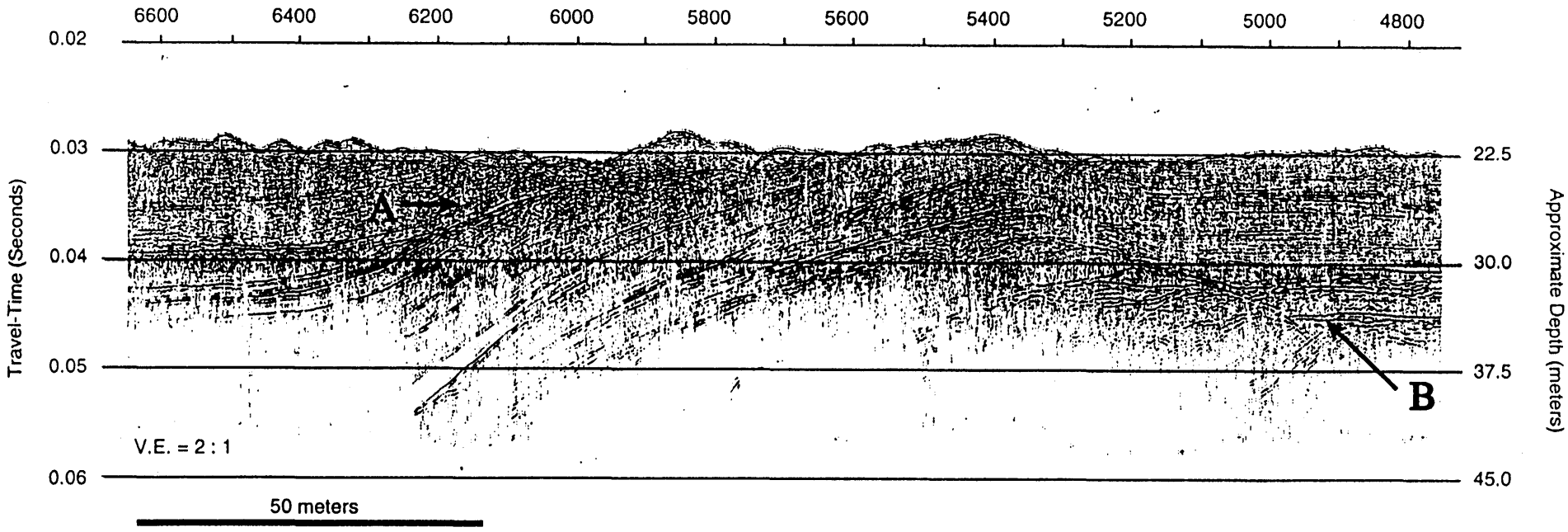

B = unconformity

A = Antiform. Unconformity is also folded here.

(4)

Seistec Very High Resolution Profile, Part I

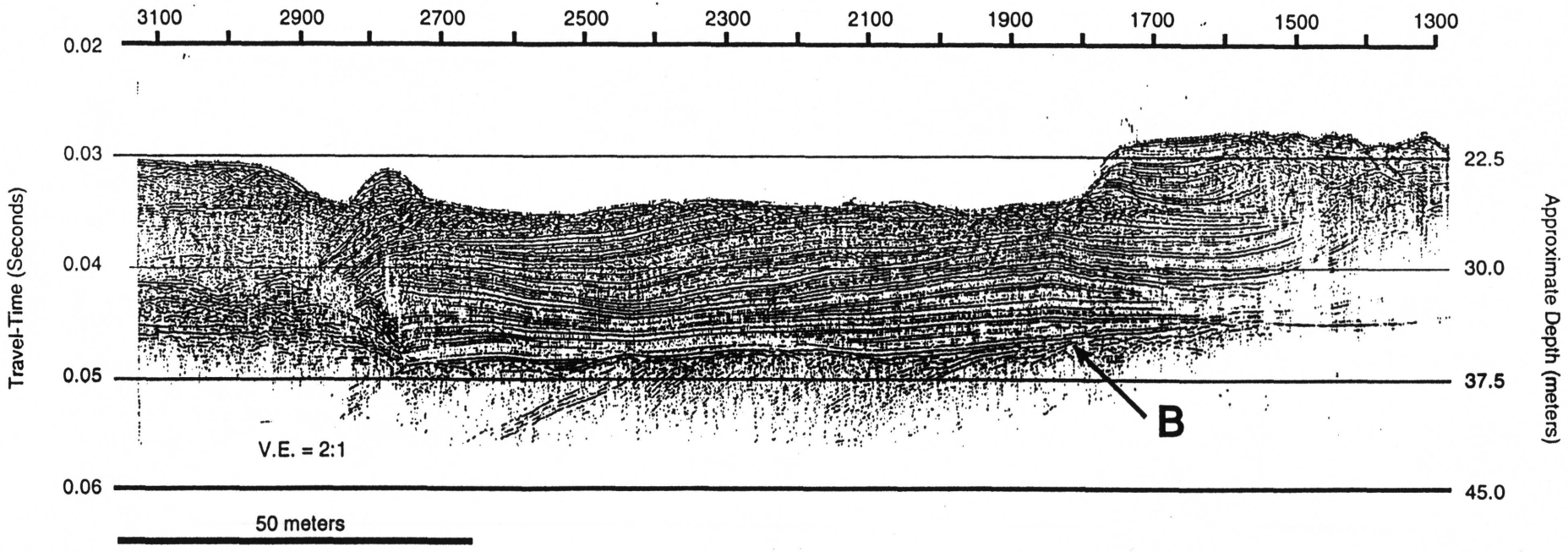

B = unconformity Age unknown

7

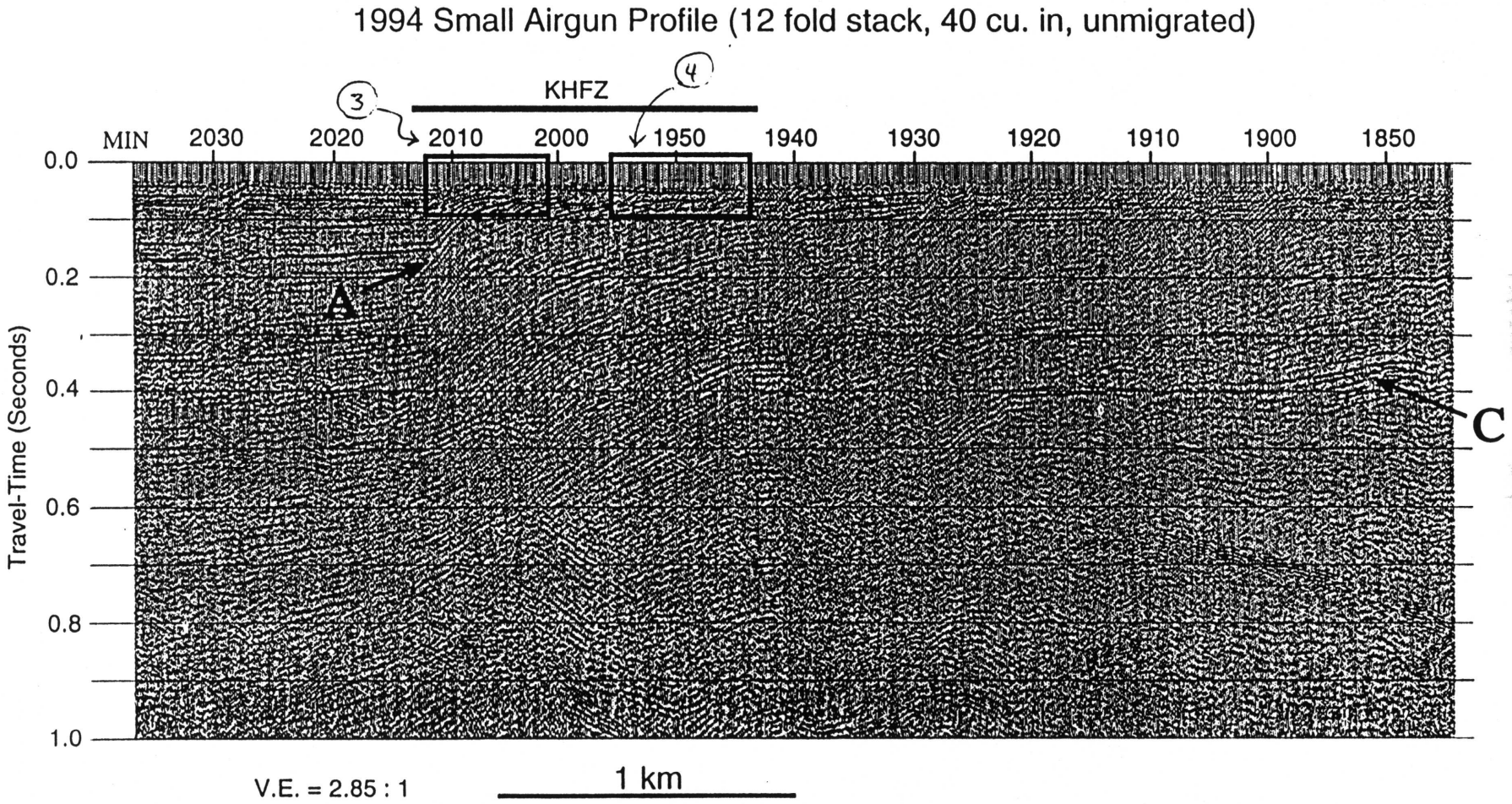
1994 Small Airgun Profile (12 fold stack, 40 cu. in, unmigrated)
KHFZ
3
4
MIN
2030
2020
2010
2000
1950
1940
1930
1920
1910
1900
1850
0.0
0.2
0.4
0.6
0.8
1.0
Travel-Time (Seconds)
A
C
V.E. = 2.85 : 1
1 km

(6)

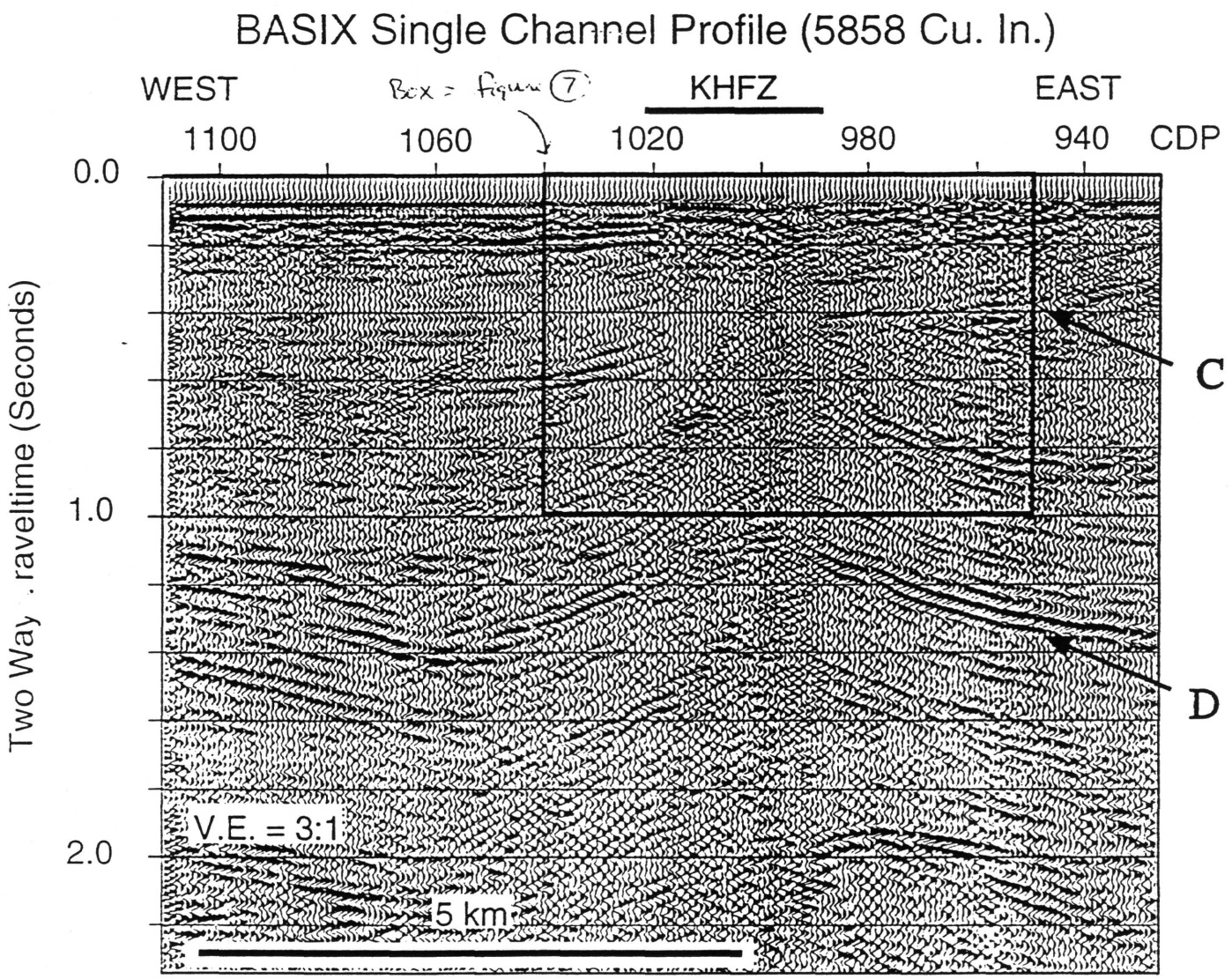
BASIX Single Channel Profile (5858 Cu. In.)
WEST
Box = figure (7)
KHFZ
EAST
1100
1060
1020
980
940
CDP
0.0
1.0
2.0
Two Way . raveltime (Seconds)
C
D
V.E. = 3:1
5 km

77

-(6) Depth converted

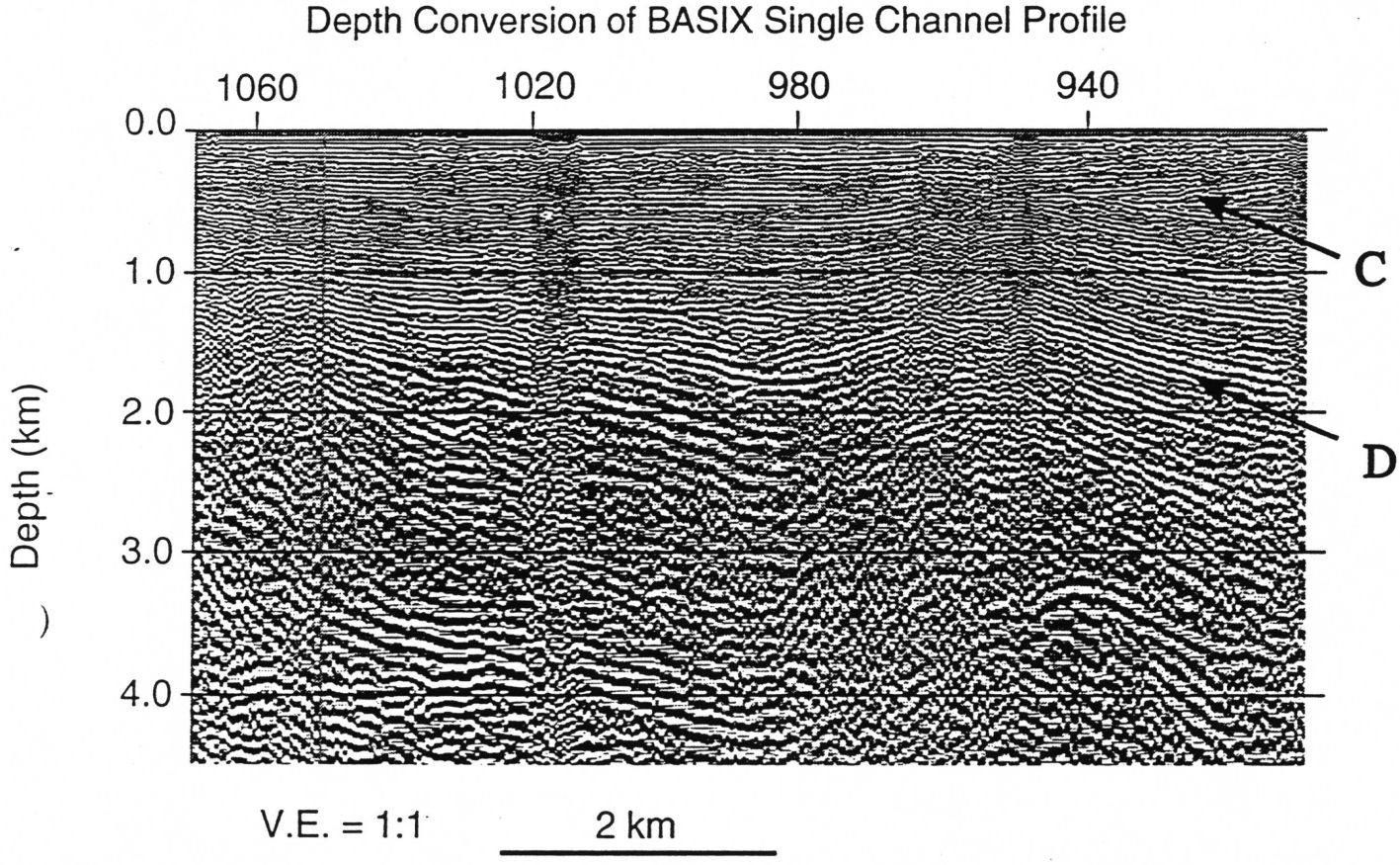

Subsurface Structure Map of the Sacramento Delta Region

Janine Weber Band, Department of Geology, University of California Berkeley

The subsurface geological structure map of the Sacramento Delta Area shows very strong evidence for active folding in several areas (marked by anticline symbols on the map). Within the Delta area, the most obvious features are the Potrero Hills and the Los Medanos Hills. Both of these features are doubly plunging anticlines related to thrust faults. The Potrero Hills are most likely a fault propagation fold, hence the overturned beds on the south side. The Los Medanos Hills overlie a complex thrust with several imbrications based on cross-sections made from tight well control (Hoffman, 1993). They also involve overturned Pleistocene Montezuma Formation on the southwest side of the fault. A large fold is seen on a seismic line that follows California Highway 12. The axis intersects the surface just north and east of the eastern end of the Potrero Hills. There is no obvious field evidence of this fold, and it may be that a recent bend of the Sacramento River has eroded and removed the upwarped sediments which may be as old as Paleocene in the core of the anticline. Smaller folds are seen lying parallel to and between the Los Medanos Anticline and Potrero Hills, the best-located fold is that beneath Ryer Island (seen on two seismic lines and well data). South of the Delta area, a small fold is developing over a wedge tip that parallels the mountain front and approximately underlies the Southern Pacific Railroad tracks between the towns of Brentwood and Tracy.

In addition to the fold axes, I mapped tiplines of thrust faults. Tiplines are the line in the subsurface where offset along a reverse or thrust fault ends. These tiplines were identified at several levels, correlated laterally to equivalent tiplines, and finally correlated laterally to faults mapped at the surface. Two well-documented tiplines are mapped along the eastern mountain front along the railroad tracks described above. One tipline is seen at 2 sec. twtt (two-way travel time), the other is seen between 3.5 and 4.0 sec twtt. The depth to the tip decreases at the ends of the fault. Tiplines parallel fold axes in the region between the Los Medanos Hills and Potrero Hills, where they appear to bottom out at 3.5 sec twtt, corresponding to approximately 2 or 3 miles depth. All the structures in this trend are likely joined along a decollement at that depth.

This portion of the map has been generated by the correlation and interpretation of seismic reflection surveys, well log data, and surface geologic data acquired through the Calcrust and BASIX programs. The author's work was supported by the University of California, Berkeley, Department of Geology and Geophysics.

Weber-Band, UCB, Sacramento Delta area

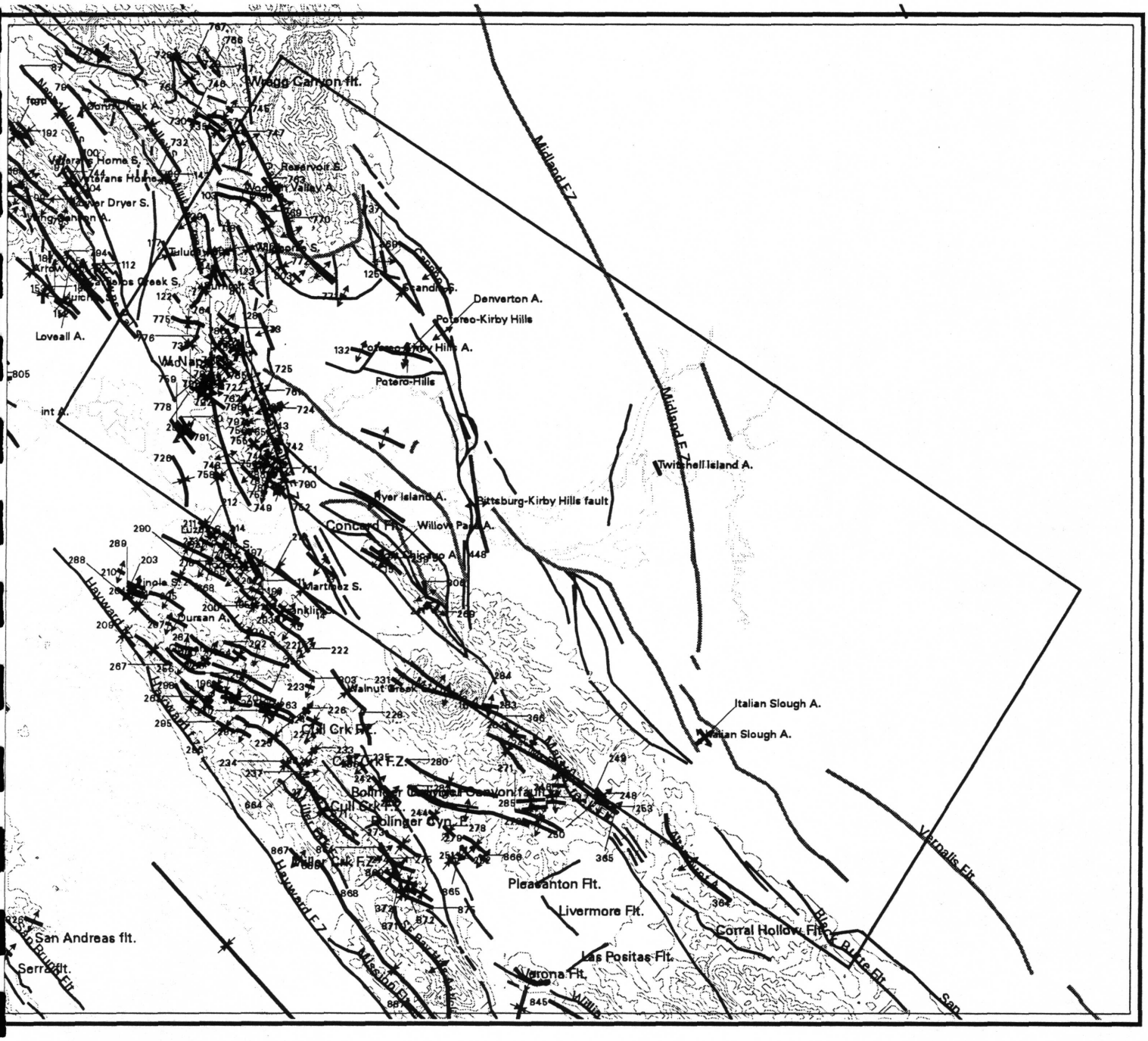

SCALE 1:600000

Weber -Band

LINEID	1024	1025	1026	1027	1028	1029	1030	1031
COMPILER	Weber-Band	Weber-Band	Weber-Band	Weber-Band	Weber-Band	Weber-Band	Weber-Band	Weber-Band
INSTITUT	U.C. Berkeley	U.C. Berkeley	U.C. Berkeley	U.C. Berkeley	U.C. Berkeley	U.C. Berkeley	U.C. Berkeley	U.C. Berkeley
SUBMISSION	6 2 95	6 2 95	6 2 95	6 2 95	6 2 95	6 2 95	6 2 95	6 2 95
STRUCTURE	Denverton Anticline	Willow Pass Anticline	Ryer Island Anticline	Italian Slough Anticline	Italian Slough Anticline	Twitchell Island Anticline		Potrero Hills
MINAGE	1	1	4	1	1	1	0	2
MAXAGE	2	2	4	2	2	2	0	3
AGECONTROL	seismic reflection	paleontologic	paleontologic	seismic reflection162	seismic reflection profile	seismic reflection		paleontologic
GEOMORPH	fluvial and lacustrine	fluvial	marine	"lacustrine, fluvial"	"lacustrine, fluvial"	"lacustrine, fluvial"		fluvial
EHORZ	2	2	0	0	0	0	0	4
CONF1	3	1	0	0	0	0	0	1.4
ERATEH	1.25	0.6	0	0	0	0	0	1.4
CONF2	3	3	0	0	0	0	0	3
ERATEV	1.9	0	0	0	0	0	0	0.43
CONF3	3	0	0	0	0	0	0	4
FOLDINIT	1.6	3.5	0	0	0	0	0	3.5
CONF4	3	1	0	0	0	0	0	3
FOLDEND	0	0	0	0	0	0	0	0
CONF5	3	0	0	0	0	0	0	3
METHOD	geologic info	balanced section						cross section
DURRAVE	1.6	3.5	0	0	0	0	0	3.5
PAPASS	no	no	no	yes	yes	no		no
DIST	19	5	0	14.5	14.5	3	0	0
ORIENTOBL	20	20	50	0	0	0		20
DISTOBL&FLT	161 G		"5, Gr"		13 Gr	3KM M		"10, G"
TREND	326	312	328	144	144	162	0	10
PLUNGE	0	0	0	0	0	0	0	0
APSTRIKE	326	312	328	144	144	162	0	10
APDIP	85	75	75	0	0	70	0	80
APDIPDR	e	n	n	e	e	W		n
CONF	definite	definite	probable	probable	probable	definite		
VERG	sw	sw	sw	sw	sw	e		s
SEGMENTED	no	yes				no		no
HALFWVL	3	0.6	2	2.5	2.5	3	0	3
FOLDDS	A	A AS	A AS	A	A	A AS		A AS
FOLDSTY	fault propagation	fault propagation	fault propagation	fault prop or bend	fault bend or fault	reactivated normal f		fault propagation
CSUBSURFAC		"Yes, Hoffman, R., 1992, Structural geology of the Concord area, in V.B. Che"						
XSECTION						"Weber-Band et al, 1995 in prep"		"Weber-Band, in prep"
DRILLHOLE	"CDOG, 4 plane by recent river scouring"	"yes, 10 holes, 1 -2 km depth"	"Yes, CDOG, 8 holes, to 8000'"	no		no		

fold style	unknown	fault propagation fold	fault propagation fold	fault bend	fault propagation	unknown		fault bend fold
Geodetic Reference				GPS Williams et al, 1994			Bulletin 181, Brooks Rogers and Day	
Subsurface data								
Structure sections	yes	Unruh and Sawyer, in progress, Crane, 1988	Unruh and Sawyer, in progress, Crane, 1988	WLA, 1995	Unruh et al, 1995	Weaver, 1949		Unruh et al, 1995
Drill Hole	unknown	Proprietary	Proprietary	yes	Unruh et al, 1995	?	Yes	Rofe, 1965; Unruh et al, 1995
Seis Reflct	unknown	Proprietary	Proprietary	Proprietary	Rameriz, 1992	Proprietary	Proprietary	Unruh and Moores, 1992; Rameriz, 1992; Unruh et al 1995;
Grav								
Historical Seismicity		Green Valley and Concord fault	Green Valley and Concord fault	Winters-Vacaville, 1892 6.4-6.7		Winters-Vacaville, 1892 6.6-6.7		yes
Mag/event								
Depth								7 km
Distrib microseis	Wong et al, 1988	Hill et al, 1991	Hill et al, 1991		Wong et al, 1988	Wong et al, 1988		Wong et al, 1988
Reference	Wong et al, 1988	Hill et al, 1991	Hill et al, 1991	Wong et al, 1988, Unruh and Moores, 1992	Wong et al, 1988	Weaver, 1949	Weaver, 1949	Wong et al, 1988
Additonal References	Wm Lettis and Assoc., 1993, Hill et al, 1991, Dibblee, numerous maps			Weaver, 1949; Bennett, 1987; Brooks et al, 1962; Eaton, 1968; Toppozada et al 1981; Thomasson et al, 1960; WLA, 1995; Unruh and Moores, 1992; Wong, 1990; Woodward-Clyde, 1989	Weaver, 1949; Brooks et al, 1962; WLA, 1995; Unruh and Moores, 1992; Loewen, 1992; Munk, 1992, Harwood and Helley, 1987; Unruh et al, 1993;	Bennett, 1987, Brooks et al, 1962, Eaton, 1986, Toppozada et al, 1981		Loewen, 1992; Munk, 1992, Harwood and Helley, 1987; Unruh et al, 1993; WLA, 1995
Extra	#	#	#	#	#	#	#	#

Rates and Styles of Quaternary Folding in the Western Great Valley and Sacramento-San Joaquin Delta Region, eastern San Francisco Bay Area

Jeffrey R. Unruh, William Lettis & Associates, Inc., 1000 Broadway, Suite 612, Oakland, CA 94607, Ph: (510) 832-3716; email: wla@netcom.com

Detailed surface mapping and analysis of seismic reflection data show that the western margin of the Sacramento Valley (the northern arm of California's Great Valley) is underlain by a system of folds and blind thrust faults that root westward beneath the northern Coast Ranges. Although stratigraphic and structural relations show that most of the contractional structures developed in latest Cretaceous or early Tertiary time (Unruh et al., 1995), many of the structures are active in the current transpressional setting and appear to be accommodating up to several mm/yr of northeast-directed shortening at a high angle to the transpressional Pacific/North American plate boundary.

Because the thrust faults in this region are blind and do not reach the ground surface, tectonic activity must be evaluated through indirect means. The surface expression of late Quaternary slip on blind thrusts beneath the southwestern Sacramento Valley includes uplift, folding and tilting of Pleistocene strata (Unruh and Moores, 1992). Additional evidence for continuing activity includes clusters of microseismicity exhibiting thrust- and reverse-faulting focal mechanisms (Wong et al., 1988). The M6.4-M6.7 1982 Winters-Vacaville earthquake in the southwestern Sacramento Valley has been attributed by several workers to slip on a blind thrust fault (Wong and Ely, 1983; Eaton, 1986). In general, seismic hazard assessments of blind thrusts in this region have combined analysis of late Cenozoic surface deformation with detailed structural analyses, including construction of kinematically-restorable cross-sections, to evaluate subsurface fault geometry and derive ranges of Quaternary slip rates (Unruh et al., 1993; Unruh et al., 1995; WLA, 1995).

To date, several late Cenozoic folds and thrust faults in the southwestern Sacremento Valley have been evaluated for Quaternary uplift and shortening rates. The Rumsey Hills, a prominent northwest-trending anticline in the northern part of the map area with crestal elevations of approximately 520-580 m, is a west-vergent fault-propagation fold developed above a blind, northeast-dipping thrust fault Ramirez (1992) concluded that approximately 1.0-1.6 km of slip occurred on the blind Rumsey Hills thrust during the past 0.5-1.0 Ma, yielding a uplift rate of approximately 0.8-1.6 mm/yr and a slip rate of approximately 1-3.5 mm/yr (1-2 mm/yr, preferred). The Dunnigan Hills, a

northeast-vergent anticline located approximately 10 km east of the Rumsey Hills, has lower crustal elevations (90-100 m) and a more subdued geomorphic expression. Detailed analysis of uplifted and deformed fluvial terraces in the Dunnigan Hills (Monk, 1992) shows that the uplift rate of this fold is approximately 0.1 mm/yr (Unruh et al., 1993), an order of magnitude lower than that of the Rumsey Hills.

These detailed studies show that the slip rates and/or shortening rates on major anticlines in the southwestern Sacramento Valley range between 1-3 mm/yr. Similar rates of contractional deformation have been obtained from analysis of Quaternary folds in the western San Joaquin Valley such as the Kettleman Hills South Dome anticline (2.5 mm/yr: Booch et al., 1993). Wakabayashi and Smith (1994) summarized available geologic and seismologic data on rates of Quaternary deformation in the western Great Valley and concluded that northeast-directed folding and thrusting in this region may accommodate most, if not all, of the ≤ 3 mm/yr of shortening normal to the transpressional Pacific/North American plate boundary permitted by regional geodetic studies.

The Potrero Hills anticline is an east-west-trending anticline in the Sacramento-San Joaquin Delta that overlies a system of south-dipping thrusts (Hector and Unruh, 1992). The orientation of the Potrero Hills anticline clearly is anomalous compared to regional northwest structural trends in the western Great Valley, implying that the direction of shortening is oblique, rather than normal, to the strike of the San Andreas system. Hector and Unruh (1992) proposed that the north-south shortening in the Potrero Hills area may be the result of a left step in the easternmost dextral faults of the San Andreas system.

Specifically, they suggested that dextral slip may be transferred from a distinct north-trending belt of strike-slip seismicity that lies along the eastern flank of Mt. Diablo, westward to the Green Valley fault across the Potrero Hills and western delta region, thus generating local north-south shortening and accounting for the anomalous east-west trend of the Potrero Hills anticline. In this interpretation, north-vergent thrust faults beneath the Potrero Hills are viewed as part of a transfer system among the easternmost faults of the San Andreas system.

South of the Delta the late Cenozoic tectonics of central Contra Costa County are dominated by growth of the west-northwest-trending, south-southwest-vergent Mt. Diablo fold-and-thrust belt (MDFTB). The Mt. Diablo anticline, which is the largest structure in the MDFTB, is approximately 25 km wide and

attains a maximum structural relief of approximately 8 km. Structural relief and amplitude of folding decrease south-southwest of Mt. Diablo. The MDFTB is bounded on the east by the dextral Greenville-Marsh Creek system, and on the west by the Calaveras and Concord faults. Unruh and Sawyer (1995) proposed that northwest dextral slip on the Greenville-Marsh Creek systems is transferred primarily to the Concord fault across a 20-km-wide restraining left-stepover. Crustal shortening in the stepover region is accommodated by growth of the MDFTB. Preliminary structural analysis indicates that the rate of late Cenozoic shortening necessary to generate uplift of the Mt. Diablo anticline (3-5 mm/yr) is comparable to the creep rate on the Concord fault (3±1 mm/yr; Galehouse, 1992), consistent with the hypothesis that northwest dextral slip probably is conserved by contractional deformation in the stepover region (Unruh and Sawyer, 1995). Additional structural analyses are planned to further test and refine this model.

The shortening rate across the MDFTB (approximately 3-5 mm/yr) is significantly greater than the 1-3 mm/yr rate of northeast-directed shortening in the southwestern Sacramento Valley. The difference in deformation rates probably accounts for the prominent geomorphic expression of Mt. Diablo relative to surrounding peaks of the northern Diablo Range. We argue that the relatively high deformation rates in central Contra Costa County are best viewed as a local phenomenon driven by strike-slip fault kinematics, rather than a measure of the component of shortening directed at a high angle to the Pacific/North American plate boundary. This interpretation is consistent with geodetic analyses that show no significant NE-directed contraction normal to faults of the San Andreas system west of the Great Valley (Lisowski et al., 1991; Williams et al., 1994). In contrast, we interpret that the northwest-trending Altamont anticline, located east of and subparallel to the dextral Greenville strike-slip fault in eastern Contra Costa County, probably accommodates a small component of NE-directed shortening normal to the plate boundary (approximately 0.3 mm/yr), and thus is kinematically analogous to northwest-striking folds in the western Sacramento Valley such as the Rumsey Hills and Dunnigan Hills.

References for Map Compilation and Text

Bennett, J.H., 1987, Winters-Vacaville earthquakes, 1892: California Geology, v. 40, p. 75-83.

Bloch, R.B., von Huene, R., Hart, P.E., and Wentworth, C.M., 1993, Style and magnitude of tectonic shortening normal to the San Andreas fault across the Pyramid Hills and Kettleman Hills South Dome, California:

Geological Society of America Bulletin, v. 105, p. 464-478.

Brooks, B.D., Rogers, D., Day, P., and Wootten, T., 1962, Field Trip 1: Sacramento Valley, *in* Bowen, O.E., ed., Geologic Guide to the Gas and Oil Fields of Northern California: California Division of Mines and Geology Bulletin, Part 4: Map 2, Geologic Map of Potrero-Kirby Hills; Map 3, Geologic Map of Putah Creek; Map 4.

Crane, R., 1988, Structural geology of the San Ramon Valley and environs, *in* R. Crane et al., eds., Field Trip Guide to the Geology of the San Ramon Valley and Environs: Northern California Geological Society, San Ramon, California, p. 1-16 and maps in Appendix 1.

Eaton, M.P., 1986, Tectonic environment of the 1892 Vacaville-Winters earthquake, and the potential for large earthquakes along the western edge of the Sacramento Valley: United States Geological Survey Open-File Report 86-370, 11 p.

Fox, K.F. Jr., Sims, J.D., Bartow, J.A., and Helley, E.J., 1973, Preliminary geologic map of eastern Sonoma County and western Napa County, California: United States Geological Survey Miscellaneous Field Studies Map MF-483.

Galehouse, J.S., 1994, Theodolite measurements of creep rates on San Francisco Bay region faults: United States Geological Survey National Earthquake Hazards Reduction Program, Summaries of Technical Reports, v. XXXV, no. I, p. 328-338.

Graymer, R.W., Jones, D.L., and Brabb, E.E., 1994, Preliminary geologic map emphasizing bedrock formations in Contra Costa County, California: a digital database: U.S.G.S. Open-File Report 94-622, 1:75,000 scale map and accompanying text.

Hector, S., and Unruh, J., 1992, Late Cenozoic blind thrusting and transpressional kinematics, Potrero Hills region, Sacramento-San Joaquin Delta, California: Program and Abstracts, American Association of Petroleum Geologists 1992 Pacific Section Convention, Sacramento, California, p. 5.

Hill, D.P., Eaton, J.P., and Jones, L.M., 1991, Seismicity, 1980-1986, *in* Wallace, R.E., ed., The San Andreas Fault System, California: U.S. Geological Survey Professional Paper 1515, p. 115-151.

Kirby, J.M., 1943, Rumsey Hills area: California Division of Mines and Geology Bulletin 118, p. 601-605.

Lisowski, M., Savage, J.C., and Prescott, W.H., 1991, The velocity field along the San Andreas fault in central and southern California: Journal of Geophysical Research, v. 96, p. 8369-8389.

Loewen, B.A., 1992, Deformation of lower Cretaceous through Tertiary strata in the Rumsey Hills-Capay Valley area: implications for late Cenozoic motion of an east-tapering underthrust wedge: M.S. thesis, University of California, Davis, 84 p.

Monk, L.P., 1992, Stratigraphy, geomorphology, soils and neotectonic interpretaion of the Dunnigan Hills, California: Ph.D. dissertation, University of California, Davis, 124 p.

Phipps, S.P., 1984, Mesozoic ophiolitic olistostromes and Cenozoic imbricate thrusting in the northern California Coast Ranges: Ph.D. dissertation, Princeton University, p. 352.

Ramirez, V.R., 1992, Geology and deep structure of the Rumsey Hills area, Sacramento Valley, California, *in* Erskine, M., Unruh, J. Lettis, W., and Bartow, A., eds., Field Guide to the tectonics of the boundary between the Coast Ranges and Great Valley of California: Guidebook 70, Pacific Section, American Association of Petroleum Geologists, p. 85-94.

Rofe', R., 1962, Dunnigan Hills gas field, California: California Division of Mines and Geology Bulletin 181, p. 119-132.

Sims, J.D., Fox, K.F. Jr., Bartow, J.A., and Helley, E.J., 1973, Preliminary geologic map of Solano County and parts of Napa, Conta Costa, Marin and Yolo counties, California: United States Geological Survey Miscellaneous Field Investigations Map MF-484, 5 sheets.

Thomasson, H.G. Jr., Olmstead, F.H., and LeRoux, E.F., 1960, Geology, water resources and usable ground-water storage capacity of part of Solano County, California: United States Geological Survey Water-Supply Paper 1464, 493 p. plus plates.

Tolman, F.B., 1943, Potrero Hills gas field: California Divsion of Mines and Geology Bulletin 118, p. 595-598.

Toppozada, T.R., Real, C.R., and Parke, D.O., 1981, Preparation of isoseismal maps and summaries of reported effects of pre- 1990 California earthquakes: California Division

of Mines and Geology Open-File Report 81-11, 182 p.

Unruh, J.R., Munk. L.P., Loewen, B.A., Moores, E.M., and Sourhard, R.J., 1993, Quaternary blind thrusting in the southwestern Sacramento Valley, California: Geological Society of America Bulletin, v. 107, p. 38-53.

Unruh, J.R., and Sawyer, T.L., 1995, Late Cenozoic growth of the Mt. Diablo fold-and-thrust belt, Contra Costa County, California, and implications for transpressional deformation of the northern Diablo Range: 1995 Pacific Section Abstracts, American Association of Petroleum Geologists and Society of Economic Paleontologists and Mineralogists, p. 47.

Wagner, D.L., and Bortugno, E.J., 1982, Geologic map of the Santa Rosa quadrangle: California Division of Mines and Geology 1°x2° series, scale 1:250,000.

Wakabayashi, J., and Smith, D.L., 1994, Evaluation of recurrence intervals, characteristic earthquakes, and slip rates associated with thrusting along the Coast Range-Central Valley geomorphic boundary: Bulletin of the Seismological Society of America, v. 84, p. 1960-1970.

William Lettis & Associates, 1993, Altamont Landfill and resource recovery facility: fault investigation for the proposed expansion area: evaluation prepared for RUST Environment and Infrastructure, Inc., 64 p.

William Lettis & Associates, 1995, Seismotectonic evaluation, Stony Gorge, East Park and Monticello Dams: prepared for the Department of the Interior, U.S. Bureau of Reclamation, Denver, Colorado, 110 p. plus appendices and plates.

Williams, S.D.P., Svarc, J.O., Lisowski, M., and Prescott, W.H., 1994, GPS measured rates of deformation in the northern San Francisco Bay Region, California, 1990-1993: Geophysical Research Letters, v. 21, p. 11511-1514.

Wong, I.G., 1990, Seismotectonics of the Coast Ranges in the vicinity of Lake Berryessa, northern California: Bulletin of the Seismological Society of America, v. 80, p. 935-950.

Wong, I.G., and Ely, R.W., 1983, Historical seismicity and tectonics of the Coast Ranges-Sierra block boundary: implications to the 1983 Coalinga earthquakes, *in* Bennet, J., and Sherburne, R., eds., The 1983 Coalinga, California Earthquakes: California Division of Mines and Geology Special Publication 66, p. 89-104.

Wong, I.G., Ely, R.W., and Kollman, A.C., 1988, contemporary seismicity and block tectonics of the northern California and central Coast Ranges-Sierran block boundary zone, California: Journal of Geophysical Research, v. 93, p. 7813-7833.

Woodward-Clyde Consultants, 1989, Seismotectonic study for Monticello Dam: prepared for Solano County Water Policy Advisory Committee, 66 p. plus Bibliography and Appendix.

Unruh, Dunnigan Hills area

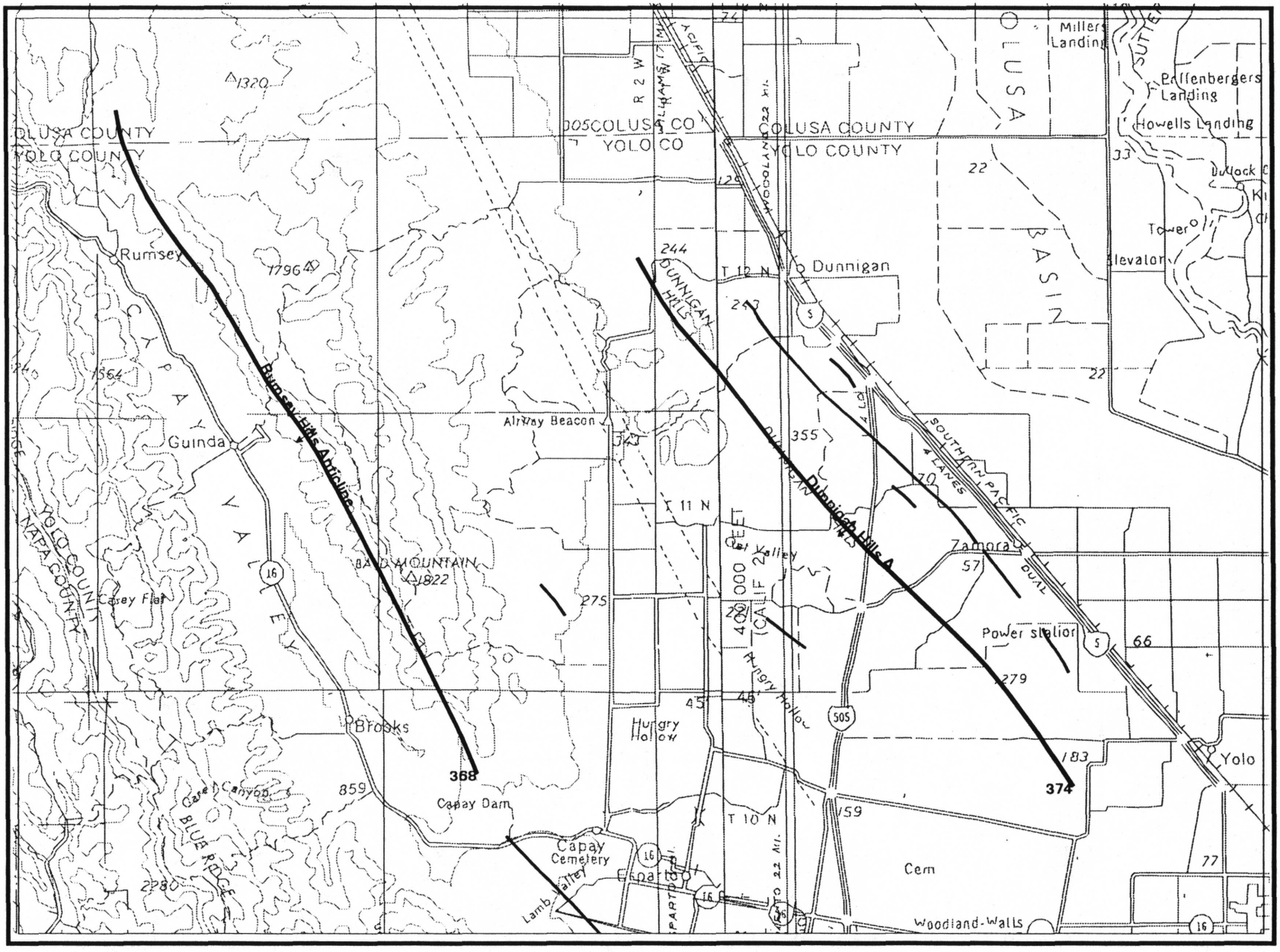

Unruh, W.Lettis and Associates, Vacaville area

SCALE 1:200000

Unruh, W.Lettis and Associates, Mt Diablo area

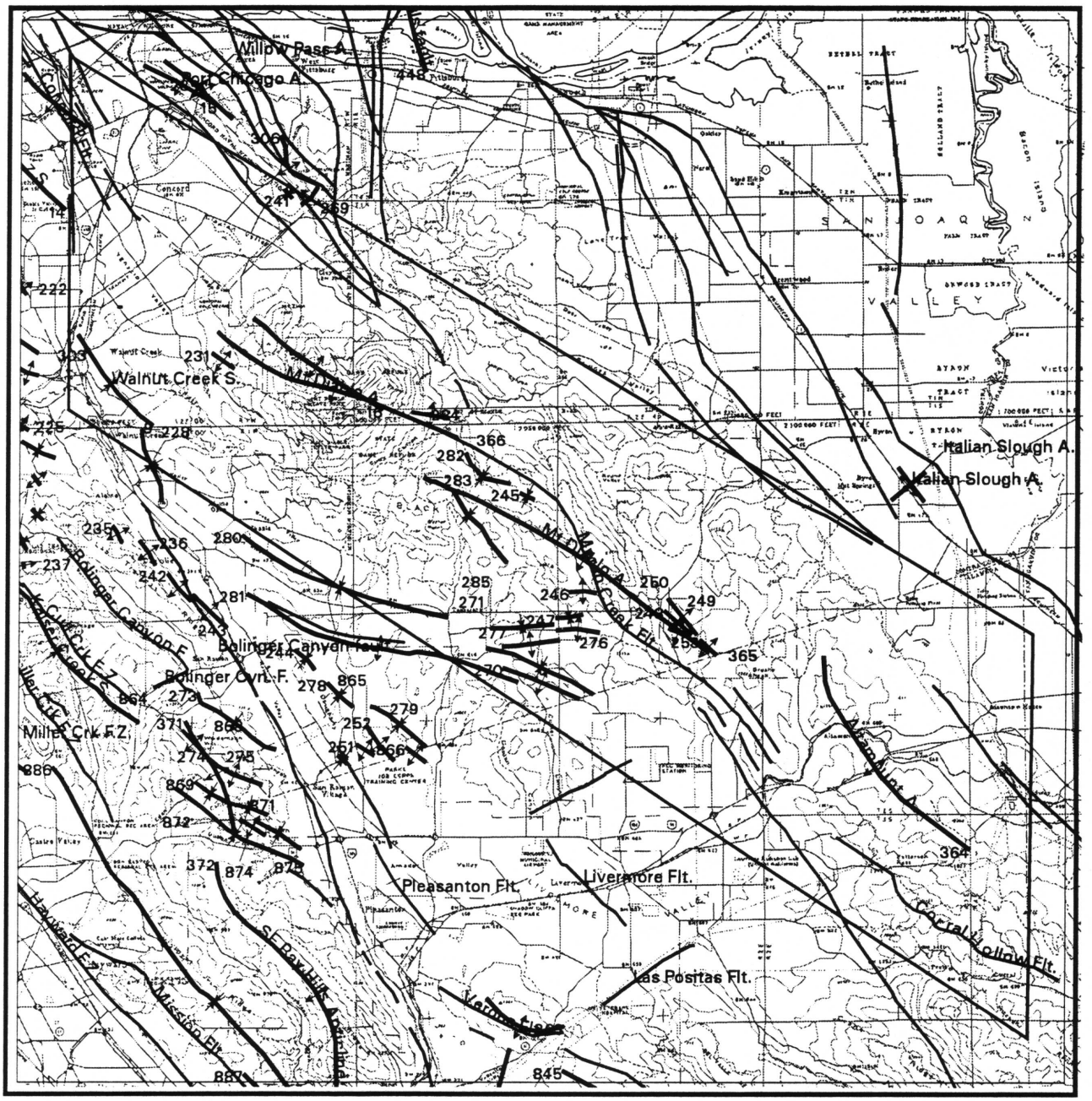

SCALE 1:300000

Unruh

Arc Ln id	364	365	366	367	368	369	370	374
Compiler(s)	Unruh, J. R.	Unruh, J. R.	Unruh, J. R.	Unruh, J. R.	Unruh, J. R.	Unruh, J. R.	Unruh, J. R.	Unruh, J. R.
Institution	WLA	WLA	WLA	WLA	WLA	WLA	WLA	WLA
D of submis	Apr 21, 95	Apr 21, 95	Apr 21, 95	Apr 21, 95	Apr 21, 95	Apr 21, 95	Apr 21, 95	Apr 21, 95
Project/Contract	1434-94-G-2463	1434-94-G-2463	1434-94-G-2463	1434-94-G-2463	1434-94-G-2463	1434-94-G-2463	1434-94-G-2463	1434-94-G-2463
Map_scale	100000	100000	100000	100000	100000	100000	100000	100000
Original_source_scale	24000	24000	24000	24000	24000	24000	40550	
Structure_Name	Altamount Anticline	Mt Diablo Anticline	Mt Diablo Anticline	Garden V., see 121	Rumsey Hills anticline	Cannon anticline	Potereo Hill - Kirby Hills	Dunnigan Hills anticline
age_min	1	2.5	2.5	1	1	6	2	1
age_max		4.5	4.5				4	
Age_control	soil stratigraphy	K/Ar on folded tephra, Graymer et al, 1994	K/Ar on folded tephra, Graymer et al, 1994	soil stratigrphy, tephra, 3.4-1.0 Ma strata deformaed (Tehama Fm.)	paleontologic, soil stratigraphy, tephra	paleontologic	K/Ar Tehama, 3.4-1.0 Ma	paleontologic, C14, soil stratigraphy
Inclined Geomorphic surface	fluvial	fluvial	fluvial		fluvial	unknown		fluvial
horiz short (km)	0.6	10	10	1	1.3			0.1
c1	3	3	3	3	2			4
Shortening rate mm/yr	0.3	3	3	1	2			0.1
c2	4	3	3	3	2			4
vert rate mm/yr	0.5	3	3	0.6	0.6			0.1
c3								
Initiation of folding (Ma)	4	2.5	2.5	0.7	0.8			0.8
c4	4	3	3	4	2			2
Termination of folding (Ma)	0	0	0	0	0			0
c 5								
Method	line-length rest, and uplift of quaternary pediments	balanced x-section	balanced x-section	cross-section	x-section			uplifted fluvial terraces
Rate ave duration	7	4	4	0.75	0.75			0.75
Para ss	yes	no	no	yes	yes	yes	No	yes
Ave dist from fault	4			7	24	15		4
Ave Ori		35	35				80	
Distance fm faults								
Ave. Trend	305	290	290	152	332	150	105	140
Plunge							15	3
Ave AP strike	305	290	290	332	332	330		320
AP dip	90	60	60	90	40			90
AP dip dir		n	n		n			
Confidence of location	Probable	Probable	Probable	Probable	Definite	Probable	Definite	Probable
Verge dir	ne	sw	sw	ne	sw	ne	sw	ne
Multi or seg	no	yes	yes	yes	yes	no?		no
Interlb ang								
Bck-lb strk	305	290	290	332	332	330		320
Bck-lb dip	20	45	45	25	20	25		3
Bck-lb dip dir	sw	ne	ne	sw	ne	sw		sw
Bck-lb dim (km sq)	45	275	275	150	240	20		50
Fr-lb strike	305	290	290	332	332	330		320
Fr-lb dip	20	80	80	35	80	47		5
Fr-lb dip dir	ne	ne	ne	ne	nw	ne		ne
Fr-lb dim (km sq)	55	210	210	225		20		25
half wvlgth (km)	10	25	25	14	10	4.2		8
fold type	A, U	A, AS	A, AS	A, AS	overturned, A, AS	A, AS	A	A, AS

SEISREFLT	"CGG seismic data, in Weber-Band et al in prep"		Basix and chevron	"CGG reflection profile, see Weber-Band et al, 1995"	"CGG and Chevron, see Weber-Band et al, 1995"	"CGG refection profile, Weber-Band et al, 1995 in prep"	Shell Oil
HISTSEIS						no	"yes,"
MAGEVENT							3
DEPTH	0	0	0	0	0	0	15
DISTRISEIS	yes			yes	yes		yes
REFERENCES			"Weber-Band, Jones, et al, 1995, Shallow tectonic wedges, active folds and reactivated faults at the eastern margin of the Coast Ranges, Sacramento Delta area, California, in prep"				

Plio-Pleistocene strain rates associated with regional folding, Sonoma area, California

A.S. Jayko, N. Green Nylen and K. M. Scharer, U.S. Geological Survey, 345 Middlefield Rd., MS-975, Menlo Park, Ca., 94025

Major Plio-Pleistocene fold structures that lie between the Rodgers Creek and West Napa fault zones in the Napa-Sonoma area were studied to estimate the minimum magnitudes of crustal shortening between major strike-slip faults during the Late Cenozoic (latest Miocene to present) . The structures studied include the Kenwood-Sonoma syncline, Napa syncline, Miyakma anticline, Rutherford anticline and Carneros fault (Weaver, 1949; Fox and others, 1973). En echelon folds apparently overlie the buried northward extension of the Carneros fault. The folds are generally open and gently plunging, or asymmetric and commonly northeast verging with steeply southwest-dipping axial planes.

The base of the Sonoma volcanics was used as a strain marker; the unit ranges in age from 2.9 and about 8 Ma (Fox, 1983). The folds are considered to postdate the top of the unit, thus are probably late Pliocene or younger. Large-scale folds with half-wavelengths of 4-5 kilometers show minimum shortening of 8 to 15% with shortening rates of about 0.1 to 0.2 mm/yr., and relative uplift rates of about o.25 to 0.5 mm/yr. Numerous small-magnitude earthquakes occur at depth beneath the mapped trace of the Miyakma and Rutherford anticlines

The fold related strain rates are generally and order of magnitude less than horizontal displacement rates determined from NA-PAC plate motion models and Quaternary fault studies.

Fox, K. F., 1983, Tectonic Setting of Late Miocene, Pliocene, and Pleistocene Rocks in Part of the Coast Ranges North of San Francisco, California: U. S. Geological Survey, Professional Paper, no. 1239,

Fox, K.F. Jr., and others, 1973, Preliminary Geologic Map of eastern Sonoma County and western Napa County, California: U.S. Geological Survey Miscellaneous Field Studies Map MF-483, 1:62, 500.

Weaver, C.E., 1949, Geology of the Coast Ranges immediately north of the San Francisco Bay region, California: Geological Society of America Memoir 35, 1:62,500.

Jayko, Sonoma area

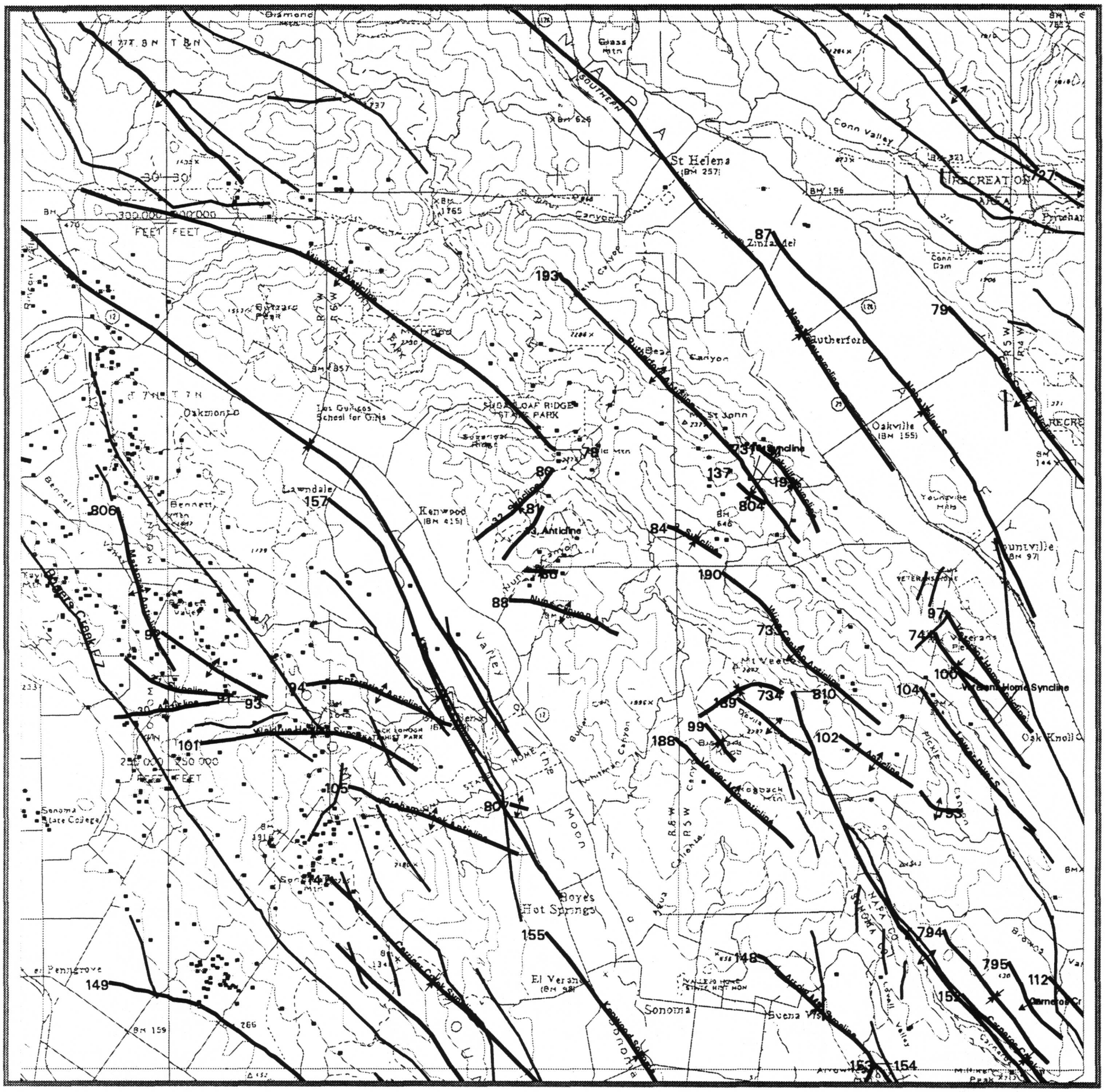

SCALE 1:160000

1 .5 0 1 2 3 4 5 6 7 MILES

1 .5 0 1 2 3 4 5 6 7 KILOMETERS

0 2 4 6 8 10 12 14 THOUSAND FEET

Jayko

LINEID	**155**	**78**
COMPILER	Jayko A, GreenNylen N, Scharer	Jayko A. S., Scharer, K.M., Platz M
INSTITUT	USGS	USGS
SUBMISSION	4/15/94	4/15/94
PROJECT	9540-10200	9540-10200
COMMAPSCALE	62500	62500
ORIMAPSCL	62500	62500
STRUCTURE	Kenwood-Sonoma Syncline	Miyakma Anticline
MINAGE	2	2
MAXAGE	5	5
AGECONTROL	Sonoma Volcanics, K-Ar	Sonoma Volcanics, K-Ar
GEOMORPH		
EHORZ	0.34	0.3
CONF1	3	3
ERATEH	0.12	0.53
CONF2	3	3
ERATEV	0.53	0.53
CONF3	3	3
FOLDINIT	3	2
CONF4	3	4
FOLDEND	0.5	0.5
CONF5	5	4
METHOD	structure sections	structure section
DURRAVE	3	3
PAPASS	no	no
TREND	128	292
PLUNGE	5	6
APSTRIKE	308	291
APDIP	88	79
APDIPDR	N	N
CONF		
VERG	sym	
SEGMENTED	no	no
ILIMBA	121	63
BLSTRIKE	317	279
BLDIP	27	25
BLDIPDR	E	N
FLSTRIKE	120	120
FLDIP	33	39
FLDIPDR	S	S
FOLDDS	S	A
REFERENCES	Weaver 1949, Fox et al 1973	Weaver 1949
ADDCOMMENTS		
EXTRA	#	#

Inverness and Point Reyes Anticlines, and Point Reyes Syncline

K. R. Lajoie, U.S. Geological survey, MS-977, Menlo Park, California, 94025

The Point Reyes peninsula lies between the right-lateral San Andreas fault and the offshore, north-dipping Point Reyes thrust fault (Figures 1 to 5). Inverness ridge and the Point Reyes headland are topographic and structural highs (Inverness and Point Reyes anticlines) separated by a partially flooded lowland, (Point Reyes syncline) (Figure 3). Inverness Ridge is the erosional remnat of an elongate anticline that formed in response to slight plate convergence at a minor bend in the San Andreas fault (Figure 4). Point Reyes headland is the erosional remnant of an anticline that formed in response to southward thrusting above the offshore Point Reyes fault (Figure 3).

BIBLIOGRAPHY

Galloway, A.J., 1977, Geology of the Point Reyes peninsula Marin County, California: California Division of Mines and Geology, Bulletin 202, p. 72, map scale 1:48,000.

McCulloch, D.S., 1983, Fault and Epicenter map in the Gulf of the Farallones area: U.S. Geological Survey Administrative Report.

Minard, C.R. Jr., 1971, Quaternary beaches and coasts between the Russian River and Drakes Bay: California University, Berkeley, Hydraulic Engineering Laboratory, HEL-2-35, 193 p.

FIGURE 1

The Point Reyes peninsula lies between the right-lateral San Andreas fault and the offshore, north-dipping Point Reyes thrust fault. Inverness ridge and the Point Reyes headland are topographic and structural highs separated by a partially flooded lowland, the Point Reyes syncline (Figures 2 through 4). Modified from McCulloch (1983).

FIGURE 2

Generalized geologic map of the Point Reyes peninsula. Cretaceous granitic rocks (Kgr), crop out along the northern part of Inverness ridge and at the Point Reyes headland. These outcrops lie along the axes of the Inverness and Point Reyes anticlines (Figure 3). Miocene sedimentary rocks (M) dip off the exposed granitic rocks toward the axis of the intervening Point Reyes syncline. The Inverness anticline is most clearly expressed in the southeast part of the peninsula where the Miocene rocks are tightly folded across the northwest-trending axis, which extends along the crest of Inverness Ridge to Tomales Point (Figure 3). This anticline reflects compressional uplift at the slight left bend in the right-lateral San Andreas fault; northwest of Point Reyes the fault strikes about N36° W, while southeast it strikes about N33° W. The subsurface extent of the Miocene rocks is not known, but they might form a buried, northwest-trending syncline with its axis lying beneath the northeastern part of Drakes Estero (Galloway, 1977) (Figure 3). Pliocene marine sedimentary rocks (P), which unconformably overlie the Miocene rocks, have been warped into gentle folds on the limbs of the Point Reyes syncline, the two most prominent being the Mendoza anticline and syncline. The axis of the Point Reyes syncline is poorly constrained because the Pliocene beds near Drakes Estero are virtually flat-lying. It is not known if the Pliocene beds originally extended over the Inverness and Point Reyes anticlines. If they did, they have been completely removed by subsequent erosion. If they did not, the two anticlines probably existed when the Pliocene beds were deposited. Quaternary marine deposits (Qt1), here tentatively correlated with the 320ka sea-level highstand, rest on an uplifted wave-cut platform, the remnants of which form flat ridge crests east and west of Drakes Estero. The extent of this terrace has not been mapped in detail, but it appears to be warped into a broad syncline. A sheet of stabilized Pleistocene dune sand (Qd1), here tentatively correlated with the 124ka sea-level highstand, occupies the topographic and structural low northeast of Drakes Estero. A complex of large, deep-seated landslides (LS) occurs in Miocene and Pliocene rocks along the southeast shore of Drakes Bay. Rapid sea-cliff erosion and the seaward dip of the beds along the southwest limb of the Inverness anticline account for the massive slope failures in this area. Geologic data modified from Minard (1971), Galloway (1977) and McCulloch (1983).

FIGURE 3

Cross section of Point Reyes peninsula showing structures delineatedmainly by Tertiary sediments. The Inverness anticline is a compressional fold reflecting crustal shortening at a minor left bend in the right-lateral San Andreas fault. Southeast of this section the Miocene beds (M) warped completely over the granitic rocks (Kgr) (Figure 2) constrain the axis of the anticline. The Point Reyes and Mendoza anticlines, and the Mendoza syncline are compressional folds in the upper plate of the offshore Point Reyes thrust fault. The southern limb of the Point Reyes anticline has been recently removed by sea-cliff erosion. The Point Reyes syncline is the broad structural low between the Mendoza and Inverness anticlines. Miocene rocks crop out prominantly on the souwest limb of the Inverness anticline, but nowhere else on the peninsula. Also, these rocks were not penetrated in an exploratory well drilled into the cresat of the Mendoza anticline. Consequently, the Miocene rocks are probably folded into a tight syncline adjacent to Inverness ridge (Galloway, 1977). If correct, this interpretation impies that the axis of synclinal folding has migrated to the southwest. Modified from Gallolway (1977). See Figure 2 for location.

FIGURE 4

Map showing late Tertiary to late Quaternary structures on Point Reyes peninsula. The Inverness anticline reflects compressional uplift at the slight left bend in the right-lateral San Andreas fault; northwest of Point Reyes the fault strikes about N37° W, while southeast it strikes about N34° W. The southeastern part of anticlinal axis is well constrained by attitudes in the Tertiary sedimentary rocks (T) (Figure 2), while the northwestern part is poorly constrained. Here the axis is drawn along the crest of Inverness ridge. The Point Reyes and Menoza anticlines and the Mendoza syncline reflect north-south compression in the upper plate of the offshore Point Reyes thrust fault; only the northern limb of the Point Reyes anticline survives above sea level, the axis and southern limb having been recently removed by sea-cliff erosion. The Inverness and Point Reyes anticlines are the dominant structures of the peninsula, the Point Reyes syncline merely being the structural low between them. The axes of the minor folds in the Tertiary rocks (T) east and west of Drakes Estero are well constrained, but the axis of the Point Reyes syncline is poorly constrained owing to

near-horizontal bedding in the Tertiary rocks undrelying the lowland between the Inverness and Point Reyes anticlines. See Figure 3 for cross section A - A. Data for the faults and minor folds modified from Galloway (1977) and McCulloch (1983).

FIGURE 5

Quaternary marine deposits (Qt1), here tentatively correlated with the 320ka sea-level highstand, rest on an uplifted wave-cut platform southwest of Drakes Estero. Flat ridge crests truncating the underlying Pliocene sediments throughout the lowland are probably remnants of this platform, which appears to be warped into a gentle syncline. The extent of the platform, and of at least one higher platform, have not been mapped in detail. Consequently, the full extent of tectonic deformation these platforms might record is not known. The Qt3 platform appears to be deformed across a minor anticline and syncline near Point Reyes (Figure 2) (Galloway, 1977), but topographic analysis suggests that the platform is erosionally dissected, not warped, in this area. However, the erosion pattern might reflect the underlying structures. A sheet of stabilized Pleistocene dune sand (Qd2), here tentatively correlated with the 124ka sea-level highstand, occurs northeast of Drakes Estero. The restricted extent of this dune field suggests that it occupies a topographic and structural low in the Qt1 platform. A broad erosional platform (Qt2), here tentatively correlated with the 124ka sea-level highstand, is well developed at Bolinas Point. The shoreline angle of this platform lies at 60m, which yields an uplift rate of 0.44m/ka. Remnants of the Qt2 platform descend to sea level east of Drakes Estero, indicating it dips southwestward toward the axis of the Point Reyes syncline. Another terrace remnant tentatively correlated with the 124ka highstand lies at 60m on the southwest side of Tomales Point, which again yields an uplift rate of 0.44m/ka. If this rate is correct, the 2m platform (Qt3) cut into the granitic rocks on both sides of Tomales Point (Minard, 1971) correlates with the 60ka sea-level highstand. More significantly though, if the rate is correct, and is applied to the entire length of Inverness ridge, the 407m summit was at sea level at about 925ka. However, the outcrop pattern of bedrock units strongly indicates that the uplift rate is variable along the ridge, and is probably greatest at the highest part of the ridge. Consequently, 0.44m/ka is probably the minimum uplift rate for the summit. Beach and dune sands tentatively correlated with the 124ka highstand crop out in the modern sea cliff at both ends of Point Reyes beach, suggesting that these areas have been uplifted relative to the area between. Collectively, all the features correlated with the 124ka highstand (Qd2 and Qt2) indicate that the major folding reflected in the Tertiary rocks (Figure 2) continued into the late Pleistocene. Geologic data modified from Minard (1971), Galloway (1977) and McCulloch (1983).

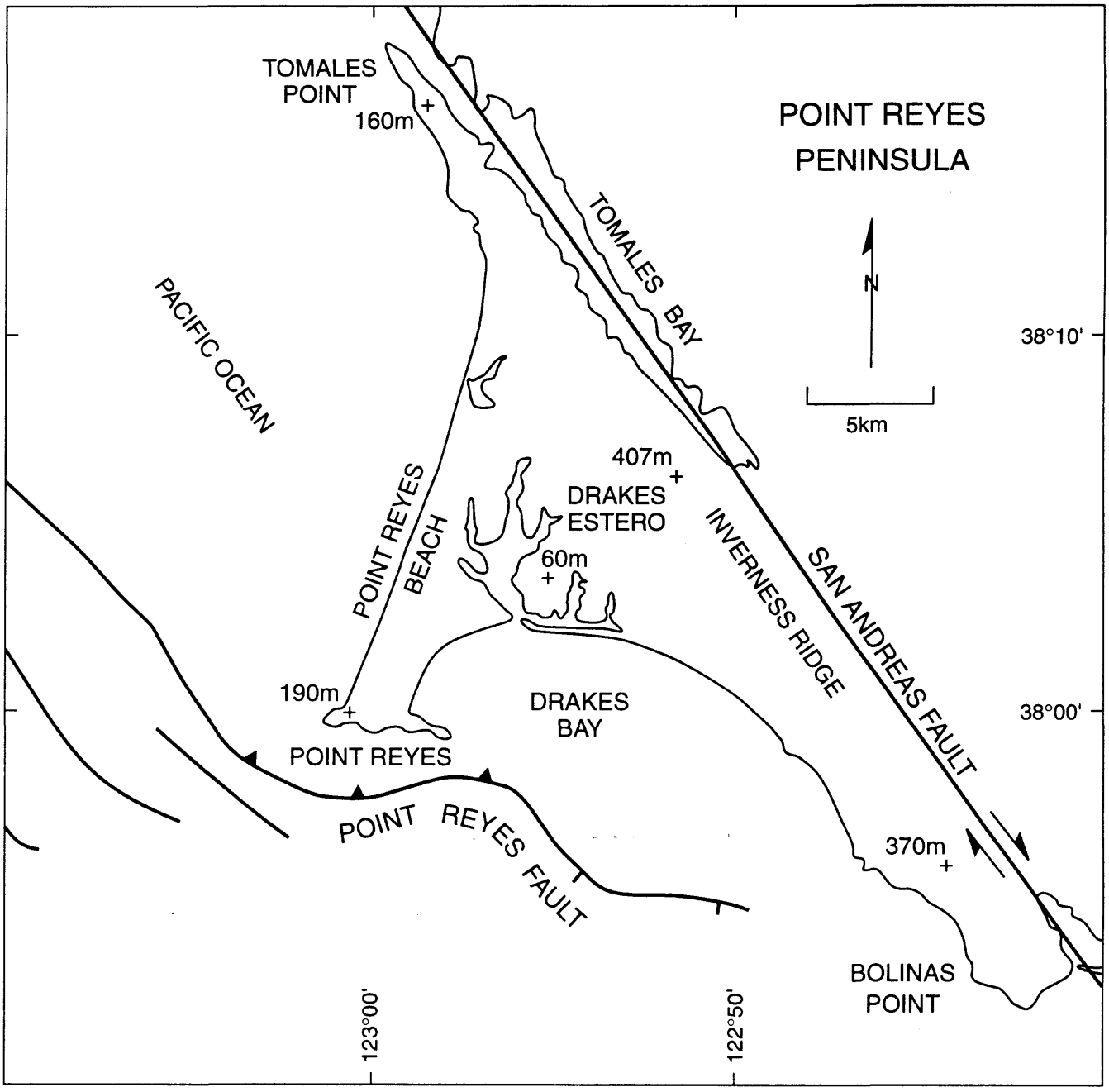
TOMALES
POINT
160m
POINT REYES
PENINSULA
TOMALES BAY
N
5km
PACIFIC OCEAN
38°10'
407m
DRAKES
ESTERO
60m
POINT REYES
BEACH
INVERNESS RIDGE
SAN ANDREAS FAULT
190m
DRAKES
BAY
38°00'
POINT REYES
POINT REYES FAULT
370m
BOLINAS
POINT
123°00'
122°50'

FIGURE 1

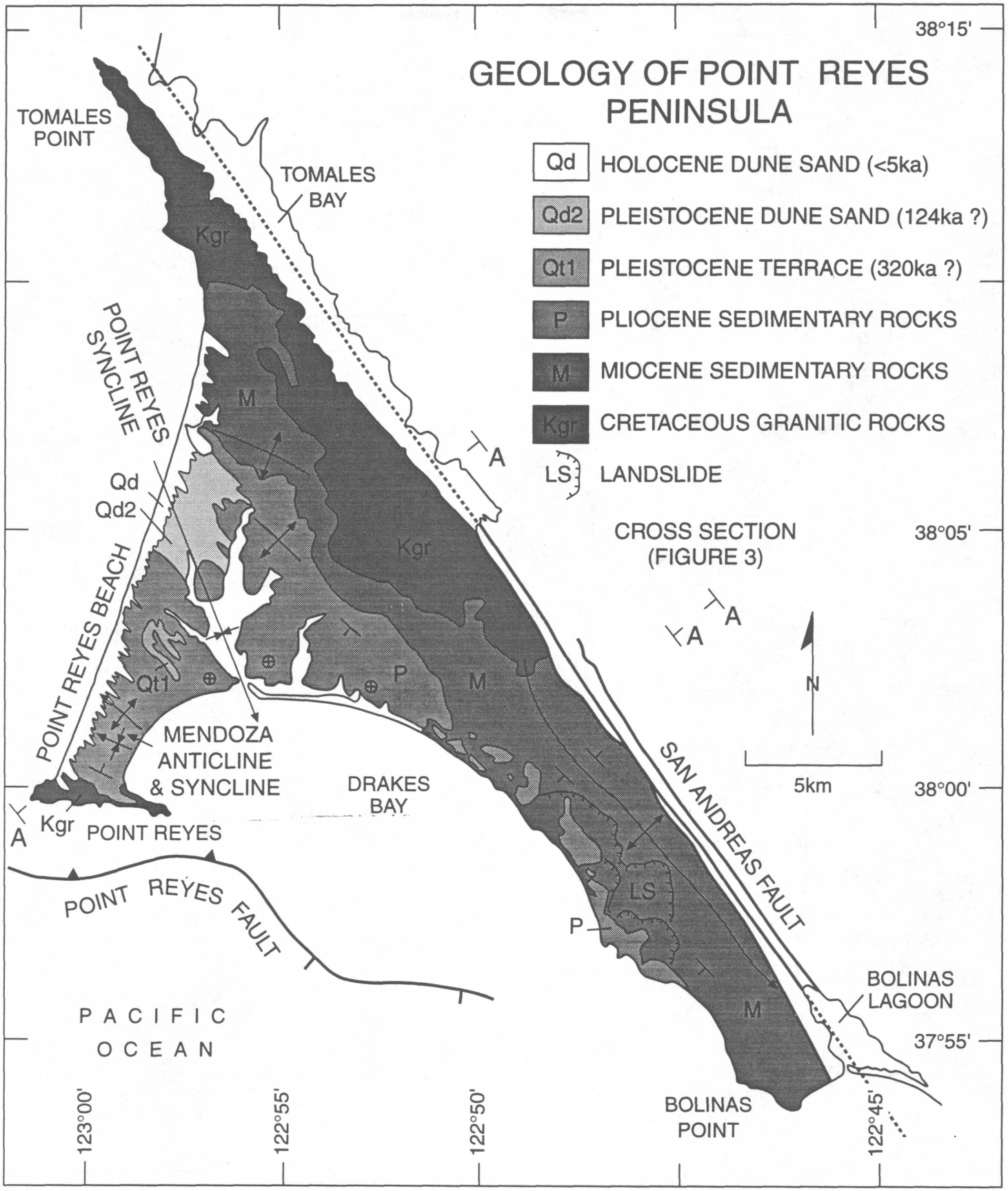
GEOLOGY OF POINT REYES PENINSULA
Qd HOLOCENE DUNE SAND (<5ka)
Qd2 PLEISTOCENE DUNE SAND (124ka ?)
Qt1 PLEISTOCENE TERRACE (320ka ?)
P PLIOCENE SEDIMENTARY ROCKS
M MIOCENE SEDIMENTARY ROCKS
Kgr CRETACEOUS GRANITIC ROCKS
LS LANDSLIDE
CROSS SECTION (FIGURE 3)
N
5km
38°15'
38°05'
38°00'
37°55'
123°00'
122°55'
122°50'
122°45'
TOMALES POINT
TOMALES BAY
POINT REYES SYNCLINE
POINT REYES BEACH
MENDOZA ANTICLINE & SYNCLINE
DRAKES BAY
POINT REYES
POINT REYES FAULT
SAN ANDREAS FAULT
BOLINAS LAGOON
BOLINAS POINT
PACIFIC OCEAN

FIGURE 2

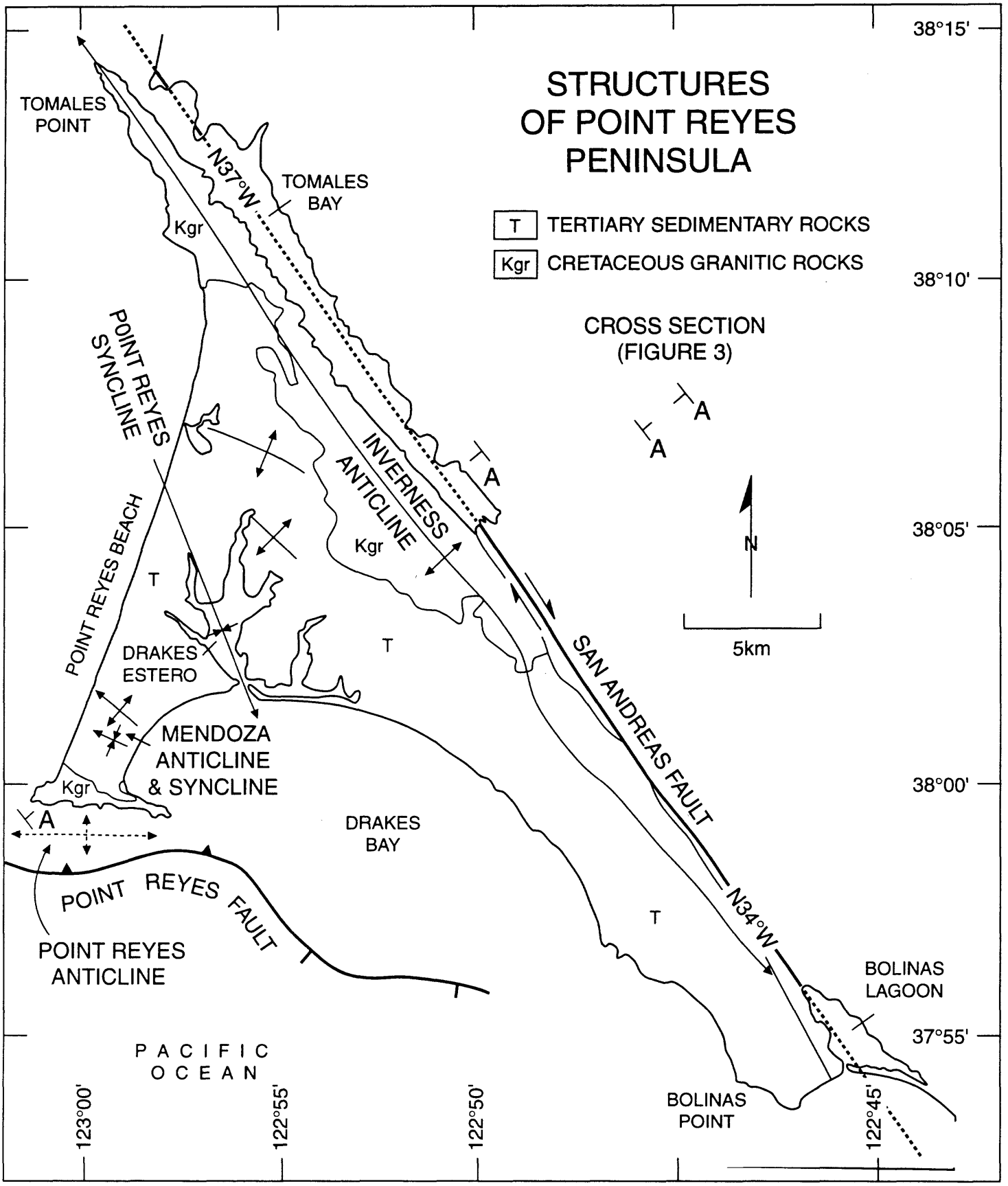
STRUCTURES
OF POINT REYES
PENINSULA
T TERTIARY SEDIMENTARY ROCKS
Kgr CRETACEOUS GRANITIC ROCKS
CROSS SECTION
(FIGURE 3)
A
A
N
5km
38°15'
38°10'
38°05'
38°00'
37°55'
123°00'
122°55'
122°50'
122°45'
TOMALES
POINT
TOMALES
BAY
N37°W
Kgr
POINT REYES
SYNCLINE
INVERNESS
ANTICLINE
POINT REYES BEACH
T
Kgr
DRAKES
ESTERO
MENDOZA
ANTICLINE
& SYNCLINE
Kgr
A
DRAKES
BAY
POINT REYES FAULT
POINT REYES
ANTICLINE
SAN ANDREAS FAULT
N34°W
BOLINAS
LAGOON
PACIFIC
OCEAN
BOLINAS
POINT

FIGURE 4

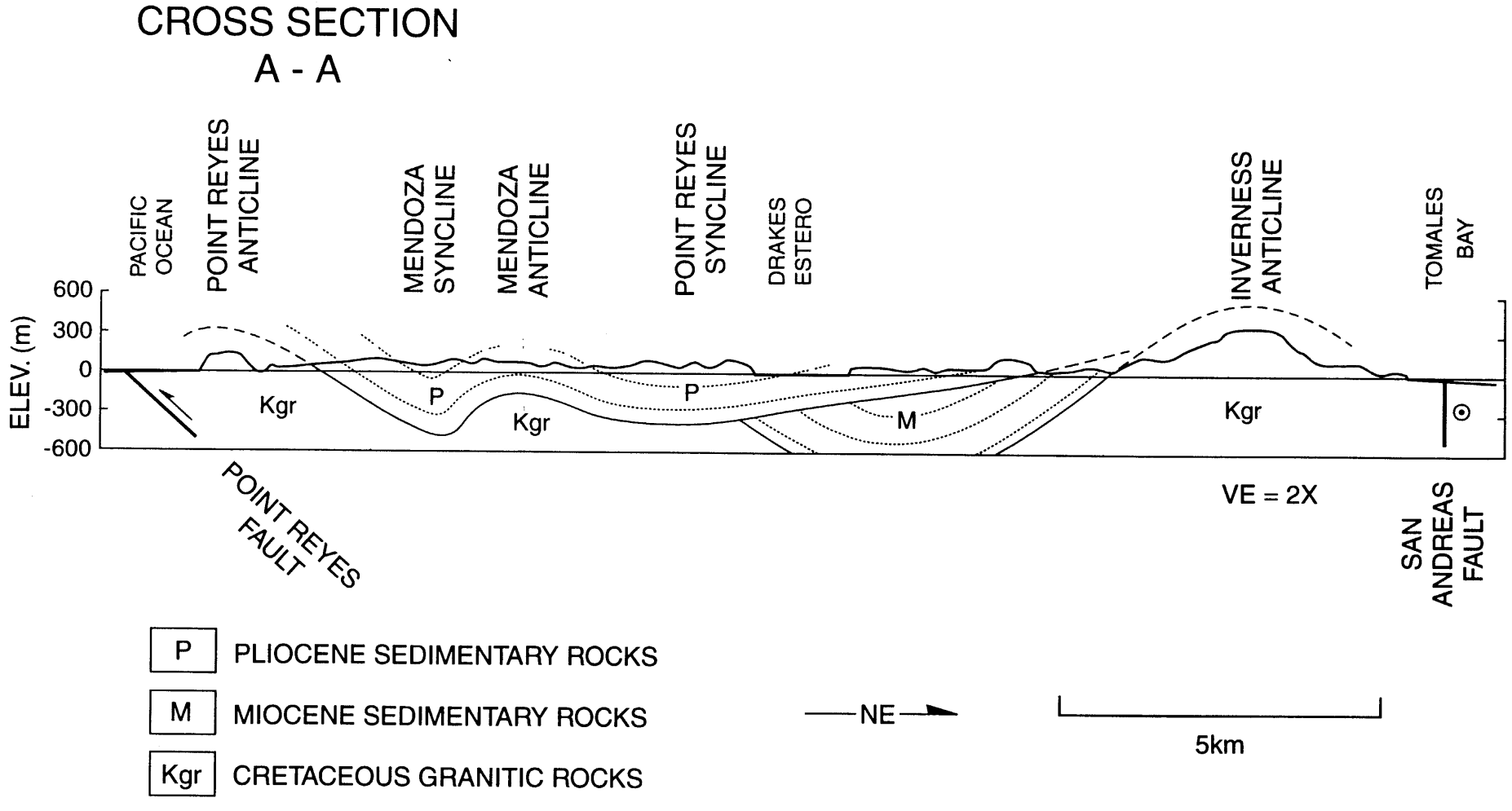
CROSS SECTION
A - A
PACIFIC OCEAN
POINT REYES ANTICLINE
MENDOZA SYNCLINE
MENDOZA ANTICLINE
POINT REYES SYNCLINE
DRAKES ESTERO
INVERNESS ANTICLINE
TOMALES BAY
ELEV. (m)
600
300
0
-300
-600
Kgr
P
Kgr
P
M
Kgr
POINT REYES FAULT
VE = 2X
SAN ANDREAS FAULT
P PLIOCENE SEDIMENTARY ROCKS
M MIOCENE SEDIMENTARY ROCKS
Kgr CRETACEOUS GRANITIC ROCKS
NE
5km

FIGURE 3

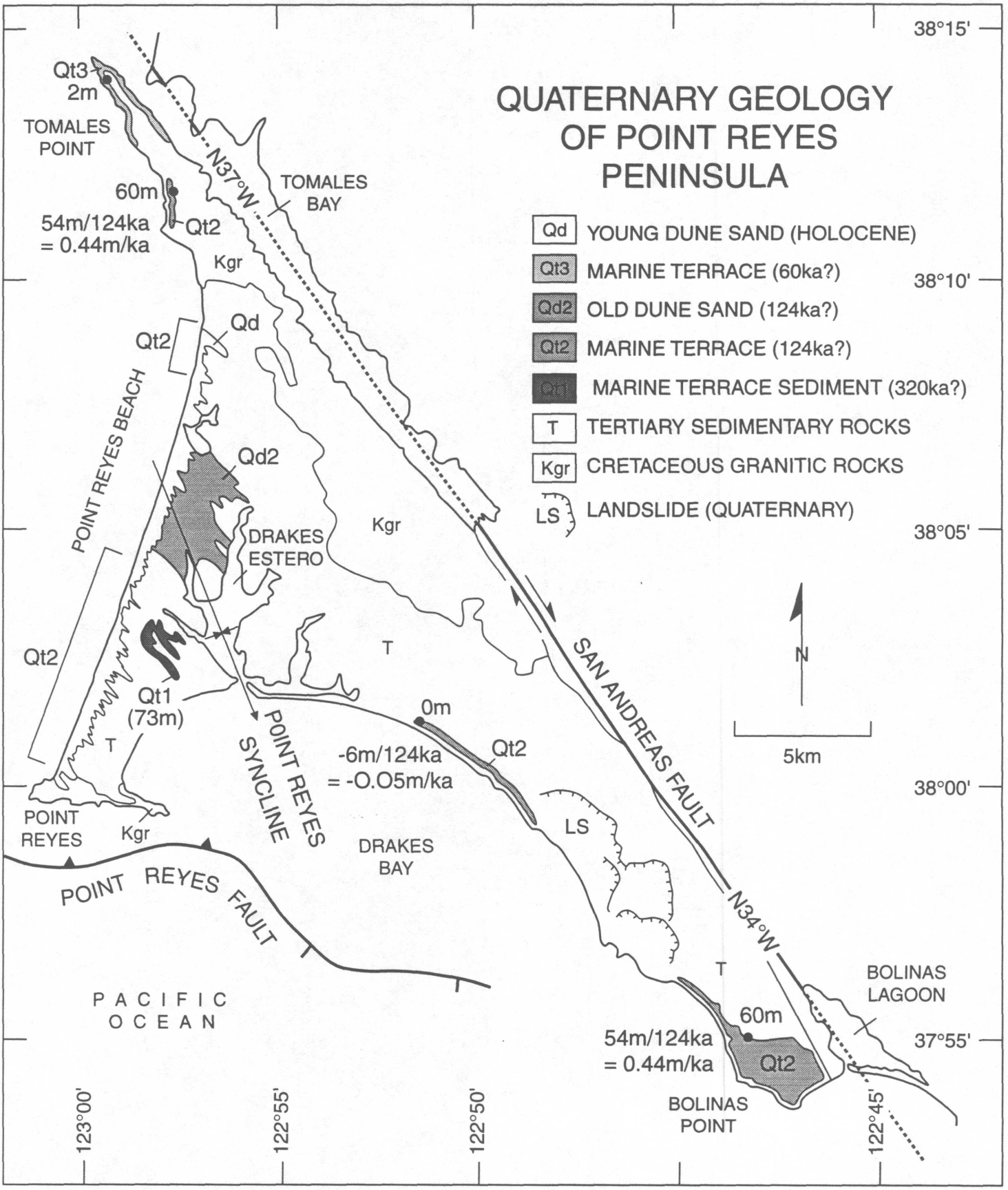
QUATERNARY GEOLOGY
OF POINT REYES
PENINSULA
Qd YOUNG DUNE SAND (HOLOCENE)
Qt3 MARINE TERRACE (60ka?)
Qd2 OLD DUNE SAND (124ka?)
Qt2 MARINE TERRACE (124ka?)
Qt1 MARINE TERRACE SEDIMENT (320ka?)
T TERTIARY SEDIMENTARY ROCKS
Kgr CRETACEOUS GRANITIC ROCKS
LS LANDSLIDE (QUATERNARY)
38°15'
38°10'
38°05'
38°00'
37°55'
123°00'
122°55'
122°50'
122°45'
Qt3
2m
TOMALES
POINT
60m
54m/124ka
= 0.44m/ka
Qt2
Kgr
N37°W
TOMALES
BAY
Qt2
Qd
POINT REYES BEACH
Qd2
DRAKES
ESTERO
Kgr
T
Qt2
Qt1
(73m)
T
POINT
REYES
Kgr
POINT REYES
SYNCLINE
0m
-6m/124ka
= -O.O5m/ka
Qt2
DRAKES
BAY
LS
SAN ANDREAS FAULT
N
5km
POINT REYES FAULT
N34°W
T
BOLINAS
LAGOON
60m
54m/124ka
= 0.44m/ka
Qt2
BOLINAS
POINT
PACIFIC
OCEAN

FIGURE 5

Lajoie

	856	895	893
Arc Ln id			
Compiler(s)	Lajoie, K. R.	Lajoie, K. R.	Lajoie, K. R.
Institution	USGS	USGS	USGS
D of submis	Feb 28, 95	Feb 28, 95	Feb 28, 95
Project/Contract	9960-11276	9960-11276	9960-11276
Map_scale	1:62,500	1:114,000; 1:24,000	1:114,000; 1:24,000
Original_source_scale	1:62,500	1:24,000	1:24,000
Structure_Name	Inverness Ridge Anticline	Half Moon Bay Syncline	Pillar Point Anticline
age_min	1	1	2
cami	pos		
age_max	5	1	2
cama	def		
Age_control	Paleontologic, geomorphic	Amino Acid	
Inclined Geomorphic surface	Marine platform, probable,marine strata definate	125 k and 5-8 k surfaces inclined	Marine terrace, Pliocene strata
c1		1	
c2		1	
vert rate mm/yr		-0.24	
Initiation of folding (Ma)		> 6000	
Rate ave, time length		125000	
Para ss	Yes	No	No
dist from fault	1 - 3 km		
Oblique to fault		yes	
Ave Ori		45	
step-over	no	no	yes?
Distance fm faults		0	
Ave. Trend	330	282	
Plunge	NW and SE	0.35	
Ave AP strike	330	282	
AP dip		90	
Confidence of location	Possible	Probable	Possible
Verge dir	NE?		
Multi or seg	Yes	Yes	Yes?
half wvlgth (km)		3 km	
fold type	anticline	syncline	anticline, asymmetric
fold style	fault-bend	fault-bend?	fault-bend?
Geodetic		none	
Reference			
Subsurface data	Yes		
Structure sections	Yes	Lajoie, 1976	

Drill Hole		Yes, local water wells, log in Lajoies files, aboutr 30 holes, 10 -40 m,depth to bedroc define deformed wave-cut platform	
Seis Reflct		no	
Grav		no	
Historical Seismicity	?	no	
Mag/event			
Depth			
Distrib microseis			
Reference	Weaver, 1949		
Additonal References	Weaver, GSA Memoir 35, Galloway, 1977, CDMG Bull 202	Lajoie, 1976; Weber and others, Lajoie and others,	Lajoie, 1976; Weber and others, Lajoie and others,

Lajoie, Point Reyes Area

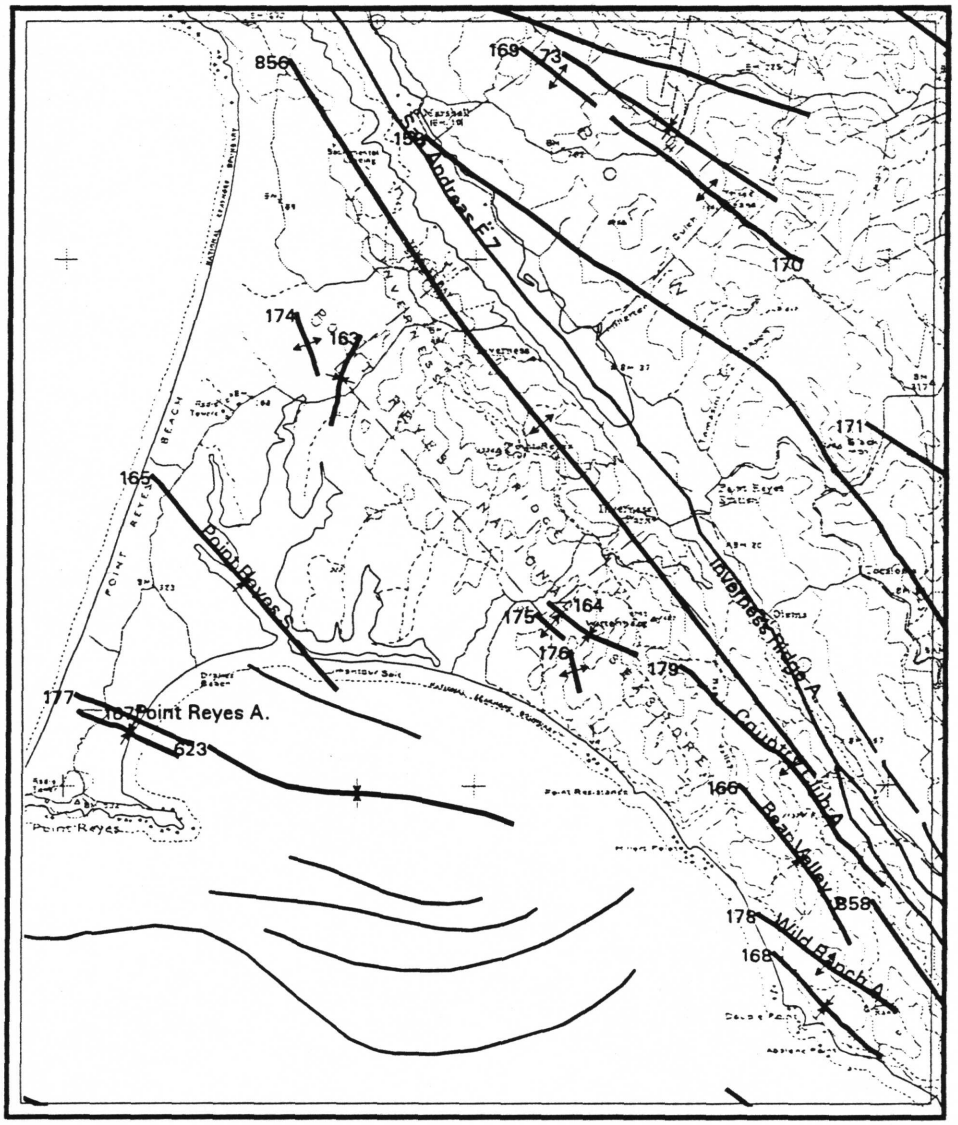

SCALE 1:200000

Napa and Sonoma Counties, north San Francisco Bay Area

Wesling, J., and Crampton, T., Geomatrix Consultants

Fox, K.F. Jr., and others, 1973, Preliminary Geologic Map of eastern Sonoma County and western Napa County, California: U.S. Geological Survey Miscellaneous Field Studies Map MF-483, 1:62, 500.

Manson, M.W., 1988, Landslide Hazards in the Cordelia-Vallejo area, Solano and Napa counties, California: D.M.G. Open-File Report 88-22, 1:24,000.

Sims, J.D., and others, 1973, Preliminary Geologic Map of Solano County and parts of Napa, Contra Costa, Marin, and Yolo counties, California: U.S. Geological Survey Miscellaneous Field Studies Map MF-484, 1:62,500.

Weaver, C.E., 1949, Geology of the Coast Ranges immediately north of the San Francisco Bay region, California: Geological Society of America Memoir 35, 1:62,500.

Geomatrix 2 on regional index map showing location of compiled areas
Wesling, Geomatrix, Glen Ellen area

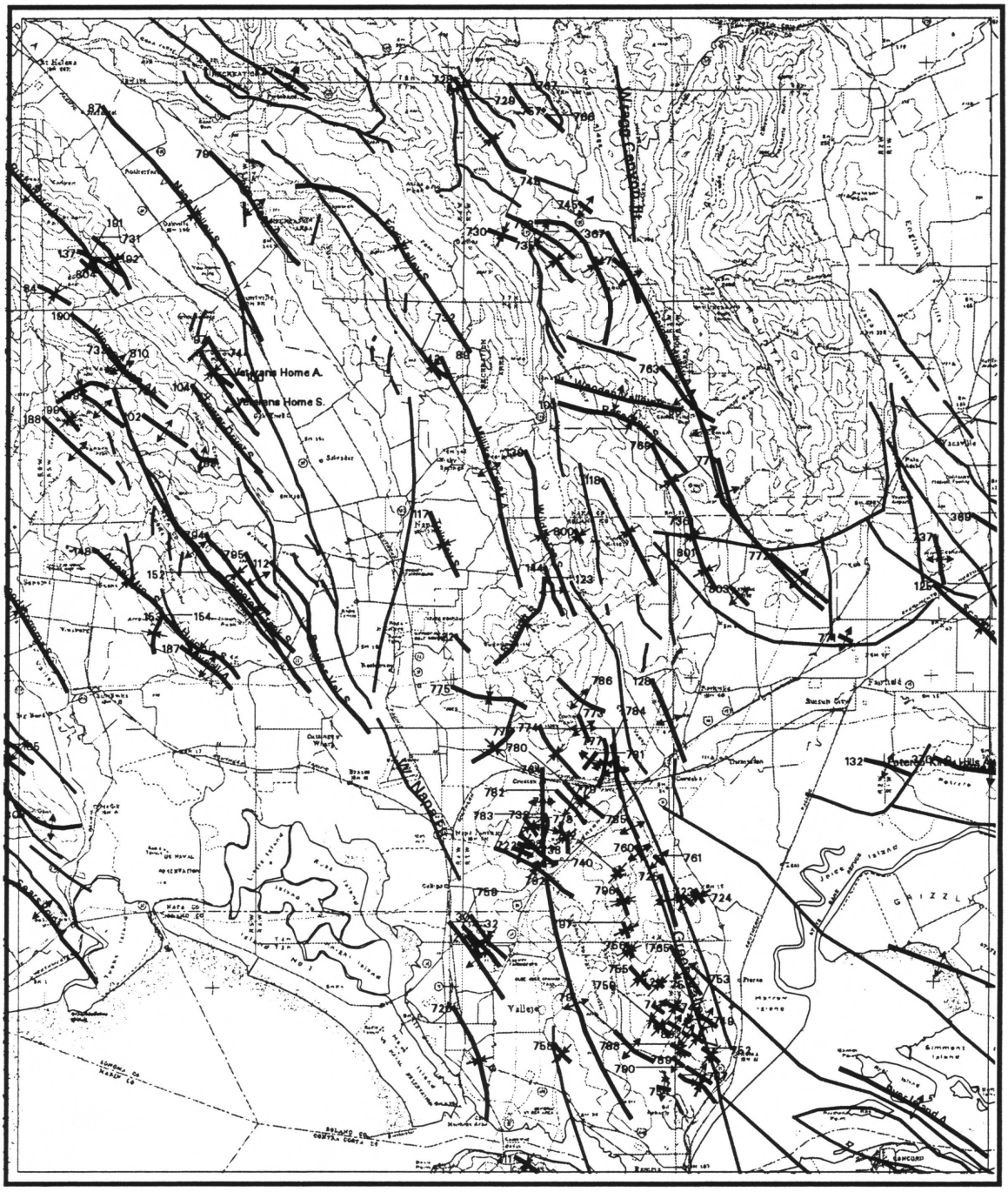

Wesling

Arc Ln id	805	806	807	808	809	810	811
Compiler(s)	Wesling, J.	Wesling, J.	Wesling, J.	Wesling, J.	Wesling, J.	Wesling, J.	Wesling, J.
Structure_Name	P9	P11		P10	Q3	Q2	Q4
age_min	4	3		3	1	1	1
age_max	6	5	7	5	3	2	3
Age_control	K/Ar, Sonoma volcanics	K/Ar, Sonoma volcanics		K/Ar, Sonoma volcanics	Glen Ellen Formation	Glen Ellen and Huichica Formation	Glen Ellen Formation
Inclined Geomorphic surface					Deformed Plio-Pleistocene deposits	fluvial and unknown	Deformed Plio-Pleistocene deposits
Para ss	no	yes		yes		yes	yes
dist from fault		1.5 Rodgers Creek		1, Rodgers Creek		0.5 Carneros fault	7-9 km
Ave Ori	40				35		
Distance fm faults	1 - 1.6, Rodgers Creek				0 -1, Rogers Creek fault		
Ave. Trend		345		145	297	240	
Plunge					25		
Ave AP strike	285	345		145		320	315
AP dip dir					ne		
Confidence of location	Possible	Possible		Possible		Possible	probable
Verge dir							ne
Multi or seg					no		
fold type	anticline	anticline	anticline	anticline	anticline	anticline	suncline
fold style	unknown	unknown		unknown		unknown	unknown

Additional Sources of Data Used in Map Compilation

Bonilla, M.G., 1971, Preliminary geologic map of the San Francisco South quadrangle and part of the Hunters Point quadrangle, California: U.S. Geological Survey Miscellaneous Field Studies Map MF-311, 1:24,000.

Bonilla, M.G., 1994, Sierra fault zone, San Francisco Peninsula, California [abs.]: EOS, American Geophysical Union Transactions, v. 75, no. 44, Supplement, p. 681. (1994 Fall Meeting, San Francisco)

Hengesh, J.V., and Wakabayashi, John, 1994, Quaternary deformation along the onshore projection of the coyote Point fault zone [abs.]: EOS, Transactions, American Geophysical Union, v. 75, no. 44, Supplement, p. 681. (1994 Fall Meeting, San Francisco).

Hunter, R.E., clifton, H.e., Hall, N.tl, Csaszar, G., Richmond, BlM., and Chin, J.L., 1984, Pliocene and Pleistocene coastal and shelf deposits of the Merced Formation and associated beds, northwest San Francisco Peninsula, california, in society of Econ9omic Paleontologists and Mineralogists Field Trip Guidebook 3, 1984 Midyear Meeting San Jose, California, p. 1-29.

Ingram, Bonnye Lynn, 1992, Paleoclimatic and paleoceanographic studies of estuarine and marine sediments using strontium isotopes: Stanford Univ. Ph.D. dissertation, 236 p.

Marvin, R.F., and Dobson, S.W., 1979, Radiometric ages: Compilation B, U.S. Geological Survey: Isochron/West, no. 26, p. 3-32.

Sarna-Wojcicki, A.M., Lajoie, K.R., Meyer, C.E., and Adam, D.P., 1991, Tephrochronologic correlation of upper Neeogene sediments along the Pacific margin, Conterminous United States, *in* Morrison, R.B., ed., Quaternary nonglacial geology; conterminous U.S.: Boulder, Colorado, Geological Society of America, The Geology of North America, v. K-2, p. 117-140.

Sarna-Wojcicki A.M., Meyer, C.E., Bowman, H.R., Hall, N.T., Russell, P.C., Woodward, M.J., and Slate, J.L., 1985, Correlation of the Rockland ash bed, a 400,000-year-old stratigraphic marker in northern California and western Nevada, and implications for middle Pleistocene paleogeography of central California: Quaternary Research, v. 23., p. 236-257.

Yancey, T.E., 1978, Stratigraphy of the Plio-Pleistocene strata in the Twelvemile Creek area, San Francisco Peninsula, California: California Academy of Sciences, Proceedings, Fourth Series, v. XLI, no. 15, p. 357-370.

Additional References:

Allen, J.E., 1946, Geology of the San Juan Bautista Quadrangle, California: California Division of Mines and Geology Bulletin 133 p. 54.

Allen, J.E., 1946, Geology of the San Juan Bautista quadrangle, CA, C.S.M.B. Bull. 133.

Alt, J.N., 1979, Analysis of repeated leveling for the Livermore Valley area, Alameda County, California [abs.]: Geological Society of America Abstracts with Programs, v. 11, p. 65-66.

Andrews et al., 1993, Journal of Geophysical Research, v. 98, no. B7, p. 12,083-12,095.

Clark, J.C., and Reitman, J.D., 1973, Oligocene stratigtrasphy tectonics and paleogeography southwest of the San Andreas fault, Santa Cruz Mountains and Gabilan Range, California Coast Ranges: U.S. Geological Survey Professional Paper 783.

Dibblee, T.W. Jr., 1975, Geologic map of the San Benito quadrangle, California: U.S. Geological Survey Open-File Report 75-394.

Dibblee, T.W. Jr., 1979, Geologic map of the Pacines quadrangle, San Benito and Monterey counties, California: U.S. Geological Survey Open-File Report 79-290.

Dibblee, T.W. Jr., 1979, Geologic map of the Tres Pinos quadrangle, San Benito and Monterey counties, California: U.S. Geological Survey Open-File Report 79-703.

Dibblee, T.W. Jr., and Brabb, E.E., 1978, Preliminary geologic map of the Chittenden Quadrangle, Santa Clara, Santa Cruz, San Benito counties, US Geological Survey Open-File Report 78-457.

Enos, Paul, 1965, Geology of the western Vallecitos Syncline, San Benito County, California: California Division of Mines and Geology Map Sheet 5, 1:31, 680.

Geomatrix Cosultants, Inc., 1991, Late Quaternary uplift along the Pajaro Riiver, southern Santa Cruz Mountains, CA, August 1991.

Hitchcock, C.S., Kelson, K.I., and Thompson, S.C., 1994, Geomorphic Investigation and deformation during the

northeastern margin of the Santa Cruz Mountains: USGS OFR 94-187.

Kelson, K.I., and Simpson, _ _ , 1944, EOS abstract.

Kelson, K.I., Simpson, G.D., Haraden, C.C., Sawyer, T.L., and Hemphill-Haley, M.A., 1993, Late Quaternary sufricial deformation of the southern East Bay Hills, San Francisco Bay Region, Calif.; Unpub. report to USGS NEHRP, award #1434-92-G2-2209, 29 p.

Rogers, T.H., 1993, Geology of Hollister and San Felipe quadrangles, San Beito, Santa Clara, and Monterey counties, California: California Division of Mines and Geology 0pen-File Report 93-01.

Rogers, T.H., 1993, Geology of the Hollister and San Felipe quadrangles, San Benito, Santa Clara, and Monterey Counties, California: California Division of Mines and Geology Open-File Report 93-01.??

Wong and Hemphill-Haley, 1992, show vertical structure to west of fold axis that has one westerly strike.

Appendix I

Confidence or assessment of activity and location

The source of uncertainties will be from establishing the geometry of the structures in two and three dimensions, from reliability of the age constrains (paleontologic and radiometric)

Confidence level	*Data Source*
Definite:	Active seismicity on blind thrust and geodetic response, Seismic reflection, drilling, good stratigraphic control on young strata, geomorphic surfaces inclined with good age control
Probable:	Stratigraphic control poor, geomorphic surfaces inclined with poor age control, undulatory concordant ridge elevations, gravity or magnetic anomaly at depth,
Possible:	Geomorphic (i.e. channel patterns, slope/sinuosity, stepped concordant ridges), topographic high, preferable orientation within present day stress field.

Map Symbols

Fold Axes	Definite	Probable	Possible
Syncline	_____	– – – – –	– · – · – · –
Anticline	_____	– – – – –	– · – · – · –
Overturned Syncline	_____	– – – – –	– · – · – · –
Overturned Anticline	_____	– – – – –	– · – · – · –
Axial Plane: strike and dip	_____	– – – – –	– · – · – · –
Fold axis: trend and plunge	_____	– – – – –	– · – · – · –

area of hinge _____

area of forelimb _____

area of back limb _____

Vergence direction _____

Inferred fault tip line of blind fault _____

Appendix II.

ACTIVE FOLD/BLIND THRUST DATABASE COMPILATION FORM

This database compilation form has been developed to help standardize the available information regarding active folding and to help identify potentially blind thrust faults. This information is being compiled in an ARC-INFO digital GIS database. The database form is organized (I-VII) with respect to the highest to lowest priority information that is useful to hazard assessment .

Description of Accompaning Map

Compiler (Last Name, First Name, Middle Initial) _____

Institution _____

Date of submission (day, month, year) _____

U.S.G.S. Contract Number or U.S.G.S. Project Number: _____

Map scale of compilation submitted for digitization: _____

Compilation scale(s) of original source materials if different from that submitted on the compilation: _____

Structure: Name or Label used on compilation: _____

I. Age Control Of Folding

A. Geologic or geomorphic evidence for age of folding:
Age of youngest inclined stratigraphic unit or age of youngest inclined surface
(Circle one or more)

1	L. Quaternary	0 - 0.75	
2	E. Quaternary	0.75 - 1.6	
3	L. Pliocene	1.6 - 3.4	(Piacenzian)
4	E. Pliocene	3.4 - 5.3	(Zanclean)
5	L Miocene	5.3 - 6.5	(Messinian)
6	Pre L Miocene	>6.5	
7	Age Unknown		

B. Source of stratigraphic age control: (check)

paleontologic:			
radiometric:	C14		
	Fission track		
	amino acid		
	soil stratigraphy		
Youngest stratigraphic unit	other: (specify) Name:		

C. Type of geomorphic surface inclined: (circle one)

M	marine	
L	lacustrine	
F	fluvial strath , tred, erosional	
U	unknown	
O	other: specify	
	aggradational, degradational	

II. Deformation Rate

	Confidence						
	High	1	2	3	4	5	Low
Minimum horizontal shortening (km): ±							
Estimated shortening rate: ±							
Vertical displacement rate (mm/yr)							
(uplift (+)/subsidence (-)) ±							
Duration of Folding							
initiation of fold activity (Ma) ±							
termination of fold activity (Ma) ±							
Method of determining rate:							
Length of time over which rate was determined							

IV. Geologic Setting

i.e.; Parallels major strike-slip fault (yes/no)

Distance from fault (name fault) _____

angle of obliquity (0-90) _____

Distance from fault (km, name fault) _____

Step-over between strike-slip faults (yes/no)

Distance from fault (km, name faults) _____

V. Description Of Fold

Axis:

Trend (0-360)	
Plunge (0-90)	

Axial Plane:

Strike (0-360)				
Dip (0-90)				
Dip Direction (circle one):	N	S	E	W

Reliability of fold axis location: (Confidence)

Circle one: Definite Probable Possible

Vergence direction: (Circle one)	N	NE	E	SE	S	SW	W	NW

Multiple or segmented folds: (Yes/no)
Interlimb angle (0-179): _____
Back limb: strike and dip _____
dimension (km sq) _____
Fore limb: strike and dip _____
dimension (km sq) _____
Half wave-length (km): _____
Fold type (s): (check one or more if known)

A	anticline
S	syncline
O	open
U	upright
I	inclined
AS	asymmetric
B	box
C	chevron
H	homocline
M	monocline

Fold style: (check one or more)

	Fault bend fold
	Fault propagation fold
	En Echelon
	Unknown

VI. Additional data sources that indicate folding:
Geodetic data:
Method:
Reference:
Subsurface data:
Structure sections available?
Reference:
Drill-hole data available: (yes/no)
Source:
Number of holes
Depth of hole
Comments:
Seismic reflection data:
Reference:
Gravity and magnetic data:
Reference:
Historical seismicity (yes/no)
Magnitude/Event
Depth (km)
Distributed micro-seismicity
Reference:
VII. Additional References:

Appendix III.a

The following information describes the field/items in the arc-info digital coverage sf_folds. The capitalized word is the arc-info item name located in the arc attribute table sf_folds.aat, this is followed by a short description of the entry into the field

FNODE
Arc-info generated field

TNODE
Arc-info generated field

LPOLY
Arc-info generated field

LENGTH
Arc-info generated field

SF_FOLDS#
Arc-info generated field

SF_FOLDS-ID

LTYPE
(Alacarte generated field) anticline certain, anticline approximately located, syncline certain, syncline approximately located

SEL
Arc-info, Alacarte, generated field

SYMB
Arc-info, Alacarte, generated field

LINEID
Arc Line identity number

COMPILER
Compiler(s)

INSTITUT
Institution

SUBMISSION
Date of submission to database

PROJECT
USGS Project or Contract number

COMMAPSCALE
Map_scale of submitted compilation

ORIMAPSCALE
Original_source_scale of data

STRUCTURE
Fold or Fault Structure_Name

MINAGE
age_min, Minimum age of structure

MAXAGE
age_max, Maximum age of structure

AGECONTROL
Source of stratigraphic or geomorphic Age_control

GEOMORPH
Inclined or otherwise deformed Geomorphic surface

EHORZ
Magnitude of horizontal strain (E) shortening (units km)

CONF1
c1, confidence in the estimate of magnitude of horizontal strain 1(high) to 5 (low)

ERATEH
Shortening rate, strain rate in the horizontal direction (units in mm/yr)

CONF2
c2, confidence in the estimate of the shortening rate, 1(high) to 5 (low)

ERATEV
Vertical displacement rate (units in mm/yr)

CONF3
c3, confidence in the estimate of the shortening rate, 1(high) to 5 (low)

FOLDINIT
Estimate of the timing of the initiation of folding (units Ma)

CONF4
c4, confidence in the estimate of the timing of the initiation of folding, 1(high) to 5 (low)

FOLDEND
Estimate of the timing of the termination of folding (Ma)

CONF5
c 5, confidence in the estimate of the timing of the termination of folding, 1(high) to 5 (low)

METHOD
Method of determining strain rates, and magnitude of displacement

DURRAVE
Lenght of time over which the displacement rate was determined or averaged

PAPASS
Does the fold parallel a strike-slip fault? (yes or no)

DIST
If the fold parallels a strike-slip fault, what is the average distance from the fault? (units km)

ORIENTOBL
If the fold does not parallel a strike-slip fault, what is its obliquity with respect to the fault.

DISTOBL&FLT

What distance does the oblique fold lie from the fault?

TREND
Average Trend of the fold (0 - 360 degrees)

PLUNGE
Plunge (0 - 90 degrees)

APSTRIKE
Average Axial Plane strike (0 -360 degrees)

APDIP
Axial Plane dip (0 -90 degrees)

APDIPDR
Axial Plane dip direction (n ne e se s sw w nw)

CONF
Confidence of location of the fold trace on the map (Definite, Probable, Possible)

VERG
Vergence direction (n ne e se s sw w nw)

SEGMENTED
Is the fold part of a larger zone or segmented? (yes or no)

ILIMBA
Interlimb angle (0 - 179 degrees)

BLSTRIKE
Back-limb strike (0 -360 degrees)

BLDIP
Back-limb dip (0 -90 degrees)

BLDIPDR
Back-limb dip direction (n ne e se s sw w nw)

BLDIM
Back-limb dimension (km sq)

FLSTRIKE
Fore-limb strike (0 -360 degrees)

FLDIP
Fore-limb dip (0 -90 degrees)

FLDIPDR
Fore-limb dip direction (n ne e se s sw w nw)

FLDIM
Fore-limb dimension (units km sq)

HALFWVL
Half wavelength of the fold (units km)

FOLDDS
fold type, anticline A, syncline, S homocline, H, upright, U, open, O gentle, G, inclined, I, asymmetric AS

FOLDSTY
fold style, fault bend fold, fault propagation fold, en echelon, unknown

GEODETICS
Geodetic data available? (yes or no)

GEODREF
Reference for geodetic data

CSUBSURFAC
Subsurface data available? (cite reference)

XSECTION
Structure sections available? (cite reference)

DRILLHOLE
Drill Hole data available? (cite reference)

SEISREFLT
Seis Reflction data available? (cite reference)

GRAVITY
Gravity data available? (cite reference)

HISTSEIS
Historical Seismicity (cite reference)

MAGEVENT
List Magnitude and name of event

DEPTH
Depth (units km)

DISTSEIS
Distributed microseismicity (cite reference)

REFERENCES
References

ADDCOMMENTS
Additonal References (cite reference)

EXTRA
Extra (This space was used to enter an arbitrary end of line character for imported file)

Col	ITEM_NAME	Width input	Out put	Type	#Decimals	
1	FNODE#	4	5	B	-	-
5	TNODE#	4	5	B	-	-
9	LPOLY#	4	5	B	-	-
13	RPOLY#	4	5	B	-	-
17	LENGTH	4	12	F	3	-
21	SF_FOLDS#	4	5	B	-	-
25	SF_FOLDS-ID	4	5	B	-	-
29	LTYPE	35	35	C	-	-
64	SEL	1	1	I	-	-
65	SYMB	3	3	I	-	-
68	LINEID	7	7	I	-	-
75	COMPILER	35	35	C	-	-
110	INSTITUT	35	35	C	-	-
145	SUBMISSION	8	8	C	-	-

153	PROJECT	25	25	C	-	-
178	COMMAPSCALE	15	15	I	-	-
193	ORIMAPSCL	15	15	I	-	-
208	STRUCTURE	50	50	C	-	-
258	MINAGE	6	6	N	2	-
264	MAXAGE	6	6	N	2	-
270	AGECONTROL	100	100	C	-	-
370	GEOMORPH	35	35	C	-	-
405	EHORZ	6	6	N	2	-
411	CONF1	3	3	N	1	-
414	ERATEH	6	6	N	2	-
420	CONF2	3	3	N	1	-
423	ERATEV	6	6	N	2	-
429	CONF3	3	3	N	1	-
432	FOLDINIT	10	10	N	5	-
442	CONF4	3	3	N	1	-
445	FOLDEND	10	10	N	5	-
455	CONF5	3	3	N	1	-
458	METHOD	35	35	C	-	-
493	DURRAVE	8	8	N	4	-
501	PAPASS	4	4	C	-	-
505	DIST	5	5	N	2	-
510	ORIENTOBL	6	6	C	-	-
516	DISTOBL&FLT	5	5	C	-	-
521	TREND	3	3	I	-	-
524	PLUNGE	2	2	I	-	-
526	APSTRIKE	3	3	I	-	-
529	APDIP	2	2	I	-	-
531	APDIPDR	3	3	C	-	-
534	CONF	15	15	C	-	-
549	VERG	4	4	C	-	-
553	SEGMENTED	4	4	C	-	-
557	ILIMBA	3	3	I	-	-
560	BLSTRIKE	3	3	I	-	-
563	BLDIP	2	2	I	-	-
565	BLDIPDR	3	3	C	-	-
568	BLDIM	8	8	N	2	-
576	FLSTRIKE	3	3	I	-	-
579	FLDIP	2	2	I	-	-
581	FLDIPDR	3	3	C	-	-
584	FLDIM	8	8	N	2	-
592	HALFWVL	8	8	N	2	-
600	FOLDDS	15	15	C	-	-
615	FOLDSTY	20	20	C	-	-
635	GEODETICS	50	50	C	-	-
685	GEODREF	75	75	C	-	-
760	CSUBSURFAC	75	75	C	-	-
835	XSECTION	75	75	C	-	-
910	DRILLHOLE	75	75	C	-	-
985	SEISREFLT	75	75	C	-	-
1060	GRAVITY	75	75	C	-	-
1135	HISTSEIS	75	75	C	-	-
1210	MAGEVENT	35	35	C	-	-
1245	DEPTH	4	4	N	1	-
1249	DISTRISEIS	75	75	C	-	-
1324	REFERENCES	200	200	C	-	-
1524	ADDCOMMENTS	200	200	C	-	-
1724	EXTRA	2	2	C	-	-

Col column number in database table
ITEM_NAME arc-info item name in .aat
Width input, field width for inputting data
Output, field with for outputting data
Type, description of type of input into field, C characters, I integers only, N numeric with #decimals specified

Appendix IIIb
The following abbreviations are found in the open-file text tables.

Arc Ln id	Arc Line identity number
Compiler(s)	
Institution	
D of submis	Date of submission to database
Project/Contract	USGS Project or Contract number
Map_scale	Map_scale of submitted compilation
Original_source_scale	
Structure_Name	Fold or Fault Structure_Name
age_min	Minimum age of structure
age_max	Maximum age of structure
Age_control	Source of stratigraphic or geomorphic Age_control
Inclined Geomorphic surface	Inclined or otherwise deformed Geomorphic surface
horiz short (km)	Magnitude of horizontal strain (E) shortening (units km)
c1	c1, confidence in the estimate of magnitude of horizontal strain 1(high) to 5 (low)
Shortening rate mm/yr	Shortening rate, strain rate in the horizontal direction (units in mm/yr)
c2	c2, confidence in the estimate of the shortening rate, 1(high) to 5 (low)
vert rate mm/yr	Vertical displacement rate (units in mm/yr)
c3	c3, confidence in the estimate of the shortening rate, 1(high) to 5 (low)
Initiation of folding (Ma)	Estimate of the timing of the initiation of folding (units Ma)
c4	c4, confidence in the estimate of the timing of the initiation of folding, 1(high) to 5 (low)
Termination of folding (Ma)	Estimate of the timing of the termination of folding (Ma)
c 5	c5, confidence in the estimate of the timing of the termination of folding, 1(high) to 5 (low)
Method	Method of determining strain rates, and magnitude of displacement
Rate ave time length	Lenght of time over which the displacement rate was determined or averaged
Para ss	Does the fold parallel a strike-slip fault? (yes or no)
dist from fault	If the fold parallels a strike-slip fault, what is the average distance from the fault? (units km)
Ave Ori	If the fold does not parallel a strike-slip fault, what is its obliquity with respect to the fault.
Distance fm faults	What distance does the oblique fold lie from the fault?
Ave. Trend	Average Trend of the fold (0 - 360 degrees)

Plunge	Plunge (0 - 90 degrees)
Ave AP strike	Average Axial Plane strike (0 -360 degrees)
AP dip	Axial Plane dip (0 -90 degrees)
AP dip dir	Axial Plane dip direction (n ne e se s sw w nw)
Confidence of location	Confidence of location of the fold trace on the map (Definite, Probable, Possible)
Verge dir	Vergence direction (n ne e se s sw w nw)
Multi or seg	Is the fold part of a larger zone or segmented? (yes or no)
Interlb ang	Interlimb angle (0 - 179 degrees)
Bck-lb strk	Back-limb strike (0 -360 degrees)
Bck-lb dip	Back-limb dip (0 -90 degrees)
Bck-lb dip dr	Back-limb dip direction (n ne e se s sw w nw)
Bck-lb dim (km sq)	Back-limb dimension (units km sq)
Fr-lb strike	Fore-limb strike (0 -360 degrees)
Fr-lb dip	Fore-limb dip (0 -90 degrees)
Fr-lb dip dr	Fore-limb dip direction (n ne e se s sw w nw)
Fr-lb dim (km sq)	Fore-limb dimension (units km sq)
half wvlgth (km)	Half wavelength of the fold (units km)
fold type	fold type, anticline A, syncline, S homocline, H, upright, U, open, O gentle, G, inclined, I, asymmetric AS
fold style	fold style, fault bend fold, fault propagation fold, en echelon, unknown
Geodetic	Geodetic data available? (yes or no)
Reference	Reference for geodetic data
Subsurface data	Subsurface data available? (cite reference)
Structure sections	Structure sections available? (cite reference)
Drill Hole	Drill Hole data available? (cite reference)
Seis Reflct	Seis Reflction data available? (cite reference)
Grav	Gravity data available? (cite reference)
Historical Seismicity	Historical Seismicity (cite reference)
Mag/event	List Magnitude and name of event
Depth	Depth (units km)
Distrib microseis	Distributed microseismicity (cite reference)
Reference or comments	
Additonal References	
Extra	Extra (This space was used to enter an arbitrary end of line character for imported file)

CONCERT WORKING GROUP FOLDS AND THRUSTS, SAN FRANCISCO BAY REGION

Angell, Micheal
Geomatrix
100 Pine St, 10th floor,
San Francisco, Ca, 94111
(415) 434-9400
angellaserve1%geomatrix_consultants@mcimail.com

Baker, Jim
Santa Clara Co.
2768 Longford Dr.,
San Jose, Ca., 95132-2235
4049
(408) 272 4554

Bakun, Bill
USGS
Menlo Park, MS 977
(415) 329-4793
bakun@andreas.wr.usgs.gov

Bonilla, M.G.
USGS
Menlo Park, MS 977
(415) 329-5615
mbonilla@isdmnl.wr.usgs.gov

Bortugno, Ed
BAREPP, Metrocenter
101 8th Street, Suite 152,
Oakland, Ca, 94607

Brabb, Earl
USGS
Menlo Park, MS 975
(415) 329-5140
ebrabb@isdmnl.wr.usgs.gov

Brocher, Tom
USGS
Menlo Park, MS 977
brocher@andreas.usgs.gov

Buising, Anna
Cal St.ate UNversity Hayward
Hayward, Ca., 94542
abuising@darwin.sci.csuhayward.edu
fax (510) 885 -2035

Bullard, Tom
Geomatrix
100 Pine St, 10th floor,
San Francisco, Ca, 94111
(415) 434-9400
tombaserve1%geomatrix_consultants@mcimail.com

Cole, Bill
Wm. Cotton & Ass.
330 Village Lane, Los Gatos, Ca.,
95030
1852
(408) 354-5542

Cotton, Bill
Wm. Cotton & Ass.
330 Village Lane, Los Gatos, Ca.,
95030
1852
(408) 354-5542

Coyle, John
Coyle Consult.
334 State St. Suite 106,
Los Altos, CA 94022
(415) 961-9980

Davis, Jim
CDMG
801 K St. MS 14-33,
Sacramento, Ca 95814

Figuers, Sandy
Norfleet Consultants
1205 East Stanley Blvd, Suite B,
Livermore, CA., 94550
(510) 606-8595

Graymer, Russell
USGS
Menlo Park, MS 975
(510) 525-8925
rgraymer@sierra.wr.usgs.gov

Griscom, Andy
USGS
Menlo Park, MS 989
(415) 329-5302
griscom@mojave.wr.usgs.gov

Hengesh, Jim
Dames & Moore
221 Main St. Suite 600,
San Francisco, Ca, 94105
(415) 243-3819 Fax 882-9261
SFOJVH@Dames.com

Hillhouse, Jack
USGS
Menlo Park
(415) 329-4909
jhillhouse@isdmnl.wr.usgs.gov

Jachens, Bob
USGS
Menlo Park, MS 989
(415) 329-5300
jachens@fourier.wr.usgs.gov

Jayko, Angela
USGS
Menlo Park, MS 975
(415) 329-4926
ajayko@isdmnl.wr.usgs.gov

Kelson, Keith
Wm Lettis & Ass.
1000 Broadway, Ste 612,
Oakland, Ca, 94607
(510) 832-3716,
FAX (510) 832-4139
wla@netcom.com

Kovach, Bob
Stanford U.
Stanford, Ca
(415) 723-4827
kov@pangea.stanford.edu

Lajoie, Ken
USGS
Menlo Park, MS 977
(415) 329-5641
lajoie@samoa.wr.usgs.gov

Lettis, Bill
Wm Lettis & Ass.
1000 Broadway, Ste 612,
Oakland, Ca, 94607
(510) 832-3716
wla@netcom.com

Lewis, Steve
USGS
Menlo Park, MS 999
(415) 354-3041
slewis@octopus.wr.usgs.gov

Lienkaemper, Jim
USGS
Menlo Park, MS 977
(415) 329-5642
jlienk@isdmnl.wr.usgs.gov

Marlow, Mike
USGS
Menlo Park, MS 999
(415) 354-3129
mmarlow@octopus.wr.usgs.gov

McCarthy, Jill
USGS
Menlo Park, MS 999
(415) 329-4776
mccarthy@octopus.wr.usgs.gov

McCrory, Pat
USGS
Menlo Park, MS 975
(415) 329-4945
pmccrory@isdmnl.wr.usgs.gov

McLaughlin, Bob
USGS
Menlo Park, MS 975
(415) 329-4925
rjmcl@isdmnl.wr.usgs.gov

Minasian, Diane

USGS
Deere Creek, MS 999
(415) 329 3082
diane@octopus.wr.usgs.gov

Murchey, Bonnie
USGS
Menlo Park, MS 915
(415) 329-4980
murchey@wr.usgs.gov

Page, Ben
Stanford University
Stanford, Ca
(415) 723-2532
page@pangea.stanford.edu

Prentice, Carol
USGS
Menlo Park, MS 977
(415) 329-5690
cprentice@isdmnl.wr.usgs.gov

Olsen, Jean
USGS
Menlo Park, MS 977
(415) 329-4779
jolsen@samoa.wr.usgs.gov

Rogers, J. David
Rogers/Pacific
396 Pacific Dr.,
Pleasant Hills, CA., 94523
7605
(510) 682-7601

Roering, Josh
Stanford U.
Stanford, Ca
roering@pangea.stanford.edu

Rymer, Mike
USGS
Menlo Park, MS 977
(415) 329-5049
mrymer@isdmnl.wr.usgs.gov

Schwartz, Dave
USGS
Menlo Park, MS 977
(415) 354-3013
dschwartz@isdmnl.wr.usgs.gov

Sims, John
USGS
12201 Sunrise Valley Drive,
Reston, VA 22092, MS 905
703-648-6722
sims@usgs.gov

Stanley, Rick
USGS
Menlo Park, MS 999
(415) 329-5651
rick@OCTOPUS.WR.USGS.GOV

Simpson, Bob
USGS
Menlo Park, MS 977
(415) 329-4865
simpson@GOLD.WR.USGS.GOV

Unruh, Jeff
Wm Lettis & Ass.
1000 Broadway, Ste 612,
Oakland, Ca, 94607
(510) 832-3716
wla@netcom.com

Wagner, Dave
CDMG
801 K St. MS 14-33,
Sacramento, CA 95814
(916) 324 7380

Wakabayashi, John
1329 Sheridan Ln.,
Hayward, Ca., 94544
(510) 887-1796

Jeff Nolan
Weber and Ass
120 Westgate Dr., Watsonville CA.,
95076
(408) 722-3580
jweber@rupture.ucsc.edu

Weber Band, Janine
UC Berkeley
U.C. Berkeley, Dept. of Geology,
Berkeley, Ca 94720
(510) 642-3993
jwband@uclink.berkeley.edu

Wentworth, Carl
USGS
Menlo Park, MS 975
(415) 329-4950
cwent@sierra.wr.usgs.gov

Wesling, John
Geomatrix
100 Pine St, 10th floor,
San Francisco, Ca, 94111
(415) 434-9400
johnwaserve1%geomatrix_consulta
nts@mcimail.com

Williams, Patrick
LBL
1 Cyclotron Rd.,
Berkeley, 94720
(510) 486-7156
plwilliams@lsl.gov

Wright, Bob
Harland, Tate and Ass.
1 Kerry St, 7th floor,
San Francisco, Ca., 94801
(415) 288-9880

Wright, Tom
Chevron (retired)
136 Jordan Ave.,
San Anselmo, 94960
(415) 456-9244

Zoback, M. L.
USGS
Menlo Park, MS 977
(415) 329-4760
zoback@andreas.wr.usgs.gov